UNIVERSITÀ DELLA CALABRIA

Dipartimento di Biologia, Ecologia e Scienze della Terra

Dottorato di Ricerca in Scienze della Vita
CICLO XXXI

Impact of DNA methylation status on plant response to Cd explored through a transcriptomic analysis

Settore Scientifico Disciplinare **BIO/01**

Coordinatore: Ch.ma Prof.ssa Maria Carmela Cerra

Supervisore: Ch.ma Prof.ssa Maria Beatrice Bitonti

Dottorando: Dott.ssa Marianna Pacenza

Table of Contents

LIST OF ABBREVIATIONS ..... **III**

ABSTRACT ..... **IX**

CHAPTER 1: INTRODUCTION **1**

1.1 DNA METHYLATION 1
1.1.1 DNA methylation: an historical overview *1*
1.1.2 DNA methylation in plants: sequence context and methylation pathways *2*
1.1.3 Molecular functions of DNA methylation in plants *6*
1.1.4 DNA methylation and its involvement in plant growth and development *8*
1.1.5 Involvement of DNA methylation in plant response to abiotic stress *11*
1.1.6 Cross-talk between epigenetic mechanisms and hormone network *13*
1.2 PHASES OF PLANTS RESPONSES TO STRESS 14
1.3 CADMIUM TOXICITY IN HIGHER PLANTS 16
1.3.1 Cadmium distribution in the environment *16*
1.3.2 Effects of cadmium exposure on plant growth and development *17*
1.3.3 Uptake and transport of Cd in higher plants *17*
1.3.4 Morphological, physiological and biochemical plant responses to Cd toxicity *19*
1.3.5 Role of phytohormones in plant response to Cd stress *21*
1.4 STUDY MODEL: *ARABIDOPSIS THALIANA* 24
1.4.1 Classification, geographical distribution and principal characteristics of Arabidopsis thaliana. *24*
1.4.2 DNA methylation landscape of the A. thaliana genome *26*
1.4.3 DNA methyltransferases-defective mutants of Arabidopsis thaliana. *27*

AIM OF THE WORK **30**

CHAPTER 2: MATERIAL AND METHODS **32**

2.1 PLANT LINES 32
2.2 GROWTH CONDITIONS 32
2.3 GERMINATION TEST 33
2.4 GROWTH PARAMETERS ANALYSIS 33
2.5 CD QUANTIFICATION 34
2.6 TOTAL RNA EXTRACTION 34
2.7 RNA-SEQ 35
2.8 PREPROCESSING AND ANALYSIS OF RNA-SEQ DATA 36
2.9 HEATMAP CONSTRUCTION 37
2.10 GENE ENRICHMENT ANALYSIS 37
2.11 ANALYSIS OF HORMONE-RELATED PATHWAYS 38
2.12 SINGLE STRAND CDNA SYNTHESIS 38
2.13 QUANTITATIVE REAL-TIME PCR (QRT-PCR) 39
2.14 LIBRARIES RESULTS VALIDATION 42
2.15 HORMONE LEVEL QUANTIFICATION 43
2.15.1 Extraction and purification *43*
2.15.2 HPLC analysis *43*
2.15.3 GC-MS analysis *43*
2.16 CONFOCAL VISUALIZATION OF GFP EXPRESSION AND SIGNAL QUANTIFICATION 44
2.17 ANALYSIS OF ROOT MERISTEM SIZE AND PATTERN 45

CHAPTER 3: RESULTS **46**

3.1 IMPACT OF CD EXPOSURE ON PLANT GROWTH AND DEVELOPMENT OF *DDC* MUTANT AND WT *A. THALIANA* SEEDLINGS. 46
3.2 QUANTIFICATION OF CD ABSORPTION IN *DDC* MUTANT AND WT SEEDLINGS OF *A. THALIANA*. 51
3.3 RNA-SEQ ANALYSIS 52
3.3.1 Analysis and Identification of Differentially Expressed Genes (DEGs) *52*
3.3.2 Gene Enrichment Analysis *55*
3.3.3 Differential expression of genes involved in hormones metabolism in ddc mutant and WT under Cd treatment *63*
3.3.3.1 Auxin 63
3.3.3.2 Cytokinins 73
3.3.3.3 Gibberellins 84
3.3.3.4 Jasmonic acid 91
3.3.3.5 Abscisic acid 95
3.3.3.6 Ethylene 107
3.3.4 Differential expression of genes involved in hormones signalling in ddc mutant and WT under Cd treatment *112*
3.3.4.1 Auxin 112
3.3.4.2 Cytokinins 114
3.3.4.3 Gibberellins 116
3.3.4.4 Jasmonic acid 118
3.3.4.5 Abscisic acid 120
3.3.4.6 Ethylene 123
3.3.4.7 Brassinosteroids 125
3.4 LIBRARIES RESULTS VALIDATION: QUANTIFICATION OF THE EXPRESSION LEVELS OF GENES RELATED TO HORMONE BIOSYNTHESIS AND SIGNALLING IN *DDC* MUTANT AND WT IN CTRL CONDITION AND UNDER CD TREATMENT BY QRT-PCR. 128
3.5 PHYTOHORMONES QUANTIFICATION IN DDC MUTANT AND WT UNDER CD TREATMENT. 131
3.5.1 IAA quantification *131*
3.5.2 GAs quantification *132*
3.5.3 JA quantification *135*
3.5.4 ABA quantification *136*
3.5.5 SA quantification *136*
3.6 HOW ARE THE DETECTED ALTERATION IN HORMONE PATHWAYS LINKED TO THE PHENOTYPE AND DIFFERENTIAL RESPONSE TO CD OF *DDC* MUTANT? 137
3.6.1 An insight into the involvement of auxin distribution pathway *137*
3.6.2 Effects of Cd toxicity on Root Apical Meristem pattern in ddc mutant and WT A. thaliana seedlings. *144*
3.6.3 Cd Impact on SCARECROW expression pattern in ddc mutant and WT A. thaliana seedlings. *149*

CHAPTER 4: DISCUSSION **153**

CHAPTER 5: CONCLUSIONS **163**

REFERENCES **165**

ACKNOWLEDGEMENTS **212**

LIST OF ABBREVIATIONS

12,13-EOT	12,13S-epoxy-octadecatrienoic acid
12-OPDA	12-oxo-phytodienoic acid
13-HPOT	13S-hydroperoxy-octadecatrienoic acid
AAO	Abscisic aldehyde oxidases
ABA	Abscisic acid
ABA-GE	ABA-glucosyl ester
ACO	1-aminocyclopropane-1-carboxylate oxidase
ACS	1-aminocyclopropane-1-carboxylate SYNTHASE
ACX	Acyl-CoA oxidase
AGO	ARGONAUTE
AHK	Histidine Kinane
AMI1	AMIDASE 1
AOC	Allene oxide cyclase
AOS	Allene oxide synthase
ARF	AUXIN RESPONSE FACTOR
ARR1	ARABIDOPSIS RESPONSE REGULATOR 1
AtBG1	ß-glucosidase
AuxREs	Auxin-responsive promoter elements
BAH	Bromo Adjacent Homology
BAK1	BRI1-ASSOCIATED RECEPTOR KINASE 1
BAM	Binary Alignment Map
BCH	ß-carotene hydroxylases
BER	Base Excision Repair
BES1	BRI1-EMS-SUPPRESSOR
BIN2	BR-INSENSITIVE 2
BR	Brassinosteroids
BR	Brassinosteroids
BRI1	BRASSINOSTEROID-INSENSITIVE 1
BSK	BRs signalling kinase
BSU1	BRI1 suppressor 1

BZR1	BRASSINAZOLE-RESISTANT 1
CAM	Crassulacean acid metabolism
CAT1	CATALASE1
CDG	Constitutive differential growth
cDNA	Complementary DNA
cDNA	Complementary DNA
CK	cytokinins
CKXs	Cytokinin oxidase/dehydrogenase enzymes
CMT	Chromomethylase
COI1	CORONATINE INSENSITIVE 1
Col-0	Columbia-0
CPS	ent-CDP synthase
CYP	Cytochrome P450 monooxygenases
cZ	*cis*-zeatin
DCL3	DICER- LIKE PROTEIN 3
ddc	*drm1 drm2 cmt3*
DDM1	DECREASED DNA METHYLATION 1
DEG	Differentially Expressed Gene
DHZR	Dihydrozeatin riboside
DMAPP	Dimethylallyl diphosphate
DME	DEMETER
DME	TRANSCRIPTIONAL ACTIVATOR DEMETER
DML2	DEMETER-LIKE 2
DML3	DEMETER-LIKE 3
DNA	Deoxyribonucleic acid
Dnmt2	DNA methyltransferase homologue 2
DRM	Domains rearranged methyltransferase
dsRNA	Double-stranded RNA
EPF2	EPIDERMAL CATTERNING FACTOR 2
ER	Endoplasmic Reticulum
ET	Ethylene
FC	Fold Change

FIE	FERTILIZATION-INDEPENDENT ENDOSPERM
FIS2	FERTILIZATION-INDEPENDENT SEED 2
FPKM	Fragments Per Kilobase Million
FWA	FLOWERING WAGENINGEN
GA	Gibberellins
GA20ox	GA 20-oxidase
GA3ox	GA 3-oxidase
GAMT	GAs methyltransferases
GFP	Green Fluorescent Protein
GGPP	Geranylgeranyl diphosphate
GO	Gene Ontology
HMA	Heavy Metal-transporting P-type ATPase
HPt	Histidine phospho¬transferase
IAA	indole-3-acetic acid
IAM	Indole-3-acetamide
IAOX	indole-3-acetaldoxime
IGP	Indole-3-glycerol phosphate
IND	Indole
INS	Indole synthase
IPA	Indole-3-pyruvic acid
IPP	C5-isopentenyl diphosphate
IPT	Adenylate isopentenyltransferase
IRT1	IRON-REGULATED TRANSPORTER 1
JA	Jasmonic acid
JAZ	Jasmonate-ZIM domain
KAO	ent-kaurenoic acid oxidase
KAT	3-ketoacyl-CoA thiolase
KO	ent-kaurene oxidase
KS	ent-kaurene synthase
KYP	KRYPTONITE
LOG	LONELY GUY
MAPKs	Mitogen-activated protein kinases

MEA	MEDEA
MEG	Maternally Expressed Gene
MES	2-N-morpholine ethane sulphonic acid
MET	Methyltransferase
Mez1	maize Ez-like gene 1
miRNA	MicroRNA
mRNA	Messenger RNA
MS	Murashige and Skoog
MT	metallotionein
NCED	9-cis-epoxycarotenoid dioxygenase
NIT	NITRILASE
NO	Nitric oxide
NPR1	NONEXPRESSER OF PATHOGENESIS-RELATED PROTEIN 1
NRAMP	Natural Resistance-Associated macrophage
OPR3	OPDA reductase 3
PA	Phaseic acid
PC	Phytochelatins
PEG	Paternally Expressed Gene
PIN	PINFORMED
PM	Plasma Membrane
POL IV	RNA Polymerase IV
POLV	RNA Polymerase V
PP2Cs	Phosphoprotein phosphatase 2Cs
PSY	Phytoene synthase
QC	Quiescent Center
qRT-PCR	Quantitative Reverse Transcriptase Polymerase Chain Reaction
RAM	Root Apical Meristem
RdDM	RNA-directed DNA methylation
RDR2	RNA- DEPENDENT RNA POLYMERASE 2
RIN transcription factor	RIPENING-INHIBITOR transcription factor
RNA	Ribonucleic acid

RNAseq	RNA sequencing
ROS	Reactive Oxygen Species
ROS1	REPRESSOR OF SILENCING 1
SA	Salicylic acid
S-AdoMet	S-adenosyl-L-methionine
SAM	Sequence Alignment Map
SAM	S-adenosylmethionine
SAM	S-adenosylmethionine
SAM	Shoot Apical Meristem
SCF	Skp-Cullin-F-box
SCN	stem cell niche
SCR	SCARECROW
sd	Standard Deviation
siRNA	Short interfering RNA
SnRK2s	SNF1-related protein kinases 2
SRA domain	SET and RING associated domain
ssRNA	Single-stranded RNA
StAR	Steroidogenic acute reg¬ulatory
TAA1	Tryptophan aminotransferase 1
TAM	Tryptamine
TDC	Tryptophan decarboxylase
T-DNA	Transfer DNA
TE	Transponsable Elements
TE	Transposable Element
TGA	TGACG Sequence-specific Binding Proteins
TIR1/AFB	TRANSPORT INHIBITOR RESPONSE/AUXIN SIGNALING F-BOX
TPL	TOPLESS
TPR	TPL-RELATED
TPS	Terpene synthase
tRNA-IPT	tRNA isopentenyltransferase
tZ	*trans*-zeatin

UGTs	O-glucosyltransferases
WT	Wild type
YUC	YUCCA
ZEP	Zeaxanthin epoxidase
ZIP	ZRT-IRT-like Proteins

ABSTRACT

Due to their sessile life style, plants are continuously exposed to a variety of abiotic and biotic stresses which could potentially hinder their growth, development, productivity and survival. In this scenario, it appears evident the relevance of epigenetic mechanisms in assuring growth plasticity to the plant and withstanding stresses through a rapid and extensive modification of gene expression in a manner that overcomes the restrictions of a highly stable DNA sequence.

Epigenome landscape is largely related to DNA methylation process, which is one of the most significant players in the control of plant responses to environmental changes and stressors. On the other hand, all these responses are also under the control of an intricate signalling network which strongly involves the phytohormones, whose action is in turn influenced by epigenetic mechanisms. Despite this information, the complex mechanisms by which DNA methylation modulates plant stress responses are yet largely unresolved, mainly with respect to heavy metal stress, for which a metal- and species-specific response was evidenced.

In order to gain further insight into these aspects, in the present work we performed a comparative transcriptomic analysis on the *drm1 drm2 cmt3 (ddc)* mutant of *A. thaliana,* defective in both maintenance and *de novo* DNA methylation, and WT plants exposed to a long lasting (21 days) Cd treatment at 25 and 50 μM concentrations. Attention was focused on Cd as one of the most toxic pollutants, widespread in both terrestrial and marine environment. The mutant was chosen as a suitable tool for investigating mechanisms and molecular processes that act in and are regulated by DNA methylation. Analyses of growth parameters and targeted cytophysiological features were also carried out.

Concerning the results, transcriptomic analysis highlighted photosynthesis, stress responses and hormone biosynthesis as the genetic pathways more impacted by Cd treatment in both *ddc* mutant and WT. All these pathways are highly relevant for plant development. A more detailed analysis carried out on the pathways related to the phytohormones suggested that, under a prolonged heavy metal exposure, plant activity was directed to enhance and/or maintain the level and signalling of hormones which are relevant in sustaining the growth (auxins, cytokinins and gibberellins) more than those of hormones specifically related to stress response (jasmonic acid, abscisic acid and salicylic acid). This could represent the plant strategy to avoid the negative effects of long-lasting

activity of stress-related hormones. Interestingly, such strategy could be more efficient in *ddc* mutant than in the WT. Indeed, likely due to a higher genome plasticity conferred to the mutant by its DNA hypomethylated status, in the *ddc* mutant the described transcriptomic differences have already been observed in the treatment with 25 μM Cd, while in the WT only in the treatment with 50 μM Cd. The outcome of this different modulation of gene expression was a better growth performance in *ddc vs* WT, as evidenced by growth parameters analysis. A tight relationship between the hormone-related transcriptomic differences and the different cyto- morphophysiological features of *ddc* mutant *vs* WT under Cd treatment was also revealed.

ABSTRACT

Le piante, a causa della loro natura sessile, sono continuamente esposte a una varietà di stress abiotici e biotici, i quali potrebbero potenzialmente ostacolare la loro crescita, sviluppo, produttività e sopravvivenza. In questo scenario, appare evidente l'importanza dei meccanismi epigenetici nell' assicurare alla pianta una certa plasticità di crescita e la capacità di tollerare situazioni stressanti, attraverso una modulazione rapida ed estesa dell'espressione genica, in modo da superare le restrizioni imposte dalla fissità dell'informazione codificata nel DNA.

Il "landscape epigenetico" di un organismo eucariotico è in gran parte correlato al processo di metilazione del DNA, che è uno dei meccanismi maggiormente coinvolti nel modulare la risposta delle piante ai cambiamenti ambientali e ai fattori di stress. D'altra parte, tutte queste risposte sono anche controllate da un intricato signalling, in cui un ruolo fondamentale è svolto dalle diverse classi di fitormoni, la cui azione è a sua volta influenzata da meccanismi epigenetici. Nonostante la vasta letteratura al riguardo, i complessi meccanismi con cui la metilazione del DNA modula le risposte della pianta allo stress rimangono ancora in larga misura incompresi, principalmente per quanto riguarda lo stress da metalli pesanti, per il quale è stata evidenziata l'esistenza di risposte metallo- e specie-specifiche.

Al fine di ottenere ulteriori informazioni riguardo questi aspetti, nel presente lavoro abbiamo effettuato un'analisi trascrittomica comparativa tra il mutante *drm1 drm2 cmt3* (*ddc*) di *A. thaliana,* difettivo sia nella metilazione di mantenimento che *de novo* del DNA e piante WT, esposti ad un trattamento prolungato (21 giorni) con Cd, alle concentrazioni di 25 e 50 μM. L'attenzione è stata focalizzata sul Cd in quanto è uno degli inquinanti più tossici, diffuso sia in ambiente terrestre che marino. Il mutante è stato scelto in quanto strumento adatto per studiare i meccanismi e i processi molecolari che agiscono e sono regolati dalla metilazione del DNA. All'analisi trascrittomica è stata inoltre associata l'analisi di alcuni parametri di crescita e di alcune mirate caratteristiche citofisiologiche.

Per quanto attiene i risultati, l'analisi trascrittomica ha evidenziato il processo di fotosintesi, la risposta allo stress e la biosintesi degli ormoni come i pathways genetici più influenzati dal trattamento col Cd, sia nel mutante che nel WT. Tutti questi pathways sono estremamente rilevanti nello sviluppo delle piante. Inoltre, il quadro emerso da un'analisi più dettagliata dei pathways relativi ai fitormoni ha portato ad ipotizzare che, nel caso di

una prolungata esposizione a metalli pesanti, l'attività delle piante venga indirizzata a migliorare e/o mantenere il livello e il signalling degli ormoni atti a sostenere la crescita (auxine, citochinine e gibberelline) più che di quelli specificamente correlati alla risposta allo stress (acido jasmonico, acido abscissico e acido salicilico). Tutto ciò potrebbe rappresentare una strategia messa in atto dalla pianta per evitare gli effetti negativi di una prolungata attività degli ormoni legati allo stress. Interessantemente, tale strategia sembrerebbe essere realizzata in modo più efficiente dal mutante. Infatti, probabilmente a causa di una maggiore plasticità del genoma conferita dallo stato ipometilato del suo DNA, nel mutante le differenze a livello del trascrittoma sono state osservate già nel trattamento con 25 µM Cd, mentre nel WT solo nel trattamento con 50 µM Cd. Questa diversa modulazione dell'espressione genica ha trovato riscontro in una migliore performance di crescita del *ddc* rispetto al WT, come evidenziato dall'analisi dei parametri di crescita. È stata inoltre osservata una stretta relazione tra le differenze trascrizionali riguardanti i pathways ormonali e le diverse caratteristiche citomorfofisiologiche del *ddc vs* WT quando trattati col Cd.

CHAPTER 1: INTRODUCTION

1.1 DNA methylation

DNA methylation refers to the covalent addition of a methyl group to the cytosine bases of DNA, to form 5-methylcitosine (He *et al.,*2011). It is one of the principal epigenetic mechanisms leading to heritable and non-heritable genome modifications, which occur beyond changes in nucleotide sequence. Like other epigenetic marks, such as the histone code, DNA methylation contributes to chromatin remodelling processes and it is involved in the regulation of gene expression (He *et al.,*2011).

DNA methylation can be found in both prokaryotes and eukaryotes. In bacteria, its major function is to act as a defence mechanism against invading phages: methylation differentiate host genome from that of the phage, which becomes preferential target of cleavage action of host restriction enzymes. It also plays an important role in DNA repair and replication (Chinnusamy and Zhu, 2009). In eukaryotes, DNA methylation is a fundamental mechanism for the maintenance of genome stability and the regulation of gene expression in response to both external and internal stimuli; as such, it plays a relevant role in plant diversity and development (Becker *et al.,*2011; Lauria and Rossi, 2011; Schmitz *et al.,*2011; Zhang *et al.,*2018).

1.1.1 DNA methylation: an historical overview

Covalent modifications of the DNA were firstly described by Hotchkiss in 1948. However, the first suggestion that DNA methylation could have some relevant biological roles, through the modulation of gene expression was made only in 1969 by Griffith and Mahler, while studying the basis of the long-term memory in the brain. In 1975, similar models for gene activity regulation and for the hereditability of DNA active or inactive status, based on the enzymatic methylation of cytosine in its sequences, were independently proposed by Riggs (Riggs, 1975) and Holliday and Pugh (1975). In particular, these authors supposed the existence of enzymes (methylases) that directly or indirectly act on specific sequences (context) modifying DNA methylation pattern and, consequently, changing gene expression. They also supposed the action of specific methylases that recognize hemi-

methylated DNA after the replication assuring the maintenance and the hereditability of DNA methylation pattern.

Unfortunately, no experimental evidence supported the brilliant models proposed by Riggs (1975) and Holliday and Pugh (1975) until the advent and the progressive upgrading of molecular techniques that allowed to screen DNA methylation in the sequences of interest. For example, the restriction of DNA with isoschizomers (i.e. enzymes that cut DNA at specific sequences context and in relation to methylation presence/absence) followed by Southern blot made possible to know whether DNA target sequences were or not methylated in the selected restriction sites. Thanks to this new technique, Doerfler (1981; 1983) finally proved the correlation between DNA methylation and gene expression modulation, discovering that the promoter regions of many inactive genes were methylated; vice versa, the corresponding active genes resulted unmethylated. Moreover, by using the 5-azacytidine, an analogue of the cytidine that inactivates the DNA methyltransferases, it was shown that 5-azacytidine reactivated silent genes, including the inactive X chromosomes (Holliday, 1991).

Over the years, additional studies and the recent genome-wide sequencing technologies allowed to gain further insights into DNA methylation pattern and role, which includes a lot of other processes, like genomic imprinting (Surani *et al.,*1984), inactivation of transposable elements (TEs) (Pray, 2008), and the control of telomere length (Chan and Blackburn, 2004).

1.1.2 DNA methylation in plants: sequence context and methylation pathways

DNA methylation can be distinguished in *de novo* methylation and maintenance methylation. *De novo* methylation consists in the methylation of DNA sequences not previously methylated (Fig. 1.1). It is involved in the rearrangement of methylation pattern during the embryogenesis and in the cell differentiation processes during development (Razin and Cedar, 1993). Maintenance methylation preserves the methylation status of symmetric (palindromic) sites after DNA duplication through recognition of hemimethylated sites and methylation of the newly synthesized filament (Finnegan and Dennis, 1993; Saze *et al.,*2003) (Fig. 1.1).

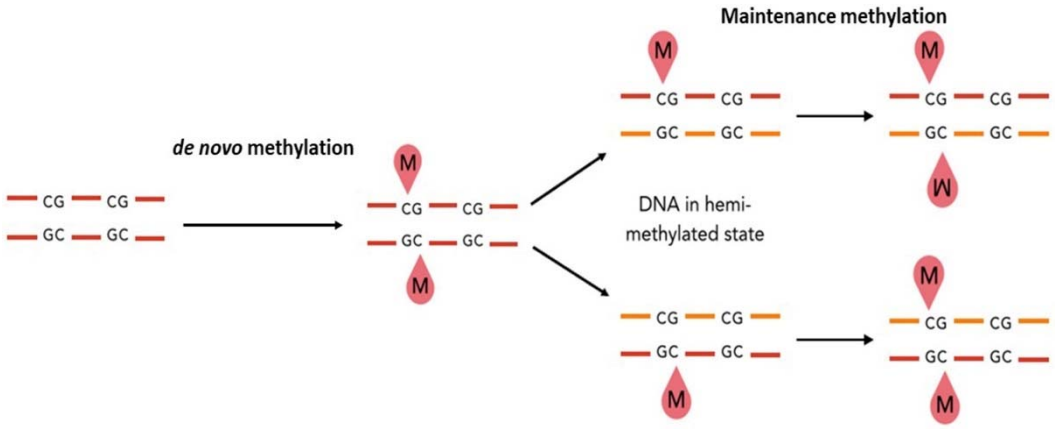

Figure 1.1: Schematic representation of *de novo* and maintenance methylation of DNA. The methyl group is indicated by the letter "M".

In animals, cytosine methylation is mainly restricted to the symmetric CpG dinucleotide, except for the embryonic stem cells (Ramsahoye *et al.,*2000), the adult mouse cortex and human brain (Lister *et al.,*2013), where CpH methylation was found. By contrast, plant DNA can be methylated in any sequence context (i.e. CG, CHG and CHH, where H is A, T or C), but most commonly in "symmetric cytosines" CpG and CpHpG (Meyer *et al.,*1994).

DNA methylation is catalysed by specific enzymes, the DNA methyltransferases, which recognise specific DNA sequences through their variable N-terminal domain and transfer a methyl group from S-adenosyl-L-methionine (S-AdoMet) to carbon 5 of cytosine residues through the activity of the C-terminal catalytic domain (Pòsfai *et al.,*1989; Kumar *et al.,*1994; Pavlopoulou and Kossida, 2007).

So far, plant DNA methyltransferases have been classified in 4 different families on the basis of their linear domain arrangement: METHYLTRANSFERASE (MET) family, CHROMOMETHYLASES (CMTs) family, DOMAINS REARRANGED METHYLTRANSFERASES (DRMs) family, and DNA METHYLTRANSFERASE HOMOLOGUE 2 (Dnmt2) family, whose role in DNA methylation has still to be further elucidated (Pavlopoulou and Kossida, 2007).

MET is the family principally involved in the maintenance of DNA methylation pattern at the symmetric CpG sites after replication events (Finnegan and Dennis, 1993; Genger *et al.,*1999). As far, in *A. thaliana*, the gene family encoding these DNA methyltransferases comprises 5 members and among them only 4 are partially

characterized (*METI, METIIa, METIIb, and METIII*). The conserved structure of these genes suggests that they were originated from one ancestral gene through a series of duplication events (Finnegan and Dennis, 1993; Genger *et al.,*1999). *METI* encodes a functional methyltransferase (Genger *et al.,*1999) expressed in both vegetative and floral tissues, with its highest expression in meristematic cells (Ronemus *et al.,*1996), while no specific function has been still attributed to the proteins encoded by the other members of this gene family (Genger *et al.,*1999).

CMTs is a family of DNA methyltransferases unique of plants, discovered by Henikoff and Comai in 1998 and characterized by the presence of a chromodomain amino acid motif between the conserved motifs II and IV. In *A. thaliana*, the gene family encoding CMTs enzymes includes 3 members, *CMT1, CMT2* and *CMT3*, originated by gene duplication events. In *A. thaliana*, *CMT1* is generally mutated or disrupted by the insertion of transposable elements (TEs) within the coding region of the gene. In both cases, the result will be the premature end of the translational process of the CMT1 protein (Henikoff and Comai, 1998). CMT2 activity seems to have an important role in keeping high levels of DNA methylation at TEs in the heterochromatic fraction (Zemach *et al*. 2013). This enzyme is principally involved, together with DRM2, in the establishment and maintenance of the asymmetrical methylation on CpHpH sites, depending on the genomic region. Namely, DRM2 catalyses CpHpH methylation at TEs, usually located in heterochromatin, or at other repeated sequences in euchromatic chromosome arms. Whereas, CMT2 catalyses CpHpH methylation at histone H1-containing heterochromatin (Huettel *et al.,*2006; Zemach *et al.,*2013; Liu *et al.,*2014), but at certain extent it can also participate in CpHpGp methylation maintenance, which is mainly catalysed by CMT3 (Lindroth *et al.,*2001; Stroud *et al.,*2014). In particular, CMT3 recognises H3K9me2 epigenetic mark and binds to the DNA nucleosome through the Bromo Adjacent Homology (BAH) domain and the chromo domains. Note that a similar recognisance mechanism is activated by the SET and RING associated (SRA) domain of KRYPTONITE (KYP, also known as SUVH4) enzyme, that catalyses the methylation of the H3K9. In such a way, CpHpG and H3K9me2 modifications reinforce each other through a positive regulatory feedback (Stroud *et al.,*2013; Du *et al.,*2014).

In *A. thaliana*, DRMs family includes DRM1and DRM2. Both these proteins mediate *de novo* methylation in all DNA sequence context (CpG, CpHpG, CpHpH) by an

RNA-directed DNA methylation process (RdDM) (Matzke and Mosher, 2014). In the canonical RdDM pathway, RNA Polymerase IV (POL IV) and RNA- DEPENDENT RNA POLYMERASE 2 (RDR2) work to produce double stranded DNA (dsDNA) which is cleaved by DICER- LIKE PROTEIN 3 (DCL3) into siRNA. These siRNAs are loaded onto ARGONAUTE (AGO) proteins and paired to complementary RNAs scaffold produced by RNA Polymerase V (POLV) to recruit DOMAINS REARRANGED METHYLASE 1 (DRM1) and DOMAINS REARRANGED METHYLASE 2 (DRM2), which methylate the DNA in a sequence-independent manner (Fig. 1.2) (Law and Jacobsen, 2010; Zhang and Zhu, 2011; Pikaard *et al.,*2012; Matzke and Mosher, 2014).

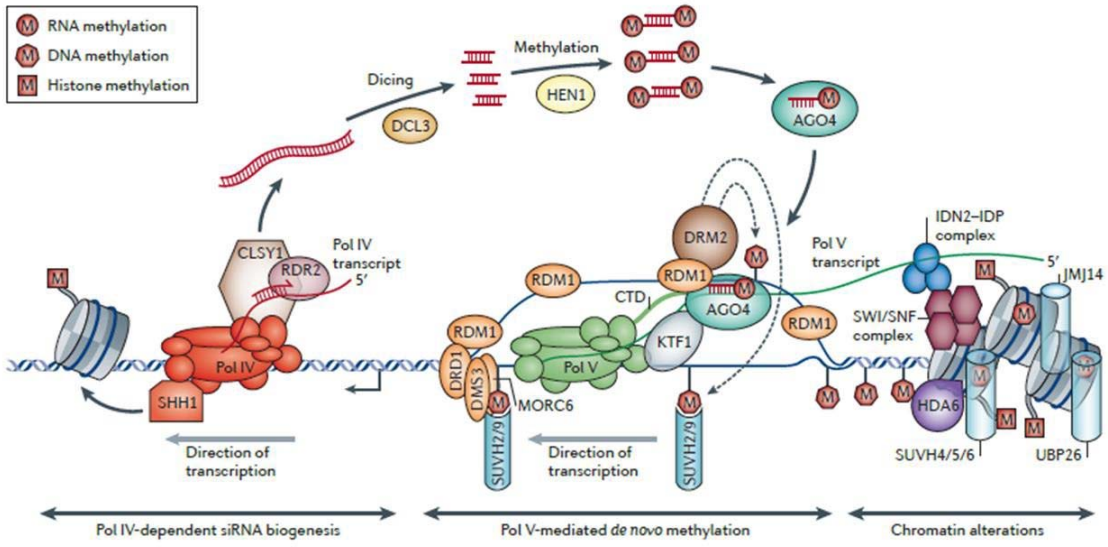

Figure 1.2: Schematic representation of the RNA-directed DNA methylation (RdDM) pathway (Matzke and Mosher, 2014).

Finally, methylome dynamics is further assured by DNA demethylation. Indeed, active DNA demethylation is extremely important for both genome-wide epigenetic reprogramming and for the activation of target gene loci during plant development (Hsieh *et al.,*2009). In particular, it consists in the enzymatic removal of methylated cytosine by the combined action of a family of DNA glycosylases including DEMETER (DME), REPRESSOR OF SILENCING 1 (ROS1), DEMETER-LIKE 2 (DML2), and DEMETER-

LIKE 3 (DML3). Subsequently, a base excision repair (BER)-dependent mechanism completes the process (Penterman *et al.,*2007; Zhu, 2009; reviewed by Li *et al.,*2018).

1.1.3 Molecular functions of DNA methylation in plants

For long time, most of the knowledge on DNA methylation in plants was obtained from studies carried out on *A. thaliana* (Zhang *et al.,*2006; Cokus *et al.,*2008).In the last decade, genome-wide sequencing technologies allowed us to obtain information on DNA methylation pattern in several other species which include important crops such as *Zea mays* (Eichten *et al.,*2013), *Solanum lycopersicum* (Fray and Zhong, 2015) and *Oryza sativa* (reviewed by Deng *et al.,*2016). In plants, DNA methylation primarily take places on transposon repeat sequences. Transposons, also called "jumping genes", are mobile elements of the genome. Based on their structure and transposition mechanism, there are two major classes of transposons: the class I transposons (or retrotransposons), that translocate from a site to another through a reverse transcription process with an RNA intermediate, resulting in an increase of the final copy number, and the class II transposons, that translocate the transposon from the integrated site to a new site of the genome, keeping the final copy number unaltered (Engels *et al.,*1990). Even though transposable elements activity contributes to genome evolution and diversity, it can also cause, depending by the site of its insertion, mutations of functional genes and/or chromosome instability (Saze *et al.,*2012). The heavy methylation state of transposons detected in several plants, preventing their expression and transposition, is addressed to avoid the risk of a bursts of transposition activity. In such a way, genome integrity and transcriptional homeostasis is assured (Pray, 2008; Zemach, 2010; Saze *et al.,*2012; Kim and Zilberman, 2014).

The presence of methylated transposons close to or within a gene can affect gene expression leading in most cases to gene silencing (Rodrigues and Zilberman, 2015). Moreover, also the promoter region and the coding regions of actively expressed genes can be methylated (Zilberman, 2008; Bewick and Schmitz, 2017). Until now, although several functions have been proposed, the exact role of gene body methylation in plants is not yet well understood (Zilberman, 2008; Takuno and Gaut, 2013; Bewick and Schmitz, 2017). More defined is, instead, the role of cytosine methylation at the gene promoter region. In this case, methylated status prevents the binding of transcription factors to their target sequences and represents a direct mechanism by which gene expression can be regulated

by DNA methylation in both mammals and plant. Therefore, increasing methylation at promoters' level results in gene silencing, whereas reduced methylation results in gene activation. (Iguchi-Ariga and Schaffner, 1989; Bell and Felsenfield, 2000; Campanero *et al.,*2000; Hark *et al.,*2000).

The inhibition of transcription by DNA methylation can occur in different ways and also involves an interplay with other epigenetic mechanisms. Indeed, transcription can be modulated: i) by inhibiting or promoting the binding of transcriptional activators or repressor, respectively ii) by promoting repressive histone modifications, like H3K9me2 methylation, and inhibiting the permissive ones, like histone acetylation. (Boyes and Bird, 1991; Henderson and Jacobsen, 2007; Zhang *et al.,*2011; Matzke and Mosher, 2014).

DNA methylation is also involved in genomic imprinting (Surani *et al.,*1984) and in the control of telomere length (Chan and Blackburn, 2008). Genomic imprinting consists in the differential activation or inactivation of alleles of a gene depending from the paternal or maternal origin of the chromosome. Namely, one of the alleles is silenced, and only the one from the other parent will be expressed. (Bajrami and Spiroski, 2016). Even though the mechanisms underlying this process aren't yet completely defined, it was observed an involvement of DNA methylation. In particular, it has been demonstrated that the repressed allele is methylated, while the active allele is unmethylated. In human, the most studied cases of methylation-related genomic imprinting deal with Prader-Willi syndrome and Angelman syndrome, associated to the imprinting on the long arm of chromosome 15 (Bajrami and Spiroski, 2016). In plants, several imprinted genes, which also show parental differences in DNA methylation, have been identified, including FERTILIZATION-INDEPENDENT SEED 2 (*FIS2)* (Jullien *et al.,*2006), FLOWERING WAGENINGEN (*FWA)* (Kinoshita *et al.,*2004), FERTILIZATION-INDEPENDENT ENDOSPERM 1 (*ZmFie1)* (Hermon, 2007), FERTILIZATION-INDEPENDENT ENDOSPERM 2 (*ZmFie2)* (Gutiérrez-Marcos *et al.,*2006) and maize E(z)-like gene 1 (*Mez1)* (Haun, 2007). However, there are some exceptions to these evidences of DNA methylation role in genomic imprinting, as in the case of the *MEDEA (MEA*) gene of *A. thaliana*. *MEA* acts as suppressor of endosperm development, and loss of function mutations could cause precocious endosperm formation before fertilization, prolonged endosperm nuclear proliferation after fertilization and embryo abortion (Grossniklaus *et al.,*1998, Kiyosue *et al.,*1999). The *MEDEA* locus is the first example of an imprinted region that doesn't

present differential DNA methylation between the silenced allele and the active allele, suggesting a DNA methylation-independent mechanism(s) and the existence of other factors that determines imprinting at the *MEA* locus (Wöhrmann *et al.,*2012).

Finally, DNA methylation is also implicated in telomere length regulation. Telomeres consists of structures formed by proteins and repetitive DNA situated at the end of the chromosomes. Both telomeric and sub-telomeric regions in the chromosome are bound to telomere binding proteins and present heterochromatinic structure (Blasco, 2007). Telomeric heterochromatin is usually devoid of functional genes, and it plays an important role in chromosome end protection and telomere length regulation (Ottaviani *et al.,*2008). When this protective structure fails, the results are chromosome degradation or fusion with neighbouring chromosomes (Chan, 2004).

One interesting evidence of the DNA methylation involvement in maintenance of telomeric heterochromatin regards the role of some telomeric repeat–containing transcripts in *A. thaliana*. These transcripts, in fact, are processed in small interfering RNAs that promote the methylation of asymmetric cytosines in telomeric (CCCTAAA)n repeats (Vrbsky *et al.,*2010). Although these siRNAs-directed mechanisms contribute to telomere length control, this process is determined and reinforced by several independent mechanisms, of which many are epigenetic ones (Vrbsky *et al.,*2010).

1.1.4 DNA methylation and its involvement in plant growth and development

In line with the above described roles of DNA methylation, this epigenetic mechanism plays a relevant role in the control of plant growth and development throughout its whole life cycle, from the gametophyte development, throughout the fecundation process, during the vegetative development until flowering, fruit formation and ripening (reviewed by Zhang *et al.,*2018).

In particular, a very complex and dynamic pattern of methylome, tightly related to other epigenetic modifications, has been assessed in *A. thaliana* during gametogenesis and fecundation (reviewed by Zhang *et al.,*2018). Indeed, the male gametophyte presents a de-repression of TEs activity, due to the global demethylation mediated by TRANSCRIPTIONAL ACTIVATOR DEMETER (DME) activity, and the down-regulation of DECREASED DNA METHYLATION 1 (DDM1) (Slotkin *et al.,*2009; Ibarra *et al.,*2012) (Fig. 1.3 A), a chromatin remodelling protein that is also required for

maintaining DNA methylation in symmetric cytosine sequences (Jeddeloh *et al.,*1999; Zemach *et al.,*2013). As a consequence, high level of siRNAs is produced from the demethylated and de-silenced transposons which accumulate in sperms (Fig. 1.3 A). After fecundation, siRNAs will be further processed through the RdDM canonical pathway, thus reinforcing the CpHpH methylation at transposons (Gehring *et al.,*2009; Ibarra *et al.,*2012; Ingouff *et al.,*2017; reviewed by Zhang *et al.,*2018) (Fig. 1.3 A). Also the central cell of female gametophyte undergoes DME-mediated global demethylation (Fig. 1.3 A); as a result, the endosperm formed following its fertilization by the sperm cell will be globally demethylated, although a reinforced CpHpH methylation at transposons will be also present due to the siRNAs activity (Gehring *et al.,*2009; Ibarra *et al.,*2012) (Fig. 1.3 A). Moreover, the endosperm is subject to gene imprinting (Pignatta *et al.,*2014; reviewed by Zhang *et al.,*2018). In the maternally expressed genes (MEGs), the maternal allele is hypomethylated, and the paternal one is methylated and repressed (Fig. 1.3 B), while in the paternally expressed genes (PEGs) the maternal allele is marked by the H3K27me3 repressive histone modification, while the paternal one presents the active modification H3K36me3 (Dong *et al.,*2017) (Fig.1.3 B).

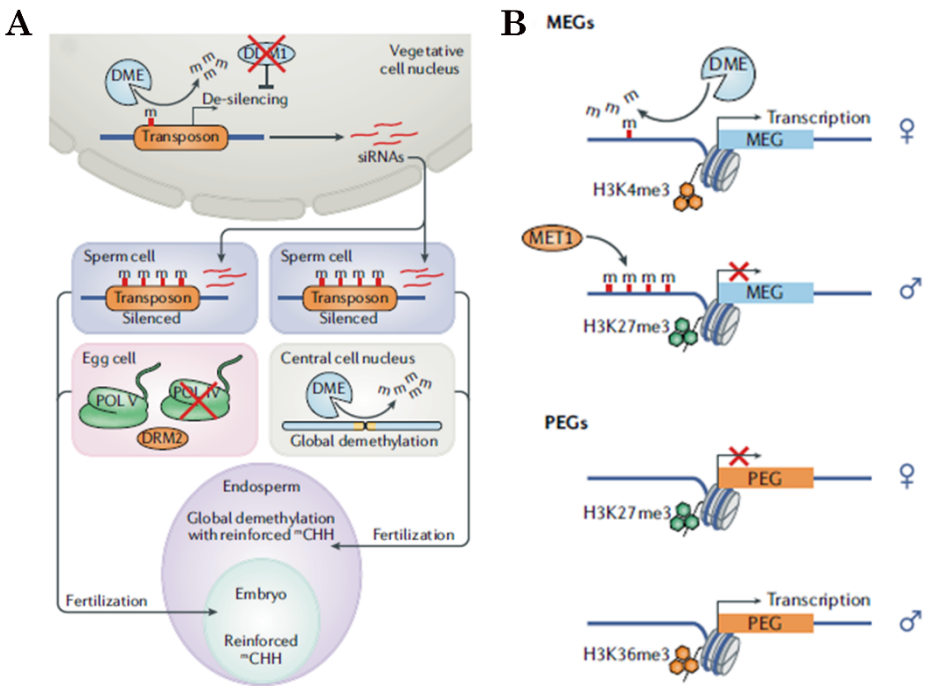

Figure 1.3: (A) In the male vegetative cell of *A. thaliana* siRNAs are produced and transported into the two sperm cells. One of the cells fertilizes the egg cell, where the siRNAs are further processed through the RdDM canonical pathway, reinforcing the CpHpH methylation. The other sperm cell fertilizes the female

central cell, globally demethylated. As a consequence, the resultant endosperm will be globally demethylated but will also present a reinforced CpHpH methylation at transposons due to the siRNAs presence. **(B)** the endosperm presents maternally expressed genes (MEGs), characterized by DNA hypomethylation and trimethylation of histone H3 lysine 4 (H3K4me3), with the paternal allele silenced by DNA hypermethylation or H3K27me3, and paternally expressed genes (PEGs), characterized by H3K36me3, whereas the maternal allele can be silenced by H3K27me3 (Zhang *et al.,*2018).

Concerning more specifically plant vegetative growth and pattern formation, DNA methylation has a crucial role. A *de novo* DNA methylation through the RdDM pathway is essential for the proliferative activity of meristems, on which plant growth relies (Kawakatsu *et al.,*2016). According to this assumption, meristem defects have been detected in *Zea mays* RdDM mutants, which display strong developmental abnormalities (Alleman *et al.,*2006; Erhard *et al.,*2009; Moritoh *et al.,*2012; Wei *et al.,*2014). Interestingly, in peach (*Prunus persica* (L.) Batsch) changes in the level of DNA methylation have been found to mark the transition of apical vegetative shoot meristem towards floral bud (Bitonti *et al.,*2002).

Methylation has been found to play a significant role also in cell differentiation. For example, a differential CpG and CpHpG methylation pattern among the division zone, transition zone, elongation zone and mature zone of developing leaves has been evidenced in *Zea mays* plants, related to the different regulation of maintenance DNA methyltransferases (Kawakatsu, *et al.,*2016). Furthermore, a different DNA methylation pattern in *Zea mays* leaves was found also in genes involved in chromatin remodelling, cell cycle progression and growth regulation. All these evidences indicate that DNA methylation has an important role in leaf growth in *Zea mays* (Candaele *et al.,*2014). In addition, in *A. thaliana* DNA methylation has been found to control stomata formation. In fact, an hypermethylation of *EPIDERMAL CATTERNING FACTOR 2* (*EPF2*) gene, whose product is a peptide ligand that represses stomata formation, leads to an over-production of stomatal lineage cells (Yamamuro *et al.,*2014).

Recently, it has been evidenced a relevant role for methylation-related epigenetic control on fruit development. In particular, it has been demonstrated that an increase of *DME-LIKE2* (*DML2*) DNA demethylase expression, is required for the activation of ripening-induced genes during *Solanum lycopersicum* fruit development. Actually, the demethylated status of the ripening-induced genes let the binding of RIPENING-

INHIBITOR (RIN) transcription factor to the promoter of these genes and consequently their transcription, that starts the ripening process (Zhong *et al.,*2013; Lang *et al.,*2017) (Fig. 1.4).

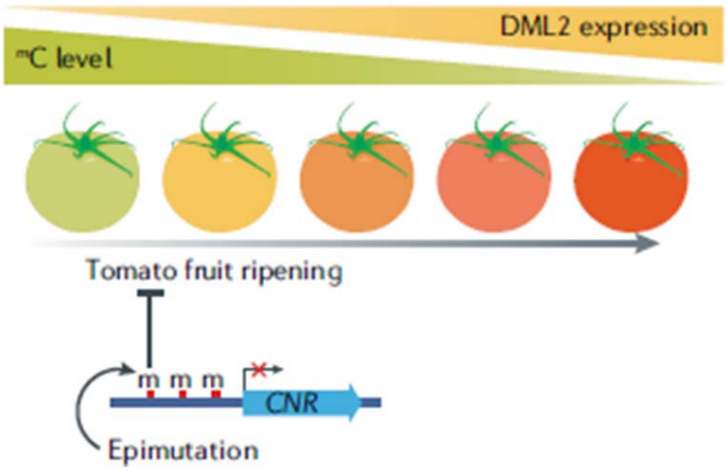

Figure 1.4: *Solanum lycopersicum* fruit ripening is accompanied by a diminution of genomic methylation and an increase of *DML2* expression (Zhang *et al.,*2018).

DNA methylation has been found to play a role also in plant growth plasticity in response to environmental condition and adaptive strategies, as evidenced in relation to the heterophylly phenomenon exhibited by the aquatic plant *Trapa natans* L. Indeed, clear differences in DNA methylation level were detected in the floating and submerged leaves produced by this plant, which are strikingly different in morphology. Namely, while the floating leaves were normally expanded, the submerged ones presented a root-like shape, likely to adapt to water presence (Bitonti *et al.,*1996).

1.1.5 Involvement of DNA methylation in plant response to abiotic stress

The role of DNA methylation in plant response to stress has been also widely investigated. Indeed, modifications in DNA methylation pattern, allowing rapid and reversible changes in the chromatin structure, can enable the activation of defence pathways through the combination of genetic and epigenetic mechanisms (Peng *et al.,*2009). Moreover, this epigenetic mechanism establishes a DNA methylation-dependent stress memory in plants in presence of a persistent stress (Jiang *et al.,*2014; Sanchez *et al.,*2014; Wibowo *et al.,*2016), principally charged to GC-rich sequences methylation, that

ensures the faithfully transfer of the "memory" to the offspring (Mathieu *et al.,*2007) (Fig. 1.5).

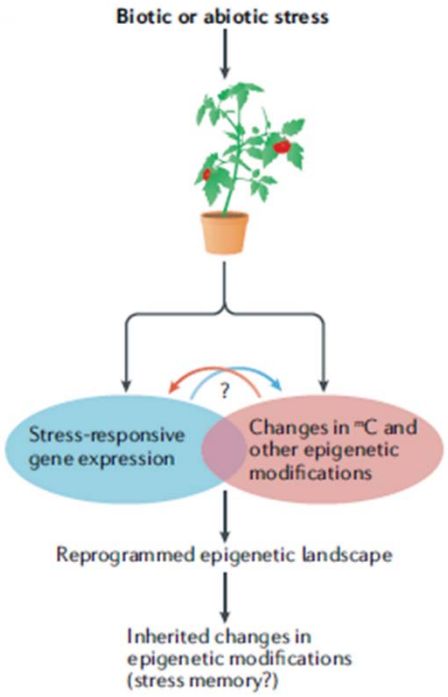

Figure 1.5: Following stress exposure, plant activate stress responsive pathways accompanied by modifications in DNA methylation status, that could be genome-wide or at specific loci level. In presence of a persistent stress, this "stress memory" genomic configuration is inherited by the next generations (Zhang *et al.,*2018).

Both biotic and abiotic stresses were found to induce modifications in DNA methylation pattern either genome-wide or at specific loci, usually associated to transcriptional regulation of genes involved in plant stress responses (Yong *et al.,*2015; Xu *et al.,*2015; Zhang *et al.,*2016) that, in turn, control important genetic functions like transcription, replication, DNA repair, gene transposition and cell differentiation (Madlung and Comai 2004; Angers *et al.,*2010; Sahu *et al.,*2013).

For example in *Zea mays*, under cold stress, the presence of methyltransferases and, consequently, the level of genomic methylation decreases. This modification seems to be organ- and site- selective, with a decrease of DNA methylation in roots in Ac/Ds transposons, suggesting a possible role for transposable elements in stress response (Shan *et al.,*2013). Whereas, in *Solanum lycopersicum* plants, cold down-regulates the expression of *DML2*, which led to a hypermethylation and silencing of genes responsible for the biosynthesis of volatile compounds, thus causing the loss of flavour of *Solanum*

lycopersicum fruits under cold storage (Zhang *et al.,*2016). In *Mesembryanthemum crystallinum* exposed to salt stress, water deficit caused by the osmotic pressure determines the switching to the Crassulacean acid metabolism (CAM) (Bohnert *et al.,*1988). This switchover to the CAM pathway is accompanied by the hypermethylation of satellite DNA, that probably enables the process thanks to the formation of chromatin structures that let the simultaneous regulation of all the genes involved (Dyachenko *et al.,*2006).

Under heavy metal stress, a reduction of DNA methylation has been detected in *Trifolium repens* L. and *Cannabis sativa* L. after exposure to nickel, cadmium and chromium (Aina *et al.,*2004), while in *Brassica napus* heavy metal exposure promotes genomic methylation (Li *et al.,*2016). An increase of DNA methylation, related to an overexpression of *PoCMT* gene was also observed in plants of *Posidonia oceanica* L. Delile exposed to Cd (Greco *et al.,*2012). These data suggest that methylome dynamic under stressful condition depends on both the plant species and the kind of heavy metal. Therefore, further studies are required to fully elucidate the network of processes that act in and are regulated by DNA methylation, mainly under stress conditions.

1.1.6 Cross-talk between epigenetic mechanisms and hormone network

In the last years, an emerging cross-talk between epigenetic modifications and the phytohormones action has been highlighted by several studies. As known, epigenetic modifications include not only DNA methylation but also histone modification, chromatin remodelling, non-coding RNAs, which interplay each other rather than act alone in the control of gene expression (reviewed by Yamamuro *et al.,*2016).

On the other hand, as above discussed, there is large evidence that epigenetic modifications, including DNA methylation, can override genetic programs in response to environmental cues, thus conferring growth plasticity to the plants and contributing to their survival strategies (Dowen *et al.,*2012). However, the biochemical signals that alter the epigenome and the transduction of such signals are still largely unknown, while the detected relationship with hormone action begins to shed light to this research field.

At this respect, available data largely deal with the involvement of histone modifications (reviewed by Yamamuro *et al.,*2016). However, some interesting evidences are emerging also in relation to DNA methylation (reviewed by Zhu, 2010; Yamamuro *et al.,*2016). For example, it has been shown that the induction of auxin responsive genes

mediated by the AUXIN RESPONSE FACTORS (ARFs) is modulated by microRNAs, histone modifications and chromatin remodelling factors (Jones-Rhoades and Bartel 2004; Mallory *et al.,*2005). In addition and very interestingly, in *met1* null allele embryos of *A. thaliana,* the distribution of auxin and its efflux carrier PIN-FORMED 1 (PIN1) resulted abnormal (Friml 2003, Weijers *et al.,*2005), although the *PIN1* gene doesn't result to be methylated in both wild type (WT) and *met1* null mutant. This result is consistent with and indirect involvement of MET1 activity in the modulation of *PIN1* expression (Xiao *et al.,*2006).

1.2 Phases of plants responses to stress

In a biological context, stress is defined as a condition related to abiotic and/or biotic factors, that exerts a disadvantageous influence on the plant and determines a significant deviation of the optimal condition of life (Taiz and Zeiger, 2003; Larcher, 2004; Cramer *et al.,*2011).

The abiotic stress factors that affect the geographical distribution of the plants, limit their productivity and threaten food security are numerous: extreme levels of light (high and low), radiation (UV-B and UV-A), temperature (high and low, that lead to chilling and freezing), water (drought, flooding, submergence), salinity (excessive Na^+), deficiency or excess of essential nutrients, gaseous pollutants (ozone, sulphur dioxide), chemical factors like extreme pH and heavy metals in the soil (Fedoroff *et al.,*2010; Pereira, 2016).

Following exposure to stress, plant response can be summarized in four distinct phases: **the alarm phase, the resistance phase, the exhaustion phase and the regeneration phase** (Lichtenthaler 1998; Larcher, 2004).

The **alarm phase**, or response phase, is characterized by a decline of one of several physiological functions, like photosynthetic performance and/or uptake and translocation of nutrient, due to the exposition to the stressful factor (Fig. 1.6). This is a crucial step for the plant, that needs to perceive promptly the deviation from their normal physiological standard and respond in a rapid and efficient manner (Lichtenthaler, 1998; Duque *et al.,*2013; Ben Rejeb *et al.,*2014). Stress sensing in plants still remains a largely unresolved topic. Namely, only few putative sensors have been so far identified, since dysfunction in one gene does not cause significant phenotypes in stress responses due to the functional redundancy of genes encoding sensor proteins (Zhu, 2016). Another reason concerns the

mechanisms of the signalling; in fact, the most common model of sensing external stimuli is based on the binding of a chemical ligand to a specific receptor. However, while it could be a suitable model for chemical stresses, it isn't the same for physical stresses such as, for example, temperature stress (Verslues *et al.,*2006).

Following stress perception, the activation of one or more signalling transduction cascades, varying depending from the different kind of stresses, determines the beginning of the **resistance phase** (Lichtenthaler, 1996; Lichtenthaler, 1998). Classically, many actions can be triggered: the activation of specific ion channels and kinase cascades (Verslues *et al.,*2005), the production of reactive oxygen species (ROS) (Dat *et al.,*2004) and the activity of phytohormones like abscisic acid (ABA), salicylic acid (SA), jasmonic acid (JA), and ethylene (ET) signalling (reviewed by Verma *et al.,*2016). All these mechanisms lead to a reprogramming of gene expression resulting in long-term metabolic and morphological adaptations addressed to increase plant tolerance and alleviate biological damages caused by stress. This allows to establish a new physiological standard (optimum stage), that corresponds to the plant *resistance maximum* (Fig. 1.6) (Lichtenthaler, 1998). If the stress dose overloads the plant capacity to put in place mechanisms for coping with it, especially during long-term stress, physiological processes slow down more and more, and inevitably vitality becomes progressively lost, causing severe damage and cell death (**exhaustion phase or end stage**) (Fig. 1.6) (Lichtenthaler, 1998). However, if the stressor agents are removed in time, before the senescence process becomes widespread, plants can regenerate themselves and, also in this case, adjust to a new physiological standard (**regeneration phase**) (Fig.1.6) (Lichtenthaler, 1996; Lichtenthaler, 1998). This new physiological standard depends from the time and the stage of exhaustion, that determines the range of minimum and maximum resistance that the plants acquire following exposure to stress. (Lichtenthaler, 1996; Lichtenthaler, 1998).

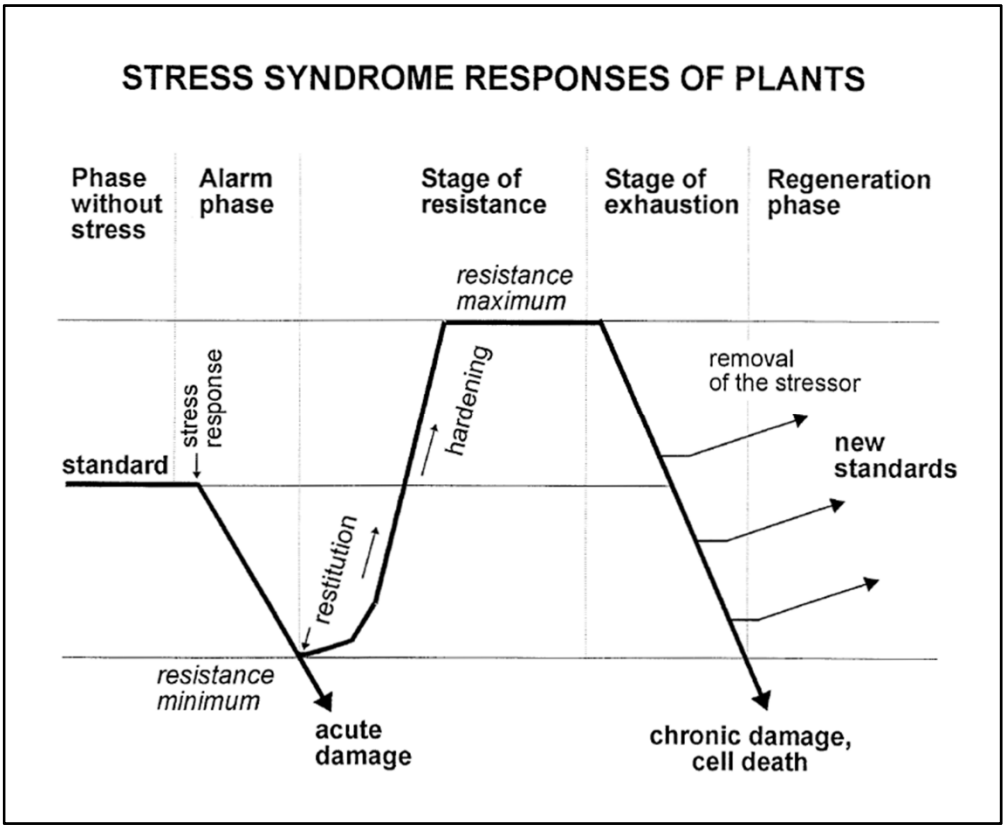

Figure 1.6: Phase sequences and responses induced in plants by stress exposure (Lichtenthaler, 1998).

1.3 Cadmium toxicity in higher plants

1.3.1 Cadmium distribution in the environment

Metals with density higher than 5 g cm^{-3} are classified as heavy metals, and they represent fiftythree of the ninety natural occurring elements (Weast, 1984). Among them, iron (Fe), molybdenum (Mo), and manganese (Mn) are fundamental micronutrients for the organisms. Zinc (Zn), nickel (Ni), copper (Cu), vanadium (Va), and chromium (Cr) are toxic elements at high concentrations, but as trace elements they are useful as components of the active sites of some enzymes, while silver (Ag), arsenic (As), mercury (Hg), lead (Pb), antimony (Sb) and cadmium (Cd) have no known metabolic and/or nutritional function and are toxic for both plants and animals (Nies, 1999).

Heavy metals are dangerous environmental pollutants, whose presence is particularly relevant in areas subjected to anthropogenic pressure. Cadmium (Cd, density = 8.6 g cm^{-3}), in particular, is a widespread heavy metal considered as one of the most significant pollutants due to its high toxicity and extreme solubility in water (Pinto *et*

*al.,*2004). In natural environment Cd is present mostly as a "guest metal" in Pb/Zn mineralization (Baker *et al.,*1990). As environment pollutant, Cd is mainly released by power stations heating systems, metal-working industries, waste incinerators, urban traffic, cement factories and as by-product of phosphate fertilizers (Sanità di Toppi e Gabbrielli, 1999). Soils containing a Cd concentration that ranges between 0.04 to 0.32 μM are classified as non-polluted, while soils with a Cd concentration varying from 0.32 to 1 μM are considered moderately polluted. When the concentration reaches 35 μM, the soil is classified as highly polluted, and only Cd hyperaccumulating species can survive in such environment (Sanità di Toppi and Gabbrielli, 1999).

1.3.2 Effects of cadmium exposure on plant growth and development

The toxic effects of Cd are well known since its absorption induces complexes changes at genetic, biochemical and physiological level in both plants and animals (Bingham *et al.,*1976; Das *et al.,*1997: Sanità di Toppi and Gabbrielli, 1999; Benavides *et al.,*2005; Greco *et al.,*2012). In particular, in plants, it has been showed that Cd alters the uptake of minerals, reducing their availability from the soil by decreasing the soil microbes population (Moreno *et al.,*2002), reduces the absorption of nitrate and its transport from root to shoot, inhibiting the nitrate reductase in the shoot (Hernandez *et al.,*1996), and inhibits Fe (III) reductase, that causes a Fe (II) deficiency (Alcàntara *et al.,*1994). Cd was also found responsible, although not directly, of Reactive Oxigen Species (ROS) production (Heyno *et al.,*2008). In addition, Cd can inhibit or enhance the activity of several enzymatic or non-enzymatic antioxidants (Salin, 1988) and increase lipid peroxidation, causing severe oxidative stress that enhance its toxic effects (Benavides *et al.,*2005). The most obvious consequence of Cd toxic effects is a reduction of plant growth due to the direct and indirect inhibition of photosynthesis, respiration and nitrogen metabolism, as well as to a reduction in water and nutrient availability (dos Santos *et al.,*2012).

1.3.3 Uptake and transport of Cd in higher plants

Cd absorption depends principally from the soil characteristics, the metal concentration in the soil and the plant species and or varieties/ecotypes. Humic acid, solid

solution and pH can modify Cd availability from the soil and, consequently, affect its absorption (Cabrera *et al.,*1988; Mench and Martin, 1991).

Cd absorption from the soil is mostly charged by root tip, and it involves three principal pathways:

i. Cd^{2+} can be absorbed through a rapid exchange with H^+ produced by the H_2CO_3 dissociation in H^+ and CO_3^- during plant respiration in the root epidermal cells and enter into the root epidermis layer through the apoplast pathway. This process is rapid and doesn't require energy (Yamaguchi *et al.,*2011);
ii. Cd^{2+} can be transported by ion channels for Fe^{2+}, Zn^{2+} and Ca^{2+} and subsequently enter the root epidermis layer through the symplastic pathway (reviewed by Song *et al.,*2017);
iii. Cd^{2+} can be chelated by molecular compounds produced by plants to enhance the availability of ions in the soil and enter the root epidermis layer through yellow stripe 1 like (YSL) proteins (Curie *et al.,*2009).

After its uptake from the root, Cd can be transported through tissues and organs via apoplastic pathway, that involves transfer through extracellular fluids and gas spaces between and within cell walls, and symplastic pathway in which water and solutes are intracellularly transferred, and it involves the ion transmembrane transport (Fig. 1.6 A) (reviewed by Song *et al.,*2017). At the level of the endodermis, metal is complexed by several ligands, such as organic acids and phytochelatins (PCs) and transported to xylem elements in the stele, through it can reach aerial organ via xylematic flow (Fig. 1.6 A, B) (Akhter *et al.,*2014). In leaves, metal transport and distribution occur through both apoplastic and symplastic pathways and Cd can be finally sequestered into extracellular and subcellular compartment (reviewed by Song *et al.,*2017), or loaded into phloematic elements that dislocate it from the shoot to the roots as a part of detoxification processes (Fig. 1.6 C) (van Belleghem *et al.,*2006).

As a result, only small amounts of Cd are transported in shoots (Sanità di Toppi and Gabbrielli, 1999), and the content of Cd in plants decreases in the order roots > stem > leaves > fruits > seeds (Blum, 1997).

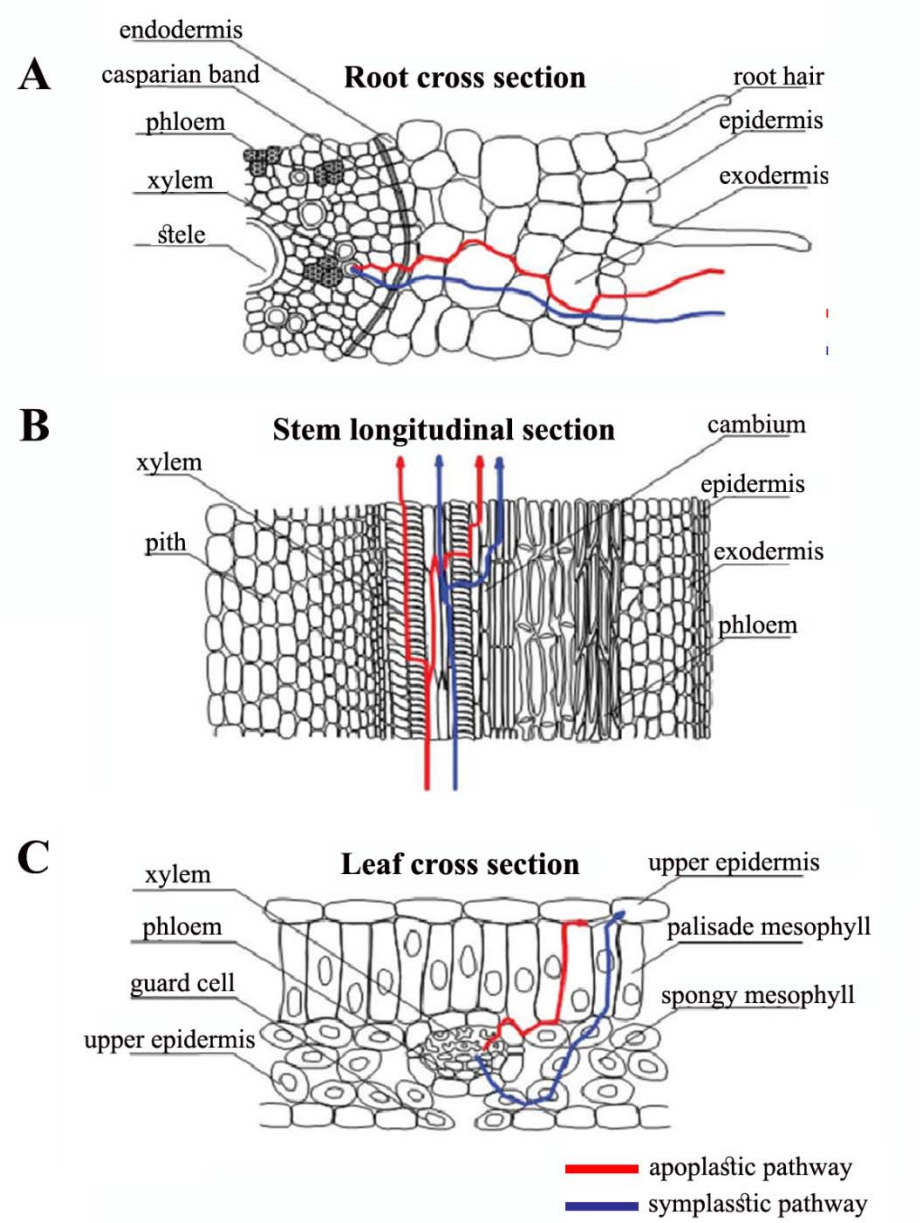

Figure 1.6 Uptake and transport of Cd through apoplastic and symplastic pathways in higher plant (A) root, (B) stem and (C) leaf (Song *et al.,*2017).

1.3.4 Morphological, physiological and biochemical plant responses to Cd toxicity

In order to withstand the heavy metals, plants adopt either of two strategies: avoidance and tolerance. Avoidance is the strategy that plant adopts at the beginning, after heavy metal exposure: it enhances the production of organic acids and chelate and sequesters Cd to prevent its access to the root cells, thus protecting the plant from the external stress influence. Tolerance mechanisms, instead, let the plant survive the effects

of an internal stress, enabling the normal functioning of physiological processes even in presence of high concentrations of toxic substances (Song *et al.,*2017).

To prevent metal uptake inside the cells, plant roots secrete exudates that have the function to chelate metals in the soil matrix (Marschner, 1995). Moreover, plants try to reduce Cd uptake by binding the metal to cellular walls, sequestering it into the apoplast or inhibiting its transport (Manara, 2012). Root cells present on their walls pectic sites, histidine groups and extracellular carbohydrates, like callose and mucilage, that bind the heavy metals and prevent their uptake into the root cells. In this way the cell wall modulates plant metal absorption (Manara, 2012).

Metal uptake and homeostasis is further modulated by the presence at the level of plasma membrane of a range of transporters like those belonging to the ZRT-IRT-like Proteins (ZIP) family transporters and the Natural Resistance-Associated macrophage (NRAMP) family proteins. Both these proteins are involved in the transport of divalent cations, such Cd^{2+} and Zn^{2+}, across membranes (Manara, 2012). ZIP transporters are necessary, but not sufficient, for the enhanced accumulation of metal ions in hyperaccumulator plants (Guerinot, 2000), while Nramp5 has been identified as a major Cd uptake transporter in *Oryza sativa* (Sasaki *et al.,*2012).

If this first line of defence fails, metal ions penetrate the cells and are conveyed to the shoots by transporters such as the Heavy Metal-transporting P-type ATPases (HMAs), that have the double functions of efflux pump, to remove metal ions from the cells, and internal transporter of Cd and Zn from the tissues to the xylem (Manara, 2012). Heavy metals can also be chelated inside plant cells by phytochelatins (PCs), metallotioneins (MTs), organic acids, amino acids and phosphate derivatives and, eventually, sequestered into the vacuole. HMA and NRAMP family transporters are also involved in this process (Manara, 2012).

Finally, when all of these mechanisms are exhausted, plants activate oxidative stress defence mechanisms based on mitogen-activated protein kinases (MAPK) signalling cascade and the synthesis of stress-related proteins and signalling molecules, like heat shock proteins, hormones and ROS, that induce the production of enzymatic and non-enzymatic antioxidants and the activation of antioxidant mechanisms (Dat *et al.,*2000).

1.3.5 Role of phytohormones in plant response to Cd stress

Recently, particular attention has been paid to the role of phytohormones in alleviating the effects of the Cd-induced toxicity, through the modulation of their level and signalling (Asgher *et al.,*2015; Bücker-Neto *et al.,*2017). In particular, it has been shown that these plant growth regulators have also a protective role against the Cd negative effects on plants by: i) regulating the antioxidative defence system and osmolytes production; ii) restricting Cd uptake in plants; iii) activating stress tolerance genes. In such a way, they enhance plant adaptation and survival (Arasimowicz-Jelonek *et al.,*2011; Masood *et al.,*2011; Piotrowska-Niczyporuk *et al.,*2012; Iqbal *et al.,*2013; Khan and Khan 2014; Asgher *et al.,*2015).

Among the various phytohormones, auxin plays a pivotal role in growth and development, being involved in cell division, elongation and differentiation (Litwack 2005; Mockaitis and Estelle, 2008; Jain and Khurana 2009; Ljung, 2013). This makes particularly interesting to study the relationship between this hormone homeostasis and heavy metal toxicity. Data in literature showed that both auxin metabolism and polar distribution are modulated by heavy metal stimuli (Wang *et al.,*2015). Under Cd exposure, a decrease in indole-3-acetic acid (IAA) content, which is the predominant representative of auxin in plants (Hu *et al.,*2013) and a down-regulation of numerous auxin-responsive genes (Weber *et al.,*2006; Van de Mortel *et al.,*2008) were detected in *A. thaliana* plants. It has been shown that such Cd effect was related to a nitric oxide (NO)-mediated reduction of PIN-FORMED 1/3/7 (PIN1/3/7) auxin efflux carrier in the meristem and the repression of IAA signalling (Yuan and Huang, 2016). Therefore, Cd exposition negatively affects IAA metabolism, transport and signalling. By contrast, an increase of IAA concentration was observed by both Sofo *et al.* (2013) and Vitti *et al.* (2013) in *A. thaliana* roots as a result of Cd-mediated up-regulation of *YUCCA2* gene and *NITRILASE* family genes (NITs), which are involved in the indole-3-acetaldoxime (IAOX) auxin biosynthetic pathway. This increase in IAA level was correlated to an enhanced lateral root formation, due to the Cd-induced suppression of primary root elongation (Besson-Bard *et al.,*2009; Fattorini *et al.,*2017).

In addition, an exogenous addition of auxin, or the stimulation of endogenous levels, was found to prevent plant growth inhibition under metal exposure and to increase heavy metal tolerance in plants (Srivastava *et al.,*2014). Even though the mechanisms

driving these responses are still poorly understood, it was suggested that auxin could enhance heavy metal tolerance by decreasing the Cd-induced disorder in membrane organization (Hac-Wydro *et al.,*2016) and/or increase metal retention in roots by fixing it to hemicellulose (Zhu *et al.,*2013). From these evidences, it's clear that auxin regulation in response to heavy metal stress is very complex and needs to be further investigated.

Regarding cytokinins, (CKs), under Cd exposure, a decrease of their level due to the enhancement of CKs oxidation/degradation was documented in *Triticum durum* (Veselov *et al.,*2003), while Cd-mediated decrease of CKs fractions (zeatin and zeatin riboside) was reported in *Glycine max* (Hashem, 2013). By contrast, just like for IAA, an increase of CKs amount was also detected in Cd-treated plants. Namely, Vitti *et al.* (2013) reported a significant increase of trans-zeatin riboside (*t-ZR*) and dihydrozeatin riboside (DHZR) in Cd-treated shoots of *A. thaliana* seedlings, while Sofo *et al.* (2013) observed an increase of *t*-ZR and DHZR in both root and shoot of *A. thaliana* seedling. Therefore, as for auxin, the emerging picture is somehow controversial. On the other hand, there is large evidence that CKs activation alleviates stress by the restoration of photosynthetic pigments and chloroplast membranes, strongly damaged by Cd, determining, in turn, an enhancement of the photosynthetic capacity. Moreover, they induce plant metabolism, leading to an increase of primary metabolite levels in Cd-treated plants (Piotrowska-Niczyporuk *et al.,*2012). An enhancement of antioxidant capacity in plants under Cd-stress after application of exogenous CKs was also reported in *Solanum melongena* (Singh and Prasad, 2014).

Concerning gibberellins (GAs), also their role in protecting plants against Cd stress has been extensively reported (Mansour and Kamel, 2005; Iqbal *et al.,*2011; Zhu *et al.,*2012; Masood and Khan, 2013; Hadi *et al.,*2014). In fact, it was shown that in *A. thaliana* GAs action alleviated Cd toxicity by reducing both NO accumulation and the expression of *IRON-REGULATED TRANSPORTER 1 (IRT1)* gene, which encodes an iron transporter, partially responsible for Cd-uptake into root cells (Zhu *et al.,*2012). Furthermore, in *Brassica juncea* plants, GAs activity decreased Cd oxidative stress, determining as a result an increase of net assimilation rate and relative growth rate (Masood and Khan, 2013).

Other evidences deal with jasmonic acid (JA) ability to protect plants against abiotic stresses (Wilen *et al.,*1994; Velitchkova and Fedina 1998; Maksymiec *et al.,*2007;

Qiu *et al.,*2014). In particular, it has been shown that JA causes the neutralization of Cd toxic effects by inducing the accumulation of osmolytes and enhancing antioxidants enzyme activity and carotenoids biosynthesis (Poonam *et al.,*2013; Chen *et al.,*2014;). Moreover, in *A. thaliana* plants this hormone was also found to up-regulate the transcription of GSH-metabolic genes and the phytochelatins accumulation, thus leading to a higher plant tolerance to Cd (Maksymiec *et al.,*2007).

Almost predictable is the involvement of abscisic acid (ABA), which is a central regulator of abiotic stress response in plants (Bartels and Sunkar, 2005; Tuteja, 2007; Danquah *et al.,*2014). High concentrations of Cd could impair water balance (Rauser and Dumbroff, 1981; Schat *et al.,*1997; Mukhopadhyay and Mondal, 2015). Therefore, under Cd stress, ABA signalling pathway induces stomatal closure which causes a suppression of transpiration flow, resulting in a restriction of transpiration and of the root-to-shoot translocation of metals (Bücker-Neto *et al.,*2017). Moreover, it was hypothesized that ABA may have a role in the activation of MAPKs signalling, thus providing Cd tolerance. Although it is already known that ABA is able to induce transient MAP kinases activity (Knetsch *et al.,*1996; Burnett *et al.,*2000), the mechanisms downstream the role of ABA in MAP kinases activation in response to heavy metal toxicity need to be further elucidated (Bücker-Neto *et al.,*2017).

Concerning ethylene, in *A. thaliana* an increase of hormone biosynthesis was detected under Cd treatment, related to an up-regulation of the expression of *ACS2* and *ACS6* genes, the main isoforms involved in Cd-induced ethylene production in *A. thaliana* (Schellingen *et al.,*2014). Evidences of the involvement of ethylene in Cd tolerance were reported also in *Brassica juncea*, where the ethylene-mediated protection of photosynthesis was related to its involvement in the regulation of glutathione (GSH) synthesis and the modulation of antioxidant system components (Masood *et al.,*2011). Ethylene-mediated Cd-tolerance was reported also in *Lycopersicon. esculentum* seedlings (Iakimova *et al.,*2008; Liu *et al.,*2008), *Allium cepa* (Maksymiec, 2011) and *Glycine max* (Chmielowska-Bąk *et al.,*2013).

An important role in Cd tolerance is also documented for salicylic acid (SA), another key hormone in plant response to stress. In particular, Shi *et al.* (2009) reported on the capacity of SA to reduce Cd uptake, enhance antioxidant activities and improve photosynthetic capacity in *Cannabis sativa*. Furthermore, under Cd stress, it was reported

that, in *Pisum sativum* plants, SA activity preserved membrane stability by modulating redox balance through up-regulation of antioxidant responses, thus safeguarding photochemical activity of chloroplast membranes and photosynthetic carboxylation reactions (Popova *et al.,*2009).

Finally, also brassinosteroids (BRs) activity was found to reduce the adverse effects of Cd stress in plants. Namely, BRs could reduce Cd toxicity on photochemical processes by reducing the damage on photochemical reaction centres and the activity of oxygen evolving centre, as well as by maintaining efficient photosynthetic electron transport (Janeczko *et al.,*2005), also through up-regulation and down-regulation of many Cd-stress responsive genes (Villiers *et al.,*2012).

Globally, literature data clearly evidence the role of the different hormone classes in plant response to stress. In some cases, like for auxin and cytokinins, results appear sometime controversial, but it must be underlined that they were derived in the context of a different experimental background related to different plant species, plant growth stage and specific treatment. Moreover, under stress condition, several cross-talks come in action between the different players of plant signalling network, making more complex the picture of plant response.

1.4 Study model: *Arabidopsis thaliana*

In 1907 Friedrich Laibach, during his PhD, described the correct chromosome number of *A. thaliana* (Laibach, 1907) and, some years later, proposed this plant as a model organism, founding the experimental *Arabidopsis* research (Laibach, 1943) that, however, began effectively only in 1980s, thanks to the opening of the Third International *Arabidopsis* Conferences at Michigan State University, that created the basis for the formation of an electronic *Arabidopsis* newsgroup (Meinke *et al.,*1998).

1.4.1 Classification, geographical distribution and principal characteristics of *Arabidopsis thaliana*.

Arabidopsis thaliana belongs to the *Brassicaceae* family (ord. Capparales) (Mitchell-Olds, 2001), and the genus *Arabidopsis* contains about 10 species native of Eurasia, North Africa and North America (Fig. 1.7). *A. lyrata* and *A. halleri*, the closest

relatives of *A. thaliana*, are diploid plants with eight chromosome pairs, while *A. thaliana* has just five chromosomes (Nasrallah *et al.,*2000).

Figure 1.7: Geographic distribution of *A. thaliana*. The red dots represent original habitat. The green color represent areas that *A. thaliana* has been naturally spread (Koornneef, 2004).

A. thaliana plants can be grown *in vitro*, in Petri plates, or *in vivo* in a greenhouse. The root, unable to establish symbiotic relationship with nitrogen-fixing bacteria, has a simple structure that makes easy its study in culture (Meinke *et al.,*1998) and the leaves are usually used to morphogenetic and cellular differentiation studies. Around 3 weeks after germination, the inflorescence forms flowers and siliques (Meinke *et al.,*1998). Flowers present four green sepals and four white petals, six stamens bearing pollen, and a central gynoecium that forms the siliques (Meinke *et al.,*1998). Self-fertilization is favored, but crossing is possible by application of pollen on the stigma surface. The siliques, when mature, can produce more than 5000 seeds of 0.5 mm for each plant (Meinke *et al.,*1998). *Arabidopsis thaliana* is an excellent biological model thanks to:

- **The short life cycle**, from the seed germination to the flowering and maturation of the first seeds, that is completed in 6 weeks (Meinke *et al.,*1998).
- **The small size,** thanks to which it can be easily grown in laboratory environments (Meinke *et al.,*1998).

- **The relatively small genome,** that makes easier the isolation and cloning of mutant loci, as well as Next Generation Sequencing analysis. *A. thaliana* genome size is of approximately 135 Mb and contains an estimated 27.000 genes encoding about 35.000 proteins (Meinke *et al.,*1998).
- **The availability of over 750 natural accessions (ecotypes)**, collected around the world, and of a great heterogeneity of mutant and transgenic constructs, thanks to the two major seed stock centers, ABCR and NASC (Meinke *et al.,*1998).
- **The easiness by which it can be transformed with a gene of interest** (Meinke *et al.,*1998)**.**

Thanks to all these advantages, *A. thaliana* became the model organism for studies of the cellular and molecular biology of flowering plants.

1.4.2 DNA methylation landscape of the *A. thaliana* genome

Most of the studies on plant DNA methylation have been performed on *A. thaliana*, which presents a rich and intricate methylation system (Gehring and Henikoff, 2008). Even though cytosines in *A. thaliana* genome can be methylated in all sequence context, the methylation frequencies in these sites aren't the same. In fact, CpG sites present the highest percentage of methylation (24%), followed by CpHpG sites (6.7%) and CpHpH sites (1.7%) (Cokus *et al.,*2008). Moreover, while transposons and repeats are usually methylated in all cytosine possible context, gene body DNA methylation is preferentially a CpG methylation (Zhang *et al.,*2006; Lister *et al.,*2008; Cokus *et al.,*2008; Takuno and Gaut, 2013).

As expected, also the distribution of DNA methylation isn't uniform through the genome, and it results to be concentrated around the centromeres and in TEs (Fig. 1.8 A, B), showing that DNA methylation preferential locations are repetitive DNA sequences, probably due to the role of this epigenetic modification in transposon inactivation (Lippman *et al.,*2003; Lippman *et al.,*2004; Zhang *et al.,*2006; Zilberman *et al.,*2007).

More than 60% of *A. thaliana* genes are completely unmethylated, around 30% of the genes contain methylated cytosines within the gene body, but not within the promoter,

and result to be moderately methylated, while 5% of the expressed genes is methylated upstream of the transcription start site (Zhang *et al.,*2006).

Finally, it was observed that the more a gene is close to the centromere, the higher is the possibility that it will be methylated, independently from its distance to TEs, suggesting a chromosome-level organization of DNA methylation distribution (Zilberman *et al.,*2007).

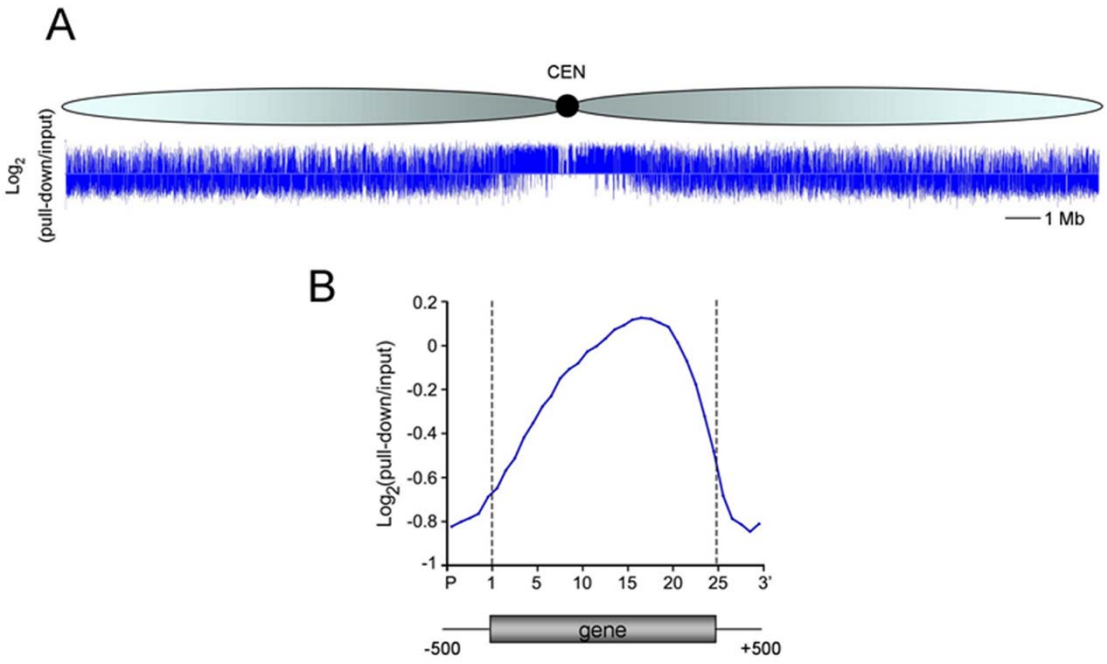

Figure 1.8: Distribution of DNA methylation in *A. thaliana*. **A)** Methylation profiling of *A. thaliana* chromosome 1. DNA methylation is present both in chromosome arms and in the centromeric region, where results to be highly concentrated. **B)** Distribution of DNA methylation within transcriptional active genes. These genes contain methylated cytosines within the gene body, but not at their 5' and 3' ends (Gehring and Henikoff, 2008).

1.4.3 DNA methyltransferases-defective mutants of *Arabidopsis thaliana*.

Currently, several DNA methylation-defective mutants of *A. thaliana* have been characterized, which are impaired in the establishment, maintenance and/or removal of DNA methylation due to the loss of function of genes encoding the different methyltransferases. Both single, double and triple mutants are available from the stock centres and therefore they have been largely used to understand DNA methylation mechanisms and its involvement in plant growth and development.

As above mentioned, MET1 is the principal responsible of the maintenance of CpG methylation throughout the *A. thaliana* genome (Finnegan and Dennis, 1993; Genger *et al.,*1999). Unlike *Dnmt1* mutant of mice, which dies during embryonal development, antisense-*MET1* transgenic plants and loss of function *met1* mutants of *A. thaliana* are viable (Finnegan *et al.,*1996; Ronemus *et al.,*1996). Interestingly, *met1* mutants show alterations in phenotype that became progressively more extreme at each subsequent inbreed (Jacobsen *et al.,*2000; Soppe *et al.,*2000; Kankel, *et al.,*2003), due to the loss or gain of endogenous gene silencing, that cause the occurrence of epimutations (Jacobsen *et al.,*2000; Soppe *et al.,*2000). Namely, *A. thaliana* T2 *met1* seedlings show reduced apical dominance and decreased fertility, moreover they display shorter roots, a decreased stature and smaller leaves with a rounded shape and curled margins toward the upper surface (Finnegan *et al*. 1996).

DDM1 it's also required for CpG methylation and gene silencing (Kakutani *et al.,*1996). Even though both MET1 and DDM1 functionality is required for full levels of CpG methylation, they show different phenotypes, and *ddm1-2 met1-1* double mutant presents additive effects on plant development compared to the single mutants, respectively (Kankel, *et al.,*2003).

As already said, CMT is a class of methyltransferases specific for plant kingdom, and *A. thaliana* contains three genes of this family: *CMT1*, *CMT2* and *CMT3* (Henikoff and Comai, 1998). While *CMT1* is expressed only at very low levels in flowers and results to be truncated in several ecotypes, *CMT2* is a putative DNA methyltransferase, and *cmt2* loss of function mutants show a loss of CpHpH methylation in heterochromatic TEs (Stroud *et al.,*2014). *CMT3* is the main methyltransferase of this family. In *cmt3* loss of function mutants, a genome-wide loss of CpHpG methylation and a reduction of asymmetric methylation at some loci was evidenced (McCallum *et al.,*2000; Bartee *et al.,*2001; Lindroth *et al.,*2001). *DRM1* and *DRM2* genes maintain the non-CG methylation in *A. thaliana* and together with *CMT3* are responsible of *de novo* methylation at both CpHpG and CpHpH sites (Cao and Jacobsen, 2002a).

The single loss of function *drm1*, *drm2* and *cmt3* mutants of *A. thaliana* and the double mutant *drm1 drm2* are morphologically similar to the wild type. These results suggest that CpHpG and CpHpH methylation are subjected to an overlapping control by DRM1, DRM2 and CMT3 (Cao and Jacobsen, 2002a, 2002b). However, this control

depends from the loci of interest, whose methylation pattern could depend to DRM activity, CMT3 activity, or both. An example is represented by *FWA* and *MEA-ISR* loci. While in the double mutant *drm1 drm2* there are no traces of asymmetric and CpHpG methylation at these loci, the single mutant *cmt3-7* showed only a reduction of CpHpG methylation. As expected, also the triple mutant *drm1 drm2 cmt3.7* doesn't show asymmetric and CpHpG methylation at *FWA* and *MEA-ISR* loci (Cao and Jacobsen, 2002a). Furthermore, *drm1 drm2 cmt3* mutant presents pleiotropic developmental defects dealing with plant size, leaf shape and seed production (Cao and Jacobsen, 2002a; Forgione *et al.,*2018 (*submitted to Plant Science*)). Since this mutant retains CpG methylation at all the sequences tested (Cao and Jacobsen, 2002a), this abnormal phenotype is caused by a reduction of non-CpG methylation.

As already described, non-CpG methylation is associated to transcriptional and post transcriptional gene silencing, and usually is implicated to viral and transposon silencing (Huettel *et al.,*2006; Zemach *et al.,*2013; Liu *et al.,*2014). Thus, defects in these defence mechanisms could cause the pleiotropic phenotype observed in the mutant. For this reason, further studies on the *drm1 drm2 cmt3* triple mutant are required to elucidate other possible biological functions that involve non-CpG methylation.

AIM OF THE WORK

As previously discussed, plants are rooted in the environment where they grow in and need to adapt to a multitude of environmental changing conditions that, if unfavourable, elicit abiotic stress (Pereira, 2016). For these reasons, during their evolution, plants developed extremely efficient signalling machinery and genetic networks to assure a high degree of growth plasticity.

Currently, the impact of abiotic stress on both ecosystems and world agriculture is very huge, causing an impressive loss of biodiversity and of the potential yield of annual crops, therefore representing the major limitation to crop production worldwide (Bray *et al.,*2000). Moreover, the global climate change, that is taking place in the last century, and the increasing human pressure, are strongly contributing to exacerbate desertification and salinization of soils all over the world, determining new threats to human health, ecosystems, and national economies (Bellard *et al.,*2012; Koyro *et al.,*2012; Asseng *et al.,*2014). For these reasons, understanding the mechanisms by which plants sense and respond to stress is becoming even more necessary in order to improve their resistance and preserve both agricultural productivity and environmental sustainability.

Within this scenario, there is increasing awareness that the epigenetic control of gene expression, assuring a rapid and extensive modulation of genome, represents a dynamic mechanism which allow the plants to adapt and withstand stressful situations. Accordingly, the involvement of DNA methylation, one of the most relevant epigenetic mechanism, in plant responses to environmental changes and stressors, has been widely assessed (reviewed by Zhang *et al.,*2018). Despite this information, the complex mechanisms by which DNA methylation modulates plant stress responses is yet largely unresolved, mainly with respect to heavy metal stress, for which a metal- and species-specific response was evidenced. Moreover, the overall picture is even more complex, since plant responses to stress are also under the control of phytohormone network, which is in turn modulated by epigenetic mechanisms.

In this context, the aim of the present work was to gain further insight into the mechanisms and molecular processes that act in and are regulated by DNA methylation under stress condition, by using the *drm1 drm2 cmt3 (ddc)* mutant of *A. thaliana,* defective in both maintenance and *de novo* DNA methylation. Attention was focused on stress

induced by heavy metals, which are dangerous environmental pollutants, and Cd was selected as one of the most toxic and widespread in both terrestrial and marine environment. In details, we performed a comparative analysis of the effects induced by the exposure to this heavy metal on *ddc* and WT plants of *A. thaliana*, exposed to a long lasting (21 days) treatment at 25 and 50 μM Cd concentrations. An integrated approach was applied by investigating: i) growth parameters by image analysis ii) transcriptome by RNA-Seq iii) cytophysiological features of root, selected as study system, being the first plant organ sensing Cd. Analyses encompassed the evaluation of: root apical meristem (RAM) size; auxin efflux carriers distribution; stem cell niche (SCN) maintenance; expression pattern of SCR transcription factors, as marker of SCN and endodermis specification.

CHAPTER 2: MATERIAL AND METHODS

2.1 Plant Lines

Seeds of *Arabidopsis thaliana* (L.) Heynh. ecotype Columbia-0 (Col-0) as control and the *drm1 drm2 cmt3.11 (ddc*) triple DNA methylation mutant in Col-0 background were used. *ddc* triple mutant was created by crossing *drm1* (SALK_021316; AT5G15380) with T-DNA insertion in the sixth exon, *drm2* (SALK_150863; AT5G14620) with T-DNA insertion in the last exon, and *cmt3.11* (SALK_148381; AT1G69770) with T-DNA insertion in the eighth intron (Henderson and Jacobsen, 2008). The seeds were purchased from the Nottingham *Arabidopsis* Stock Centre (NASC, http://*Arabidopsis*.info/).

2.2 Growth Conditions

Seeds were surface sterilized by incubation in 70% ethanol (EtOH) for 2 minutes, then in 5% sodium hypochlorite solution (NaClO) and 0.05% Tween 20 for 10 minutes. Finally, they were thoroughly washed in water 5 times for 5 minutes each. After sterilization, seeds were sown in Petri dishes containing half-strength MS medium (Murashige and Skoog, 1962) including vitamins (glycine 2 mg/l, myo-inositol 100 mg/l, nicotinic acid 0.5 mg/l, pyridoxine HCl 0.5 mg/l, thiamine HCl 0.1 g/l), 1% sucrose, 0.5 g/l 2-N-morpholine ethane sulphonic acid (MES), 8 g/l agar. MS medium pH was set to 5.7 with KOH 1N.

The plated seeds were stratificated at 4°C for 48 h to ensure uniform germination, and then incubated in a growth chamber at 21°C, under long day condition (16h/8 day/night) with white light (neon fluorescent tubes “Radium NL Spectralux, cool white”, 100 μmol m^{-2} s^{-1}) and 50% relative humidity.

For Cd treatment, seeds were placed in a medium supplemented with Cd (25 μM and 50 μM) as $CdCl_2$. In particular, $CdCl_2$ was dissolved in sterile water and 100 mM stocks were prepared. An aliquot of this stock solution was added directly to the germination medium immediately before placing it in the Petri dishes to prepare the desired Cd concentrations.

2.3 Germination test

For germination test, 100 seeds coming from different batches of *A. thaliana* WT and *ddc* mutant were sterilized and sown in the same Petri dish, containing control (Ctrl) and Cd enriched medium (25 and 50 µM respectively). After stratification at 4°C for 48 h, the plates were transferred in the growth chamber as above described. The germination status of the seeds was checked daily, up to 5 days after sowing. Three independent replicates were performed. Data were statistically evaluated by Student's *t*-test (*$p \leq 0.05$; **$p \leq 0.01$; ***$p \leq 0.001$), performed between *ddc vs* WT subjected to the same treatment.

2.4 Growth parameters analysis

For root length analysis and lateral root investigation, *A. thaliana* seedlings of WT and *ddc* mutant germinated in the above described conditions and grown in a vertical position were used. Root length was monitored every 2 days until 21 days after germination (DAG) by scanning the plates and analysing the resulting images through the open source processing program ImageJ (https://imagej.net). The number of lateral roots was counted by observing single plants by stereomicroscope (Leica IC80 HD). Subsequently, the images of the plates were acquired by scanner and primary root length was measured by using ImageJ software (https://imagej.nih.gov/ij/). Finally, lateral root density was calculated by dividing the number of lateral roots by the primary root length for each root.

For rosette analysis, 21 DAG *A. thaliana* seedlings of WT and *ddc* mutant germinated in the above described conditions and grown in round Petri dishes (140 x 20 mm) were used. Seedlings were collected at 21 DAG, corresponding to the period necessary for our samples to reach the last step of leaf development that, according to Boyes *et al.* (2001), is characterized by the presence of 14 rosette leaves > 1mm length. Leaf series was obtained by placing *ddc* mutant and WT leaves on large square plates containing 1% plant tissue agar in distilled water. Incisions were made to make the leaves fully expanded, when necessary. Measures were taken by scanning the plates and analysing the resulting images through the open source processing program ImageJ (https://imagej.nih.gov/ij/).

For all the above described analyses, three independent replicates were performed (n = 45). For root length and leaf area, statistical analysis was performed by using Student's *t*-test

(*$p \leq 0.05$; **$p \leq 0.01$; ***$p \leq 0.001$) between *ddc vs* WT subjected to the same treatment. For lateral root density, statistical analysis was performed by using two-way ANOVA with Tukey post hoc test ($p \leq 0.05$) after Shapiro–Wilk normality test. Means with the same letter are not significantly different at $p \leq 0.05$.

2.5 Cd quantification

For Cd quantification, 21 DAG *A. thaliana* seedlings of WT and *ddc* mutant, germinated and grown in the above described conditions, were used. As described by Liu *et al.* (2015), the seedlings were rinsed with deionized water and oven dried at 65°C. Subsequently, the plant material was weighted and digested with HNO_3:H_2O_2 at high pressure in a sealed microwave digestion oven. After this digestion, samples were diluted with 5% HNO_3 (in ultra-pure water) to a final volume of 50 ml and the Cd concentration in the solution was measures via graphite furnace atomic absorption spectrometry (GFAAS- Hitachi z-2000, Japan). Three independent replicates were performed. Statistical analysis was performed by using two-way ANOVA with Tukey post hoc test ($p \leq 0.05$) after Shapiro–Wilk normality test. Means with the same letter are not significantly different at $p \leq 0.05$.

2.6 Total RNA extraction

Arabidopsis thaliana seedlings of WT and *ddc* mutant germinated and grown in the above described conditions and sampled at 21 DAG were used. Seedlings were frozen with liquid nitrogen and grinded with mortar and pestle and about 100 mg of the obtained powder were used for total RNA extraction by using the RNeasy Plant Mini kit (Qiagen, Hilden, Germany) according to the manufacturer's instructions. Briefly, the powder was transferred to 2 ml microcentrifuge tube. 450 µl of RLT buffer, previously added with 10 µl/ml of β-mercaptoethanol, were put in the microcentrifuge tube and vortexed vigorously. The lysate was transferred in the QIAshredder spin column (lilac) placed in a 2 ml collection tube, both provided by the extraction kit, and centrifuged at 14.000 rpm (full speed) for 2 minutes. The supernatant of the obtained flow-through was transferred in another microcentrifuge tube, being careful to not disturb the celldebris pellet, and the supernatant was precipitated by adding 0.5 volume of absolute ethanol (EtOH). The

solution was quickly mixed by pipetting and transferred, together with any precipitate that may have formed, to a RNeasy spin column (pink) placed in a 2 ml collection tube (provided by the extraction kit) and centrifuged at 10.000 rpm for 15 seconds. On column DNase digestion (RQ1 RNase-Free Dnase, Cat. Nr. M6101) was performed to eliminate DNA contamination, by adding a mix of 8 µl of RQ1 buffer, 8 µl DNase (8 unit) and 64 µl of RNase free water previously prepared directly on the membrane of the RNeasy spin column (pink). After 15 minutes of incubation, the spin column membrane was washed with 350 µl of Buffer RW1, and the sample was centrifuged at 10.000 rpm for 15 seconds. Subsequently, 500 µl Buffer RPE were added to purify the membrane and the sample was centrifuged at 10.000 rpm for 15 seconds, followed by three additional washing with 500 µl, 350 µl and 300 µl with the same buffer. In order to remove residual ethanol which may interfere with downstream reactions, a centrifugation at full speed for 1 minute was applied. The RNeasy spin column was transferred into a new 1.5 ml collection tube (supplied) and 30 µl RNase-free water were added directly on the spin column membrane. Finally, the sample was centrifuged at 10,000 rpm for 1 minute to elute the RNA. For transcriptomic analysis, the extracted RNA was quantified by using the Qubit RNA BR (Broad-Range) Assay Kit, used with the Qubit 3.0 Fluorometer (Thermo Fisher Scientific), while its integrity was checked by using an Agilent 2100 Bioanalyzer (Agilent Technologies). Only RNA samples with an RNA integrity number ≥ 8 were used in subsequent analyses.

2.7 RNA-seq

cDNA libraries were constructed from 1 µg of total RNA, using the Illumina's TruSeq Stranded Total RNA Sample Preparation Kit (Illumina, San Diego, CA, USA), according to the manufacturer's protocol. The quality of the obtained libraries and the fragments length were verified on the Bioanalyzer 2100 by using an Agilent 2100 DNA 1000 Kit and quantified by fluorimetry using the dsDNA HS (High sensitivity) Assay kit (Q232854) on Qubit 3.0 Fluorometer (Thermo Fisher Scientific).The sequencing of the cDNA libraries was carried out on Illumina Genome Analyzer IIx (SCS v2.10) platform, generating a total of 29.4 Giga reads of 50 bp paired-end reads.

2.8 Preprocessing and analysis of RNA-seq data

Original reads were generated from RNA-Seq by 50-bp pair-ended sequencing. Reads in FASTQ format were inspected using FASTQC program (http://www.bioinformatics.babraham.ac.uk/projects/fastqc/). For each sample (WT Ctrl, WT 25 µM Cd, WT 50 µM Cd, *ddc* Ctrl, *ddc* 25 µM Cd, *ddc* 50 µM Cd) only reads with Phred quality score Q > 30 (Q30 Quality Score) were taken into account, whose proportion ranged from 90 to 95 % (90.4%, 91.4%, 94.7%, 94.0%, 94.3%, 95.0% in the different samples, respectively), for a total of 29.4 Giga reads (93.3% of the total obtained reads) (Fig. 2.1). Sub-sequences, low quality reads and other impurities were removed-to obtain clean reads for the analysis by using Trim Galore (http://www.bioinformatics.babraham.ac.uk/projects/trim_galore/) (Annese *et al.,*2018). Next, *Arabidopsis* TAIR 10 gene sequences database was used to match the clean reads (allowing for two mismatched bases). Only the alignment that resulted unique and concordant in Sequence Alignment Map (SAM) format were converted in the binary BAM format by SAMtools and basic statistics were calculated using Picard tools (CollectRnaSeq Metrics.jar) (http://picard.sourceforge.net/). The obtained results were used for subsequent analyses. Transcriptome quantification and differential expression of coding and non-coding RNA was performed using CuffDiff2 (http://cufflinks.cbcb.umd.edu/) software version 2.1.1, as described in Annese *et al.* (2018).

Gene expression levels were calculated using the rescue method (or Cufflinks method) to calculate FPKM (Roberts *et al.,*2011). Bioinformatic analysis was performed by multiple pairwise comparisons of gene expression levels (i) in *ddc* mutant *vs* WT under both Ctrl and Cd-treated conditions (*ddc vs* WT- Ctrl, *ddc vs* WT -25 µM Cd, *ddc vs* WT -50 µM Cd); (ii) in WT treated at either 25 or 50 µM Cd *vs* WT grown in Ctrl condition (25 µM Cd *vs* Ctrl –WT, 50 µM Cd *vs* Ctrl –WT); iii) in *ddc* mutant treated at either 25 or 50 µM Cd *vs ddc* grown in Ctrl condition (25 µM Cd *vs* Ctrl – *ddc*, 50 µM Cd *vs* Ctrl – *ddc*). Differentially expressed genes (DEGs) were selected on the basis of fold change (FC) ($5 \geq |\log_2 FC| \geq 2$ and FDR ≤ 0.01).

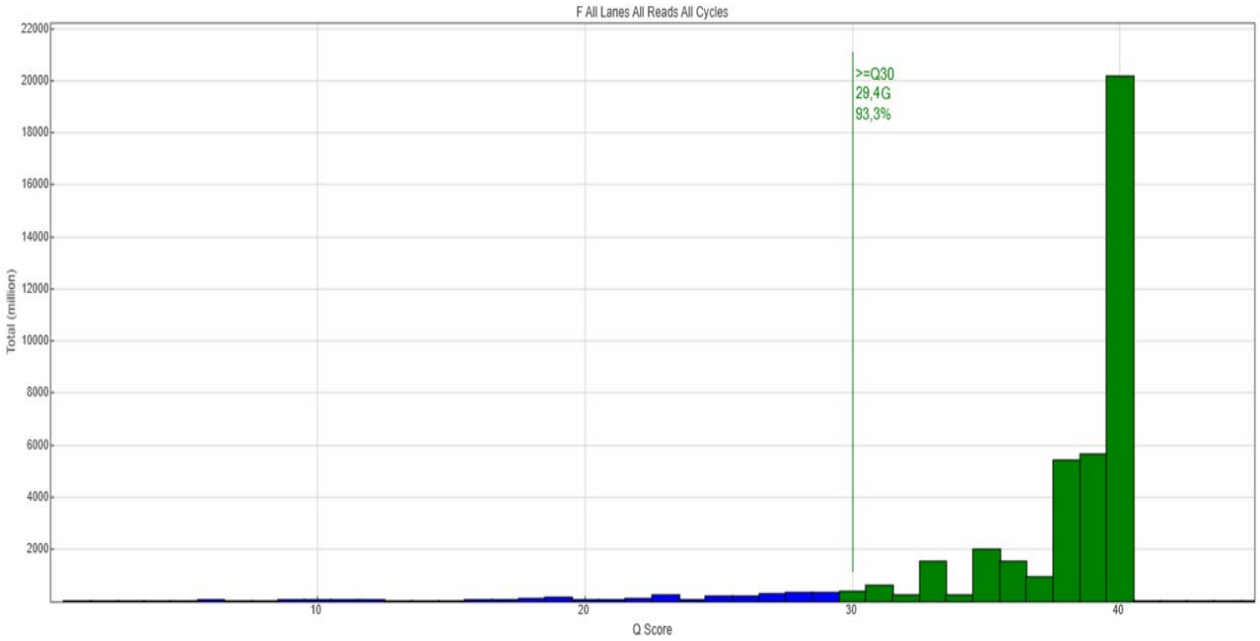

Figure 2.1: Total QScore Distribution. In all analysed libraries, a total of 93.3% of the obtained reads (29.4 Giga reads) passed the Q30 quality score threshold and were used for subsequent analyses.

2.9 Heatmap construction

A global visualization of the obtained data was provided by the heatmap created from the FPKM values of the total DEGs found in all the different pairwise comparisons analysed in this work. The heatmap was created by using the R package gplot (https://cran.r-project.org/package=gplots).

2.10 Gene Enrichment analysis

Generally, one of the problems of high-throughput experiments is the biological interpretation of the large gene clusters obtained. A largely used strategy, applied also in this work, consists into the use of ontology sources, that classify the knowledge on gene function in a controlled vocabulary applicable to all the organisms.

In particular, a functional annotation analysis of the detected DEGs was performed by using Gene Ontology (GO) annotations, which provides definitions of gene product properties based on three different domains: Cellular Component, Molecular Function and Biological Process (Ashburner *et al.,*2000; http://www.geneontology.org/).

As known, the GO terms are structured in a complex, not linear relationship, that doesn't guarantee a static and unique position into the hierarchical structure for each term

(Bindea *et al.,*2009). Moreover, the large amount of information causes, for close related terms, a high degree of redundancy. More importantly, analysing all the DEGs found without performing any previous statistical selection could bias the data interpretation and the identification of the genes and pathways involved in a particular phenotype/phenomenon object of study (Bindea *et al.,*2009).

To overcome, at least partially, these limitations, a Gene Enrichment analysis was performed on DEGs by using ClueGO plug-in of the Cytoscape software (Shannon *et al.,*2003). This bioinformatic source filters the terms grouping those which share similar associated genes and creating, as a final output, large clusters of genes of non-redundant biological terms in a functionally grouped network (Bindea *et al.,*2009).

In particular, a Gene Enrichment analysis, based on biological process ontology and KEGG database information, was performed through the selection of over-represented GO terms in each comparison analysed in this work. Namely, ClueGO automatically determined the significance of each term and group by the calculation of a Bonferroni-corrected P-value using the hypergeometric distribution (Bindea *et al.,*2009); only the GO terms with a P-value ≤ 0.05 were selected and used in the subsequent analyses.

2.11 Analysis of hormone-related pathways

Hormone-related pathways analysis was performed by using the online tool Plant MetGenMAP (http://bioinfo.bti.cornell.edu/cgibin/MetGenMAP/home.cgi). This Web-based system allows the final user to explore large-scale gene expression data-set and identify the significantly altered biochemical pathways and biological processes in a rapid and efficient way, through intuitive visualization and robust statistical tests (Joung *et al.,*2009).

2.12 Single Strand cDNA synthesis

Total RNA extraction was performed by using the RNeasy Plant Mini kit (Qiagen, Hilden, Germany) according to the manufacturer's instructions, as above described. First-strand cDNA synthesis was performed by SuperScript™ III Invitrogen USA, according to the manufacturer's instructions. A reaction mix containing 1 µg of total RNA, 1 µl of oligo$(DT)_{20}$ (50 µM), 1 µl of 10 mM dNTPmix and DEPC-treated water up to 10 µl was incubated at 65 °C for 5 minutes and then put on ice for at least 1 minute. Subsequently,

a cDNA Synthesis mix, containing 2 µl 10x RT buffer, 4 µl 25 mM $MgCl_2$, 2 µl 0,1 M DDT, 1 µl RNaseOUT (40 U/µl) and 1 µl SuperScript™ III RT (200 U/µl) was added to the previous reaction mix and incubated at 50 °C for 50 minutes. The reaction was terminated at 85 °C for 5 minutes and the samples were chilled on ice. Eventual residual RNA was digested by adding 1 µl of RNase H and incubated at 37 °C for 20 minutes.

2.13 Quantitative Real-Time PCR (qRT-PCR)

Primers used for qRT-PCR analysis were designed using Primer-BLAST online tool (https://www.ncbi.nlm.nih.gov/tools/primer-blast/) (Ye *et al.,*2012). According to Bruno *et al.* (2017), primers pairs where selected on the basis of their: (a) robustness: successful amplification over a range of annealing temperatures, (b) specificity: generation of a single significant peak in the melting curve, and (c) consistency: highly reproducible Ct values within the reactions of a triplicate. Only the ones with an average efficiency between 0.95 and 1.0. were used. The housekeeping gene *AT2G28390* (*MONENSIN SENSITIVITY1, SAND*) was used as a normalization control. This gene was selected from independent trials of several housekeeping genes as the one that produced the most reproducible results across various cDNAs, as also described by Remans *et al.* (2008). The primer sequences are reported in Table 2.1 and Table 2.2.

Quantitative real-time PCR (qRT-PCR) was performed using STEP ONE instrument (Applied Biosystems). According to Bruno *et al.* (2017), amplification reactions were prepared in a final volume of 20 µL, containing: 2.5 µl Power SYBR® Green PCR Master Mix (Applied Biosystems), 1 µl each primer (0.5 µM final concentration) and cDNA (25 ng). All reactions were run in triplicate in 48-well reaction plates and negative controls were included. The cycling parameters were as follows: 95°C for 10 min, followed by 40 cycles of 95°C for 10 seconds and 60°C for 30 seconds. Melting curve analysis was also performed. The results were analysed using STEP One Software 2.0 (Applied Biosystems), by using the "Comparative Ct method", also known as ΔΔCt method (Rao *et al.,*2013). Statistical analysis was performed by using two-way ANOVA with Tukey post hoc test ($p \leq 0.05$) after Shapiro–Wilk normality test. Means with the same letter are not significantly different at $p \leq 0.05$;

Table 2.1: Primers used in qRT-PCR for libraries results validation. Gene description was obtained from the freely accessible database STRING (Search Tool for the Retrieval of Interacting Genes/Proteins, https://string-db.org) (von Mering *et al.,*2005).

Locus	Description	Gene Name	Primer FW	Primer BW
AT4G32540	YUCCA 1; Involved in auxin biosynthesis. Belongs to the set of redundant YUCCA genes probably responsible for auxin biosynthesis in shoots.	*YUC1*	5'-TGGTCTTGCCACTTCAGCAT-3'	5'-GCGTAGGACTCAAGGTAGGC-3'
AT3G62980	TRANSPORT INHIBITOR RESPONSE 1; Auxin receptor that mediates Aux/IAA proteins proteasomal degradation and auxin-regulated transcription. Plays a role in ethylene signaling in roots.	*TIR1*	5'-CTACGCGAGCTGAGAGTGTT-3'	5'-GGAAGCGAGTCATGTTGGGA-3'
AT2G01830	WOODEN LEG; Principal component in CK signalling. Functions as a histidine kinase and transmits the stress signal to a downstream MAPK cascade.	*AHK4*	5'-GCTGCAGGAGCTCTCAAGAA-3'	5'-AGGTCGCGTGTATCACATCC-3'
AT1G79460	GA REQUIRING 2; Catalyzes the conversion of ent-copalyl diphosphate to the gibberellin precursor ent-kaur-16-ene	*GA2*	5'-CTCGCGTTAAAGAAGTGGGG-3'	5'-AGCCCAATGGAATCGTCAGA-3'
AT1G14920	DELLA protein GAI; Probable transcriptional regulator that acts as a repressor of the gibberellins (GAs) signalling pathway. Its activity is probably regulated by other phytohormones such as auxin and ethylene.	*GAI*	5'-ACGGTAACGGCATGGATGAG-3'	5'-CGACGGAGGATTAAGGTCGG-3'
AT1G20510	OPC-8-0 CoA ligase1; Contributes to jasmonic acid biosynthesis by initiating the beta-oxidative chain shortening of its precursors.	*OPCL1*	5'-ATTCCCCGTCGTTTGTCTCT-3'	5'-CACGATCGGGAGCTTCTTTG-3'

AT1G19180	Protein TIFY 10A; Repressor of jasmonate responses.	*JAZ1*	5'-CCTGATGTCAATGGAACTTTAGGC-3'	5'-TGGTGCAGTTTGAGACTCTGG-3'
AT3G14440	NINE-CIS-EPOXYCAROTENOID DIOXYGENASE 3; Catalyzes the first step of abscisic-acid biosynthesis from carotenoids, in response to water stress.	NCED 3	5'-CGGTTTCTGGGAGATGGCTT-3'	5'-GGCTTAACAACAATGGCGGG-3'
AT2G27150	ABSCISIC-ALDEHYDE OXIDASE 3; It catalyse the final step in abscisic acid biosynthesis in leaves and in seeds.	*AAO3*	5'-TGGTTGCTTATGGTCTCGGT-3'	5'-AACACAGCAAAGCCTAACGG-3'
AT2G19590	ACC OXIDASE 1; Key enzyme involved in ethylene biosynthesis.	*ACO1*	5'-ACGTTTTACAATCCGGCTGG-3'	5'-GCTGAATCCGCATTTCCCAT-3'
AT3G20770	ETHYLENE-INSENSITIVE3; Probable transcription factor acting as a positive regulator in the ethylene response pathway.	*EIN3*	5'-GCTTACCGTATGGAGCAGCA-3'	5'-TGGACTGTGGGTTGAAGCAG-3'
AT4G39400	BRASSINOSTEROID INSENSITIVE 1; Receptor with a dual specificity kinase activity acting on both serine/threonine- and tyrosine-containing substrates.	BRI1	5'-GCACGCAAAACTGCGGATTA-3'	5'-TATCCCTGACCCGGCTTGTA-3'
AT1G64280	Regulatory protein NPR1; Key positive regulator of the SA-dependent signaling pathway that negatively regulates JA-dependent signaling pathway. Controls the onset of systemic acquired resistance (SAR).	*NPR1*	5'-TTGTTTATCTGGCCGCCGAA-3'	5'-TTCTCGCTGACAAAACGCAC-3'
AT5G13320	AVRPPHB SUSCEPTIBLE 3; It is involved in both basal and induced resistance	*PBS3*	5'-GAGGTTGTGAGGACGGGTTC-3'	5'-GTGGCCCTCCAAGAACCAAA-3'

	in a SA-dependent manner.			
AT2G28390	*MONENSIN SENSITIVITY1;* SAND family protein.	*SAND*	5'-AACTCTATGCAGCATTTGATCCACT-3'	5'-TGATTGCATATCTTTATCGCCATC-3'

Table 2.2: Primers used in qRT-PCR for auxin transporter genes. Gene description was obtained from the freely accessible database STRING (Search Tool for the Retrieval of Interacting Genes/Proteins, https://string-db.org) (von Mering *et al.,*2005).

Locus	Description	Gene Name	Primer FW	Primer BW
AT1G73590	PIN-FORMED 1; Component of the auxin efflux carrier. It's involved in the basipetal auxin transport. Mediates the formation of auxin gradient which is required to ensure correct organogenesis.	*PIN1*	5'-CTTCTTATGCCGTTGGCCTC-3'	5'-CACCGCAGTGCTAAGAATGTC-3'
AT1G23080	PIN-FORMED 7; Component of the auxin efflux carrier. Mediates the initial auxin gradient which contributes to the establishment of the apical-basal axis in early embryogenesis.	*PIN7*	5'- ATTGCGTGTGGCCATTGTTC-3'	5'- CCTGTACTCAAGATTGCGGGA-3'

2.14 Libraries results validation

In order to confirm the results obtained by the transcriptomic analysis, 14 key genes involved in hormone homeostasis and signalling (Table 2.1) were selected for validation, that was carried out by qRT-PCR. As RNA-sequencing and qRT-PCR produce relative gene expression measures, one of the samples (WT grown in Ctrl condition) was chosen as reference, to which all the others were compared to obtain the $\log_2$ (FC) values used to evaluate concordance in gene expression by Pearson correlation coefficient calculation (Annese *et al.,*2018).

2.15 Hormone level quantification

2.15.1 Extraction and purification

Plant material was ground in a mortar with 80 % MeOH (1:5 w/v). [13C6]-IAA (Cambridge Isotopes Laboratories Inc., Andover, MA), [2H6]-ABA (OlChemlm Ltd., Olomouc, Czech Republic), [2H4]-SA (CDN Isotopes Inc., Quebec, Canada) and [2H5]-JA (CDN Isotopes Inc.) and deuterated GAs ([17,17- 2H2]-GA9, [17,17- 2H2]-GA4, [17,17- 2H2]-GA34, [17,17- 2H2]-GA7, [17,17- 2H2]-GA51, [17,17- 2H2]-GA19, [17,17- 2H2]-GA20, [17,17- 2H2]-GA29, [17,17- 2H2]-GA1, [17,17- 2H2]-GA8, [17,17- 2H2]-GA3, [17,17- 2H2]-GA5, obtained from Dr. L. N. Mander, Australian National University, Canberra, Australia), 50 ng each, were added as internal standards. Methanolic extracts were centrifuged (4000·g; 5 minutes), surnatants were collected and pellets were eluted with 80 % MeOH. The extraction was repeated three times. After adjusting the pH at 2.8, the methanol was evaporated under vacuum at 35 °C and the aqueous phase was partitioned with ethyl acetate (1:1 v/v). For GAs purification, the extracts were also dried and suspended in 0.3-0.5 ml of distilled water with 0.01% acetic acid and 10% methanol (Fambrini *et al.,*2015; Scartazza *et al.,*2017).

2.15.2 HPLC analysis

JA, SA, ABA, GAs and IAA were separated by reversed phase HPLC as described by Fiorini *et al.* (2016) by using a Kontron instrument (Kontron Instruments, Munich, Germany) equipped with a variable wavelength UV detector SpectroMonitor 3100 (Milton Roy, Florida, USA) operating at 214 nm at a flow rate=1 ml min^{-1}. Samples were applied to a 150 mm×4.6 mm i.d. column, packed with Hypersil C18 particle size 5µm (Thermo Fisher Scientific Inc., Waltham, MA, USA). Each fraction was dried in a rotary evaporator and resolved in MeOH for GC-MS analysis.

2.15.3 GC-MS analysis

After drying, samples were trimethylsilylated with 10µl of N,O-bis(trimethylsilyl) trifluoroacetamide (BSTFA) containing 1 % trimethylchlorosilane (TMCS) (Pierce, Rockford, IL, USA) at 70 °C for 1 hour and finally analysed by GC-MS. Quantitative

determination of IAA, ABA, SA, GA and JA was performed by using a Saturn 2200 quadrupole ion trap mass spectrometer coupled to a CP-3800 gas chromatograph (Varian Analytical Instruments, WalnutCreek, CA, USA) equipped with a Mega 1MS capillary column (30 m×0.25 mm i.d., 0.25 m film thickness)(Mega, Milano, Italy), as described by Fiorini *et al.* (2016). Plant hormones were identified by comparing full mass spectra with standard compounds. The concentration of each plant hormone in the extracts was determined from the peak area ratio of labelled and non-labelled ions of internal standard and endogenous hormone, respectively. Final data were means of three biological replicates.

2.16 Confocal Visualization of GFP Expression and signal quantification

Green fluorescent protein (GFP) expression was monitored in seedlings of the transgenic lines of *A. thaliana* auxin-induced *pDR5::GFP* (Ottenschläger *et al.,*2003) *pPIN1::PIN1-GFP*, *pPIN7::PIN7-GFP* (Blilou *et al.,*2005) *pSCR::SCR-GFP* (Sabatini *et al.,*1999) in WT roots. For the *ddc* mutant, *pDR5::GFP*, *pPIN1::PIN1-GFP*, *pPIN7::PIN7-GFP* and the *pSCR::SCR-GFP* reporter genes were introgressed in *ddc* through crosses with the transgenic WT lines. Third generation seeds from two independent homozygous mutant lines, which exhibited the same phenotype of the parental *ddc*, were used, and the homozygous lines were selected by polymerase chain reaction (PCR) using T-DNA primers, designed following the instructions of the Salk institute genomic analysis laboratory (http://signal.salk.edu/tdnaprimers.2.html), and gene-specific primer pairs, as described by Forgione (2016) and Forgione *et al. (*2018; *submitted to Plant Science*).

A Leica inverted TCS SP8 confocal scanning laser microscope with a 40x oil immersion objective was used to obtain median longitudinal sections of the root samples. The detection of GFP was performed with the excitation peak centred at about 488 nm and an emission peak wavelength of 509 nm.

As described by Bruno *et al.* (2017), measurements of GFP signal intensity were carried out on the root apex of 8 DAG seedlings of the transgenic lines *pDR5::GFP, ddc X pDR5::GFP, pPIN1::PIN1-GFP*, *ddc X pPIN1::PIN1-GFP, pPIN7::PIN7-GFP* and *ddc X pPIN7::PIN7-GFP*. Measurements were performed separately on the different zones of the root apex: calyptra, root apical meristem (RAM) and transition zone (TZ) until

about 500 μm from the junction calyptra-root apex. Signal intensity measurements were carried out with Leica Application Suite X software (LAS X) for a minimum of 50 seedlings for each sample. The experiment was performed in triplicate and statistical analysis was performed by using two-way ANOVA with Tukey post hoc test ($p \leq 0.05$) after Shapiro–Wilk normality test. Means with the same letter are not significantly different at $p \leq 0.05$.

2.17 Analysis of root Meristem Size and pattern

For the root meristem size analysis, WT and *ddc* seedlings of *A. thaliana,* germinated and grown for 8 DAG in the above described conditions, were stained with propidium iodide following the MPS-PI-staining protocol (Truernit *et al.,*2008). Namely, the seedlings were fixed in a solution of 50% methanol and 10% acetic acid and incubated at 4°C for at least 12 hours. Subsequently, the seedlings were washed with water and incubated in a solution of 1% periodic acid at room temperature for 40 minutes. Next, seedlings were washed again with water and incubated in Schiff reagent with propidium iodide (100 mM sodium metabisulphite, 0.15 N HCl, 100 mg/ml propidium iodide) until plants were visibly stained (this step usually takes 1 or 2 hours). Finally, the samples were put on microscope slides and covered with a chloral hydrate solution (4 g chloral hydrate, 1 ml glycerol, and 2 ml water). Samples were observed after waiting for at least 24 hours, in order to allow the mounting solution to set (Truernit *et al.,*2008).

A Leica inverted TCS SP8 confocal scanning laser microscope with a 40x oil immersion objective was used to obtain median longitudinal sections of the root samples. Excitation and emission wavelength were 600 and 640 nm, respectively. Root meristem size evaluation was performed by measuring the distance and the number of cortex cells in a file extending from the QC to the first elongated cortex cell (Dello Ioio *et al.,*2007; Perilli and Sabatini, 2010; Bruno *et al.,*2017). Three independent replicates were performed, and for each sample a minimum of 70 seedlings was analysed. Data were statistically evaluated by using two-way ANOVA with Tukey post hoc test ($p \leq 0.05$) after Shapiro–Wilk normality test. Means with the same letter are not significantly different at $p \leq 0.05$.

CHAPTER 3: RESULTS

3.1 Impact of Cd exposure on plant growth and development of *ddc* mutant and WT *A. thaliana* seedlings.

First of all, to test the viability of the seeds in a Cd-enriched environment, a germination test was performed by sowing *ddc* mutant and WT seeds of *Arabidopsis thaliana:* (i) on growth medium added with 25 or 50 µM Cd; (ii) on growth medium without Cd as control (Ctrl).

For all the samples, the maximum percentage of germination was achieved at 2 days after sowing, corresponding to a value higher than 95% (Fig. 3.1). However, under Ctrl condition, the germination percentage at the 1st day after sowing was significantly lower in *ddc* mutant compared to the WT (Fig. 3.1); from the 2nd day after sowing until the end of the germination test (5 days after sowing), the percentage of germination was still lower in *ddc* than in the WT, although the difference was not any more significant (Fig. 3.1). By contrast, under Cd treatment, at the 1st day after sowing the percentage of germination was higher in *ddc* mutant than in WT whatever concentration was considered (Fig. 3.1); thereafter, the percentage of germination was significantly higher in the mutant than in WT only at 50 µM Cd concentration (Fig. 3.1).

These results showed that Cd exposure affected the germinative energy more than capacity of both WT and *ddc* seeds in a dose-dependent way. However, this effect was lower on mutant than WT seeds.

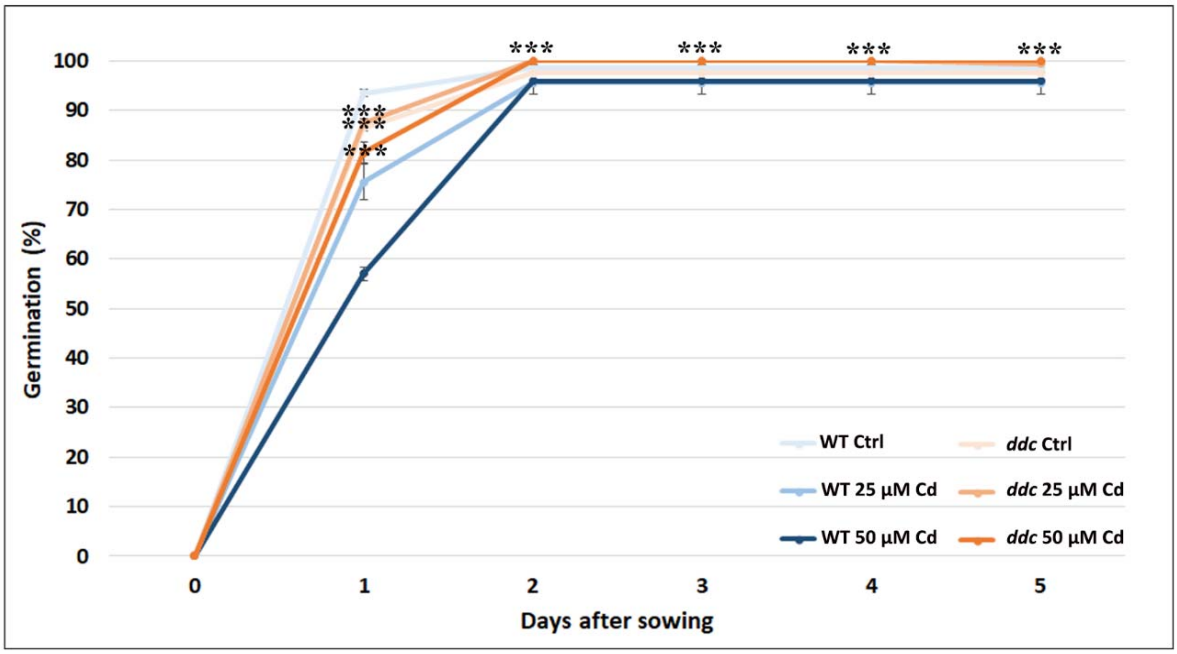

Figure 3.1: Germination percentage of *ddc* and WT *A. thaliana* seeds (i) on growth medium added with 25 or 50 µM Cd; (ii) on growth medium without Cd as control (Ctrl); under long day light regime. The results represent the mean value (± standard deviation) of three independent biological replicates (n = 100). Asterisks indicate significant pairwise differences using Student's t-test (*p ≤ 0.05; **p ≤ 0.01; ***p ≤ 0.001), performed between *ddc vs* WT subjected to the same treatment.

In order to evaluate the effects of Cd on plant growth and development, WT and *ddc* seedlings of *A. thaliana* were germinated and grown as above described. Primary root length, lateral root density and leaves area were selected as growth parameter to be analysed.

Primary root growth was monitored from germination up to 21 days after germination (DAG). It was observed that, in Ctrl condition, primary root was lightly shorter in *ddc* mutant compared to the WT (Fig. 3.2 A, B). Following Cd exposure, starting from the 6th DAG, a significant dose-dependent inhibition of root growth was observed both in the WT and *ddc* mutant (Fig. 3.2 A). However, the Cd inhibitory effect was higher on the WT than on *ddc* seedlings, especially at 25 µM Cd concentration. In fact, at 21 DAG, root length of WT seedlings treated with 25 and 50 µM Cd was about two and three folds shorter as compared to Ctrl condition, respectively (Fig. 3.2 A, B). By contrast, root length of *ddc* mutant treated with 25 and 50 µM Cd was only 1.2 and 2.6 folds shorter as compared to Ctrl condition, respectively. Consequently, at the end of Cd exposure, root resulted to be significantly longer in the *ddc* mutant than in WT (Fig. 3.2 A, B).

A

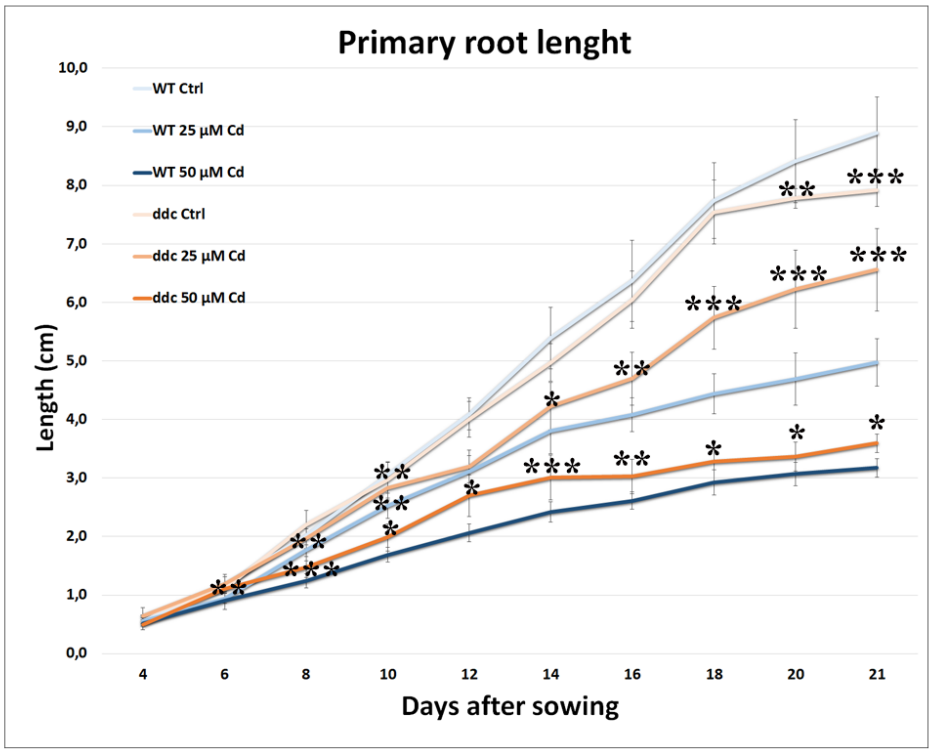
Primary root lenght
WT Ctrl
WT 25 µM Cd
WT 50 µM Cd
ddc Ctrl
ddc 25 µM Cd
ddc 50 µM Cd
Length (cm)
Days after sowing
10,0
9,0
8,0
7,0
6,0
5,0
4,0
3,0
2,0
1,0
0,0
4
6
8
10
12
14
16
18
20
21

B

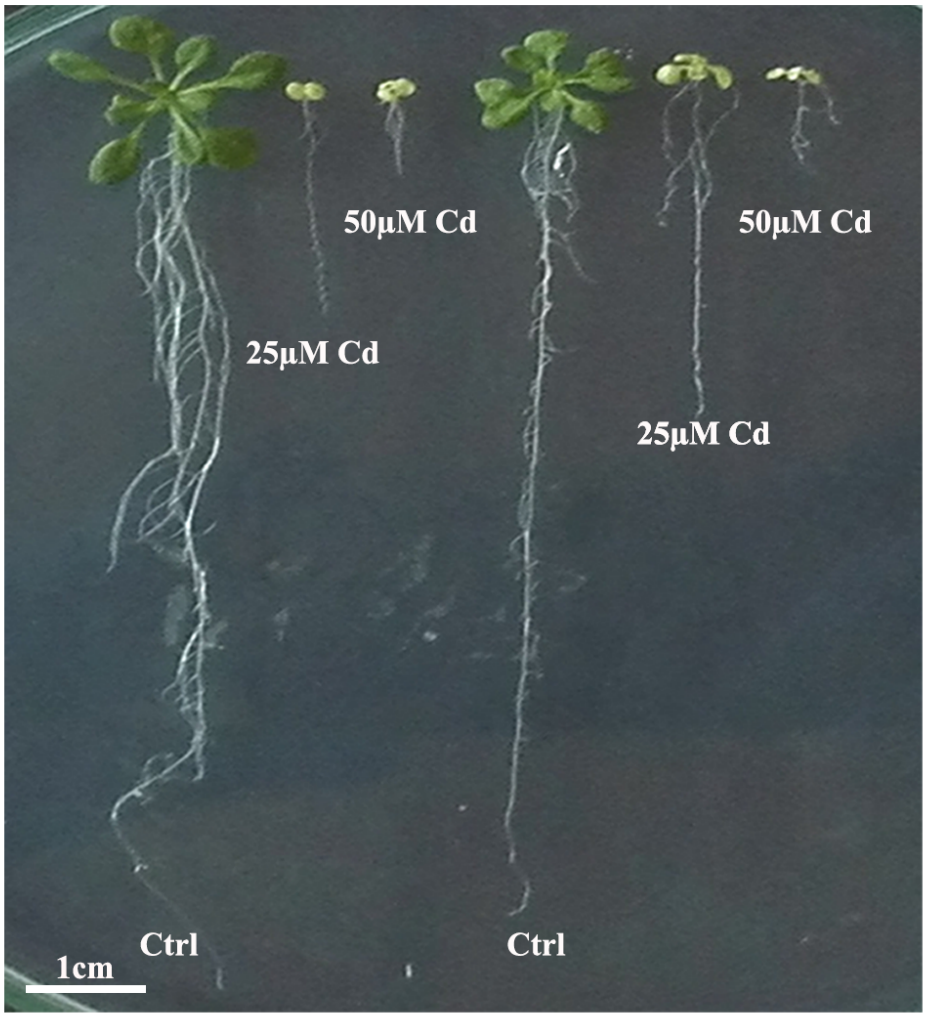
WT
ddc
50µM Cd
25µM Cd
50µM Cd
25µM Cd
Ctrl
Ctrl
1cm

Figure 3.2: (A) Primary root length of WT and *ddc* seedlings of *A. thaliana*, monitored up to 21 days after germination (DAG) every two days from germination. The seedlings germinated and grown under long day condition: (i) on growth medium added with 25 or 50 µM Cd; (ii) on growth medium without Cd as control (Ctrl). The results represent the mean value (± standard deviation) of three independent biological replicates (n = 45). Asterisks indicate significant pairwise differences using Student's t-test (*p ≤ 0.05; **p ≤ 0.01; ***p ≤ 0.001), performed between *ddc vs* WT subjected to the same treatment. **(B)** Picture of WT and *ddc* mutant seedlings of *A. thaliana* grown under the above described conditions at 21 DAG.

Concerning lateral root density (lateral root number/primary root length), no differences were evidenced between the *ddc* triple mutant and the WT grown in Ctrl condition (Fig. 3.3). A higher lateral root density was instead observed in *ddc* and WT Cd-treated seedlings compared to their respective seedlings grown under Ctrl condition (Fig. 3.3), evidencing that Cd treatment induced an increase of lateral root formation. No differences in lateral root density were detected between *ddc* mutant and WT seedlings treated with Cd (Fig. 3.3).

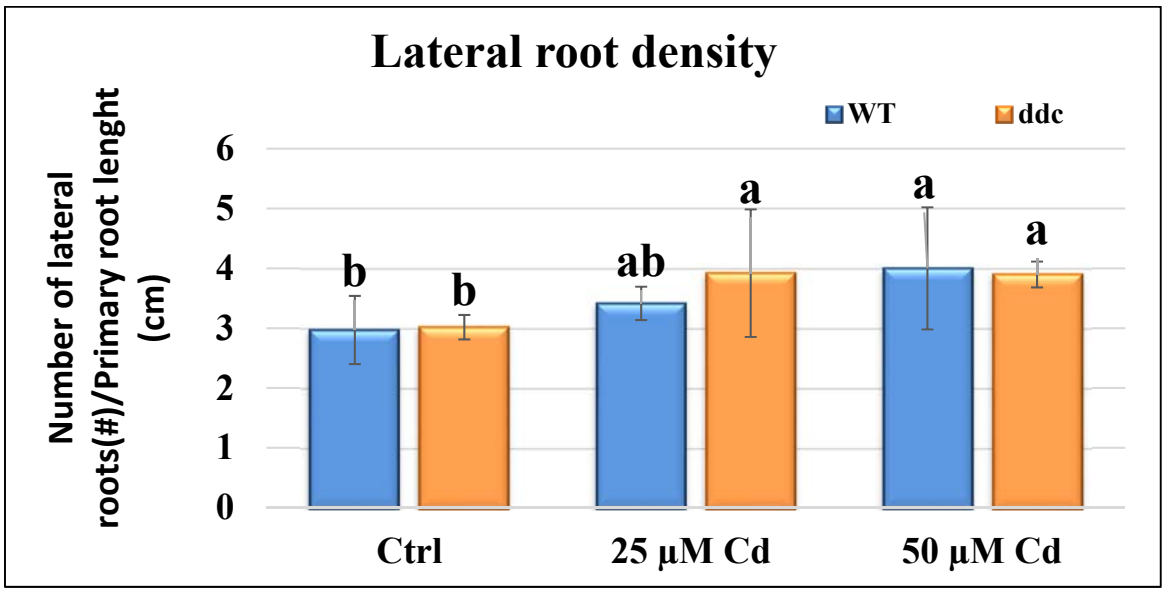

Figure 3.3: Lateral root density (number of lateral roots (#)/primary root length (cm)) of WT and *ddc* seedlings of *A. thaliana* germinated and grown for 21 DAG in long day condition: (i) on growth medium added with 25 or 50 µM Cd; (ii) on growth medium without Cd as control (Ctrl). The results represent the mean value (± standard deviation) of three independent biological replicates (n = 45). Statistical analysis was performed by using two-way ANOVA with Tukey post hoc test ($p \leq 0.05$) after Shapiro–Wilk normality test. Means with the same letter are not significantly different at $p \leq 0.05$.

Rosette size was estimated by analysing leaf number and area in seedlings collected at 21 DAG, corresponding to the period necessary for our samples to complete the leaf development (Boyes *et al.,*2001). We observed that Cd induced a significant dose-dependent inhibition of rosette development, at major extent in the WT than in *ddc* mutant (Fig. 3.4 A, B). Indeed, in Ctrl condition, a complete leaf series was formed by both *ddc* mutant and WT, but the area of the majority of the leaves was significantly smaller in the mutant compared to WT (Fig. 3.4 A, B). By contrast, in 25 µM Cd treated seedlings, both the number of leaves and their area were greater in the mutant than in the WT, while under the highest Cd treatment the differential impact on *ddc vs* WT was evident only with respect to the number of leaves, which was higher in the former than in the latter (Fig. 3.4 A, B).

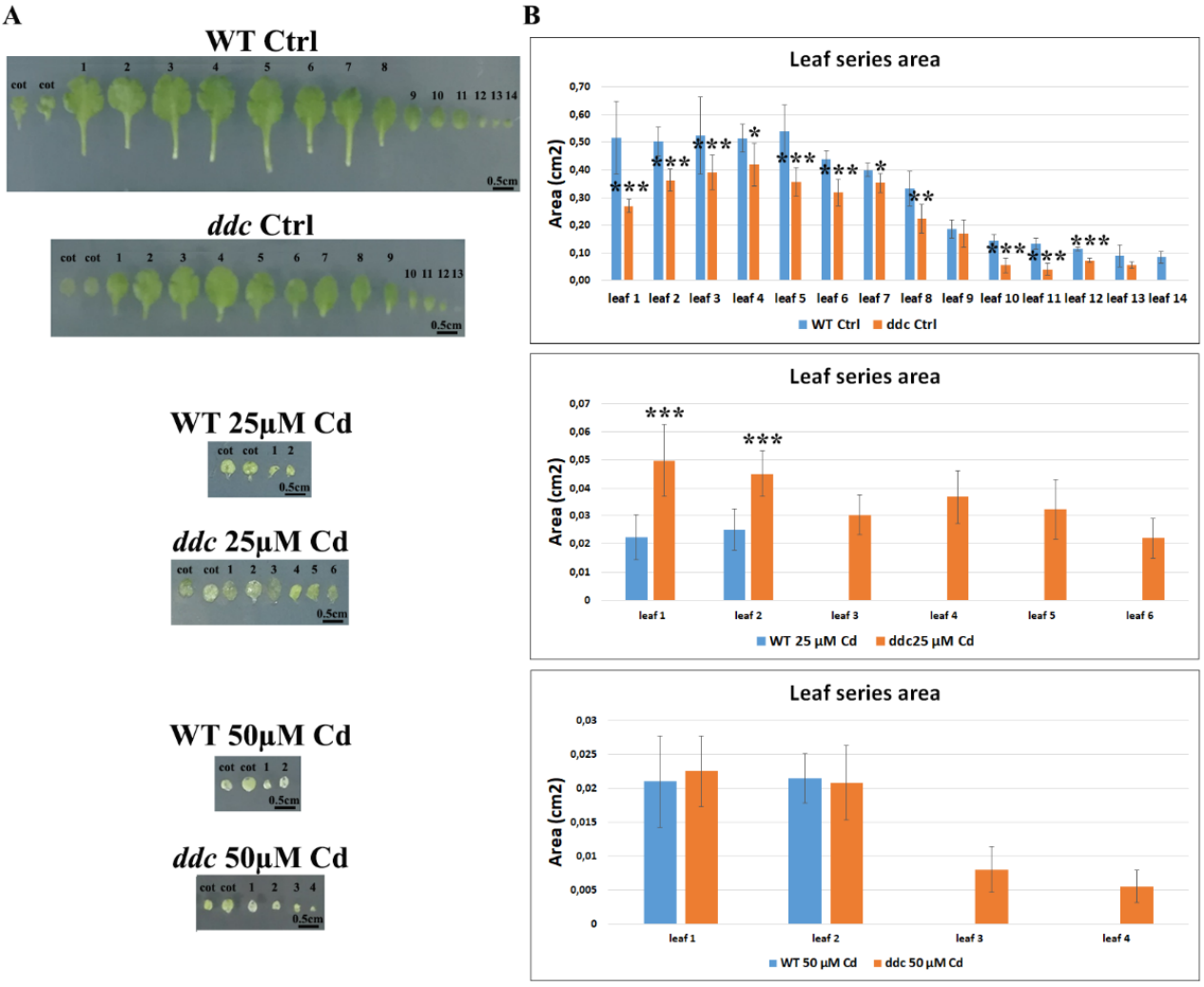

Figure 3.4: (A) Picture of rosette leaf series and **(B)** rosette leaf area (cm^2) of WT and *ddc* seedlings of *A. thaliana*, germinated and grown for 21 DAG in long day condition: (i) on growth medium added with 25 or

50 µM Cd; (ii) on growth medium without Cd as control (Ctrl). The results represent the mean value (± standard deviation) of three independent biological replicates (n = 45). Asterisks indicate significant pairwise differences using Student's t-test (*p ≤ 0.05; **p ≤ 0.01; ***p ≤ 0.001), performed between *ddc vs* WT subjected to the same treatment.

3.2 Quantification of Cd absorption in *ddc* mutant and WT seedlings of *A. thaliana.*

The differential growth performance observed in the mutant and the WT under Cd treatment prompted us to investigate whether it could be related to a different rate of Cd absorption, and a quantification of Cd accumulated inside the tissues/cells was carried out in WT and *ddc* seedlings of *A. thaliana*, germinated and grown for 21 DAG as above described.

A dose-dependent accumulation of this heavy metal was observed in both the mutant and the WT (Fig. 3.5). Interestingly, under 25 µM Cd treatment *ddc* mutant accumulated significantly more Cd than the WT (Fig. 3.5). This result clearly indicated that globally the better growth performance of *ddc* mutant compared to WT when treated with Cd was not dependent on a lower Cd absorption. Hence, it could be envisaged that more complex factors and mechanisms were involved.

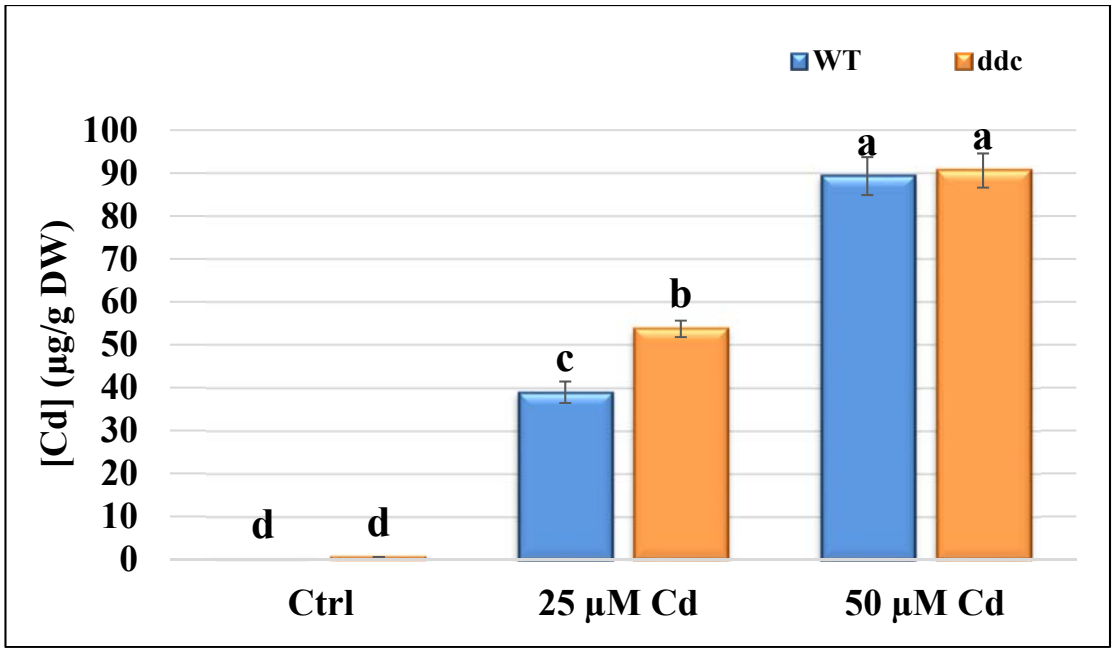

Figure 3.5: Cd amount in WT and *ddc* seedlings of *A. thaliana*, germinated and grown for 21 DAG in long day condition: (i) on growth medium added with 25 or 50 µM Cd; (ii) on growth medium without Cd as

control (Ctrl). The results represent the mean value (± standard deviation) of three independent biological replicates (n = 45). Statistical analysis was performed by using two-way ANOVA with Tukey post hoc test ($p \leq 0.05$) after Shapiro–Wilk normality test. Means with the same letter are not significantly different at $p \leq 0.05$.

3.3 RNA-seq Analysis

In order to gain some insights into the molecular factors and mechanisms underlying the differences in growth performance of *ddc* and WT seedlings under Cd treatment, a transcriptomic approach was used. RNA-Seq analysis was performed on seedlings of *A. thaliana* WT and *ddc* mutant, germinated and grown in long day condition for 21 DAG: (i) on growth medium added with 25 or 50 µM Cd; ii) on growth medium without Cd as control (Ctrl).

The aim was to explore whether a global DNA hypomethylation, like in the *ddc* mutant, could result into a different response to Cd-induced stress through a differential modulation of gene expression and, consequently, a differential metabolic reconfiguration, as compared to the methylation landscape of the WT genome.

3.3.1 Analysis and Identification of Differentially Expressed Genes (DEGs)

Gene expression levels were calculated using the rescue method (or Cufflinks method) to calculate Fragments Per Kilobase Million (FPKM) (Roberts *et al.,*2011). Bioinformatic analysis was performed by multiple pairwise comparisons of gene expression levels (i) in *ddc* mutant *vs* WT under both Ctrl and Cd-treated conditions (*ddc vs* WT- Ctrl, *ddc vs* WT -25 µM Cd, *ddc vs* WT -50 µM Cd); (ii) in WT treated at either 25 or 50 µM Cd *vs* WT grown in Ctrl condition (25 µM Cd *vs* Ctrl –WT, 50 µM Cd *vs* Ctrl –WT); iii) in *ddc* mutant treated at either 25 or 50 µM Cd *vs ddc* grown in Ctrl condition (25 µM Cd *vs* Ctrl – *ddc*, 50 µM Cd *vs* Ctrl – *ddc*) (Fig. 3.6 A, B).

Differentially expressed genes (DEGs) were selected on the basis of fold change (FC) ($5 \geq |\log_2 FC| \geq 2$ and $FDR \leq 0.01$). It was evident that, in Ctrl condition, relatively few genes were differentially expressed in *ddc vs* WT (338 DEGs, Fig. 3.6 A). Moreover, we could also observe that Cd treatment impacted on gene expression in *ddc* mutant and WT seedlings, although at a different extent. Indeed, the number of DEGs in *ddc* 25 µM Cd *vs ddc* Ctrl (2242 DEGs, Fig. 3.6 A) was higher than the number of DEGs observed in

WT 25 µM Cd *vs* WT Ctrl (715 DEGs, Fig. 3.6 A). As expected, in each sample (i.e. *ddc* mutant and WT) the highest number of DEGs (2261 and 2508 for WT and *ddc*, respectively) was found in the comparisons between the seedlings treated with the highest Cd concentration *vs* seedlings grown in Ctrl condition (Fig. 3.6 A).

When comparing *ddc* and WT seedling exposed to the same Cd concentration, it was observed that under 25 µM Cd treatment, DEGs number in *ddc vs* WT increased (980 DEGs, Fig. 3.6 A), as compared to that observed under Ctrl condition. Notably, few genes (only 212 DEGs, Fig. 3.6 A) resulted differentially expressed in the comparison *ddc vs* WT-50 µM Cd, suggesting that mostly of the mechanisms that come in action to counteract Cd effects are shared between the mutant and the WT.

Additional information was derived by analysing the fraction of DEGs up- and down-regulated. In particular, under Ctrl condition most of the DEGs were down-regulated in *ddc* mutant *vs* WT (66.6%, Fig. 3.6 B). A widespread down-regulation of gene expression was induced by Cd exposition in both *ddc* and WT seedlings, as evidenced when comparing treated seedlings *vs* their respective controls. In these cases, the percentage of down-regulated genes ranged from 61.4% to 69.9% (Fig. 3.6 B). A high percentage of down-regulated DEGs (73.4%, Fig. 3.6 B) was also found in the comparison *ddc vs* WT -25 µM Cd, while the majority of the DEGs resulted up-regulated (71.2%, Fig. 3.6 B) in the comparison *ddc vs* WT -50 µM Cd. Globally, these observations suggested that under Cd stress *ddc* mutant underwent to a differential modulation of gene expression as compared to the WT.

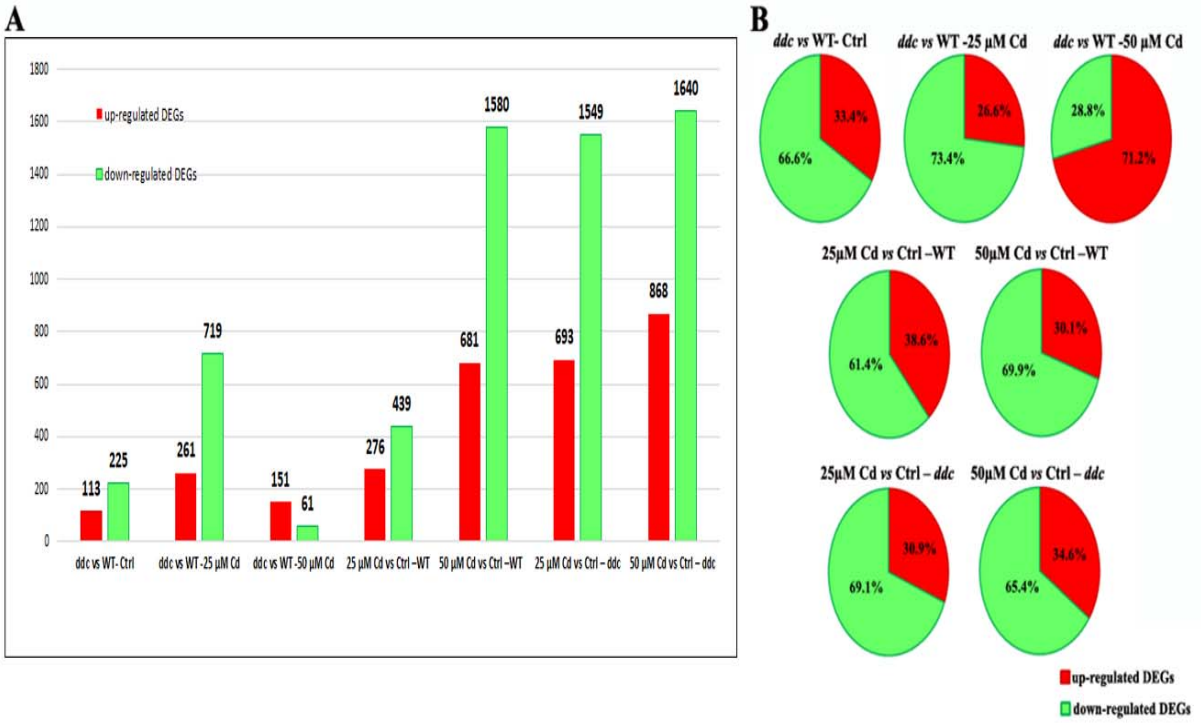

Figure 3.6: (A) Number and **(B)** percentage of up and down-regulated DEGs in all the multiple pairwise comparisons of gene expression levels.

An intuitive visualization of the obtained data was provided by the heatmap (Fig. 3.7) created by using FPKM values of the total DEGs found in all the different pairwise comparisons analysed in this work. Genes with higher expression levels are shown in red, whereas genes with lower expression levels are shown in blue. It was clear that samples are divided in two different groups. The first group included *ddc* and WT samples under Ctrl condition, which exhibited a very similar pattern of gene expression, and WT sample exposed to 25 µM Cd, which exhibited an expression pattern lightly different from the previous ones (Fig. 3.7). In a specular way, the second group was composed by *ddc* and WT samples exposed to 50 µM Cd, which exhibited a very similar pattern of gene expression but different from the first group, and *ddc* sample exposed to 25 µM Cd that presented a gene expression pattern lightly different from the previous ones (Fig. 3.7).

Globally, from the heatmap it was clear that Cd impacted on gene expression; in the framework of this impact, gene expression pattern was largely shared between *ddc* mutant and WT, under both Ctrl condition and 50 µM Cd treatment. Very intriguingly, under 25 µM Cd-treatment, the response of *ddc* mutant was completely different from that of the WT (Fig. 3.7).

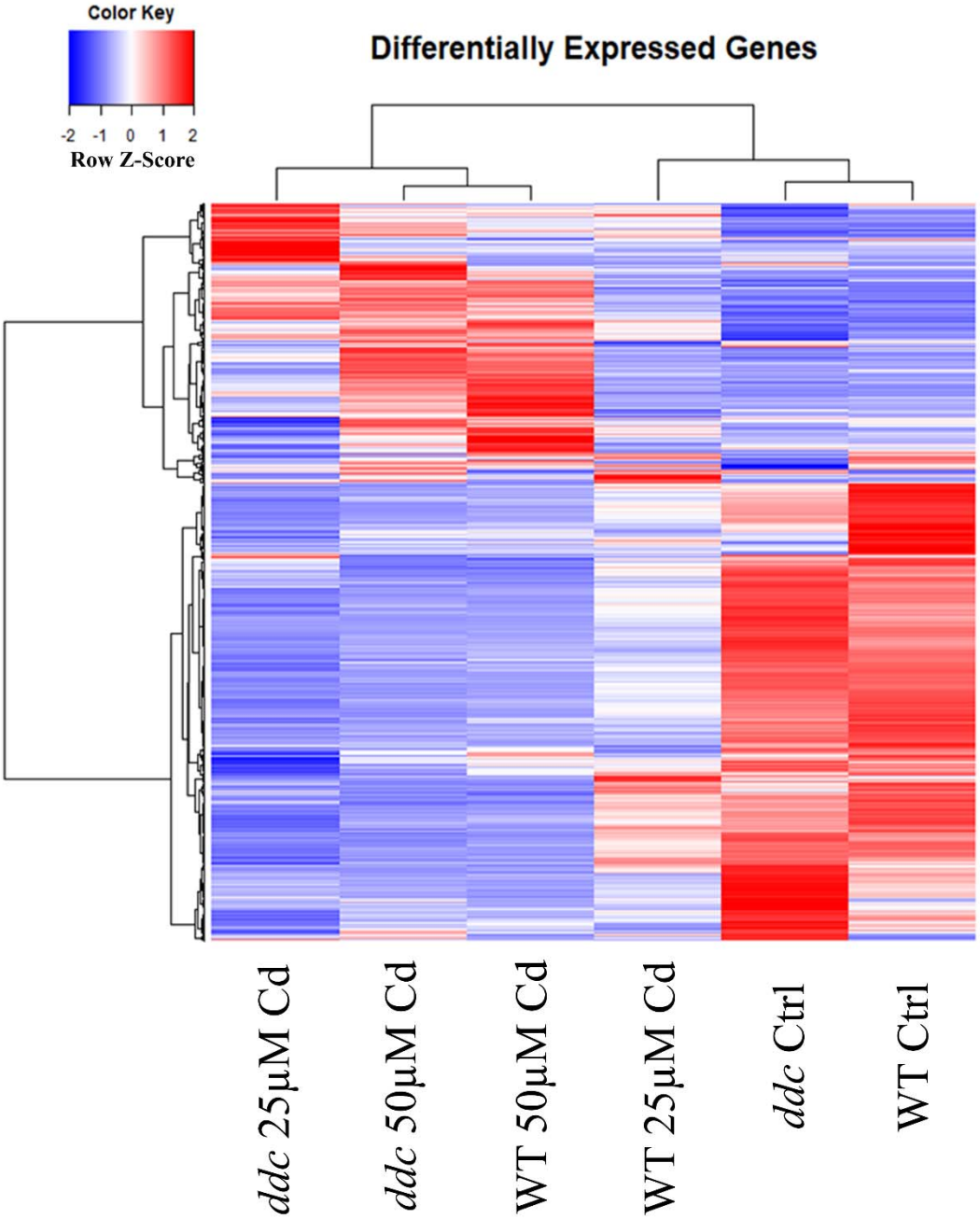

Figure 3.7: Heatmap of differentially expressed genes in the six analysed RNA-seq libraries. Genes with higher expression levels are shown in red, whereas genes with lower expression levels are shown in blue.

3.3.2 Gene Enrichment Analysis

A Gene Enrichment analysis, based on biological process ontology and KEGG database information, was performed through the selection of over-represented GO terms in each comparison analysed in this work, by using ClueGO plug-in of the Cytoscape

software (Bindea *et al.,*2009). Namely, ClueGO automatically determined the significance of each term and group by the calculation of a Bonferroni-corrected p-value using the hypergeometric distribution (Bindea *et al.,*2009); only the GO terms with a p-value ≤ 0.05 were selected and used in the subsequent analyses. Results are illustrated in Fig. 3.8 A-G.

Briefly, in Ctrl condition, a significant down-regulation of genetic pathways related to jasmonic acid (JA) biosynthesis and signalling, and an up-regulation of genetic pathways related to photosynthetic process was detected in the *ddc* mutant compared to the WT (Fig. 3.8 A). Concerning Cd effect, under 25 µM Cd treatment, a significant down-regulation of genetic pathways related to jasmonic acid, glucosinolate and unsaturated fatty acid metabolism, flavonoid biosynthesis, cellular response to nitric oxide, starvation and light intensity was induced in WT seedlings. In the same sample, oxidative phosphorylation, photosynthesis and valine, leucine and isoleucine degradation genetic pathways were significantly up-regulated (Fig. 3.8 B). A down-regulation of several genetic pathways was observed in WT seedlings also under 50 µM Cd treatment, which in this case involved photosynthesis, different carbohydrate metabolism, root development-related processes, exocytosis-related processes, phenylpropanoid biosynthesis and cell walls formation-related processes, glucosinolate metabolism, cellular response to hormone stimulus, plant hormone signal transduction and hormone-mediated signalling pathways, in particular ethylene, abscisic acid, gibberellic acid and cytokinins-activated signalling (Fig. 3.8 C).

In *ddc* mutant, 25 µM Cd treatment was found to induce a down-regulation of almost all enriched genetic pathways. These included photosynthesis, carbohydrate metabolism, glucosinolate metabolism, phenylpropanoid biosynthesis, spindle organization, nonphotochemical quenching, plastoquinone biosynthesis and cellular response to light and salt stress. In the same sample, genetic pathways related to the response to absence of light and sucrose, the propanoate metabolism and the degradation of valine, leucine and isoleucine were significantly up-regulated (Fig. 3.8 D). Under 50 µM Cd, in *ddc* mutant a significant down-regulation of the following genetic pathways was observed: photosynthesis, hemicellulose, lignine and glucosinolate, xiloglucans, phenylpropanoid metabolism, cell wall modifications, brassinosteroids, auxin and abscisic acid metabolism, auxin polar transport, response to blue light, water deprivation and lipids, non-photochemical quenching and cellular response to hormones. Pathways involved in

cellular response to freezing, regulation of leaf senescence, response to red light, regulation of chlorophyll biosynthesis, ethylene signalling and its regulation, regulation of signal transduction processes were up-regulated (Fig. 3.8 E).

When comparing *ddc vs* WT under 25 µM Cd treatment, it was found a significant down-regulation of genetic pathways related to glucosinolate and cyanoaminoacid metabolism, phenylpropanoid biosynthesis, plant hormone signal transduction, cotyledon vascular tissue pattern formation and spindle organization, while cellular response to hypoxia was up-regulated (Fig. 3.8 F). In the same comparison, under 50 µM Cd, only a significant up-regulation of genetic pathways related to photosynthesis and oxidative phosphorylation pathways was found (Fig. 3.8 G).

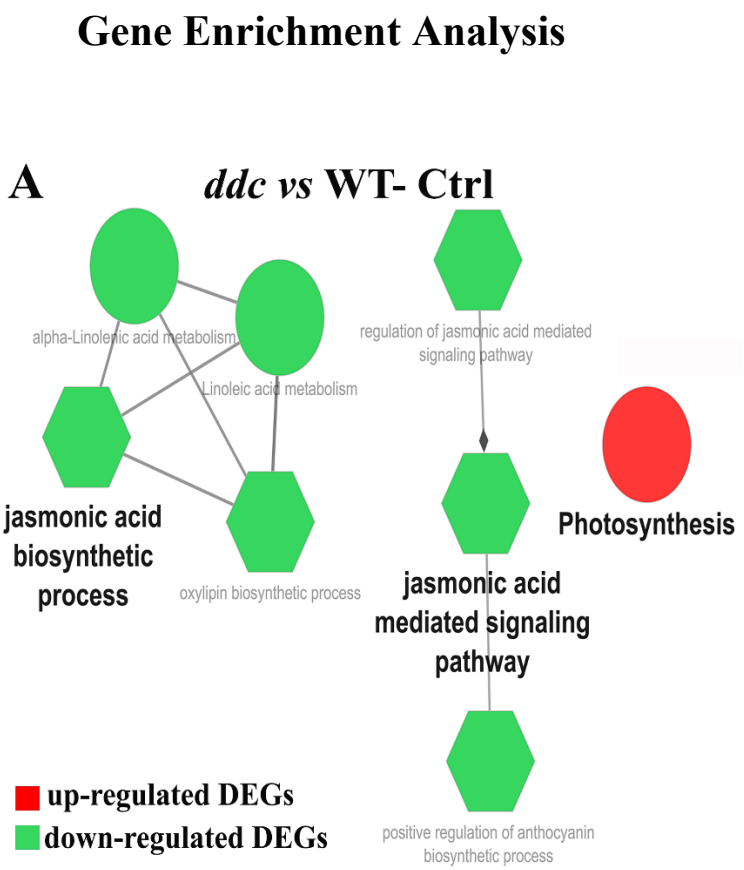

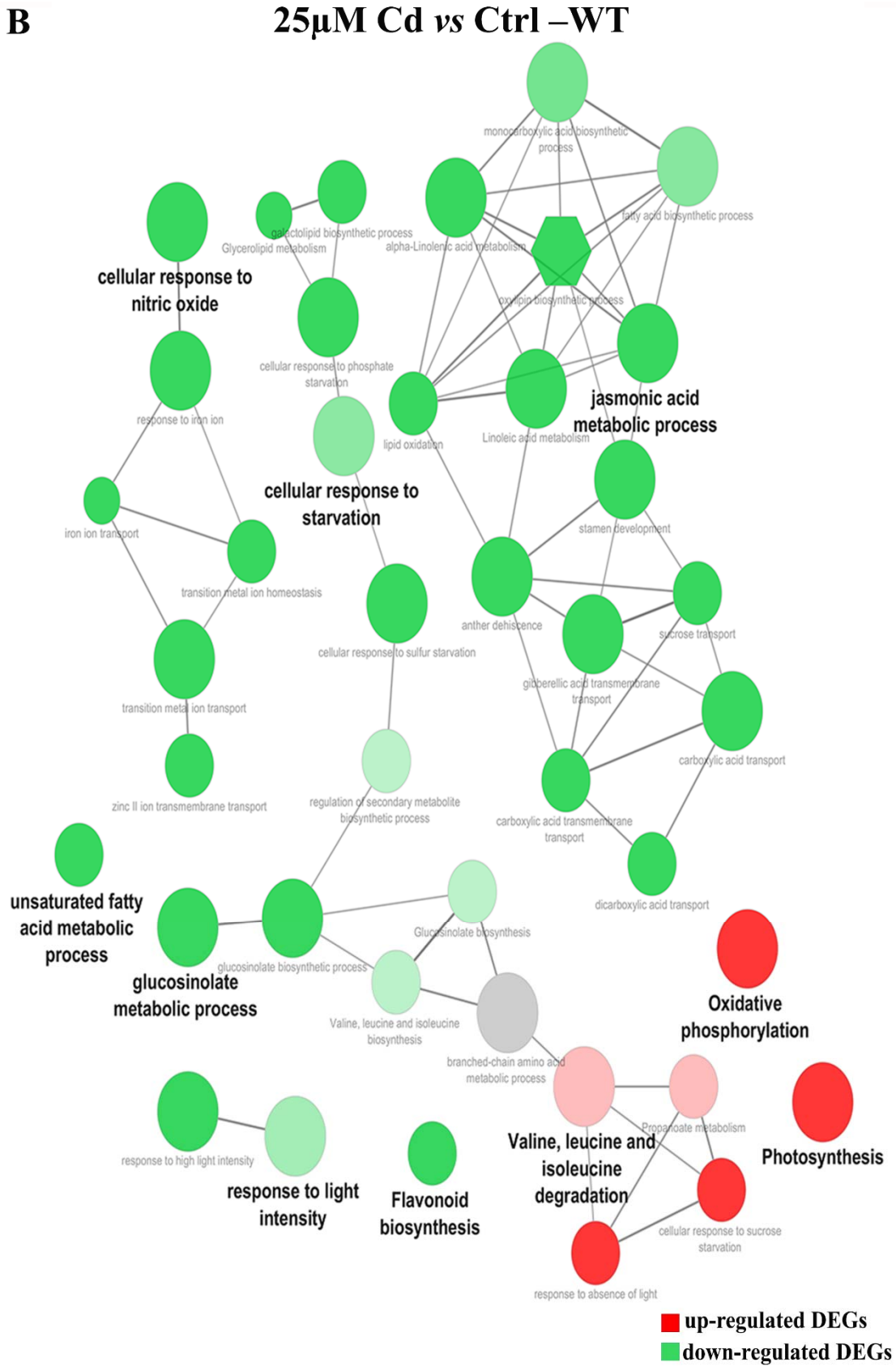
B
25µM Cd *vs* Ctrl –WT
monocarboxylic acid biosynthetic process
fatty acid biosynthetic process
galactolipid biosynthetic process
Glycerolipid metabolism
alpha-Linolenic acid metabolism
oxylipin biosynthetic process
cellular response to nitric oxide
cellular response to phosphate starvation
response to iron ion
jasmonic acid metabolic process
lipid oxidation
Linoleic acid metabolism
cellular response to starvation
iron ion transport
stamen development
transition metal ion homeostasis
anther dehiscence
sucrose transport
cellular response to sulfur starvation
gibberellic acid transmembrane transport
transition metal ion transport
carboxylic acid transport
zinc II ion transmembrane transport
regulation of secondary metabolite biosynthetic process
carboxylic acid transmembrane transport
dicarboxylic acid transport
unsaturated fatty acid metabolic process
Glucosinolate biosynthesis
glucosinolate biosynthetic process
glucosinolate metabolic process
Oxidative phosphorylation
Valine, leucine and isoleucine biosynthesis
branched-chain amino acid metabolic process
Propanoate metabolism
Photosynthesis
response to high light intensity
Valine, leucine and isoleucine degradation
response to light intensity
Flavonoid biosynthesis
cellular response to sucrose starvation
response to absence of light
up-regulated DEGs
down-regulated DEGs

C **50µM Cd *vs* Ctrl –WT**

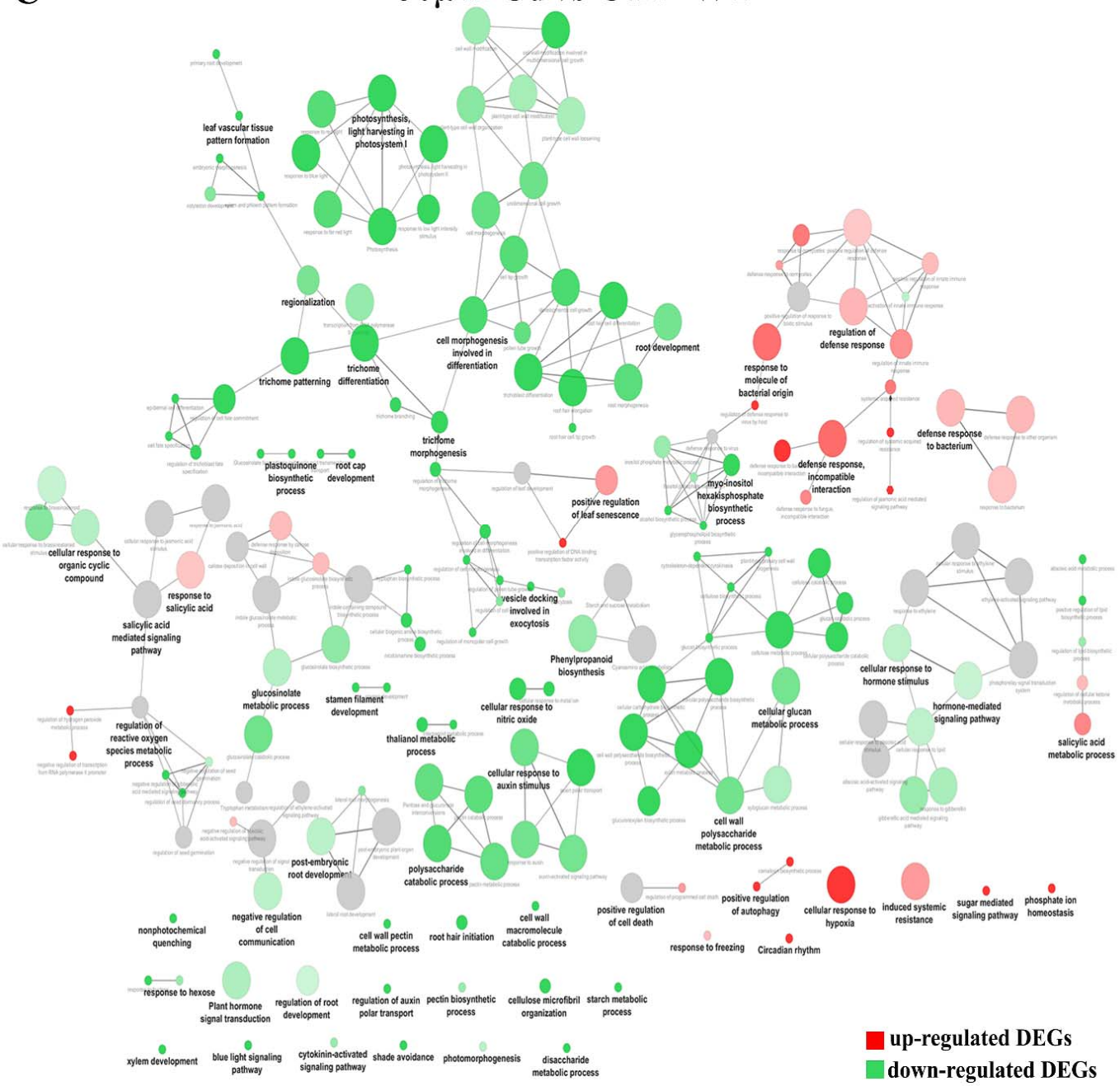

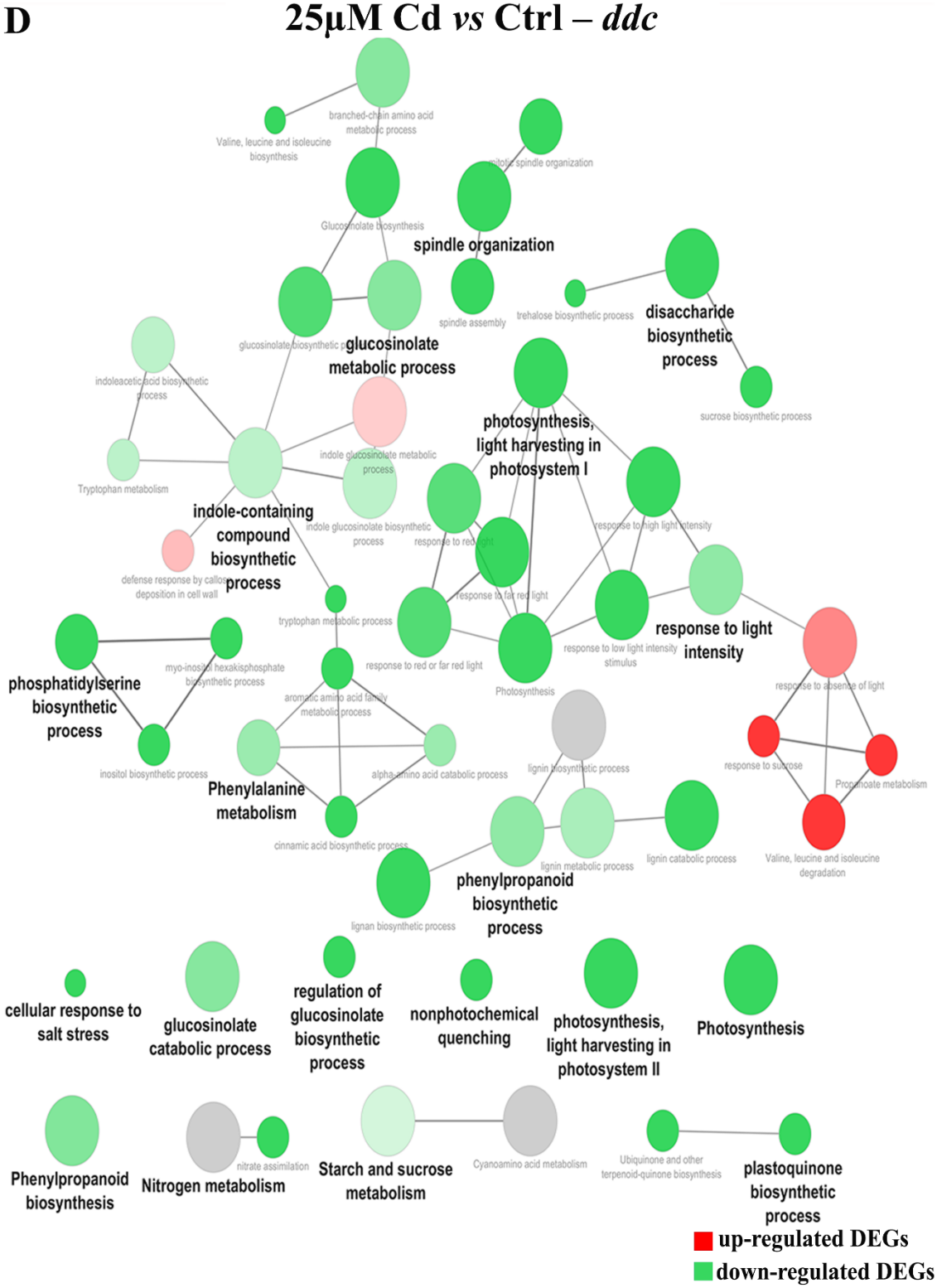
D
25µM Cd vs Ctrl – ddc
branched-chain amino acid metabolic process
Valine, leucine and isoleucine biosynthesis
mitotic spindle organization
Glucosinolate biosynthesis
spindle organization
spindle assembly
trehalose biosynthetic process
disaccharide biosynthetic process
sucrose biosynthetic process
glucosinolate biosynthetic process
glucosinolate metabolic process
indoleacetic acid biosynthetic process
indole glucosinolate metabolic process
photosynthesis, light harvesting in photosystem I
Tryptophan metabolism
indole glucosinolate biosynthetic process
response to high light intensity
response to red light
indole-containing compound biosynthetic process
defense response by callose deposition in cell wall
response to far red light
tryptophan metabolic process
response to low light intensity stimulus
response to light intensity
response to red or far red light
Photosynthesis
response to absence of light
myo-inositol hexakisphosphate biosynthetic process
phosphatidylserine biosynthetic process
aromatic amino acid family metabolic process
lignin biosynthetic process
response to sucrose
Propanoate metabolism
inositol biosynthetic process
alpha-amino acid catabolic process
Phenylalanine metabolism
cinnamic acid biosynthetic process
lignin metabolic process
lignin catabolic process
Valine, leucine and isoleucine degradation
phenylpropanoid biosynthetic process
lignan biosynthetic process
cellular response to salt stress
glucosinolate catabolic process
regulation of glucosinolate biosynthetic process
nonphotochemical quenching
photosynthesis, light harvesting in photosystem II
Photosynthesis
Phenylpropanoid biosynthesis
nitrate assimilation
Nitrogen metabolism
Starch and sucrose metabolism
Cyanoamino acid metabolism
Ubiquinone and other terpenoid-quinone biosynthesis
plastoquinone biosynthetic process
up-regulated DEGs
down-regulated DEGs

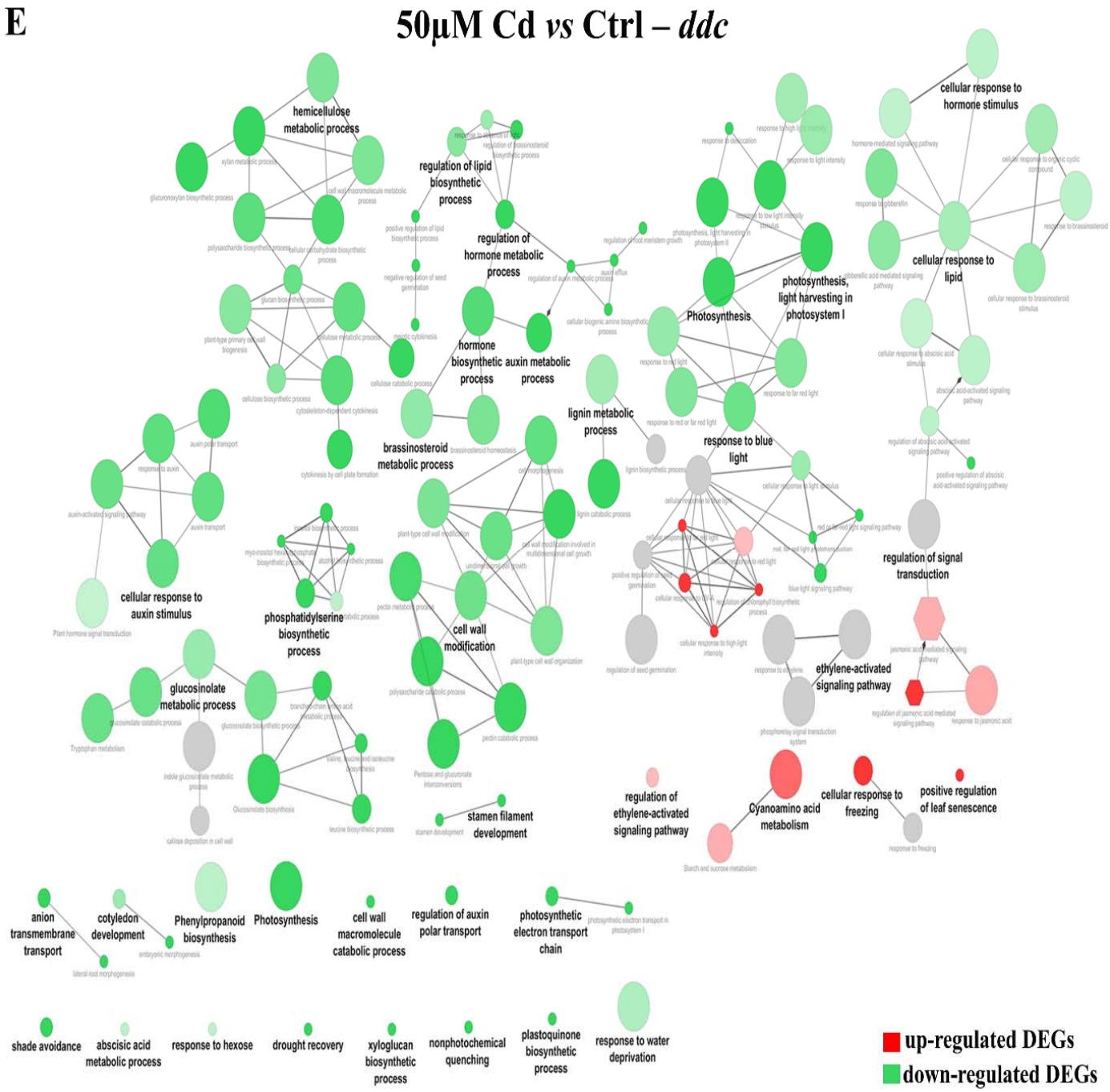
E
50µM Cd vs Ctrl – ddc
hemicellulose metabolic process
regulation of lipid biosynthetic process
regulation of hormone metabolic process
hormone biosynthetic process
auxin metabolic process
brassinosteroid metabolic process
lignin metabolic process
cellular response to auxin stimulus
phosphatidylserine biosynthetic process
cell wall modification
glucosinolate metabolic process
stamen filament development
Photosynthesis
photosynthesis, light harvesting in photosystem I
response to blue light
cellular response to hormone stimulus
cellular response to lipid
regulation of signal transduction
ethylene-activated signaling pathway
regulation of ethylene-activated signaling pathway
Cyanoamino acid metabolism
cellular response to freezing
positive regulation of leaf senescence
anion transmembrane transport
cotyledon development
Phenylpropanoid biosynthesis
Photosynthesis
cell wall macromolecule catabolic process
regulation of auxin polar transport
photosynthetic electron transport chain
shade avoidance
abscisic acid metabolic process
response to hexose
drought recovery
xyloglucan biosynthetic process
nonphotochemical quenching
plastoquinone biosynthetic process
response to water deprivation
up-regulated DEGs
down-regulated DEGs

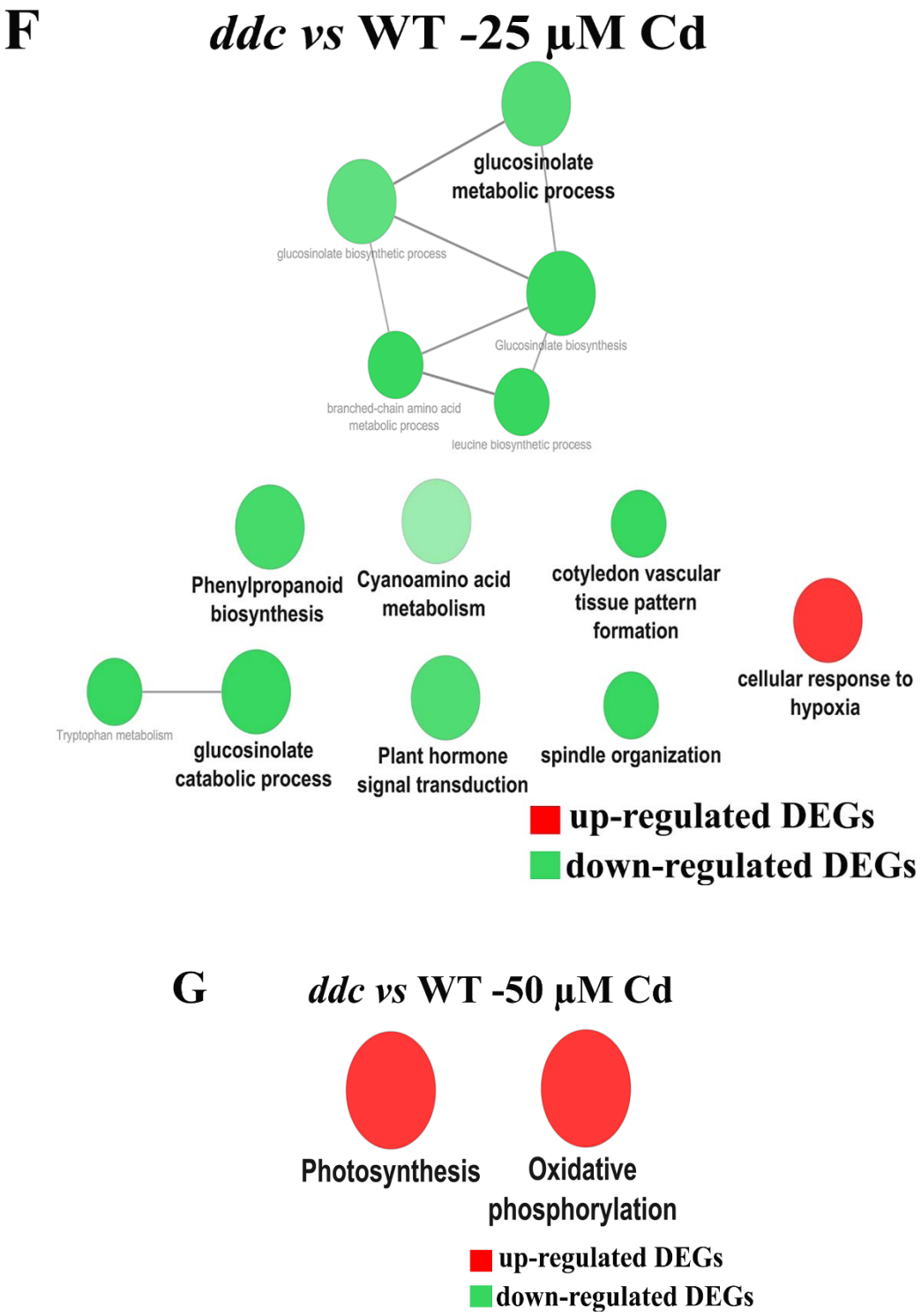

Figure 3.8: Gene Enrichment analysis of the DEGs found in the comparisons **(A)** *ddc vs* WT- Ctrl **(B)** 25 µM Cd *vs* Ctrl –WT, **(C)** 50 µM Cd *vs* Ctrl –WT, **(D)** 25 µM Cd *vs* Ctrl – *ddc*, **(E)** 50 µM Cd *vs* Ctrl – *ddc*, **(F)** *ddc vs* WT -25 µM Cd, **(G)** *ddc vs* WT -50 µM Cd. The analyses were performed by using ClueGO plugin of Cytoscape software (Bindea *et al.,*2009), and the enriched genes were selected on the basis of the calculation of Bonferroni-corrected p-value by using the hypergeometric distribution. The up-regulated genes are shown in red, while the down-regulated ones are shown in green.

On the whole, it was evident that in both *ddc* mutant and WT seedlings the genetic pathways more impacted by Cd treatment were those related to photosynthesis, hormones biosynthesis and signalling and stress response. (Fig. 3.8 A-G). All these pathways are relevant for plant development, suggesting that the differential growth performance of *ddc* mutant and WT plants to Cd stress could be directly or indirectly related to the modulation of these pathways.

In the first instance, in the present work, we analysed in more details genetic pathways related to the different hormone classes, since these signal molecules, beside their role in plant development, are also strongly involved in plant response to stress.

3.3.3 Differential expression of genes involved in hormones metabolism in *ddc* mutant and WT under Cd treatment.

In order to describe and discuss smoothly the obtained results, a brief description of hormones biosynthetic and catabolic pathways will be included as boxes in the sections dedicated to each hormone.

3.3.3.1 Auxin

Box 1

Auxin biosynthetic pathway

Auxin is a critical plant hormone which modulates diverse processes and tropic responses, thus it is indispensable for plant growth. Indole-3-acetic acid (IAA) is the key auxin in most plants (Davies, 2004). Two major pathways for IAA biosynthesis have been proposed in plants: the tryptophan (Trp)-independent and Trp-dependent pathways (Woodward and Bartel, 2005; Chandler, 2009; Normanly, 2010).

IAA Trp-independent pathway is not a major route for IAA biosynthesis and likely its precursors are indole-3-glycerol phosphate or indole. Recently, an important role in this pathway has been payed to a cytosolic indole synthase (INS), which catalyses the conversion of indole-3-glycerol phosphate (IGP) in indole (IND), a putative precursor of IAA in the cytosol (Wang *et al.,*2015) (Fig. B1). However, little is known about the subsequent reactions dealing with IND conversion into IAA (Kasahara, 2016).

Four principal pathways have been proposed for Trp-dependent IAA biosynthetic pathways: (i) the indole-3-pyruvic acid (IPA); (ii) the indole-3-acetaldoxime (IAOX) pathway (iii) the tryptamine (TAM) pathway and the (iv) the indole-3-acetamide (IAM) pathway (Woodward and Bartel, 2005; Pollmann *et al.,*2006; Mano *et al.,*2010; Zhao, 2010) (Fig. B1).

The IPA pathway [Trp → IPA → IAA] is the principal IAA biosynthetic pathway in *A. thaliana*, and also the first complete and universally conserved IAA biosynthetic pathway in plants (reviewed by

Kasahara, 2016). *TAA1/TIR2* gene encodes tryptophan aminotransferase 1 (TAA1), which acts in the first step of the IPA pathway (Stepanova *et al.,*2008; Tao *et al.,*2008; Yamada *et al.,*2009), while YUCCA (YUC) family genes encode flavin-containing monooxygenases (11 in *A. thaliana*, with partial overlapping functions) that catalyse the second and rate-limiting step of the pathway (Mashiguchi *et al.,*2011; Stepanova *et al.,*2011) (Fig. B1).

IAOX pathway [Trp→ IAOx → IAN or IAM → IAA] plays an auxiliary role in IAA biosynthesis in Brassicaceae family (Zhao *et al.,*2002; Sugawara *et al.,*2009; Kong *et al.,*2015; Kasahara, 2016). The conversion from Trp to IAOX is catalysed by cytochrome P450 monooxygenases CYP79B2 and CYP79B3 (Hull *et al.,*2000; Mikkelsen *et al.,*2000; Zhao *et al.,*2002). IAM and indole-3-acetonitrile (IAN) have been proposed as possible IAA precursors and the NITRILASE (NIT) family of enzymes has been proposed to convert IAN to IAA in *A. thaliana* and *Zea mays* (Bartel *et al.,*1994; Kriechbaumer *et al.,*2007) (Fig. B1).

IAA biosynthesis from Trp can also happen through the TAM pathway [Trp → TAM → N-hydroxyl-TAM → IAAld → IAA]. The possible active enzymes in these pathways are tryptophan decarboxylases (TDCs), that can convert Trp to TAM (Woodward and Bartel, 2005; Mano and Nemoto, 2012) and aldehyde oxidases (AAO), which catalyse the conversion of IAAld to IAA (Sekimoto *et al.,*1997; Seo *et al.,*1998) (Fig. B1). However, until now there are not enough evidences that confirm the role of these enzymes in IAA biosynthesis (Kasahara, 2016).

Finally, the IAM pathway [Trp → IAM → IAA] is the last proposed pathway for IAA biosynthesis in plants. Although in *A. thaliana* and *Nicotiana tabacum* AMIDASE 1 (AMI1) is capable to convert IAM to IAA *in vitro* (Nemoto *et al.,*2008; Mano and Nemoto, 2012), no direct evidence of its role in IAA biosynthesis has been yet found (Kasahara, 2016) (Fig. B1).

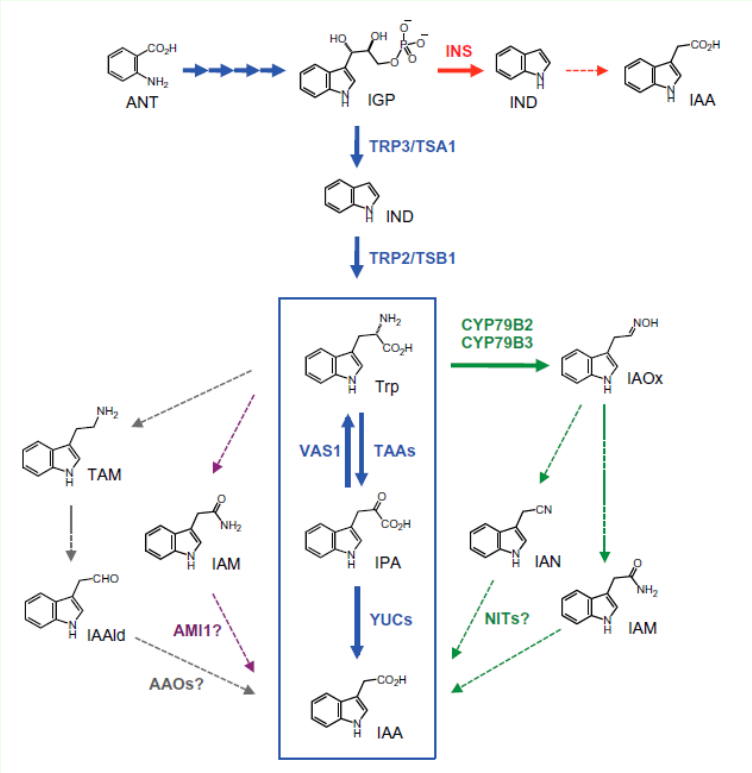

Figure B1: IAA biosynthetic pathways in *A. thaliana*. The Trp-independent pathway is shown in red, the common Trp biosynthesis and IPA pathway (in the box) are shown in blue, the IAOx pathway in *A. thaliana* is shown in green, the IAM pathway is shown in purple, the TAM pathway is shown in gray. Characterized enzymatic steps are in bold typeface. Enzymatic steps to be clarified are shown by dashed arrows. TRP3/TSA1: Trp synthase α-subunit and TRP2/TSB1: Trp synthase β-subunit (Kasahara, 2016).

Principal auxin conjugation pathways

In *A. thaliana*, IAA is present at 90% as amide linkages, approximately 10% as ester-linked conjugates and approximately 1 % as free IAA (Normanly *et al.,*1993; Tam *et al.,*2000), while Me-IAA represents a small, although important, proportion in the total IAA pool (Abbas *et al.,*2018). While glycosylation inactivates IAA, the conjugate forms IAA–Ala and IAA–Leu function in supplying free IAA (Östin *et al.,*1998; Barratt *et al.,*1999), whereas IAA–Asp and IAA–Glu have a role in IAA catabolism (Östin *et al.,*1998). The enzymes that conjugate IAA to amino acids are encoded by members of the *GH3* family of auxin-induced genes (Staswick *et al.,*2002; Staswick and Tiryaki, 2004; Kasahara, 2016). IAA methylation is catalysed by an IAA carboxyl methyltransferase (IAMT).

Concerning the auxin biosynthetic pathways (Box 1, Fig. B1), transcriptomic data evidenced that under Ctrl condition there were no differences between *ddc* mutant and WT (comparison ***ddc vs* WT- Ctrl)** (Fig. 3.9 A). Moreover, data also showed that Cd exposition determined a down-regulation of IPA genetic pathway and an up-regulation of the IAOX pathway in both mutant and WT, although in the latter such differences were observed only under 50 µM Cd (comparisons: **25 µM Cd *vs* Ctrl – WT; 50 µM Cd *vs* Ctrl – WT; 25 µM Cd *vs* Ctrl – *ddc*; 50 µM Cd *vs* Ctrl – *ddc)*** (Fig. 3.9 B, C). In particular, under 25 µM Cd, *ddc* mutant presented:

- a slight down-regulation of the IPA pathway related to the down-regulation of *TAA1* and *YUC5* genes;
- an overall up-regulation of the IAOX genetic pathway mainly related to the up-regulation of *CYP71A13* and *NIT2*, while *CYP79B3* was down-regulated and *CYP72B2*, which acts redundantly with *CYP79B3,* didn't undergo to any differential expression (comparison **25 µM Cd *vs* Ctrl – *ddc)*** (Fig. 3.9 B).

When comparing the effect of 25 µM Cd treatment on *ddc* mutant *vs* WT, the only significant difference involved *TAA1* gene, whose expression was down-regulated in the mutant (comparison ***ddc vs* WT -25 µM Cd)** (Fig. 3.9 B).

Interestingly, under 50 µM Cd exposure *ddc* mutant and WT underwent to a similar alteration of their expression profile consisting in:

- a down-regulation of IPA genetic pathway related to a down-expression of *YUC2* in both samples and of *YUC5* and *YUC9* in *ddc* and WT, respectively (Fig. 3.9 C);
- a strong up-regulation of IAOX pathway related to the up-regulation of *CYP71A12, CYP71A13, NIT2* and *NIT4,* while only *CYP71A16* was down-regulated (comparisons: **50 µM Cd *vs* Ctrl –WT*;* 50 µM Cd *vs* Ctrl – *ddc***) (Fig. 3.9 C).

As expected, under 50 µM Cd no differences were found between *ddc* and WT (comparison ***ddc vs* WT -50 µM Cd)** (Fig. 3.9 C).

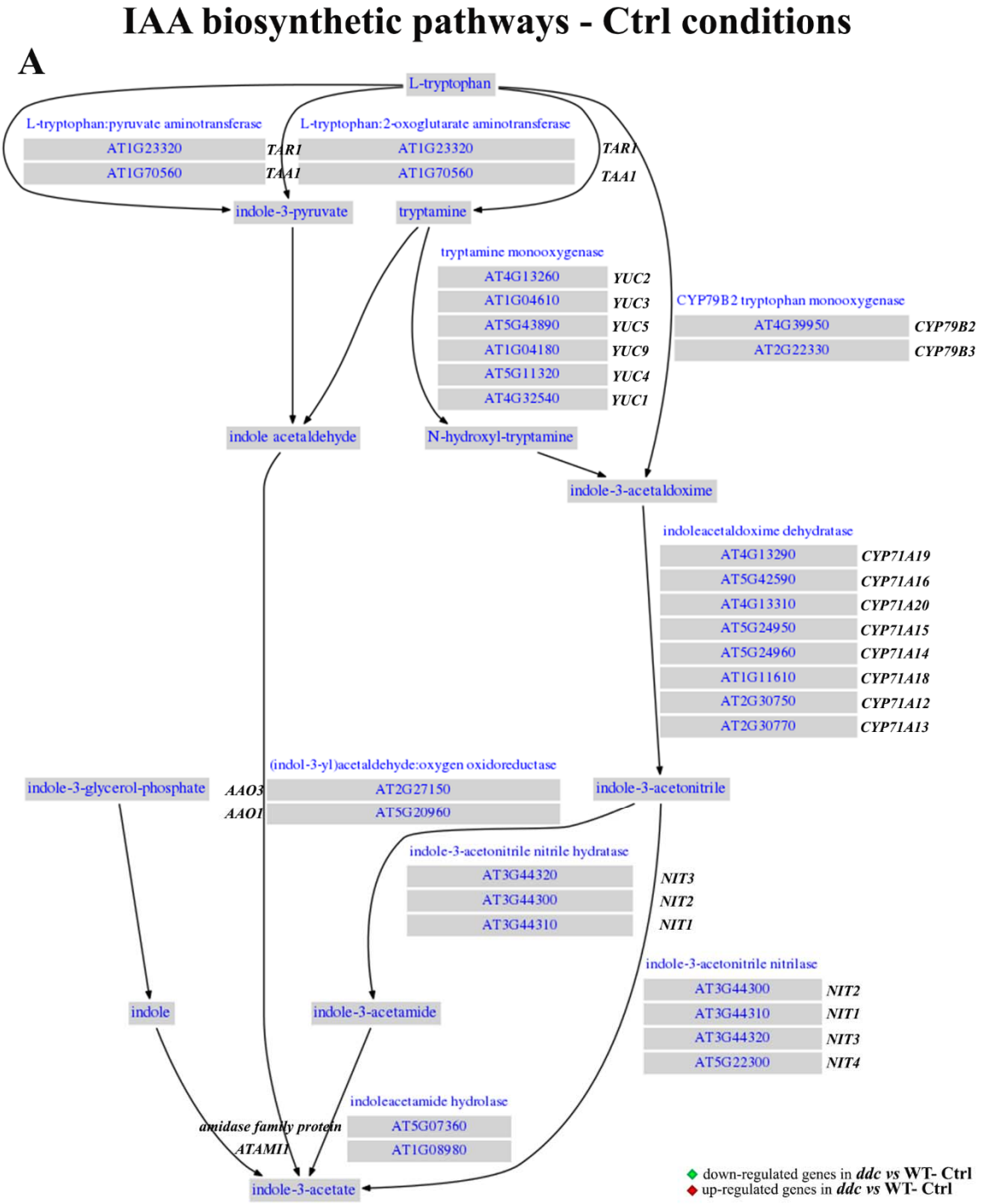
IAA biosynthetic pathways - Ctrl conditions
A
L-tryptophan
L-tryptophan:pyruvate aminotransferase
AT1G23320
TAR1
AT1G70560
TAA1
L-tryptophan:2-oxoglutarate aminotransferase
AT1G23320
TAR1
AT1G70560
TAA1
indole-3-pyruvate
tryptamine
tryptamine monooxygenase
AT4G13260
YUC2
AT1G04610
YUC3
AT5G43890
YUC5
AT1G04180
YUC9
AT5G11320
YUC4
AT4G32540
YUC1
CYP79B2 tryptophan monooxygenase
AT4G39950
CYP79B2
AT2G22330
CYP79B3
indole acetaldehyde
N-hydroxyl-tryptamine
indole-3-acetaldoxime
indoleacetaldoxime dehydratase
AT4G13290
CYP71A19
AT5G42590
CYP71A16
AT4G13310
CYP71A20
AT5G24950
CYP71A15
AT5G24960
CYP71A14
AT1G11610
CYP71A18
AT2G30750
CYP71A12
AT2G30770
CYP71A13
(indol-3-yl)acetaldehyde:oxygen oxidoreductase
indole-3-glycerol-phosphate
AAO3
AT2G27150
AAO1
AT5G20960
indole-3-acetonitrile
indole-3-acetonitrile nitrile hydratase
AT3G44320
NIT3
AT3G44300
NIT2
AT3G44310
NIT1
indole-3-acetonitrile nitrilase
AT3G44300
NIT2
AT3G44310
NIT1
AT3G44320
NIT3
AT5G22300
NIT4
indole
indole-3-acetamide
indoleacetamide hydrolase
amidase family protein
AT5G07360
ATAMI1
AT1G08980
indole-3-acetate
down-regulated genes in ddc vs WT- Ctrl
up-regulated genes in ddc vs WT- Ctrl

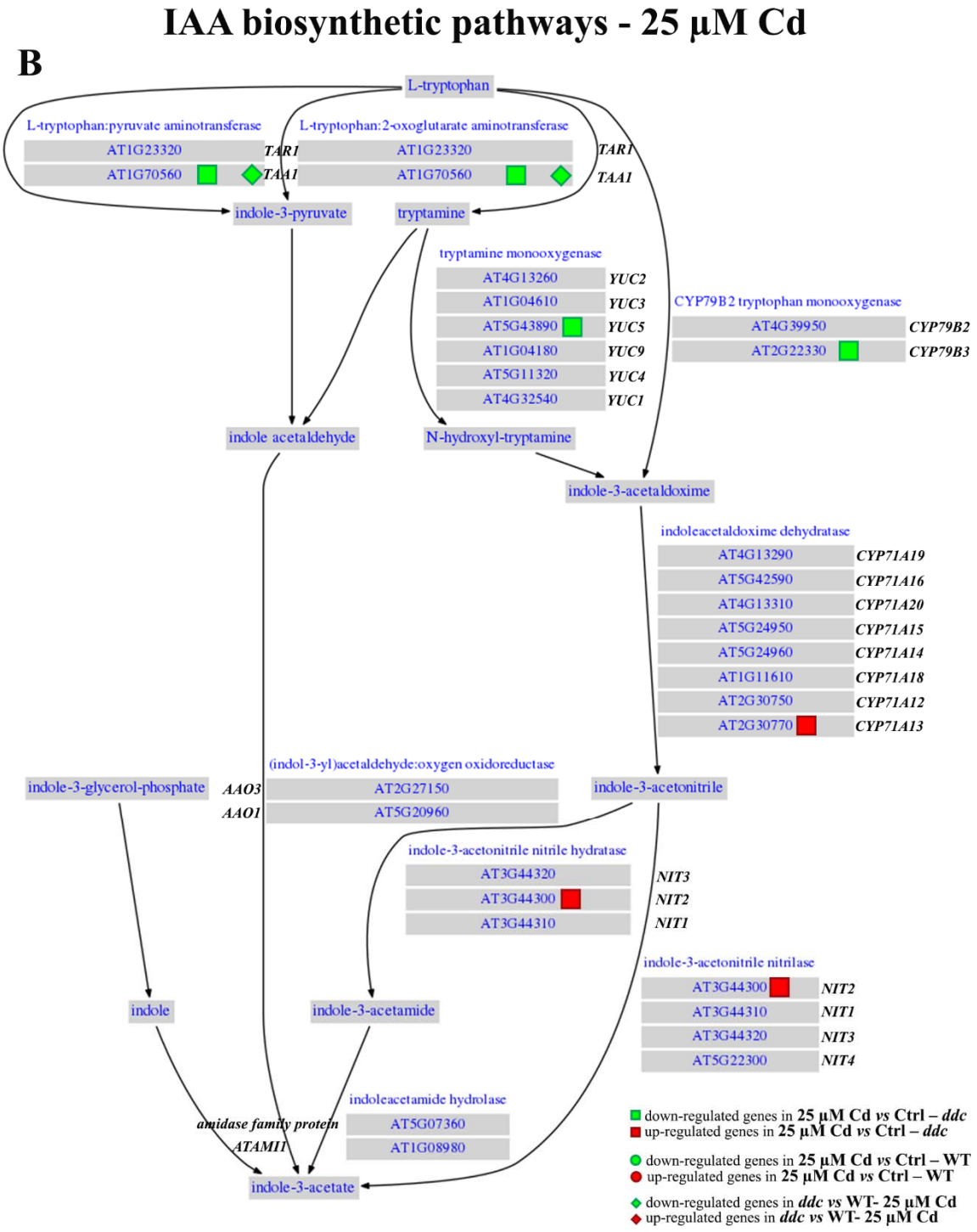
IAA biosynthetic pathways - 25 µM Cd
B
L-tryptophan
L-tryptophan:pyruvate aminotransferase
AT1G23320
TAR1
AT1G70560
TAA1
L-tryptophan:2-oxoglutarate aminotransferase
AT1G23320
TAR1
AT1G70560
TAA1
indole-3-pyruvate
tryptamine
tryptamine monooxygenase
AT4G13260
YUC2
AT1G04610
YUC3
AT5G43890
YUC5
AT1G04180
YUC9
AT5G11320
YUC4
AT4G32540
YUC1
CYP79B2 tryptophan monooxygenase
AT4G39950
CYP79B2
AT2G22330
CYP79B3
indole acetaldehyde
N-hydroxyl-tryptamine
indole-3-acetaldoxime
indoleacetaldoxime dehydratase
AT4G13290
CYP71A19
AT5G42590
CYP71A16
AT4G13310
CYP71A20
AT5G24950
CYP71A15
AT5G24960
CYP71A14
AT1G11610
CYP71A18
AT2G30750
CYP71A12
AT2G30770
CYP71A13
(indol-3-yl)acetaldehyde:oxygen oxidoreductase
indole-3-glycerol-phosphate
AAO3
AT2G27150
AAO1
AT5G20960
indole-3-acetonitrile
indole-3-acetonitrile nitrile hydratase
AT3G44320
NIT3
AT3G44300
NIT2
AT3G44310
NIT1
indole-3-acetonitrile nitrilase
AT3G44300
NIT2
AT3G44310
NIT1
AT3G44320
NIT3
AT5G22300
NIT4
indole
indole-3-acetamide
indoleacetamide hydrolase
amidase family protein
ATAMI1
AT5G07360
AT1G08980
indole-3-acetate
down-regulated genes in 25 µM Cd vs Ctrl – ddc
up-regulated genes in 25 µM Cd vs Ctrl – ddc
down-regulated genes in 25 µM Cd vs Ctrl – WT
up-regulated genes in 25 µM Cd vs Ctrl – WT
down-regulated genes in ddc vs WT- 25 µM Cd
up-regulated genes in ddc vs WT- 25 µM Cd

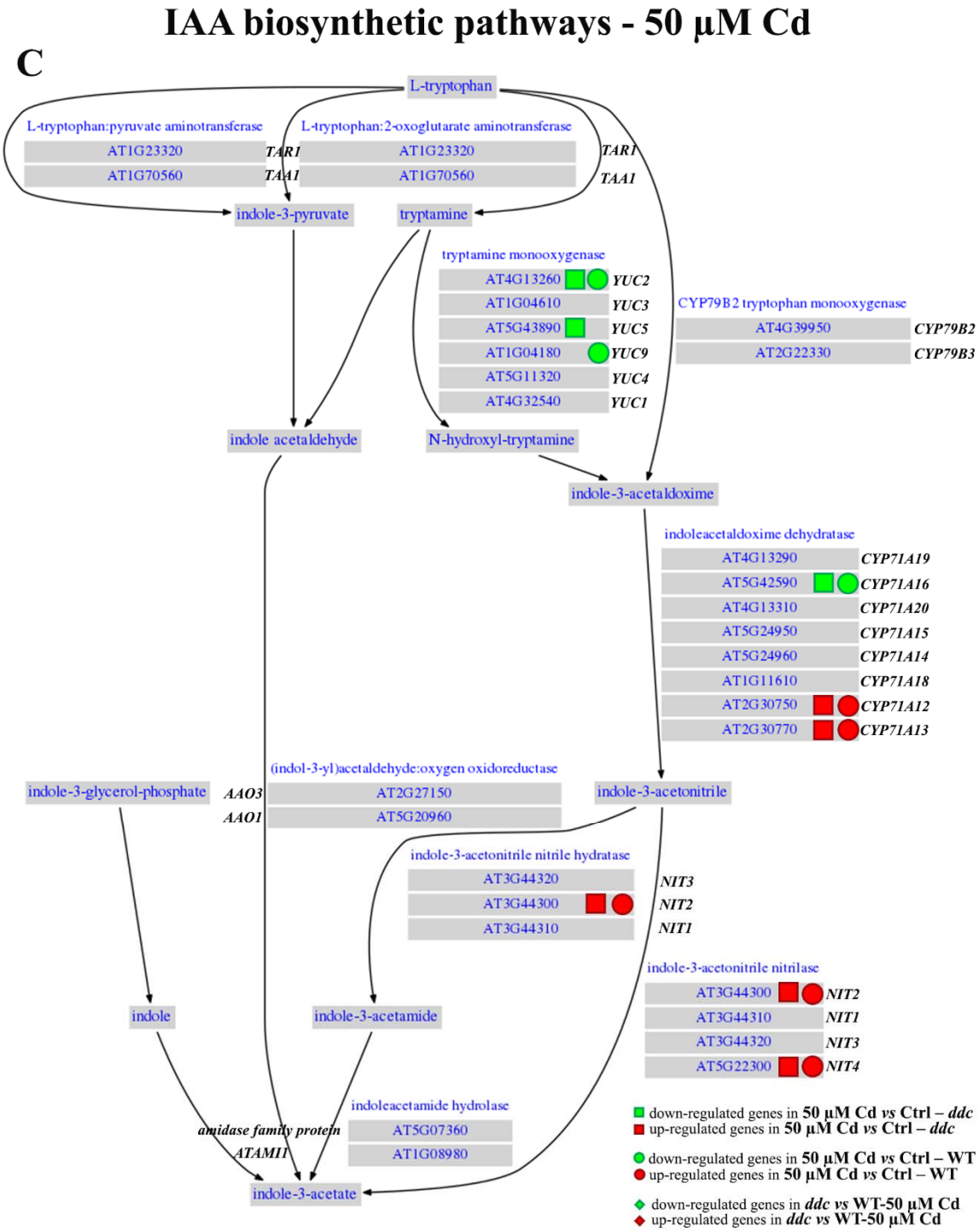

Figure 3.9: Genes differentially expressed (DEGs) along the pathway of auxin biosynthesis in *ddc* and WT seedlings identified through a transcriptomic approach. Seedlings grown **(A)** in Ctrl condition, **(B)** under treatment with 25 µM Cd and **(C)** 50 µM Cd.

In addition to biosynthesis, auxin homeostasis /level is also dependent on several other processes including both oxidative degradation (Zhao *et al.*,2013) and amino acid,

sugar or peptides conjugation (Jackson *et al.,*2002; Staswick *et al.,*2005; Tognetti *et al.,*2010) and methylation (Abbas *et al.,*2018).

Transcriptomic data dealing with the genetic pathway involved in auxin conjugation (Box 1) showed that under Ctrl condition it wasn't differentially regulated in the *ddc* mutant compared to the WT (***ddc vs* WT- Ctrl)** (Fig. 3.10 A; Fig. 3.11 A). Data also showed that, when exposed to 25 µM Cd treatment, WT didn't undergo to any significant difference concerning indole-3-acetyl-amino acid production, while a slightly down-regulation of the methyl-indole-3-acetate production, involving *MES18* gene was observed (**25 µM Cd *vs* Ctrl –WT)** (Fig. 3.10 B; Fig. 3.11 B). By contrast, in *ddc* mutant 25 µM Cd concentration was found to induce a strong down-regulation of genes related to both auxin conjugates production (*GH3.3, GH3.14,* and *YDK1*) and methylation (*MES7* and *MES17),* with the exception of *MES16* which was up-regulated (**25 µM Cd *vs* Ctrl – *ddc)*** (Fig. 3.10 B; Fig. 3.11 B).In addition, transcriptomic data also showed that under 25 µM Cd treatment a down-regulation of genes involved both in auxin conjugates production (*GH3.3* and *YDK1*) and auxin methylation (*MES7* and *MES17)* occurred in *ddc* mutant compared to the WT (***ddc vs* WT -25 µM Cd)** (Fig. 3.10 B; Fig. 3.11 B)

Under 50 µM Cd, differential expression was observed only for genes involved in auxin methylation, such as *IAM1* and *MES16,* which were down-regulated and up-regulated, respectively (comparisons: **50 µM Cd *vs* Ctrl –WT; 50 µM Cd *vs* Ctrl – *ddc)*** (Fig. 3.11 C). As expected, no significative differences were found when comparing *ddc* mutant *vs* WT under 50 µM Cd (comparison ***ddc vs* WT -50 µM Cd)** (Fig. 3.11 C).

Globally, results dealing with auxin-related genetic pathways showed that Cd impacted on IAA biosynthetic pathway in a quite similar way in *ddc* and WT, inducing a global down-regulation of the IPA pathway and an up-regulation of IAOX pathway. Notwithstanding, only in *ddc* mutant this effect was already evident at 25 µM Cd concentration. Moreover, genetic pathways related to the production of IAA amino acid conjugates was affected by Cd treatment only in *ddc* mutant (Fig. 3.10; Fig. 3.11).

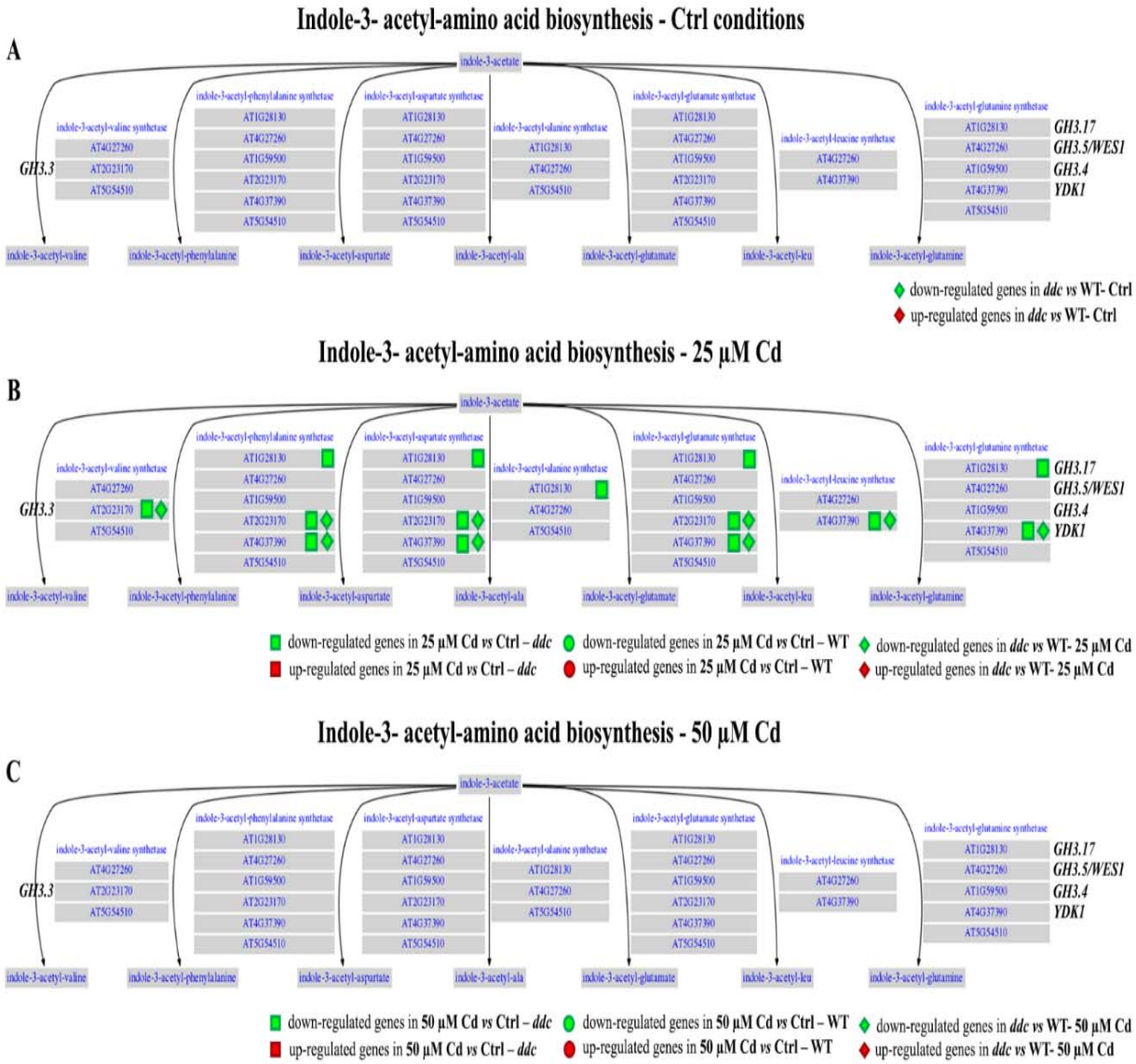

Figure 3.10: Gene expression analysis, performed through a transcriptomic approach, of DEGs involved in auxin conjugation (indole-3-acetyl-amino acid biosynthesis) in *ddc* and WT. Seedling grown **(A)** in Ctrl condition, **(B)** under treatment with 25 µM Cd and **(C)** 50 µM Cd.

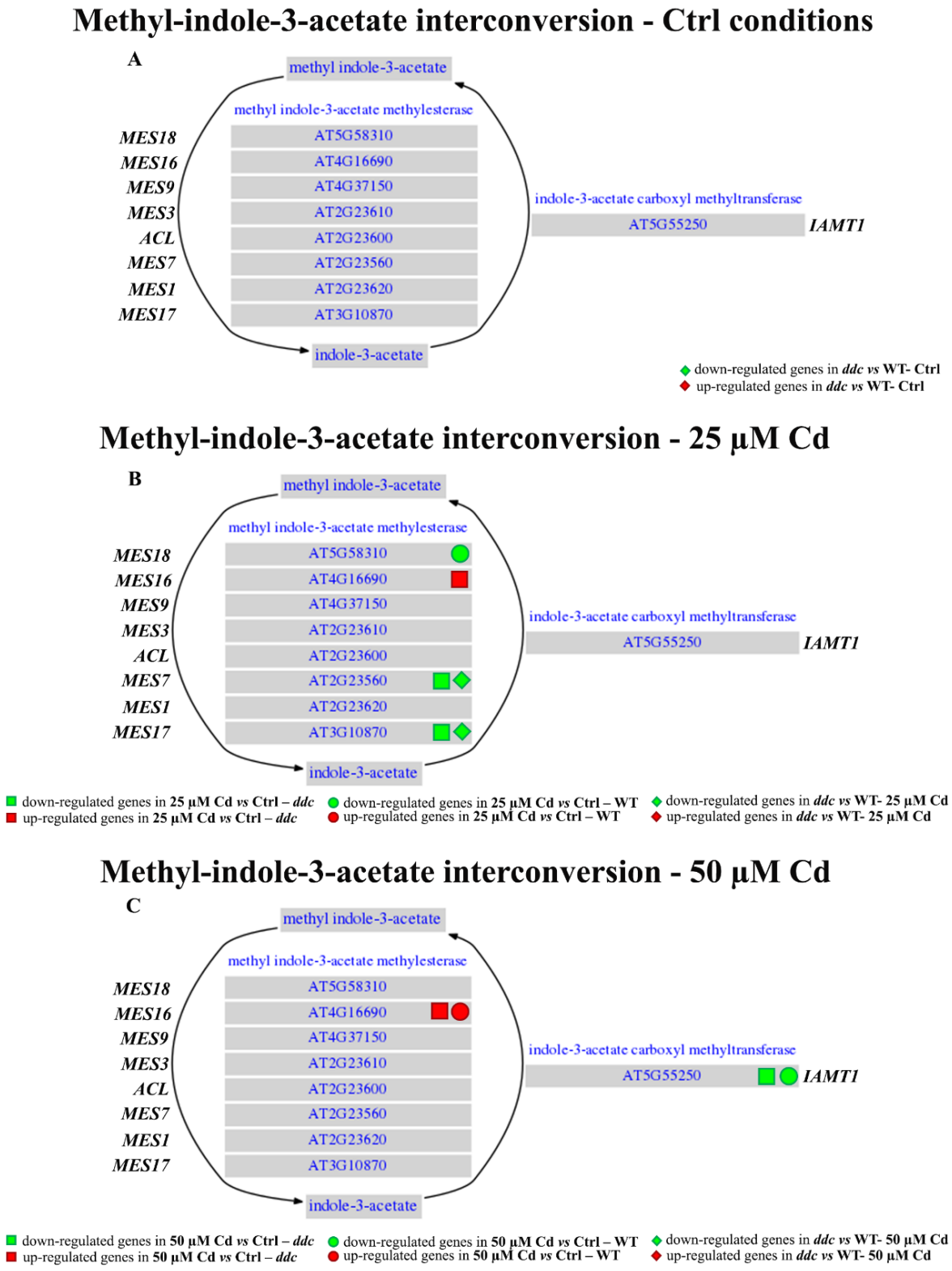

Figure 3.11: Gene expression analysis, performed through a transcriptomic approach, of DEGs involved in auxin conjugation (methyl-indole-3-acetate interconversion) in *ddc* and WT. Seedling grown **(A)** in Ctrl condition, **(B)** under treatment with 25 µM Cd and **(C)** 50 µM Cd.

3.3.3.2 Cytokinins

Box 2

Cytokinins biosynthetic pathways

Cytokinins (CKs) are involved in many aspects of plant growth and development, promoting cell division and differentiation. Moreover, they play an important role in biotic and abiotic stress response (Argueso *et al.,*2012).

CKs are adenine derivatives that carry an isoprene-derived or an aromatic side chain at the N^6 position of the purine (Feng *et al.,*2017). These hormones are classified, based on the N^6-chain structure, in aromatic CKs, that present a benzyl or hydroxybenzyl group at the N^6-position and isoprenoid CKs, which have an isopentenyl side chain at the N^6-position (Martin *et al.,*2001; Mok and Mok, 2001).

Isoprenoid CKs are the most represented in plant tissue and include: N^6-(Δ2-isopentenyl)-adenine (iP); *trans*-zeatin (*t*Z), the most abundant active cytokinin in *A. thaliana*; *cis*-zeatin (*cZ*) whose activity is mostly limited (Spichal *et al.,*2004; Romanov *et al.,*2006; Heyl *et al.,*2012; Kieber and Schaller, 2013, 2014).

This CKs class can be synthetized through two different pathways: the tRNA degradation pathway and the *de novo* pathway.

In the tRNA degradation pathway, tRNA isopentenyltransferase (tRNA-IPT) transfers an isopentenyl unit from dimethylallyl diphosphate (DMAPP) to the N^6 of the nucleotide adjacent to the 3′-end of the anticodon in the tRNA to produce *cZ* (Fig. B2). In *A. thaliana*, tRNA IPTs involved in this pathway are encoded by *AtIPT2* and *AtIPT9* genes (Miyawaki *et al.,*2006; Sakamoto *et al.,*2006).

In *de novo* pathway, adenylate isopentenyltransferase (*IPT*) enzyme family catalyses the first and rate-limiting reaction of isoprenoid CKs biosynthesis (Taya *et al.,*1978), by transferring a prenyl moiety from dimethylallyl diphosphate (DMAPP) to the N^6 position of ATP, ADP, or, rarely in *A. thaliana*, AMP, to produce iP riboside 5′-tri-, di-, or monophosphate (iPRTP, iPRDP, or iPRMP), respectively (Fig. B2). iPRTP, iPRDP and iPRMP can be subsequently converted to *t*Z by CYP735A cytochrome P450 enzymes, while nucleosides are directly converted into the free CKs base by the LONELY GUY (LOG) family of enzymes (Kurakawa *et al.,*2007) (Fig. B2).

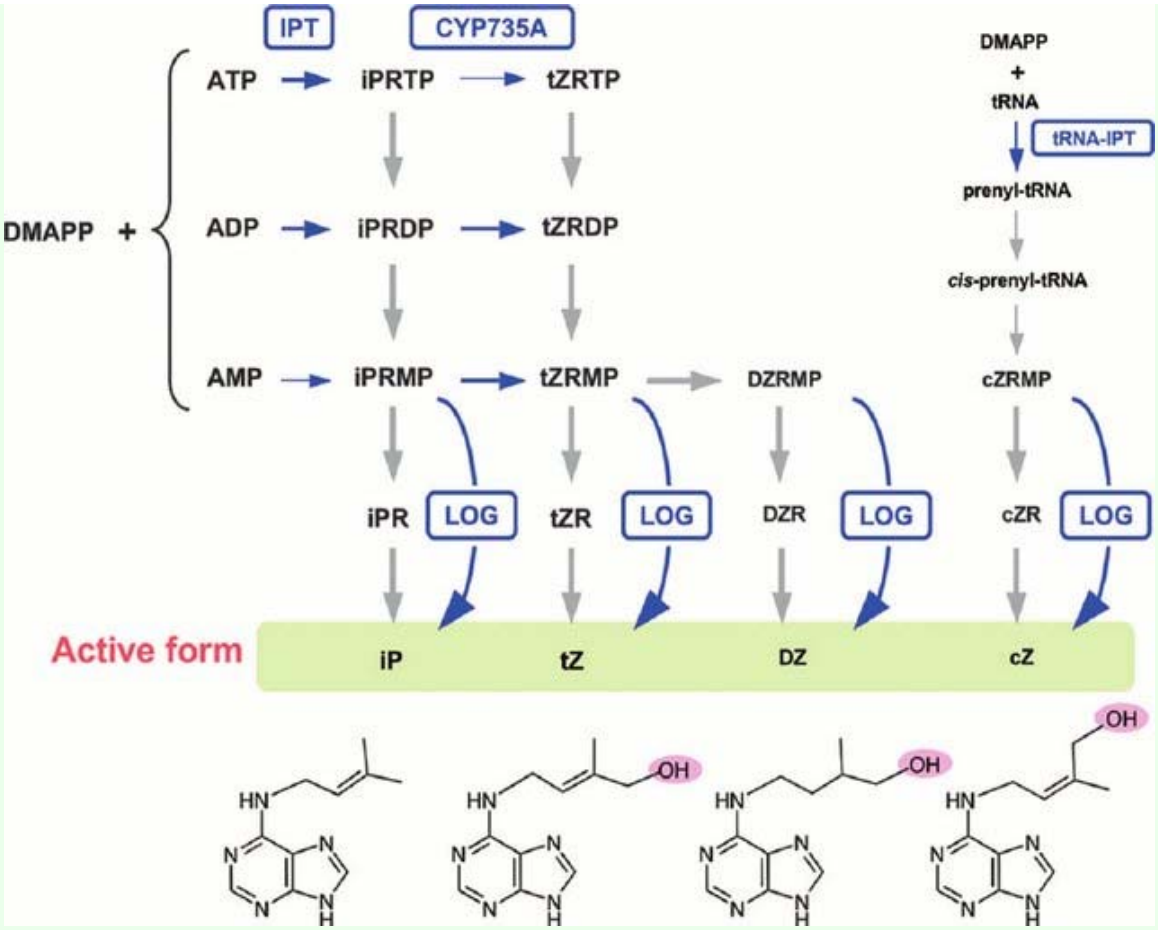

Figure B2: Cytokinin biosynthesis in higher plants. In the *de novo* pathway, IPT catalyses the first reaction of isoprenoid CKs biosynthesis to produce iPRTP, iPRDP, or iPRMP by transferring a prenyl moiety from DMAPP to ATP, ADP, or AMP. iPRTP, iPRDP, or iPRMP can be subsequently converted to *tZ* by CYP735A, while nucleosides are directly converted into the free CKs by LOG. In the tRNA degradation pathway, tRNA-IPT transfers an isopentenyl unit from DMAPP to the N^6 of the nucleotide adjacent to the 3′-end of the anticodon in the tRNA to produce *cZ* (Hirose *et al.,*2008).

Cytokinins degradation and conjugation pathways

Cytokinin cleavage is carried out by cytokinin oxidase/dehydrogenase enzymes (CKXs), that irreversibly degrade CKs (Feng *et al.,*2017). CKs glycosylation is distinguished in *N*-glycosylation and *O*-glucosylation. *N*-glycosylation occurs on the nitrogens at positions N3 N7 or N9 of the purine ring and in *A. thaliana* it is catalysed by UGT76C1 and UGT76C2 enzymes (Hou *et al.,*2004; Wang *et al.,*2011). Since *N*-glucosyl hydrolases have not been identified, this mechanism is thought to inactivate CKs excess in a definitive way (Feng *et al.,*2017). *O*-glucosylation is catalysed by zeatin *O*-glucosyltransferases (UGTs) (Dixon *et al.,*1989; Veach *et al.,*2003) and UGT85A1 showed to be particularly active in this pathway (Jin *et al.,*2013). Inactive *tZ-O*-glucoside serves as stable storage and transport form of the hormone, that can be re-converted in active CKs by β-glucosidases (Brzobohaty *et al.,*1993).

Concerning genes involved in CKs biosynthesis (Box 2, Fig. B2) as a general picture, no significative differences were evidenced by transcriptome analysis in most of the comparisons. The only exception deals with the down-regulation of *IPT3* and *IPT5* in WT plants under 50 μM Cd treatment (comparison **50 μM Cd *vs* Ctrl –WT)** (Fig. 3.12 C). Note that these genes catalyse a rate-limiting reaction along the biosynthetic pathway of *trans*-zeatin, which is the most relevant active cytokinin.

A

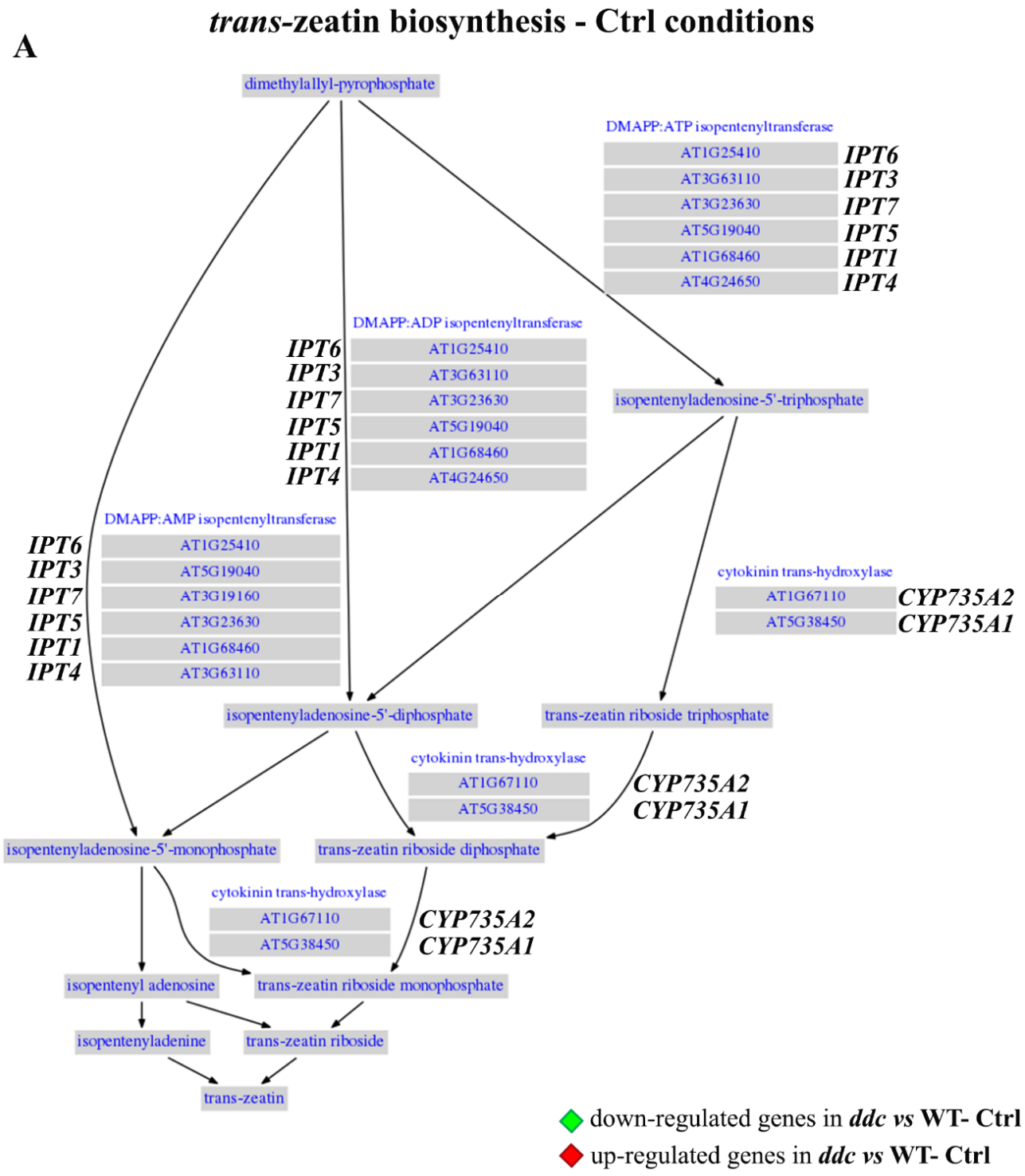
trans-zeatin biosynthesis - Ctrl conditions
dimethylallyl-pyrophosphate
DMAPP:ATP isopentenyltransferase
AT1G25410 IPT6
AT3G63110 IPT3
AT3G23630 IPT7
AT5G19040 IPT5
AT1G68460 IPT1
AT4G24650 IPT4
DMAPP:ADP isopentenyltransferase
IPT6 AT1G25410
IPT3 AT3G63110
IPT7 AT3G23630
IPT5 AT5G19040
IPT1 AT1G68460
IPT4 AT4G24650
isopentenyladenosine-5'-triphosphate
DMAPP:AMP isopentenyltransferase
IPT6 AT1G25410
IPT3 AT5G19040
IPT7 AT3G19160
IPT5 AT3G23630
IPT1 AT1G68460
IPT4 AT3G63110
cytokinin trans-hydroxylase
AT1G67110 CYP735A2
AT5G38450 CYP735A1
isopentenyladenosine-5'-diphosphate
trans-zeatin riboside triphosphate
cytokinin trans-hydroxylase
AT1G67110
AT5G38450
CYP735A2
CYP735A1
isopentenyladenosine-5'-monophosphate
trans-zeatin riboside diphosphate
cytokinin trans-hydroxylase
AT1G67110
AT5G38450
CYP735A2
CYP735A1
isopentenyl adenosine
trans-zeatin riboside monophosphate
isopentenyladenine
trans-zeatin riboside
trans-zeatin
down-regulated genes in ddc vs WT- Ctrl
up-regulated genes in ddc vs WT- Ctrl

B

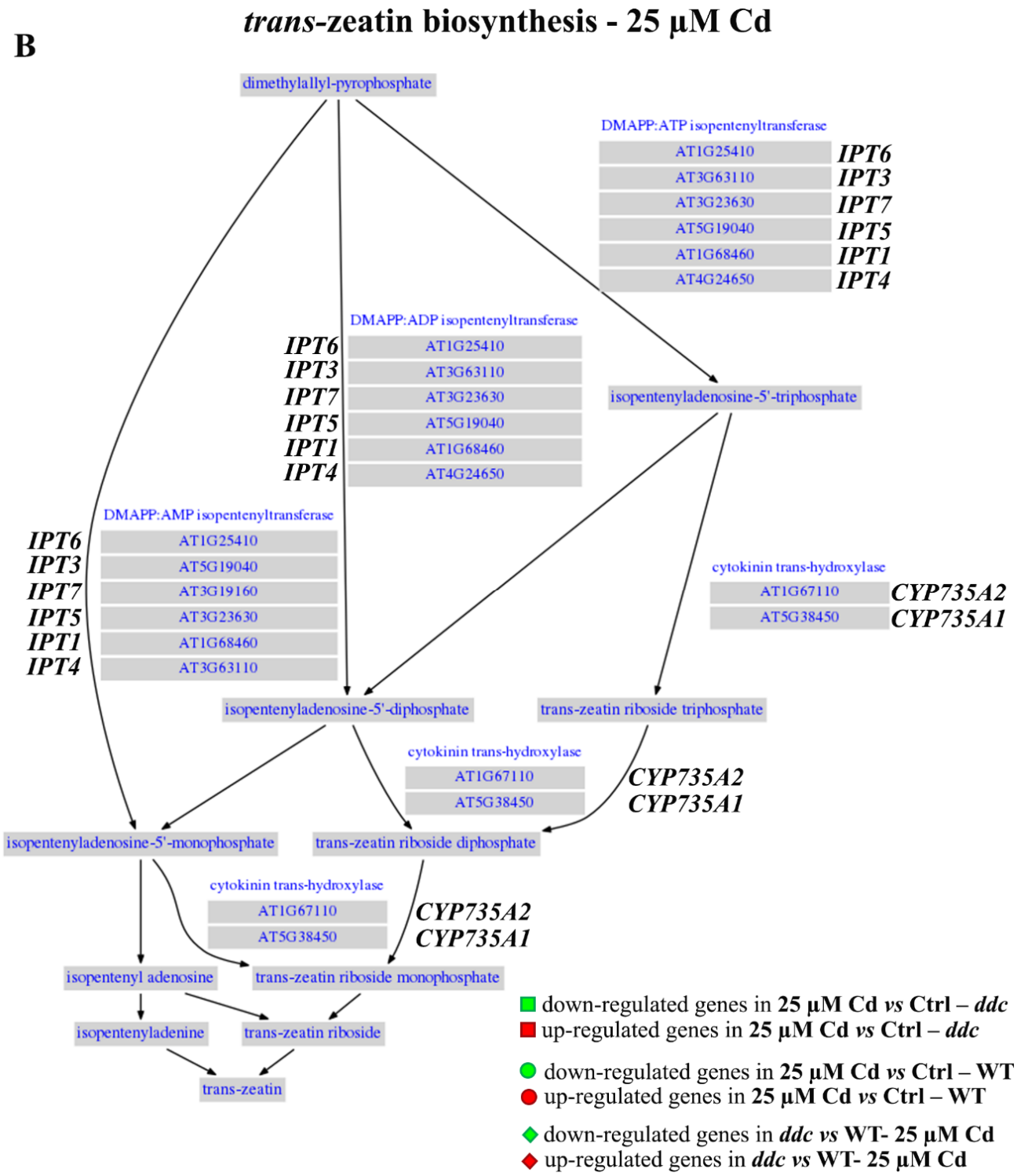
trans-zeatin biosynthesis - 25 µM Cd
dimethylallyl-pyrophosphate
DMAPP:ATP isopentenyltransferase
AT1G25410 IPT6
AT3G63110 IPT3
AT3G23630 IPT7
AT5G19040 IPT5
AT1G68460 IPT1
AT4G24650 IPT4
DMAPP:ADP isopentenyltransferase
IPT6 AT1G25410
IPT3 AT3G63110
IPT7 AT3G23630
IPT5 AT5G19040
IPT1 AT1G68460
IPT4 AT4G24650
isopentenyladenosine-5'-triphosphate
DMAPP:AMP isopentenyltransferase
IPT6 AT1G25410
IPT3 AT5G19040
IPT7 AT3G19160
IPT5 AT3G23630
IPT1 AT1G68460
IPT4 AT3G63110
cytokinin trans-hydroxylase
AT1G67110 CYP735A2
AT5G38450 CYP735A1
isopentenyladenosine-5'-diphosphate
trans-zeatin riboside triphosphate
cytokinin trans-hydroxylase
AT1G67110
AT5G38450
CYP735A2
CYP735A1
isopentenyladenosine-5'-monophosphate
trans-zeatin riboside diphosphate
cytokinin trans-hydroxylase
AT1G67110
AT5G38450
CYP735A2
CYP735A1
isopentenyl adenosine
trans-zeatin riboside monophosphate
isopentenyladenine
trans-zeatin riboside
trans-zeatin
down-regulated genes in 25 µM Cd vs Ctrl – ddc
up-regulated genes in 25 µM Cd vs Ctrl – ddc
down-regulated genes in 25 µM Cd vs Ctrl – WT
up-regulated genes in 25 µM Cd vs Ctrl – WT
down-regulated genes in ddc vs WT- 25 µM Cd
up-regulated genes in ddc vs WT- 25 µM Cd

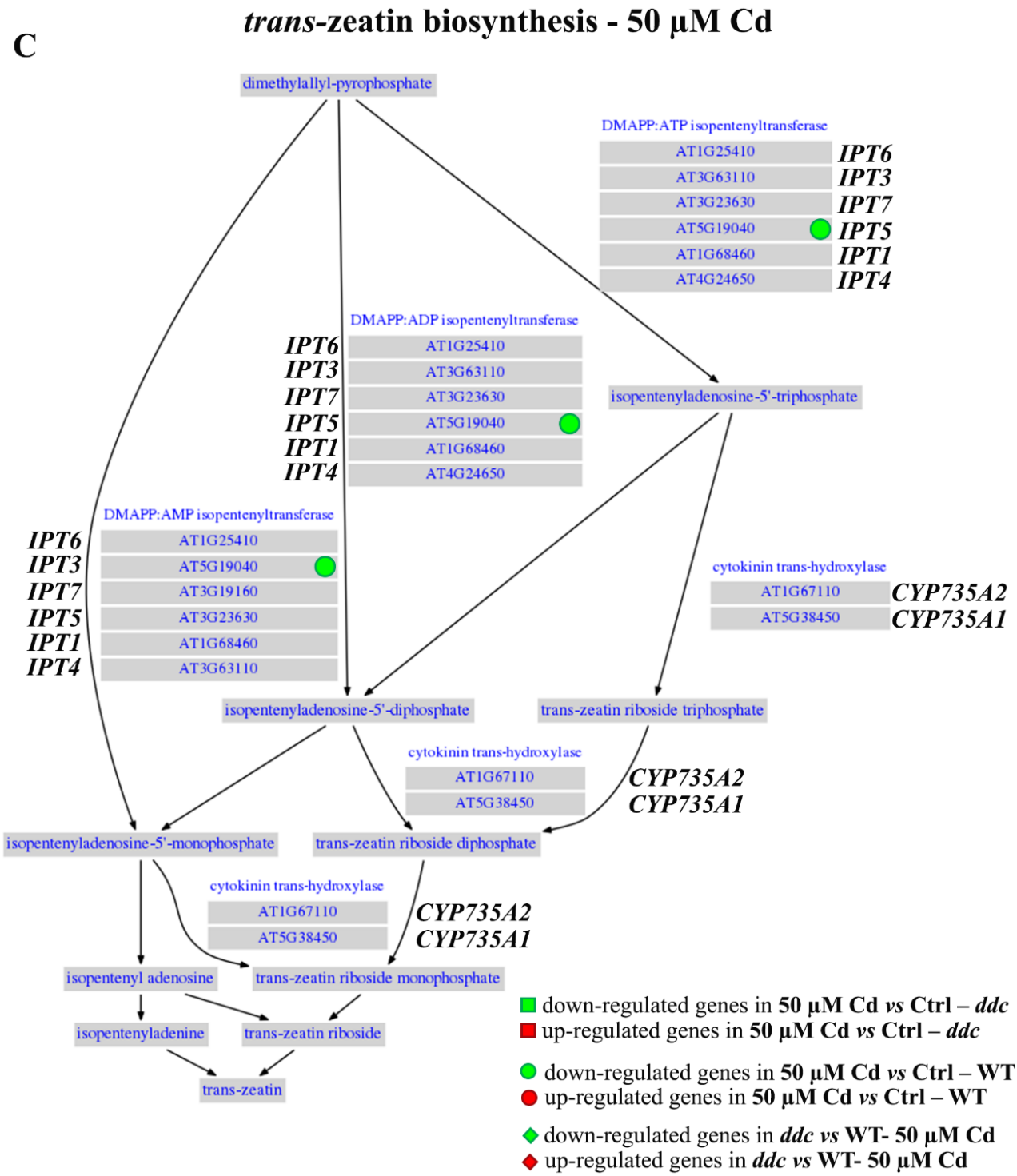

Figure 3.12: Genes differentially expressed (DEGs) along the pathway of *trans*-zeatin biosynthesis in *ddc* and WT seedlings identified through a transcriptomic approach. Seedling grown **(A)** in Ctrl condition, **(B)** under treatment with 25 µM Cd and **(C)** 50 µM Cd.

Some relevant differences were instead observed for genes involved in cytokinin catabolism or conjugation, which occurs through cleavage by cytokinin oxidases or glycosylation, respectively. Both these processes play a role in controlling active cytokinin level in plants.

Following Cd treatment, genes encoding cytokinin-oxidases enzymes (*CKX5* and *CKX6)* resulted down-regulated in *ddc* mutant at both 25 and 50 µM Cd concentration (comparison **25 µM Cd *vs* Ctrl – *ddc***; **50 µM Cd *vs* Ctrl – *ddc)*** (Fig. 3.13 B, C). Interestingly, at 25 µM Cd the *CKX5* gene was down-regulated also in *ddc* mutant compared to WT (***ddc vs* WT -25 µM Cd)** (Fig. 3.13 B).

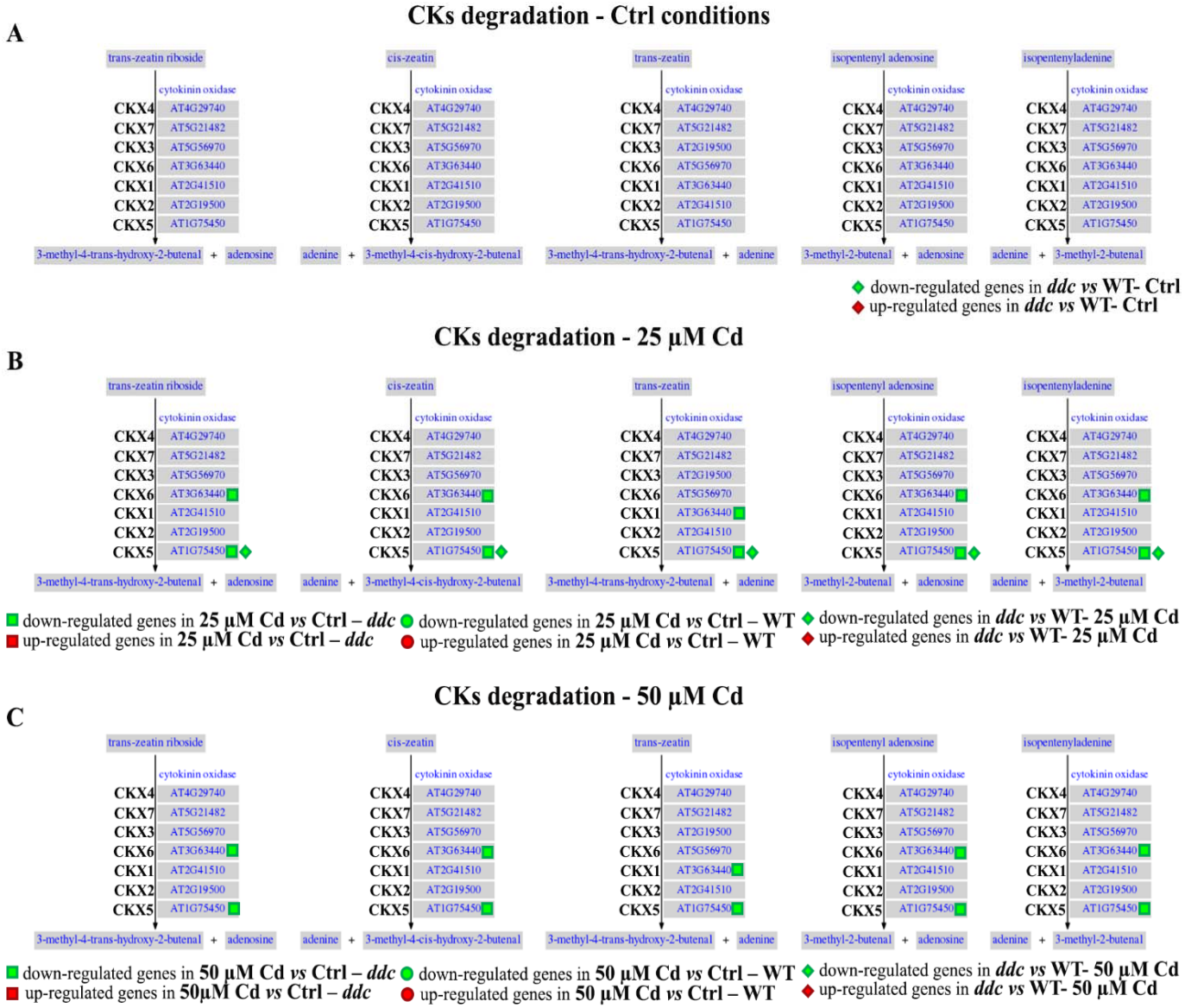

Figure 3.13: Genes differentially expressed (DEGs) along the pathway of cytokinins degradations in *ddc* and WT seedlings identified through a transcriptomic approach. Seedling grown **(A)** in Ctrl condition, **(B)** under treatment with 25 µM Cd and **(C)** 50 µM Cd.

As for cytokinin glycosylation pathways, under Ctrl condition no differences were detected between *ddc vs* WT (comparison ***ddc vs* WT- Ctrl)** (Fig. 3.14 A) but, following Cd treatment, gene expression highly differed in the two samples. Namely, in 25 µM Cd-treated seedlings, an up-regulation of *UGT73C5* and *UGT72C1* genes, which works in both N^7- and N^9-glycosylation pathways, was observed in *ddc* (comparison **25 µM Cd *vs* Ctrl – *ddc)*** and WT (comparison **25 µM Cd *vs* Ctrl –WT)** (Fig. 3.14 B)**,** respectively. Notably, under 25 µM Cd treatment, both these genes were up-regulated also in *ddc vs* WT (***ddc vs* WT -25 µM Cd)** (Fig. 3.14 B).

Following 50 µM Cd treatment, in both *ddc* (comparison **50 µM Cd *vs* Ctrl – *ddc*)** and WT (comparison **50 µM Cd *vs* Ctrl –WT*)*** (Fig. 3.14 C), the only differences dealt with the *UGT73C5* gene which was up-regulated with respect to Ctrl condition**.** As expected, no differences were found in *ddc vs* WT (comparison ***ddc vs* WT -50 µM Cd)** (Fig. 3.14 C).

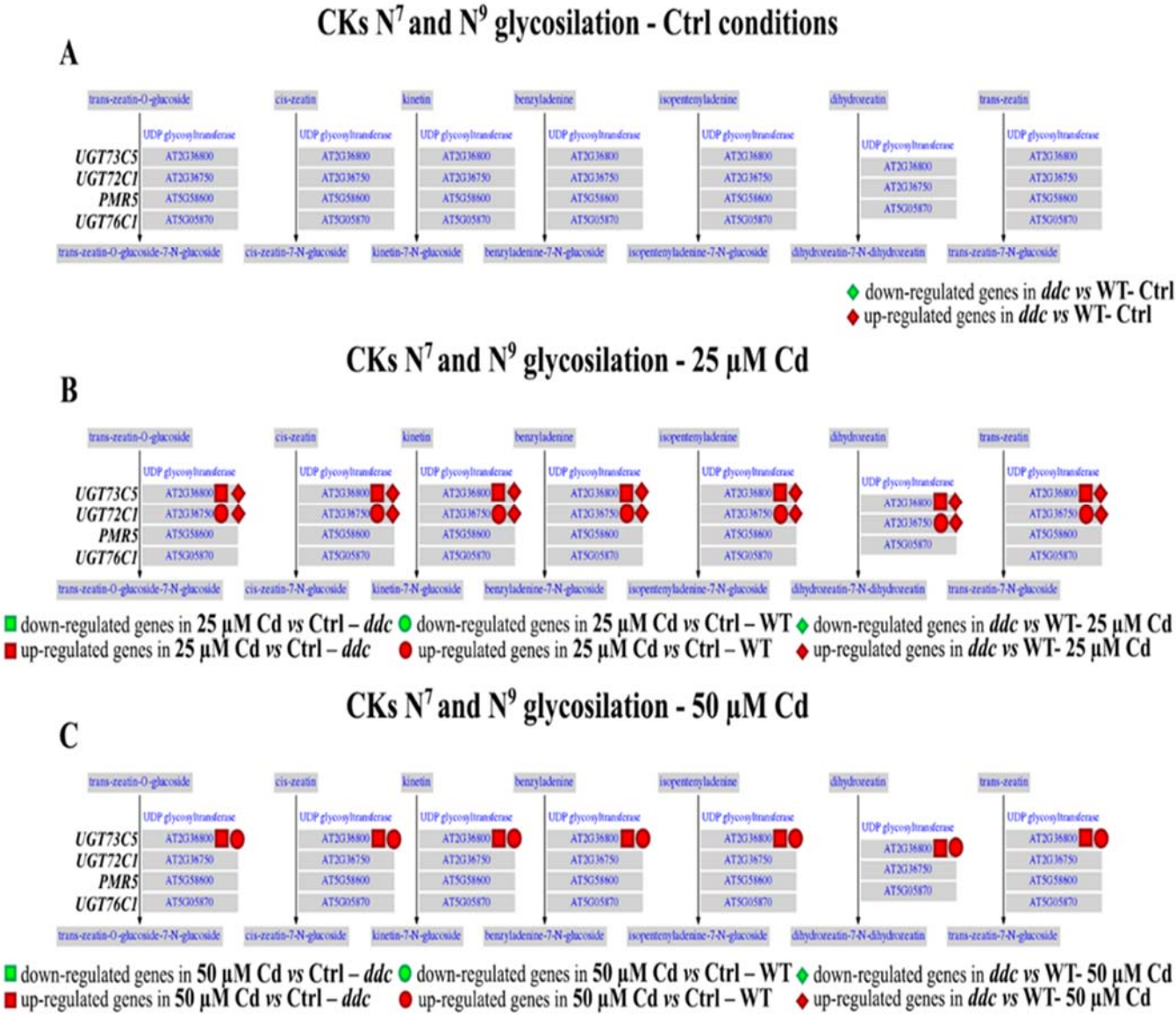

Figure 3.14: Genes differentially expressed (DEGs) along the pathway of cytokinin N^7- and N^9-glucoside biosynthesis in *ddc* and WT seedlings identified through a transcriptomic approach. Seedling grown **(A)** in Ctrl condition, **(B)** under treatment with 25 µM Cd and **(C)** 50 µM Cd.

A higher Cd impact was observed on the genetic pathway related to cytokinin *O*-glycosylation. In fact, under 25 µM Cd treatment, only the *UGT72C1* gene was up-regulated in the WT (comparison **25 µM Cd *vs* Ctrl –WT)** (Fig. 3.15 B), whereas in *ddc* mutant up-regulation event involved the following 7 genes: *AT3G36780, UGT73C7, UGT73C6, UGT87A2, AT2G36770, UGT73C5 and UGT85A1*) (comparison **25 µM Cd *vs* Ctrl – *ddc)*** (Fig. 3.15 B). Moreover, under 25 µM Cd this pathway resulted strongly up-regulated in *ddc* mutant compared to the WT through the overexpression of the following

genes: *UGT76E12, UGT73C6, AT2G36770, UGT72C1 and UGT73C5* (comparison ***ddc vs* WT-25 µM Cd)** (Fig. 3.15 B)**.**

Following 50 µM Cd treatment, pathway related to cytokinin *O*-glycosylation exhibited quite similar expression pattern in *ddc* mutant and WT: in both samples *AT2G36780, UGT73C7, UGT73C6, UGT87A2, AT2G36770, UGT73C5* and *UGT85A1* genes were up-regulated and *AT5G38010* was down-regulated as compared to Ctrl condition (comparisons: **50 µM Cd *vs* Ctrl –WT*; 50* µM Cd *vs* Ctrl – *ddc)*** (Fig. 3.15 C)**.** No differences were observed under 50 µM Cd treatment between *ddc* mutant and WT (comparison ***ddc vs* WT -50 µM Cd)** (Fig. 3.15 C).

In summary, Cd negatively affected genetic pathway related to *trans*-zeatin biosynthesis only in WT exposed at 50 µM Cd concentration. By contrast, in both *ddc* mutant and WT, under Cd treatment the genetic pathways related to cytokinin inactivation were enhanced. Nonetheless and very interestingly, in *ddc* mutant a down-regulation of genetic pathway related to cytokinin cleavage was also induced under Cd exposure.

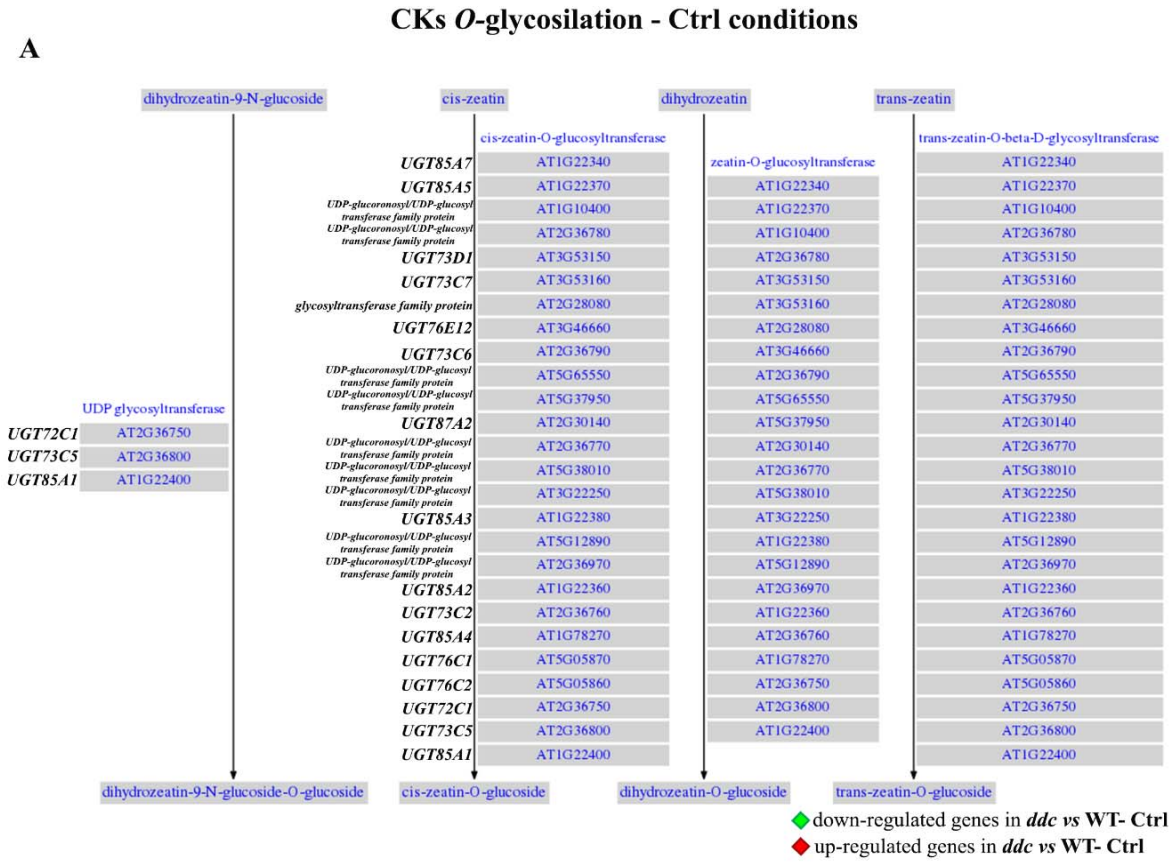

B

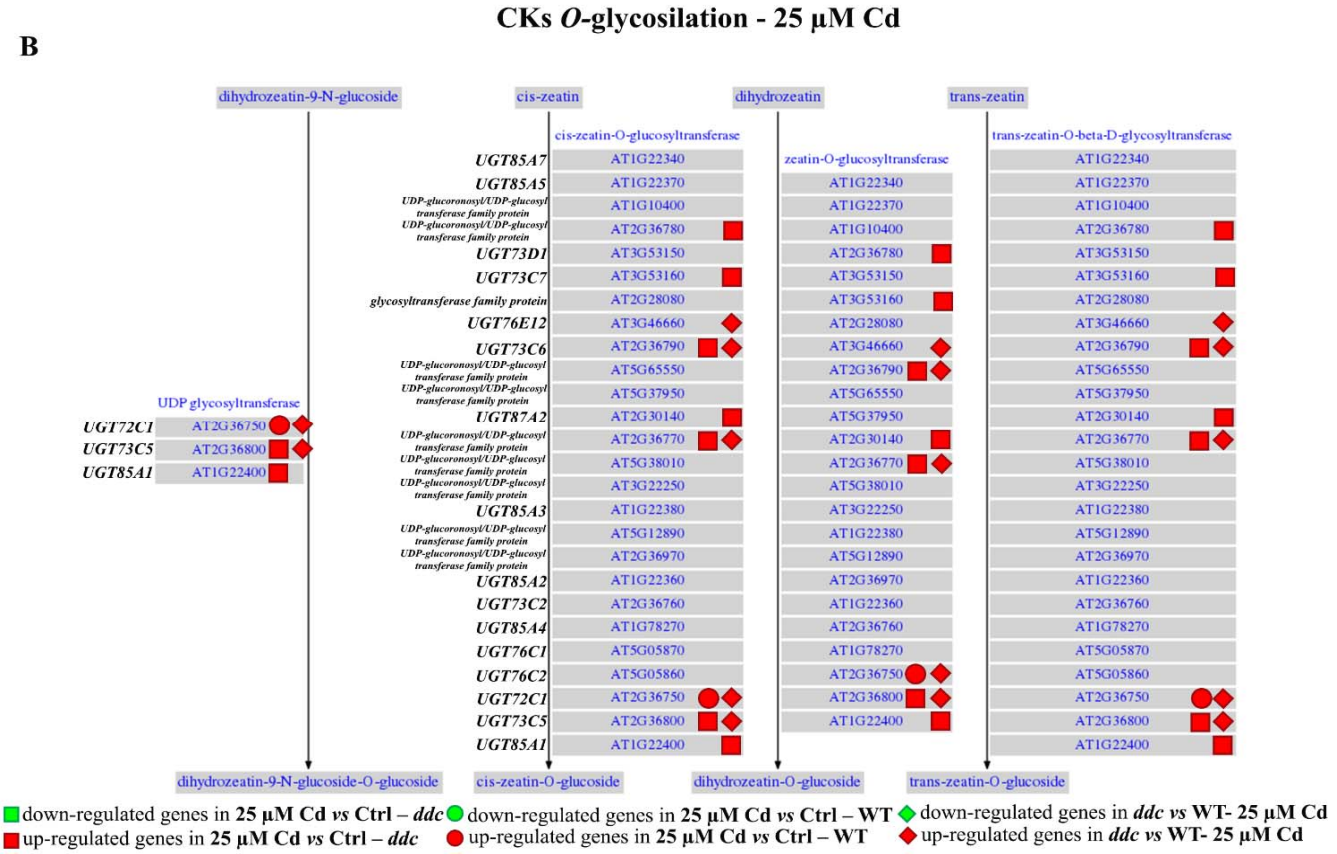
CKs O-glycosilation - 25 µM Cd
dihydrozeatin-9-N-glucoside
cis-zeatin
dihydrozeatin
trans-zeatin
cis-zeatin-O-glucosyltransferase
zeatin-O-glucosyltransferase
trans-zeatin-O-beta-D-glycosyltransferase
UGT85A7 AT1G22340
UGT85A5 AT1G22370
UDP-glucoronosyl/UDP-glucosyl transferase family protein AT1G10400
UDP-glucoronosyl/UDP-glucosyl transferase family protein AT2G36780
UGT73D1 AT3G53150
UGT73C7 AT3G53160
glycosyltransferase family protein AT2G28080
UGT76E12 AT3G46660
UGT73C6 AT2G36790
UDP-glucoronosyl/UDP-glucosyl transferase family protein AT5G65550
UDP-glucoronosyl/UDP-glucosyl transferase family protein AT5G37950
UGT87A2 AT2G30140
UDP-glucoronosyl/UDP-glucosyl transferase family protein AT2G36770
UDP-glucoronosyl/UDP-glucosyl transferase family protein AT5G38010
UDP-glucoronosyl/UDP-glucosyl transferase family protein AT3G22250
UGT85A3 AT1G22380
UDP-glucoronosyl/UDP-glucosyl transferase family protein AT5G12890
UDP-glucoronosyl/UDP-glucosyl transferase family protein AT2G36970
UGT85A2 AT1G22360
UGT73C2 AT2G36760
UGT85A4 AT1G78270
UGT76C1 AT5G05870
UGT76C2 AT5G05860
UGT72C1 AT2G36750
UGT73C5 AT2G36800
UGT85A1 AT1G22400
UDP glycosyltransferase
UGT72C1 AT2G36750
UGT73C5 AT2G36800
UGT85A1 AT1G22400
dihydrozeatin-9-N-glucoside-O-glucoside
cis-zeatin-O-glucoside
dihydrozeatin-O-glucoside
trans-zeatin-O-glucoside
down-regulated genes in 25 µM Cd vs Ctrl – ddc
up-regulated genes in 25 µM Cd vs Ctrl – ddc
down-regulated genes in 25 µM Cd vs Ctrl – WT
up-regulated genes in 25 µM Cd vs Ctrl – WT
down-regulated genes in ddc vs WT- 25 µM Cd
up-regulated genes in ddc vs WT- 25 µM Cd

C

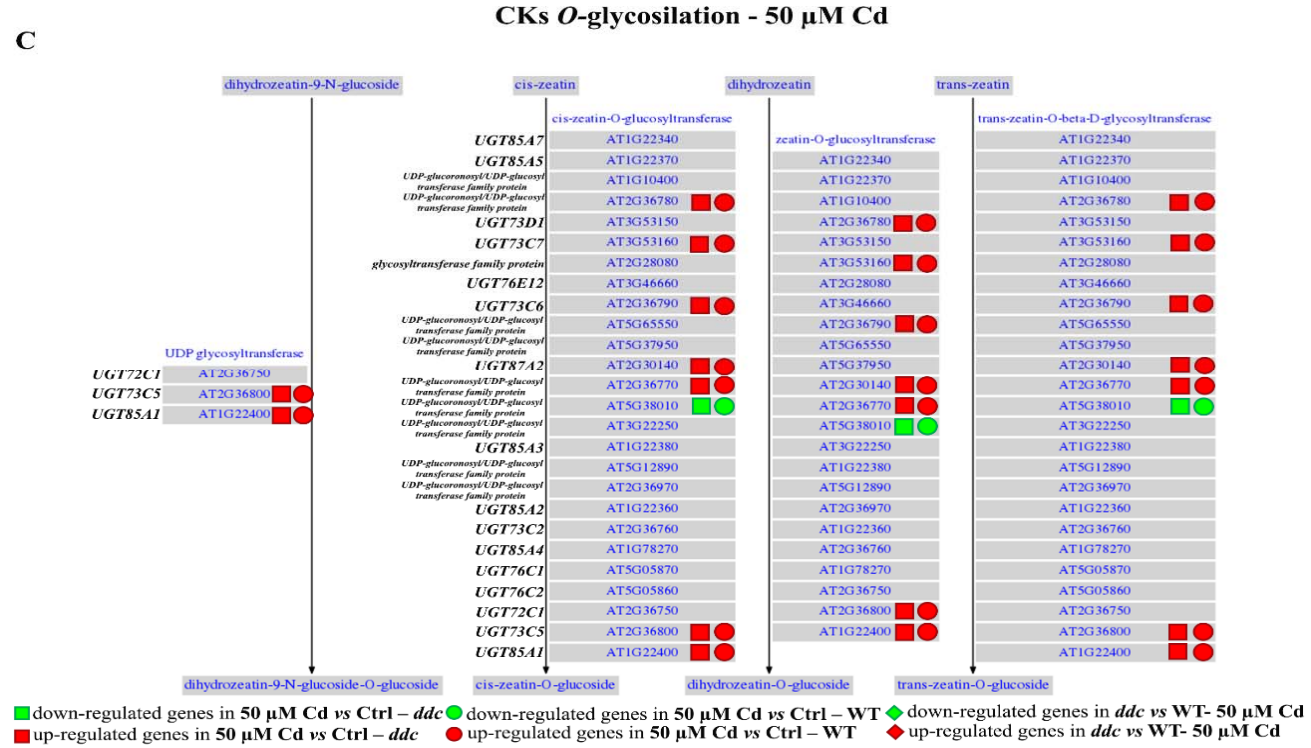
CKs O-glycosilation - 50 µM Cd
dihydrozeatin-9-N-glucoside
cis-zeatin
dihydrozeatin
trans-zeatin
cis-zeatin-O-glucosyltransferase
zeatin-O-glucosyltransferase
trans-zeatin-O-beta-D-glycosyltransferase
UGT85A7 AT1G22340
UGT85A5 AT1G22370
UDP-glucoronosyl/UDP-glucosyl transferase family protein AT1G10400
UDP-glucoronosyl/UDP-glucosyl transferase family protein AT2G36780
UGT73D1 AT3G53150
UGT73C7 AT3G53160
glycosyltransferase family protein AT2G28080
UGT76E12 AT3G46660
UGT73C6 AT2G36790
UDP-glucoronosyl/UDP-glucosyl transferase family protein AT5G65550
UDP-glucoronosyl/UDP-glucosyl transferase family protein AT5G37950
UGT87A2 AT2G30140
UDP-glucoronosyl/UDP-glucosyl transferase family protein AT2G36770
UDP-glucoronosyl/UDP-glucosyl transferase family protein AT5G38010
UDP-glucoronosyl/UDP-glucosyl transferase family protein AT3G22250
UGT85A3 AT1G22380
UDP-glucoronosyl/UDP-glucosyl transferase family protein AT5G12890
UDP-glucoronosyl/UDP-glucosyl transferase family protein AT2G36970
UGT85A2 AT1G22360
UGT73C2 AT2G36760
UGT85A4 AT1G78270
UGT76C1 AT5G05870
UGT76C2 AT5G05860
UGT72C1 AT2G36750
UGT73C5 AT2G36800
UGT85A1 AT1G22400
UDP glycosyltransferase
UGT72C1 AT2G36750
UGT73C5 AT2G36800
UGT85A1 AT1G22400
dihydrozeatin-9-N-glucoside-O-glucoside
cis-zeatin-O-glucoside
dihydrozeatin-O-glucoside
trans-zeatin-O-glucoside
down-regulated genes in 50 µM Cd vs Ctrl – ddc
up-regulated genes in 50 µM Cd vs Ctrl – ddc
down-regulated genes in 50 µM Cd vs Ctrl – WT
up-regulated genes in 50 µM Cd vs Ctrl – WT
down-regulated genes in ddc vs WT- 50 µM Cd
up-regulated genes in ddc vs WT- 50 µM Cd

Figure 3.15: Genes differentially expressed (DEGs) along the pathway of cytokinin *O*-glycosylation in *ddc* and WT seedlings identified through a transcriptomic approach. Seedling grown **(A)** in Ctrl condition, **(B)** under treatment with 25 µM Cd and **(C)** 50 µM Cd.

3.3.3.3 Gibberellins

Box 3

Gibberellins biosynthetic pathways

Gibberellins (GAs) are tetracyclic diterpenoid phytohormones that modulate plant growth and development along all its life cycle, from seed germination to promotion of cell division and elongation and flowering induction (Sun and Gubler, 2004; Sun, 2011; Vera-Sirera *et al.,*2016). Moreover, they play an important role also in biotic and abiotic stress responses (Yang *et al.,*2008; Daviere and Achard, 2016). Despite the huge number of GAs identified until now (more than 136 different GAs), only few of them are biologically active, namely GA_1, GA_3, GA_4 and GA_7 (Sakamoto *et al.,*2004; Plackett *et al.,*2011; Hedden and Sponsel, 2015). In most plant species, GA_1 and GA_4 are the major active GAs and, in particular, GA_4 shows a stronger bioactivity that GA_1 in *A. thaliana* and *Oryza sativa* (Cowling *et al.,*1998; Magome *et al.,*2013; Nomura *et al.,*2013).

GAs biosynthesis is carried forward in three different subcellular compartments: the plastids, the endomembrane system and the cytosol (Yamaguchi, 2008; Han and Zhu, 2011; Hedden and Thomas, 2012). The conversion of geranylgeranyl diphosphate (GGDP) to *ent*-kaurene is the first stage of GAs biosynthesis and occurs in plastids. It is a two-steps reaction catalysed by the *ent*-CDP synthase (CPS) and *ent*-kaurene synthase (KS), two terpene synthase (TPSs) enzymes that in *A. thaliana* are encoded by the genes *CPS* (also known as *GA1*) and *KS* (or *GA2*), respectively. These genes are present in single copy and their expression isn't feedback-regulated by GA-signalling pathway activity (reviewed by Gao *et al.,*2017).

The second stage of GAs biosynthesis occurs first in the plastid envelope, and later in the endoplasmic reticulum (ER), where *ent*-kaurene is converted in GA_{12} by *ent*-kaurene oxidase (KO) (Helliwell *et al.,*1998, 1999) and *ent*-kaurenoic acid oxidase (KAO) activity (Helliwell *et al.,*2001a, b; Regnault *et al.,*2014). *KO* gene (*GA3* in *Arabidopsis*), like *CPS* and *KS*, isn't feedback-regulated by GAs, and these genes expression has a role in the control of early GA biosynthesis (Hedden and Phillips, 2000; Olszewski *et al.,*2002).

In the last GAs biosynthesis steps, that occur in the cytosol, GA 20-oxidase (GA20ox) and GA 3-oxidase (GA3ox) convert GA_{12} and GA_{53} (produced by GA_{12} 13-hydroxylation) in GA intermediates and active GAs along two parallel branches: the non-13-hydroxylation branch, that leads to the production of 13-H GAs like the bioactive GA_4, and the 13-hydroxylation branch that leads to the production of 13-OH GAs like the bioactive GA_1 (Yamaguchi, 2008; reviewed by Gao *et al.,*2017).

GA20ox enzymes are responsible for the production of GA_9 in the non-13-hydroxylation branch, and the production of GA_{20} by using GA_{19} as substrate in the 13-hydroxylation branch. GA_9 and GA_{20} are the precursors of bioactive GAs (Lange *et al.,*1994; Hedden and Phillips, 2000; Yamaguchi, 2008). These

inactive precursors will be hydroxylated by GA3ox enzymes to form GA_4 and GA_1, respectively (Yamaguchi, 2008).

GAs inactivation pathways

The most studied GAs inactivation pathway, the 2β-hydroxylation, is catalysed by GA2oxs (Yamaguchi and Kamiya, 2000; Lo *et al.,*2008; Huang *et al.,*2010; Shan *et al.,*2014;), which are divided in two different classes: the C_{19}-GA2ox and the C_{20}-GA2ox. The C_{19}-GA2ox catalyse deactivation of the bioactive GA_4 and GA_1 by converting them in GA_{34} and GA_8, respectively. This enzymatic family also catalyse the conversion of GA_9 and GA_{20}, direct precursors of GA_4 and GA_1, into GA_{51} and GA_{29} gibberellin catabolites (reviewed by Gao *et al.,*2017). The C_{20}-GA2ox enzymes use GA_{12} and GA_{53} as substrates to form GA_{110} and GA_{97} (reviewed by Gao *et al.,*2017). Active GAs can also be deactivated through a methylation process, catalysed in *A. thaliana* by two GAs methyltransferases, GAMT1 and GAMT2, to generate inactive GAs methyl esters (Varbanova *et al.,*2007). However, there are still uncertainties regarding this mechanism, that needs to be further elucidated.

Concerning GAs genetic pathways, under Ctrl condition the pathways related to their biosynthesis (Box 3) showed similar expression pattern in *ddc* and WT (comparison ***ddc vs* WT- Ctrl)** (Fig. 3.16 A; Fig. 3.17 A). As for Cd effects, a significant down-regulation of *GA2* gene was found in *ddc* mutant treated with 25 µM Cd (comparison **25 µM Cd *vs* Ctrl – *ddc)*** (Fig. 3.16 B). It is worth to underline that this gene encodes the *ent*-kaurene synthase, a pivotal enzyme along the early biosynthetic GAs pathways, that ends with the GA_{12} formation. Under 25 µM Cd, *GA2* gene resulted to be down-regulated also in *ddc* mutant as compared to the WT (***ddc vs* WT -25 µM Cd)** (Fig. 3.16 B).

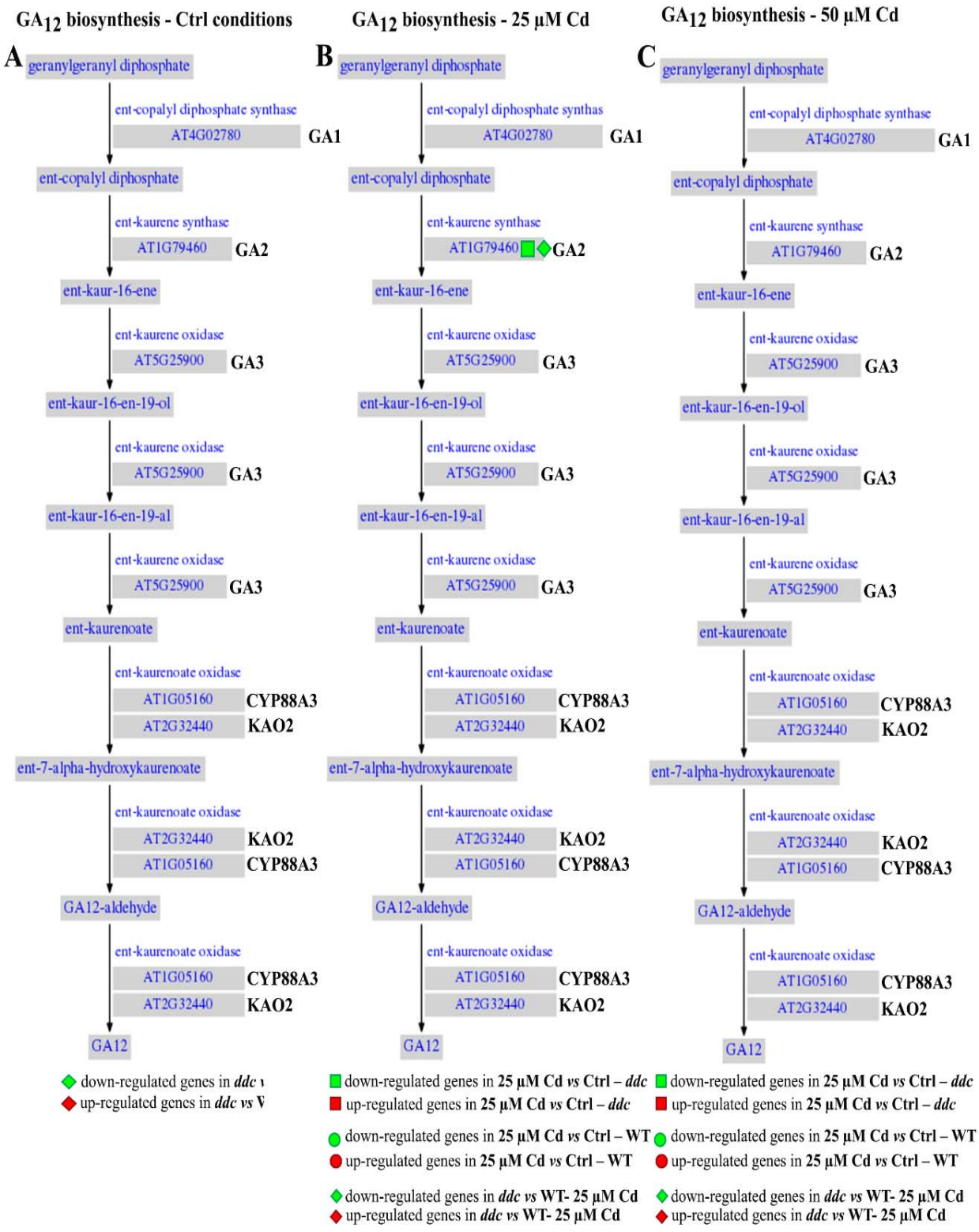

Figure 3.16: Genes differentially expressed (DEGs) along the pathway of GA_{12} biosynthesis in *ddc* and WT seedlings identified through a transcriptomic approach. Seedling grown **(A)** in Ctrl condition, **(B)** under treatment with 25 µM Cd and **(C)** 50 µM Cd.

Some other differences were detected for the GAs biosynthesis superpathway, that comprehends the reactions that synthetize bioactive GAs from GA_{12}. Under 25 µM Cd treatment, this pathway wasn't differentially regulated in WT (comparison **25 µM Cd *vs* Ctrl –WT)** (Fig. 3.17 B), while in *ddc* a down-regulation of *GA4* gene, a key gene along the pathway, was observed (comparison **25 µM Cd *vs* Ctrl – *ddc)*** (Fig. 3.17 B). No significant differences were found in *ddc vs* WT (comparison ***ddc vs* WT -25 µM Cd)** (Fig. 3.17 B). Interestingly, at 50 µM Cd concentration both *ddc* and WT showed a down-regulation of *GA5* gene (comparison **50 µM Cd *vs* Ctrl –WT*;* 50 µM Cd *vs* Ctrl – *ddc)*** (Fig. 3.17 C). As expected on the basis of other comparisons, no differences were found in *ddc* mutant *vs* WT (comparison ***ddc vs* WT -50 µM Cd)** (Fig. 3.17 C).

A

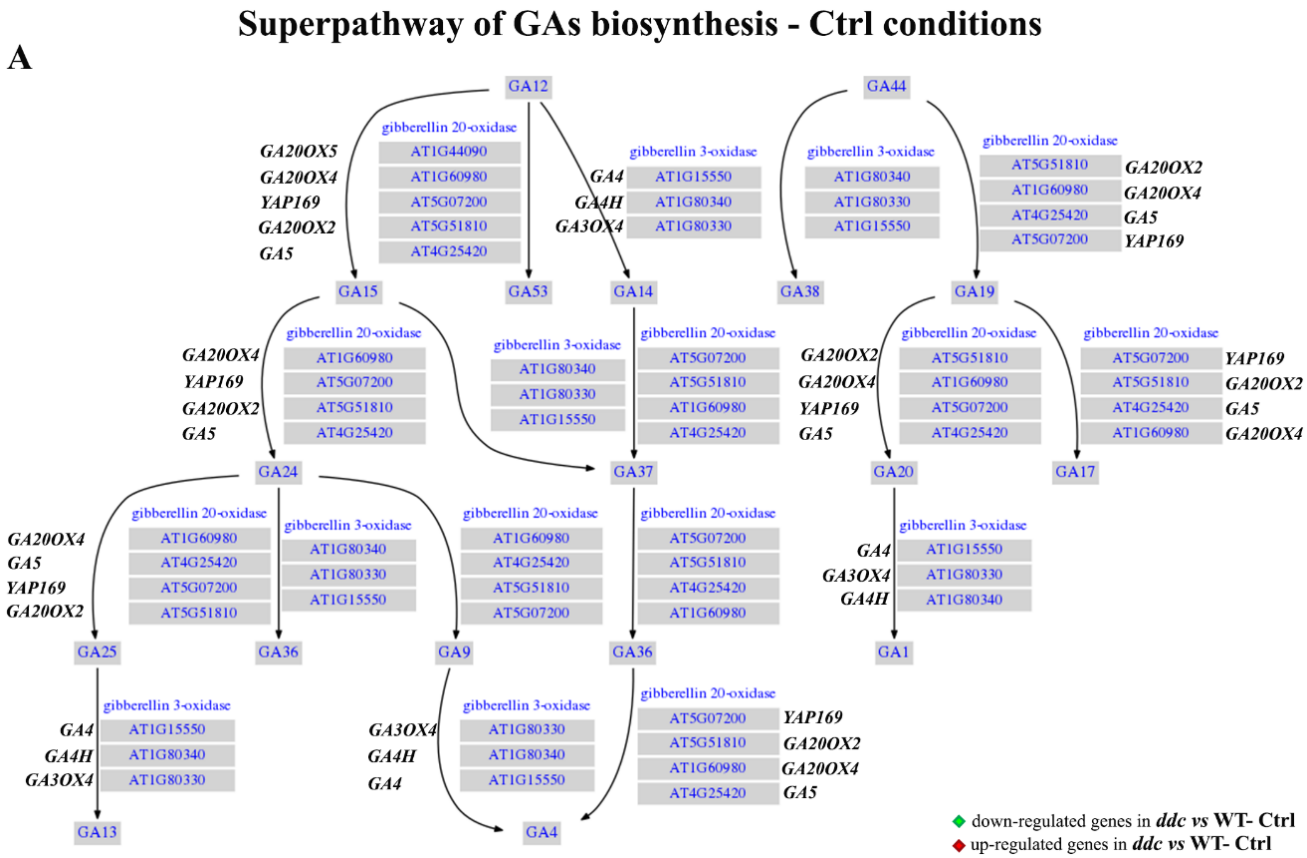

B

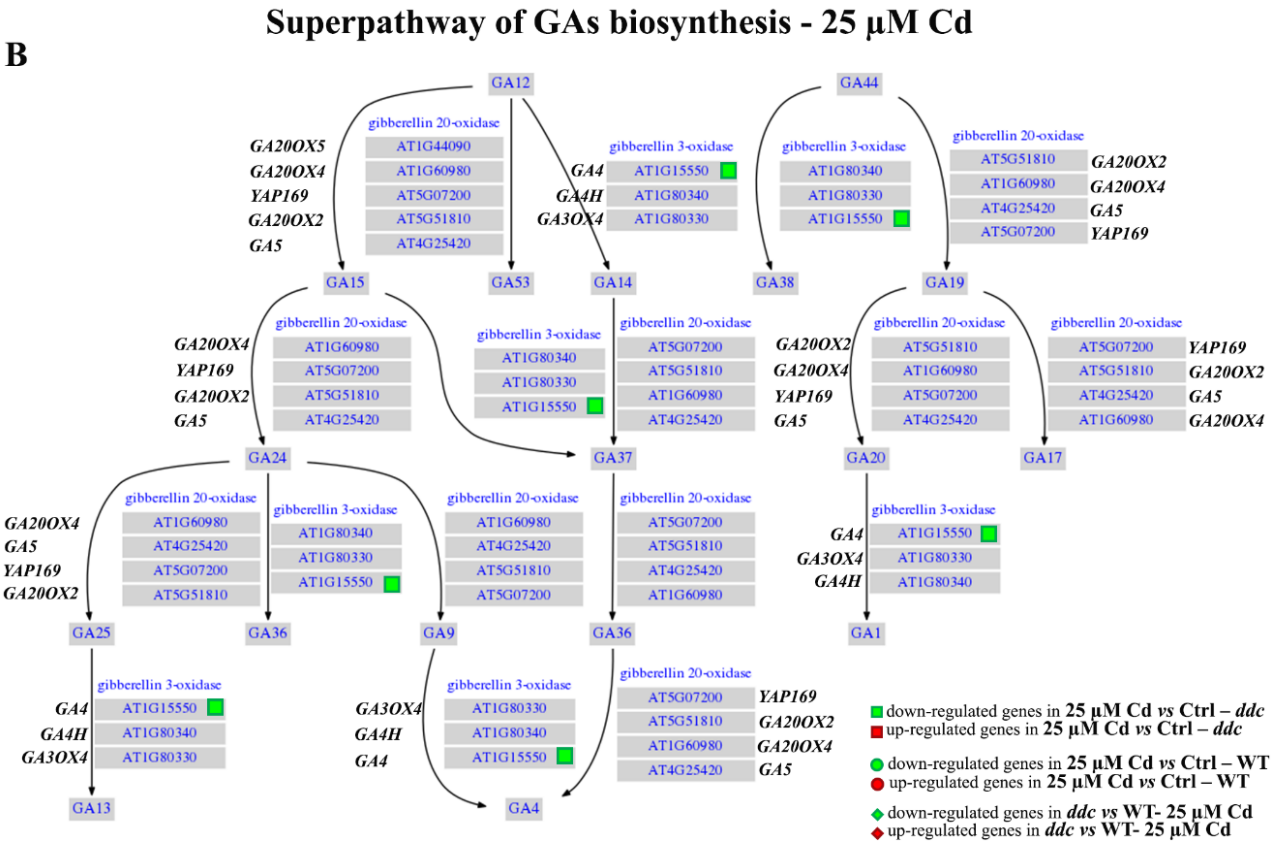
Superpathway of GAs biosynthesis - 25 µM Cd
GA12
GA44
GA15
GA53
GA14
GA38
GA19
GA24
GA37
GA20
GA17
GA25
GA36
GA9
GA36
GA1
GA13
GA4
gibberellin 20-oxidase
gibberellin 3-oxidase
AT1G44090
AT1G60980
AT5G07200
AT5G51810
AT4G25420
AT1G15550
AT1G80340
AT1G80330
GA20OX5
GA20OX4
YAP169
GA20OX2
GA5
GA4
GA4H
GA3OX4
down-regulated genes in 25 µM Cd vs Ctrl – ddc
up-regulated genes in 25 µM Cd vs Ctrl – ddc
down-regulated genes in 25 µM Cd vs Ctrl – WT
up-regulated genes in 25 µM Cd vs Ctrl – WT
down-regulated genes in ddc vs WT- 25 µM Cd
up-regulated genes in ddc vs WT- 25 µM Cd

C

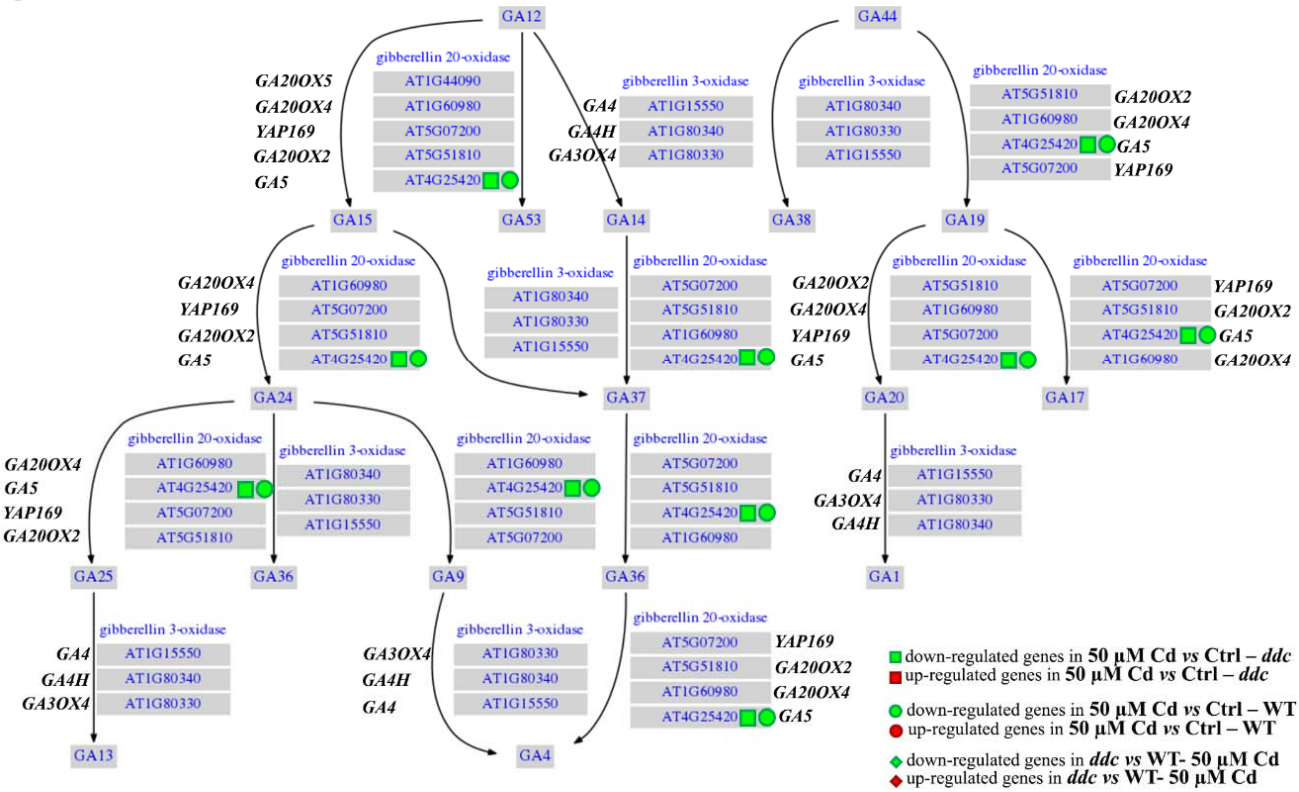
Superpathway of GAs biosynthesis - 50 µM Cd
GA12
GA44
GA15
GA53
GA14
GA38
GA19
GA24
GA37
GA20
GA17
GA25
GA36
GA9
GA36
GA1
GA13
GA4
gibberellin 20-oxidase
gibberellin 3-oxidase
AT1G44090
AT1G60980
AT5G07200
AT5G51810
AT4G25420
AT1G15550
AT1G80340
AT1G80330
GA20OX5
GA20OX4
YAP169
GA20OX2
GA5
GA4
GA4H
GA3OX4
down-regulated genes in 50 µM Cd vs Ctrl – ddc
up-regulated genes in 50 µM Cd vs Ctrl – ddc
down-regulated genes in 50 µM Cd vs Ctrl – WT
up-regulated genes in 50 µM Cd vs Ctrl – WT
down-regulated genes in ddc vs WT- 50 µM Cd
up-regulated genes in ddc vs WT- 50 µM Cd

Figure 3.17: Genes differentially expressed (DEGs) along the pathway of GAs biosynthetic superpathway in *ddc* and WT seedlings identified through a transcriptomic approach. Seedling grown **(A)** in Ctrl condition, **(B)** under treatment with 25 µM Cd and **(C)** 50 µM Cd.

Data dealing with the genetic pathways controlling endogenous GAs levels by inactivation (Box 6) provided some other interesting information. In particular, no differences were observed between *ddc* mutant and WT under Ctrl condition (comparison ***ddc vs* WT- Ctrl)** (Fig. 3.18 A), while a differential response was induced by Cd treatment. Namely, following 25 µM Cd two members of the gene family encoding the GA2ox enzymes, *DAO2* and *AOP1,* were down-regulated only in *ddc* mutant (comparison **25 µM Cd *vs* Ctrl – *ddc)*** (Fig. 3.18 B). A down-regulation of these genes was also observed when comparing the expression pattern of both *ddc* and WT under this Cd concentration (comparison ***ddc vs* WT -25 µM Cd)** (Fig. 3.18 B).

Altogether, GAs results evidenced that the pathways related to their biosynthesis were down-regulated by Cd treatment more rapidly in *ddc* mutant than in WT. In fact, at 25 µM Cd a down-regulation of early GAs biosynthetic pathway was observed in the mutant together with a down-regulation of GAs biosynthesis superpathway, which in the WT resulted affected only at 50 µM Cd concentration.

A

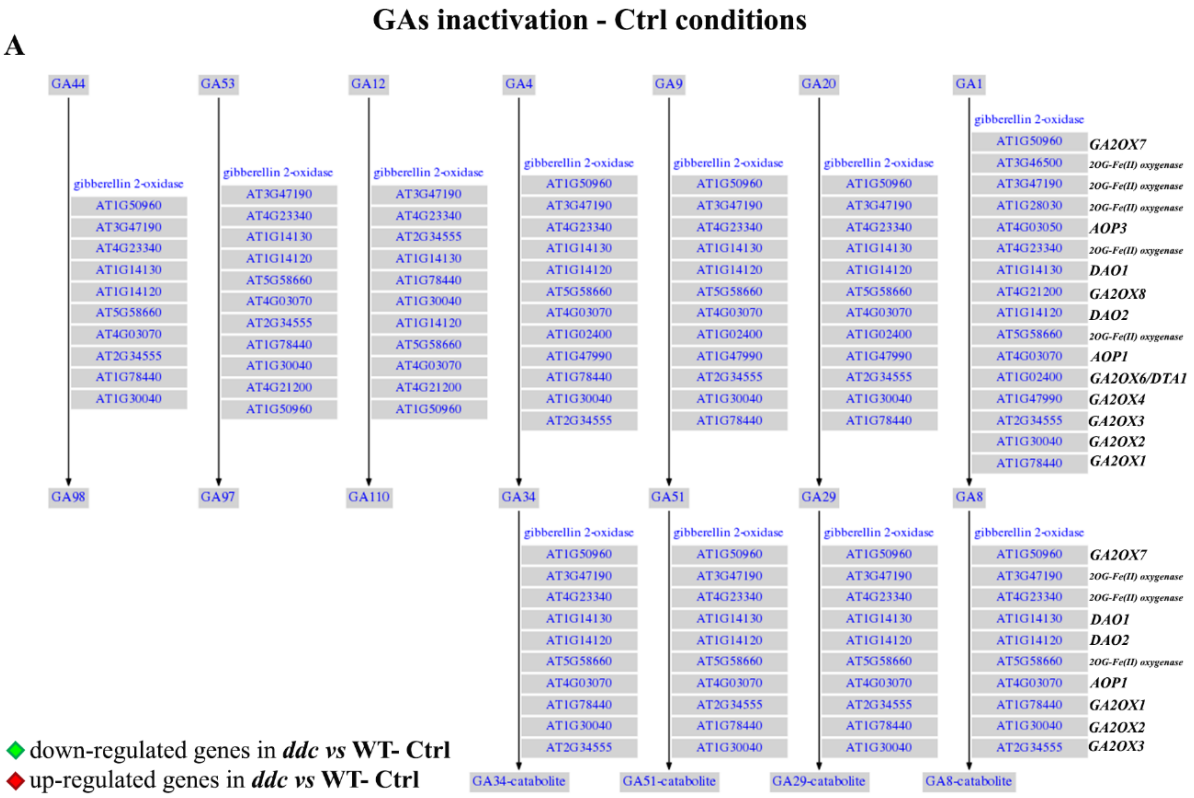
GAs inactivation - Ctrl conditions
GA44
GA53
GA12
GA4
GA9
GA20
GA1
gibberellin 2-oxidase
AT1G50960
AT3G47190
AT4G23340
AT1G14130
AT1G14120
AT5G58660
AT4G03070
AT2G34555
AT1G78440
AT1G30040
AT3G47190
AT4G23340
AT1G14130
AT1G14120
AT5G58660
AT4G03070
AT2G34555
AT1G78440
AT1G30040
AT4G21200
AT1G50960
AT3G47190
AT4G23340
AT2G34555
AT1G14130
AT1G78440
AT1G30040
AT4G21200
AT1G50960
AT1G50960
AT3G47190
AT4G23340
AT1G14130
AT1G14120
AT5G58660
AT4G03070
AT1G02400
AT1G47990
AT1G78440
AT1G30040
AT2G34555
AT1G50960
AT3G47190
AT4G23340
AT1G14130
AT1G14120
AT5G58660
AT4G03070
AT1G02400
AT1G47990
AT2G34555
AT1G30040
AT1G78440
AT1G50960
AT3G47190
AT4G23340
AT1G14130
AT1G14120
AT5G58660
AT4G03070
AT1G02400
AT1G47990
AT2G34555
AT1G30040
AT1G78440
AT1G50960
AT3G46500
AT3G47190
AT1G28030
AT4G03050
AT4G23340
AT1G14130
AT4G21200
AT1G14120
AT5G58660
AT4G03070
AT1G02400
AT1G47990
AT2G34555
AT1G30040
AT1G78440
GA2OX7
2OG-Fe(II) oxygenase
2OG-Fe(II) oxygenase
2OG-Fe(II) oxygenase
AOP3
2OG-Fe(II) oxygenase
DAO1
GA2OX8
DAO2
2OG-Fe(II) oxygenase
AOP1
GA2OX6/DTA1
GA2OX4
GA2OX3
GA2OX2
GA2OX1
GA98
GA97
GA110
GA34
GA51
GA29
GA8
AT1G50960
AT3G47190
AT4G23340
AT1G14130
AT1G14120
AT5G58660
AT4G03070
AT1G78440
AT1G30040
AT2G34555
AT1G50960
AT3G47190
AT4G23340
AT1G14130
AT1G14120
AT5G58660
AT4G03070
AT2G34555
AT1G78440
AT1G30040
AT1G50960
AT3G47190
AT4G23340
AT1G14130
AT1G14120
AT5G58660
AT4G03070
AT2G34555
AT1G78440
AT1G30040
AT1G50960
AT3G47190
AT4G23340
AT1G14130
AT1G14120
AT5G58660
AT4G03070
AT1G78440
AT1G30040
AT2G34555
GA2OX7
2OG-Fe(II) oxygenase
2OG-Fe(II) oxygenase
DAO1
DAO2
2OG-Fe(II) oxygenase
AOP1
GA2OX1
GA2OX2
GA2OX3
GA34-catabolite
GA51-catabolite
GA29-catabolite
GA8-catabolite
down-regulated genes in ddc vs WT- Ctrl
up-regulated genes in ddc vs WT- Ctrl

B

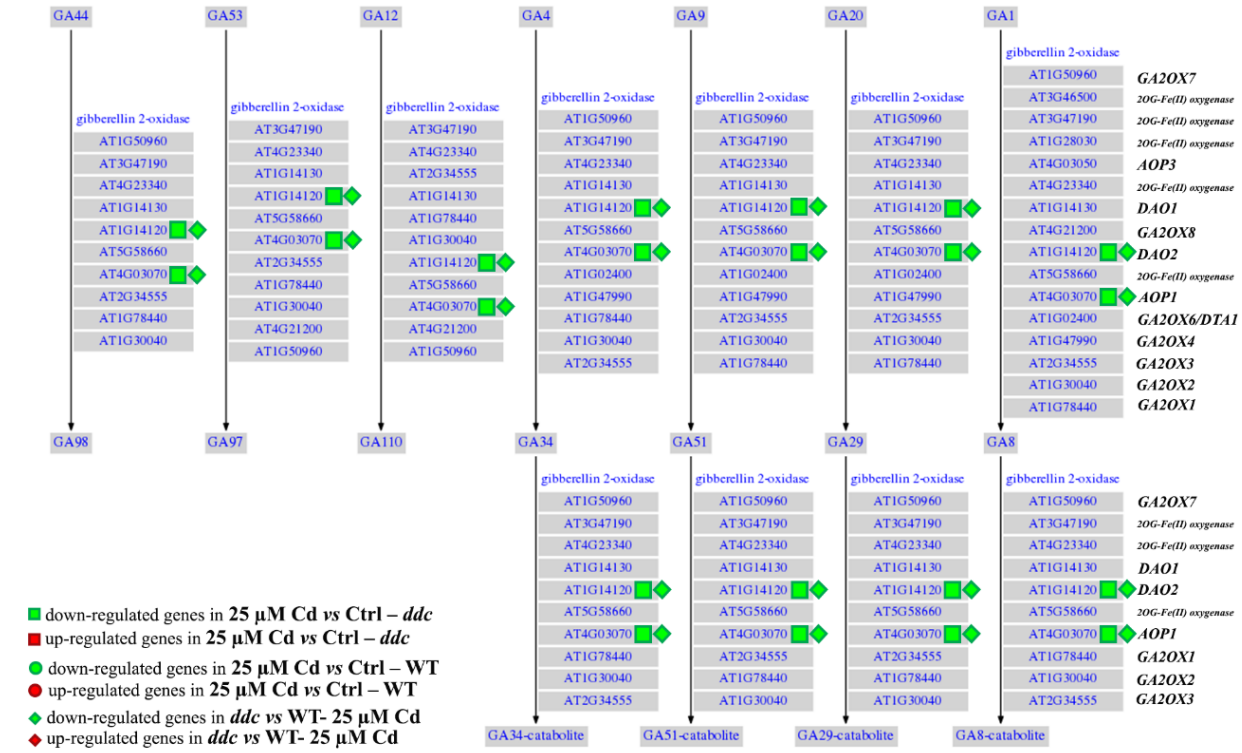
GAs inactivation - 25 µM Cd
GA44
GA53
GA12
GA4
GA9
GA20
GA1
gibberellin 2-oxidase
AT1G50960
AT3G47190
AT4G23340
AT1G14130
AT1G14120
AT5G58660
AT4G03070
AT2G34555
AT1G78440
AT1G30040
AT3G47190
AT4G23340
AT1G14130
AT1G14120
AT5G58660
AT4G03070
AT2G34555
AT1G78440
AT1G30040
AT4G21200
AT1G50960
AT3G47190
AT4G23340
AT2G34555
AT1G14130
AT1G78440
AT1G30040
AT4G21200
AT1G50960
AT1G50960
AT3G47190
AT4G23340
AT1G14130
AT1G14120
AT5G58660
AT4G03070
AT1G02400
AT1G47990
AT1G78440
AT1G30040
AT2G34555
AT1G50960
AT3G47190
AT4G23340
AT1G14130
AT1G14120
AT5G58660
AT4G03070
AT1G02400
AT1G47990
AT2G34555
AT1G30040
AT1G78440
AT1G50960
AT3G47190
AT4G23340
AT1G14130
AT1G14120
AT5G58660
AT4G03070
AT1G02400
AT1G47990
AT2G34555
AT1G30040
AT1G78440
AT1G50960
AT3G46500
AT3G47190
AT1G28030
AT4G03050
AT4G23340
AT1G14130
AT4G21200
AT1G14120
AT5G58660
AT4G03070
AT1G02400
AT1G47990
AT2G34555
AT1G30040
AT1G78440
GA2OX7
2OG-Fe(II) oxygenase
2OG-Fe(II) oxygenase
2OG-Fe(II) oxygenase
AOP3
2OG-Fe(II) oxygenase
DAO1
GA2OX8
DAO2
2OG-Fe(II) oxygenase
AOP1
GA2OX6/DTA1
GA2OX4
GA2OX3
GA2OX2
GA2OX1
GA98
GA97
GA110
GA34
GA51
GA29
GA8
AT1G50960
AT3G47190
AT4G23340
AT1G14130
AT1G14120
AT5G58660
AT4G03070
AT1G78440
AT1G30040
AT2G34555
AT1G50960
AT3G47190
AT4G23340
AT1G14130
AT1G14120
AT5G58660
AT4G03070
AT2G34555
AT1G78440
AT1G30040
AT1G50960
AT3G47190
AT4G23340
AT1G14130
AT1G14120
AT5G58660
AT4G03070
AT2G34555
AT1G78440
AT1G30040
AT1G50960
AT3G47190
AT4G23340
AT1G14130
AT1G14120
AT5G58660
AT4G03070
AT1G78440
AT1G30040
AT2G34555
GA2OX7
2OG-Fe(II) oxygenase
2OG-Fe(II) oxygenase
DAO1
DAO2
2OG-Fe(II) oxygenase
AOP1
GA2OX1
GA2OX2
GA2OX3
GA34-catabolite
GA51-catabolite
GA29-catabolite
GA8-catabolite
down-regulated genes in 25 µM Cd vs Ctrl – ddc
up-regulated genes in 25 µM Cd vs Ctrl – ddc
down-regulated genes in 25 µM Cd vs Ctrl – WT
up-regulated genes in 25 µM Cd vs Ctrl – WT
down-regulated genes in ddc vs WT- 25 µM Cd
up-regulated genes in ddc vs WT- 25 µM Cd

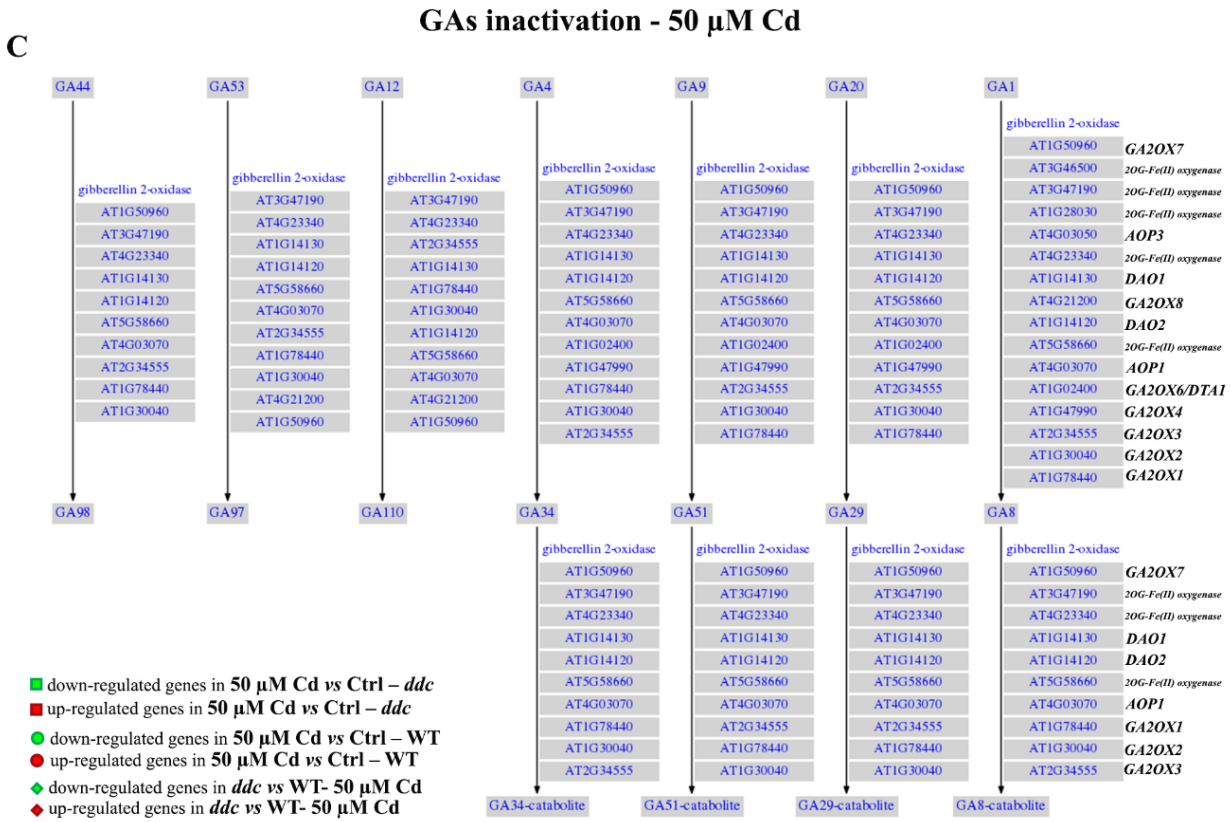

Figure 3.18: Genes differentially expressed (DEGs) along the pathway of gibberellins inactivation superpathway in *ddc* and WT seedlings identified through a transcriptomic approach. Seedling grown **(A)** in Ctrl condition, **(B)** under treatment with 25 µM Cd and **(C)** 50 µM Cd.

3.3.3.4 Jasmonic acid

Box 4

Jasmonic acid biosynthetic pathways

Jasmonic acid (JA) is a major immunity hormone involved in defence response and promotion of reproductive development by repressing the vegetative growth (reviewed by Zhai *et al.,*2017). The first step of JA biosynthesis occurs in the chloroplast and is catalysed by lypoxigenase enzyme family (LOX), that oxygenate free *α*-linoleic acid (18:3) to produce 13(*S*)-hydroperoxy-octadecatrienoic acid (13-HPOT) (Fig. B3) (reviewed by Zhai *et al.,*2017). In *A. thaliana*, LOX2 is mainly involved in JA production induced by wounding (Bell *et al.,*1995; Glauser *et al.,*2009; Schommer *et al.,*2008), LOX3 and LOX4 are involved in flowers development (Caldelari *et al.,*2011), while LOX6 is involved in stress-induced JA production, mainly wounding and drought-related stresses (Chauvin *et al.,*2012; Grebner *et al.,*2013).

13-HOPT is successively converted by allene oxide synthase (AOS) in 12,13(*S*)-epoxy-octadecatrienoic acid (12,13-EOT), an unstable allene oxide that is cyclized by allene oxide cyclase (AOC) to the 9*S*, 13*S* isomer of 12-oxo-phytodienoic acid (12-OPDA) and exported to the peroxisome, where it

becomes the substrate of OPDA reductase 3 (OPR3) to produce 3-oxo-2-(2′(Z)-pentenyl)-cyclopentane-1-octanoic acid (OPC-8:0) (Fig. B3) (Sanders *et al.,*2000; Stintzi and Browse, 2000).

To complete JA biosynthesis, three β-oxidation cycles are necessary. These steps are catalysed by acyl-CoA oxidase (ACX), the multifunctional protein (MFP), and 3-ketoacyl-CoA thiolase (KAT), which are core enzymes of the β-oxidation cycle (Li *et al.,*2005; Schilmiller *et al.,*2007). The final product of these reaction will be the (+)-7-*iso*-JA (Fig. B3).

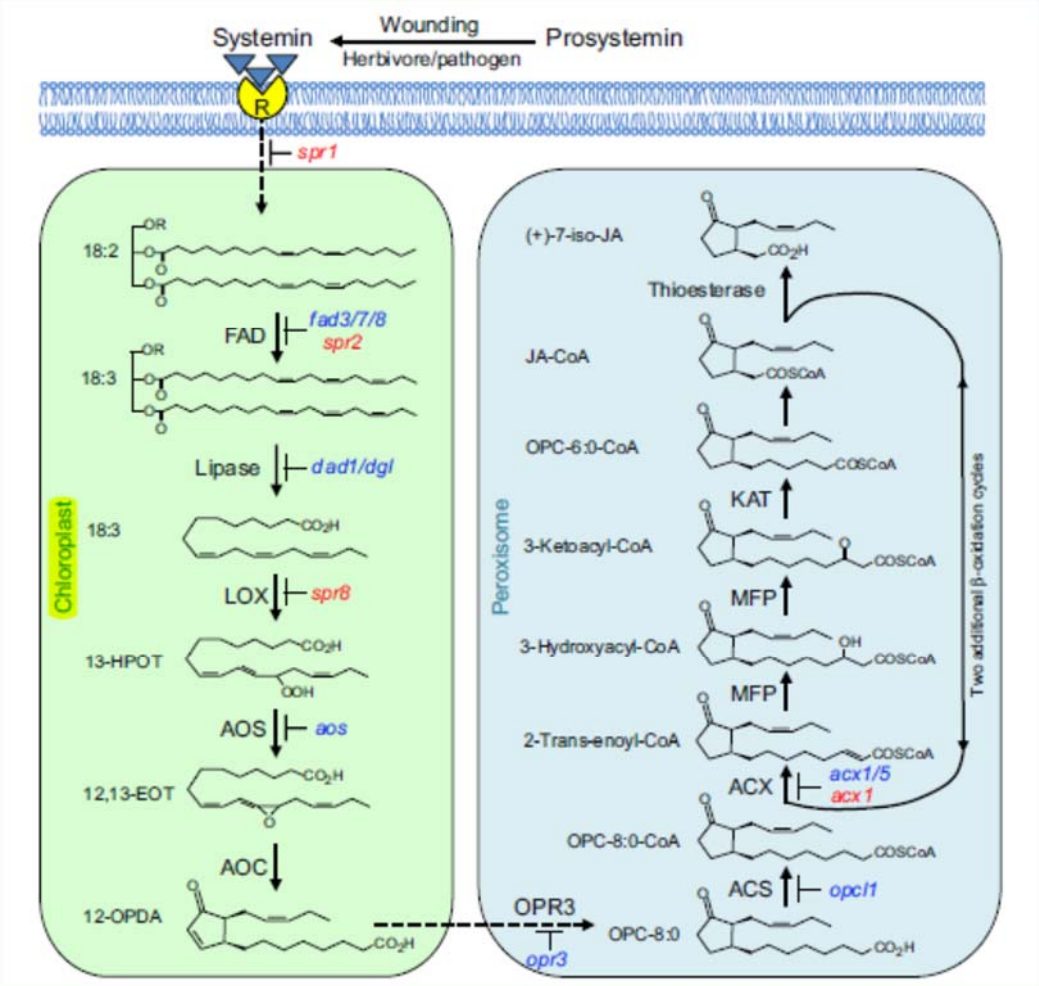

Figure B3: Jasmonic acid (JA) biosynthesis in *A. thaliana via* the octadecanoid pathway. The first step of JA biosynthesis occurs in the chloroplast, and it's catalysed by LOX, to produce 13-HPOT. Subsequently, 13-HPOT is converted by AOS into 12,13-EOT, an unstable allene oxide that, in presence of AOC, is cyclized to 12-OPDA and exported to the peroxisome, where it becomes the substrate of OPR3 to produce OPC-8:0. To complete JA biosynthesis, three β-oxidation cycles, catalysed by ACX, MFP and KAT, are necessary. The final product of these reaction will be the (+)-7-*iso*-JA.

Legend: 12,13- EOT, 12,13(S)-epoxy-octadecatrienoic acid; 13-HOPT, 13(S)-hydroperoxy-octadecatrienoic acid; ACS, acyl-CoA synthetase; ACX, acyl-CoA oxidase; FAD, fatty acid desaturases; KAT, 3-ketoacyl-CoA thiolase; MFP, multifunctional protein; OPR3, OPDA reductase 3 (Zhai *et al.,*2017).

Differences in expression pattern of genetic pathway related to JA biosynthesis were also observed in *ddc* compared to WT starting from Ctrl condition (comparison ***ddc vs* WT- Ctrl)** (Fig. 3.19 A). Namely, a general down-regulation of *LOX2, LOX3, LOX4 AOC1, AOC2* and *OPR3* genes, working in the first steps in JA biosynthesis, was clearly evident in the mutant (Fig. 3.19 A). Concerning Cd effect, in the WT the exposure to 25 µM Cd concentration was found to induce a down-regulation of the following 8 genes, *LOX2, LOX3, LOX4, AOS, AOC1, AOC2, OPR3* and *KAT5* (comparison **25 µM Cd *vs* Ctrl –WT)**. Whereas, in *dcc* mutant *LOX3, LOX5, AOS* and *KAT5* genes also resulted down-regulated, but *LOX4* was up-regulated (comparison **25 µM Cd *vs* Ctrl – *ddc)*** (Fig. 3.19 B). However, under this Cd concentration (25 µM) no differences were found when comparing *ddc* mutant *vs* WT (comparison ***ddc vs* WT -25 µM Cd)** (Fig. 3.19 B).
When 50 µM Cd concentration was used, only *LOX5* and *AOS* were down-regulated in the WT, (comparison **50 µM Cd *vs* Ctrl –WT),** while the *ddc* showed a down-regulation of *LOX5* and an up-regulation of *LOX4* and *OPR1* genes (comparison **50 µM Cd *vs* Ctrl – *ddc)*** (Fig. 3.19 C). Also under this treatment, no differences were found when comparing *ddc* mutant *vs* WT under this Cd concentration (50 µM) (comparison ***ddc vs* WT -50 µM Cd)** (Fig. 3.19 C).

Globally, the emerging picture is that Cd affects JA biosynthesis in WT more than *ddc* whatever concentration was applied.

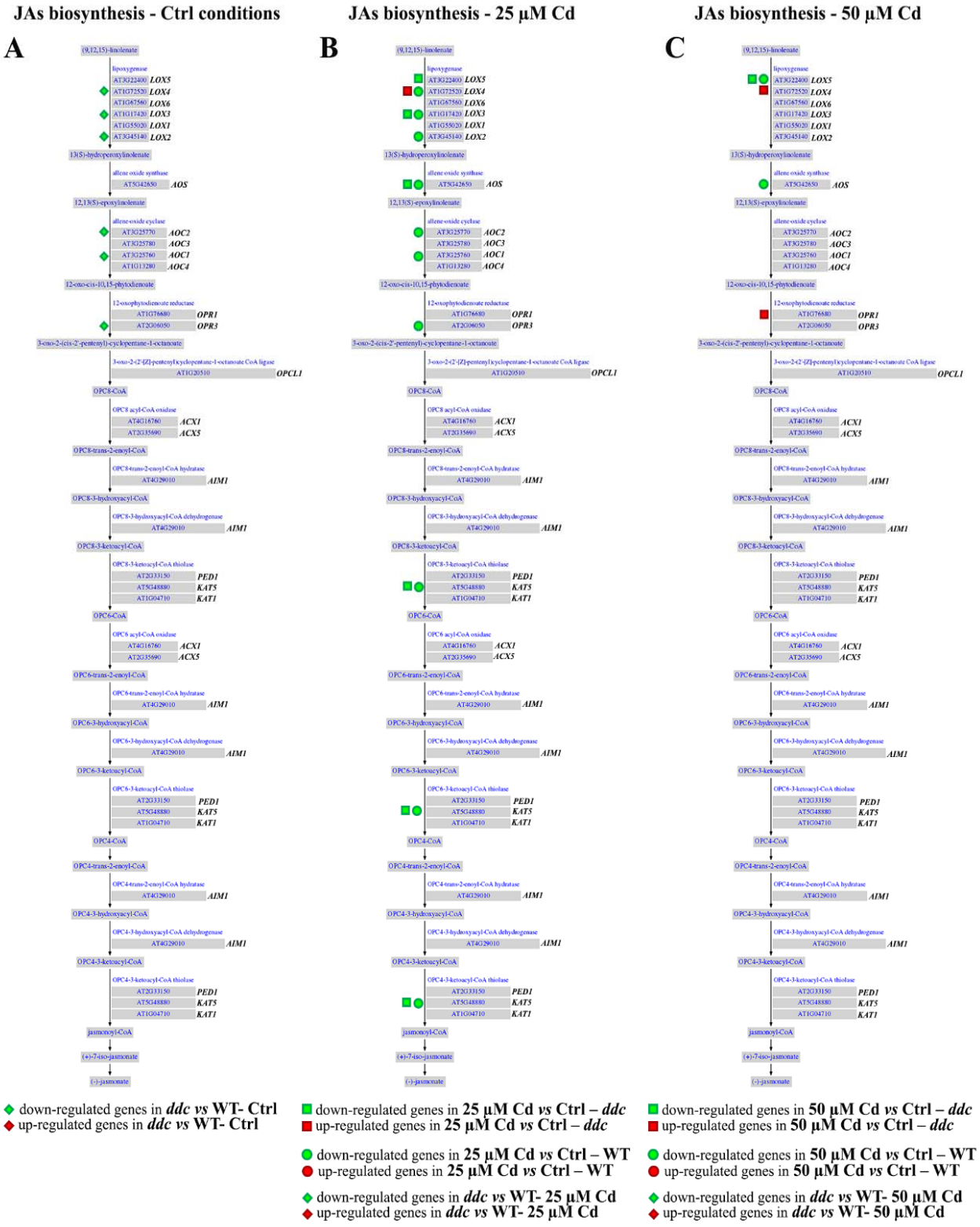

Figure 3.19: Genes differentially expressed (DEGs) along the pathway of jasmonic acid biosynthesis in *ddc* and WT seedlings identified through a transcriptomic approach. Seedling grown **(A)** in Ctrl condition, **(B)** under treatment with 25 µM Cd and **(C)** 50 µM Cd.

3.3.3.5 Abscisic acid

Box 5

Abscisic acid biosynthetic pathway

Abscisic acid (ABA) is a 15-carbon (C15) terpenoid hormone which regulate plant resistance to abiotic stress such as drought, salinity, and low temperature, and participate in plant growth and development mechanisms such as embryo development and seed maturation, seed dormancy and germination, seedling establishment, vegetative development, root growth, stomatal movement, flowering, pathogen response, and senescence (reviewed by Finkelstein, 2013).

The first step of ABA biosynthesis occurs in plastids and consists in the geranylgeranyl diphosphate (GGPP) biosynthesis through the addition of three C5-isopentenyl diphosphate (IPP) molecules to dimethylallyl diphosphate. Two GGPP molecules are condensed by phytoene synthase (PSY) to form C40-phytoene, that is converted in either α- or β-carotene by subsequent desaturation, isomerization, and cyclization step. Only β-carotene can be further metabolized into ABA via zeaxanthin. In *A. thaliana*, two genes (*BCH1* and *BCH2*) encode β-carotene hydroxylases enzymes, that catalyse β-carotene conversion in zeaxanthin, that will be further processed to produce all-*trans*-violaxanthin by zeaxanthin epoxidase (ZEP), that will be later converted in 9′-*cis*-neoxanthin or 9-*cis*-violaxanthin (Rock and Zeevaart, 1991; Barrero *et al.,*2005; reviewed by Li *et al.,*2017).

The oxidative cleavage of 9′-*cis*-neoxanthin and/or 9-*cis*-violaxanthin to produce xanthonin, an intermediate with physiological properties like ABA, is catalysed by *9-cis*-epoxycarotenoid dioxygenase (NCED) (Nambara and Marion-Poll, 2005).

Afterwards, xanthoxin is transferred to the cytoplasm and converted to abscisic aldehyde by a short-chain dehydrogenase/reductase (SDR)-like enzyme encoded by *ABA2* gene in *A. thaliana* (Cheng *et al.,*2002; Gonzalez-Guzman *et al.,*2002), while the final step is catalysed by abscisic aldehyde oxidases family (AAOs) enzymes (Bittner *et al.,*2001; Xiong *et al.,*2001).

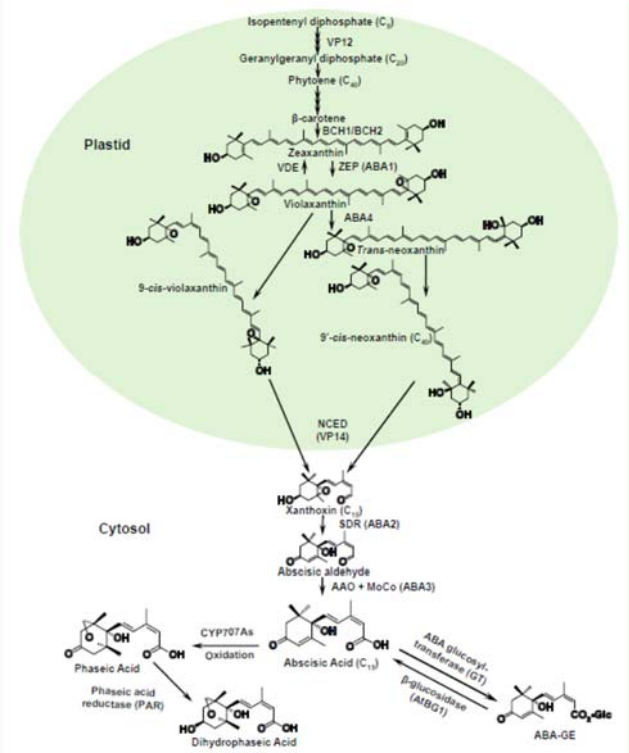

Figure B4: Abscisic acid metabolic pathways in plants. The first step of ABA biosynthesis occurs in plastids and consists in the geranylgeranyl diphosphate (GGPP) biosynthesis through the addition of three C5-isopentenyl diphosphate (IPP) molecules to dimethylallyl diphosphate. Two GGPP molecules are condensed by PSY to form C40-phytoene and, subsequently, in β-carotene, that will be further metabolized into ABA via zeaxanthin. Later, zeaxanthin, will be further processed by ZEP to produce all-*trans*-violaxanthin that will be later converted in 9′-*cis*-neoxanthin or 9-*cis*-violaxanthin, which will be converted by NCED in xanthonin. Afterwards, xanthoxin is transferred to the cytoplasm and converted to abscisic aldehyde by a short-chain dehydrogenase/reductase (SDR)-like enzyme. The final step is catalysed by AAOs, to produce ABA (Li *et al.,*2017).

ABA catabolic pathways

ABA catabolism involves hydroxylation to regulate hormones levels *in vivo* (reviewed in Nambara and Marion-Poll, 2005). 8′-hydroxylation is the predominant ABA catabolic pathway (Cutler and Krochko, 1999). This pathway is catalysed by 8′-hydroxylase enzyme, encoded in *A. thaliana* by *CYP707A* gene. The reaction leads to the formation of 8′-hydroxy-ABA, that spontaneously rearranges itself in phaseic acid (PA), that will be further catabolised in dihydrophaseic acid (Kushiro *et al.,*2004; Saito *et al.,*2004; Okamoto *et al.,*2006).

Both ABA and its catabolites can be subjected to conjugation reaction catalysed by glucosyl transferases. The most common product of ABA glucosylation is the physiologically inactive ABA-glucosyl ester (ABA-GE), that is a potential storage/transport form which hydrolysis by β-glucosidase (AtBG1 in *A. thaliana*) could release free ABA when and where needed (Lee *et al.,*2006; Xu *et al.,*2012).

Concerning genetic pathway related to ABA (Box 5, Fig. B4), in Ctrl condition the biosynthetic pathway wasn't differentially modulated in *ddc* compared to WT (comparison ***ddc vs* WT- Ctrl)** (Fig. 3.20 A). After Cd treatment only one gene along the pathway, *NCED3*, resulted down-regulated both in the mutant and the WT whatever concentration was considered (comparisons: **25 µM Cd *vs* Ctrl –WT; 25 µM Cd *vs* Ctrl – *ddc;* 50 µM Cd *vs* Ctrl –WT; 50 µM Cd *vs* Ctrl – *ddc)*** (Fig. 3.20 B, C). All the other multiple pairwise comparison analysed didn't show any significant difference (comparisons: ***ddc vs* WT - 25 µM Cd; *ddc vs* WT -50 µM Cd)** (Fig. 3.20 B, C).

A

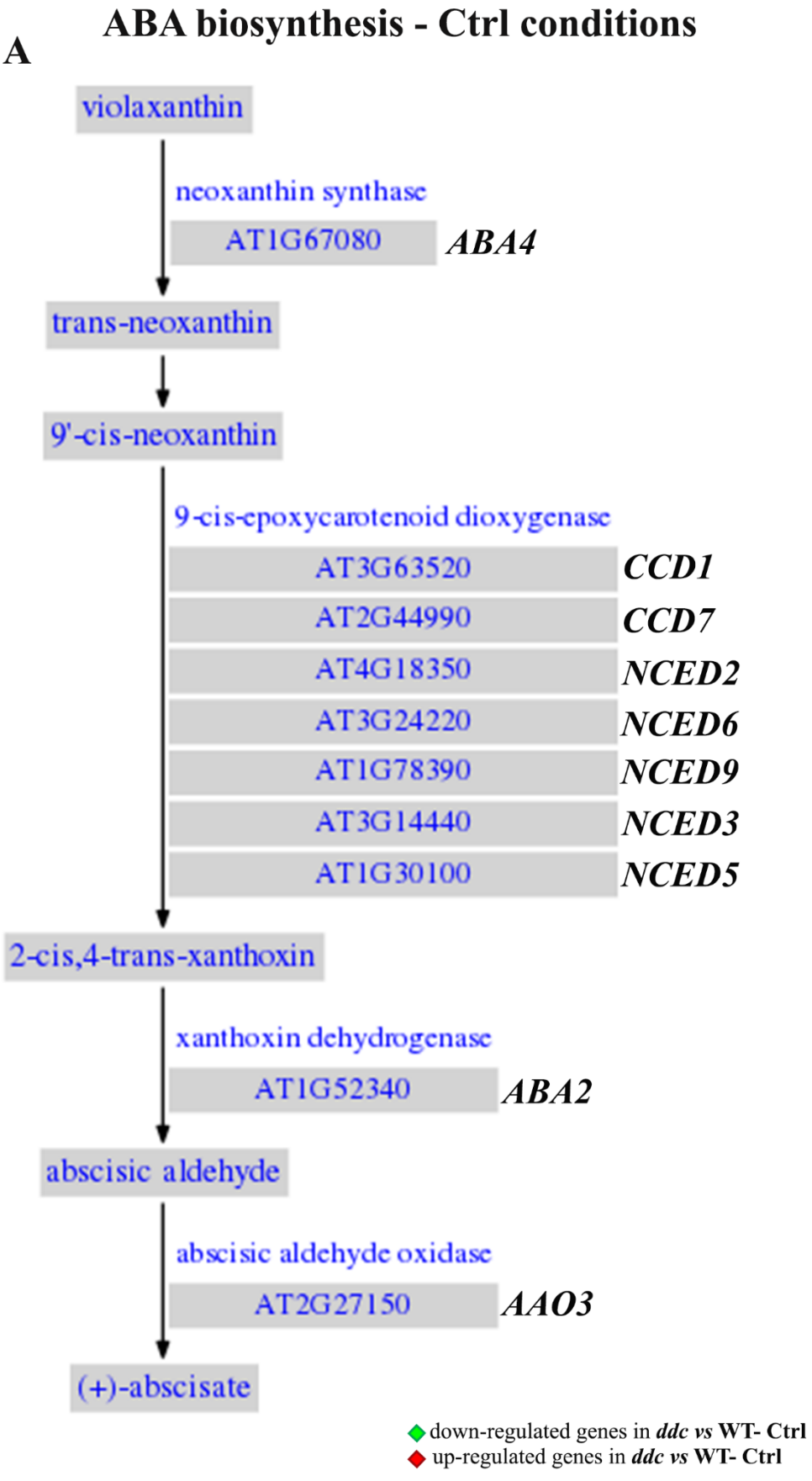
ABA biosynthesis - Ctrl conditions
violaxanthin
neoxanthin synthase
AT1G67080
ABA4
trans-neoxanthin
9'-cis-neoxanthin
9-cis-epoxycarotenoid dioxygenase
AT3G63520
CCD1
AT2G44990
CCD7
AT4G18350
NCED2
AT3G24220
NCED6
AT1G78390
NCED9
AT3G14440
NCED3
AT1G30100
NCED5
2-cis,4-trans-xanthoxin
xanthoxin dehydrogenase
AT1G52340
ABA2
abscisic aldehyde
abscisic aldehyde oxidase
AT2G27150
AAO3
(+)-abscisate
down-regulated genes in ddc vs WT- Ctrl
up-regulated genes in ddc vs WT- Ctrl

B

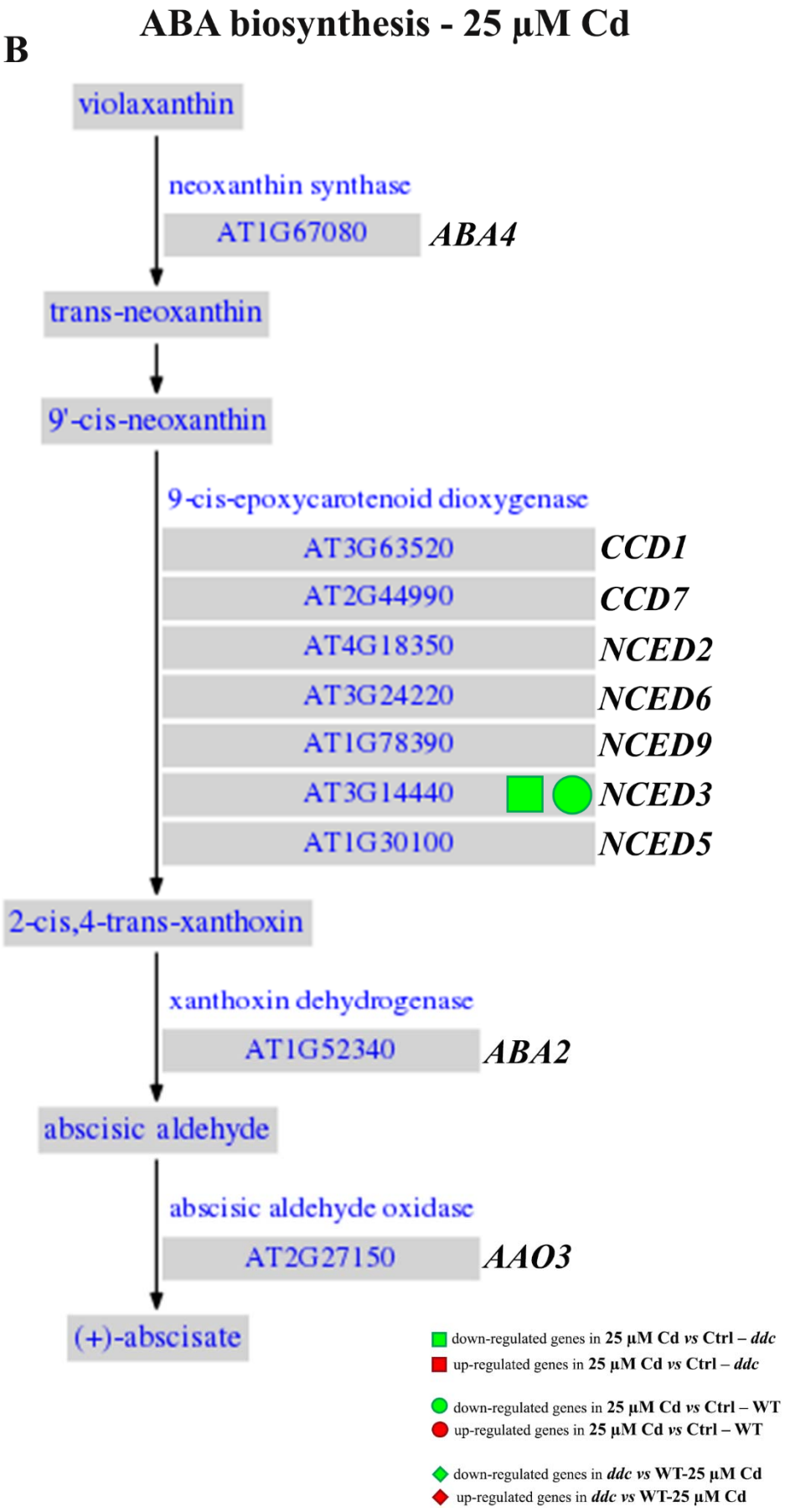
ABA biosynthesis - 25 µM Cd
violaxanthin
neoxanthin synthase
AT1G67080
ABA4
trans-neoxanthin
9'-cis-neoxanthin
9-cis-epoxycarotenoid dioxygenase
AT3G63520
CCD1
AT2G44990
CCD7
AT4G18350
NCED2
AT3G24220
NCED6
AT1G78390
NCED9
AT3G14440
NCED3
AT1G30100
NCED5
2-cis,4-trans-xanthoxin
xanthoxin dehydrogenase
AT1G52340
ABA2
abscisic aldehyde
abscisic aldehyde oxidase
AT2G27150
AAO3
(+)-abscisate
down-regulated genes in 25 µM Cd vs Ctrl – ddc
up-regulated genes in 25 µM Cd vs Ctrl – ddc
down-regulated genes in 25 µM Cd vs Ctrl – WT
up-regulated genes in 25 µM Cd vs Ctrl – WT
down-regulated genes in ddc vs WT-25 µM Cd
up-regulated genes in ddc vs WT-25 µM Cd

C

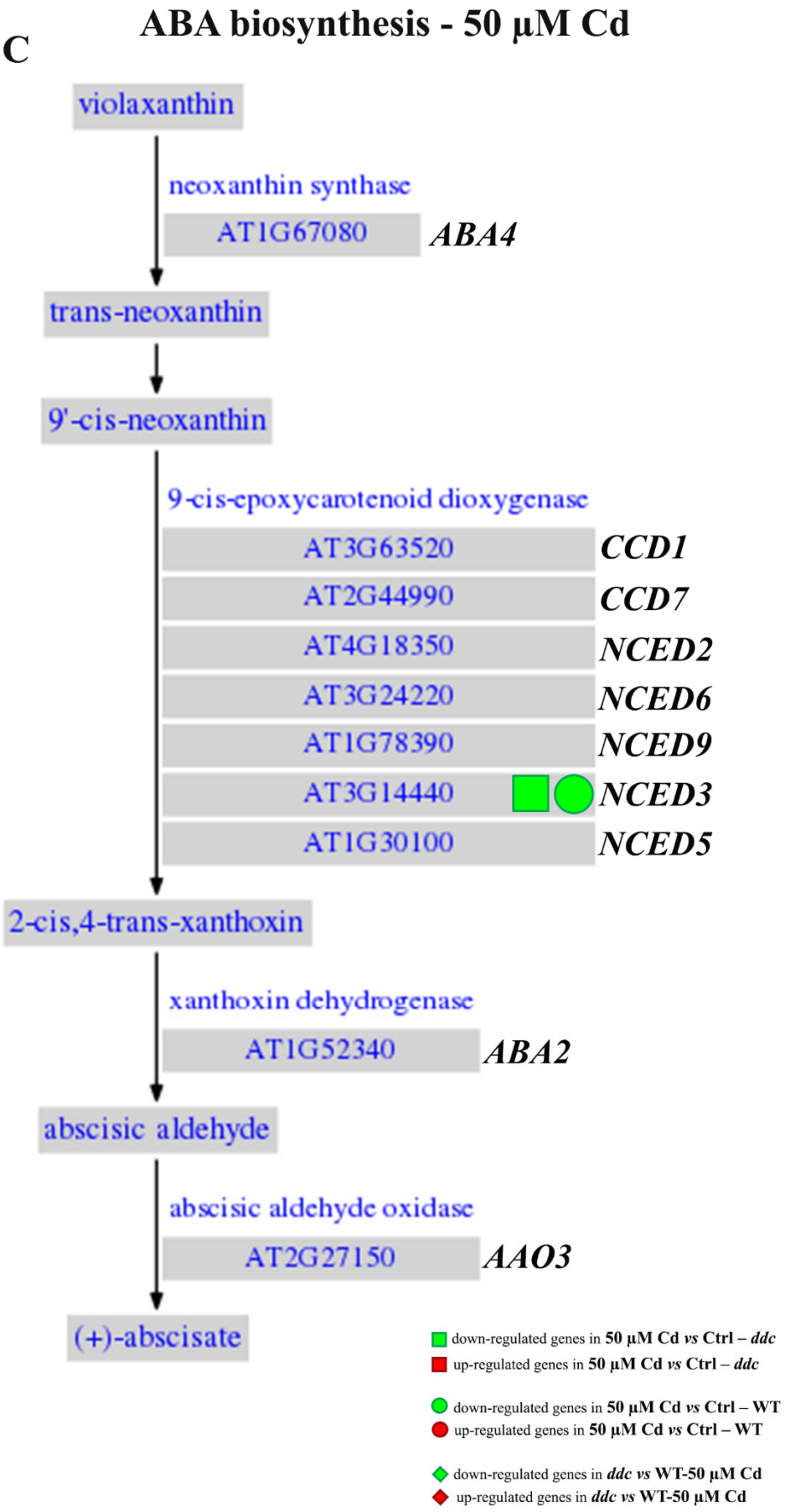
ABA biosynthesis - 50 µM Cd
violaxanthin
neoxanthin synthase
AT1G67080
ABA4
trans-neoxanthin
9'-cis-neoxanthin
9-cis-epoxycarotenoid dioxygenase
AT3G63520
CCD1
AT2G44990
CCD7
AT4G18350
NCED2
AT3G24220
NCED6
AT1G78390
NCED9
AT3G14440
NCED3
AT1G30100
NCED5
2-cis,4-trans-xanthoxin
xanthoxin dehydrogenase
AT1G52340
ABA2
abscisic aldehyde
abscisic aldehyde oxidase
AT2G27150
AAO3
(+)-abscisate
down-regulated genes in 50 µM Cd vs Ctrl – ddc
up-regulated genes in 50 µM Cd vs Ctrl – ddc
down-regulated genes in 50 µM Cd vs Ctrl – WT
up-regulated genes in 50 µM Cd vs Ctrl – WT
down-regulated genes in ddc vs WT-50 µM Cd
up-regulated genes in ddc vs WT-50 µM Cd

Figure 3.20: Genes differentially expressed (DEGs) along the pathway of abscisic acid biosynthesis in *ddc* and WT seedlings identified through a transcriptomic approach. Seedling grown **(A)** in Ctrl condition, **(B)** under treatment with 25 µM Cd and **(C)** 50 µM Cd.

Under Ctrl condition, also the genetic pathways related to ABA catabolism did not show different expression pattern in *ddc vs* WT (comparison ***ddc vs* WT- Ctrl)** (Fig. 3.21 A). Under 25 µM Cd treatment no differential expression of genes involved in the degradation pathway was observed in the WT (comparison **25 µM Cd *vs* Ctrl –WT)** (Fig. 3.21 B), while *ddc* mutant showed a down-regulation of *CYP707A3* gene (comparison **25 µM Cd *vs* Ctrl – *ddc)*** (Fig. 3.21 B). Moreover, at 25 µM Cd concentration, along this pathway also *CYP707A2* resulted down-regulated when comparing *ddc vs* WT (comparison ***ddc vs* WT -25 µM Cd)** (Fig. 3.21 B). Both these genes are involved in the degradative production of phaseic acid along the pathway. An up-regulation of ABA degradation pathway was instead observed in both *ddc* and WT at 50 µM Cd-concentration, which involved in the WT only the *CYP707A4* gene (comparison **50 µM Cd *vs* Ctrl –WT)** and in the *ddc* mutant both *CYP707A2* and *CYP707A4* genes (comparisons: **50 µM Cd *vs* Ctrl –WT; 50 µM Cd *vs* Ctrl – *ddc)*** (Fig. 3.21).

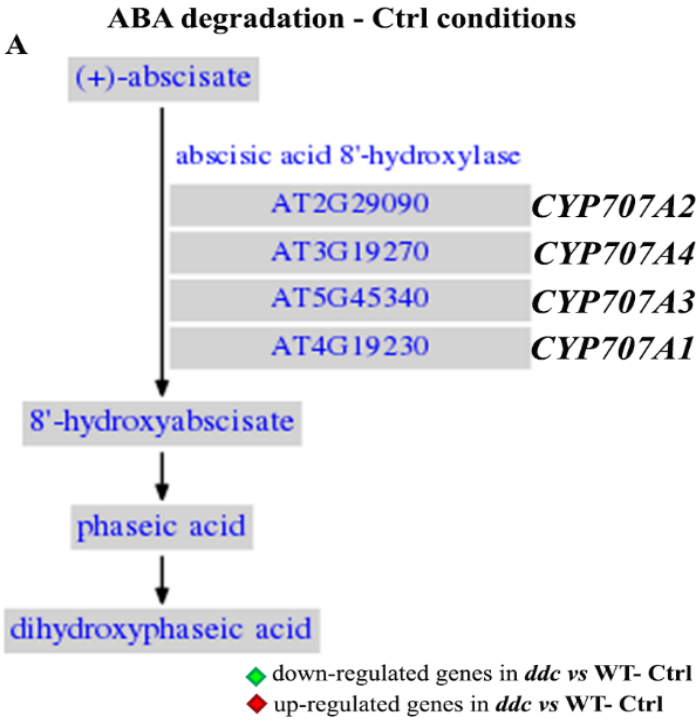

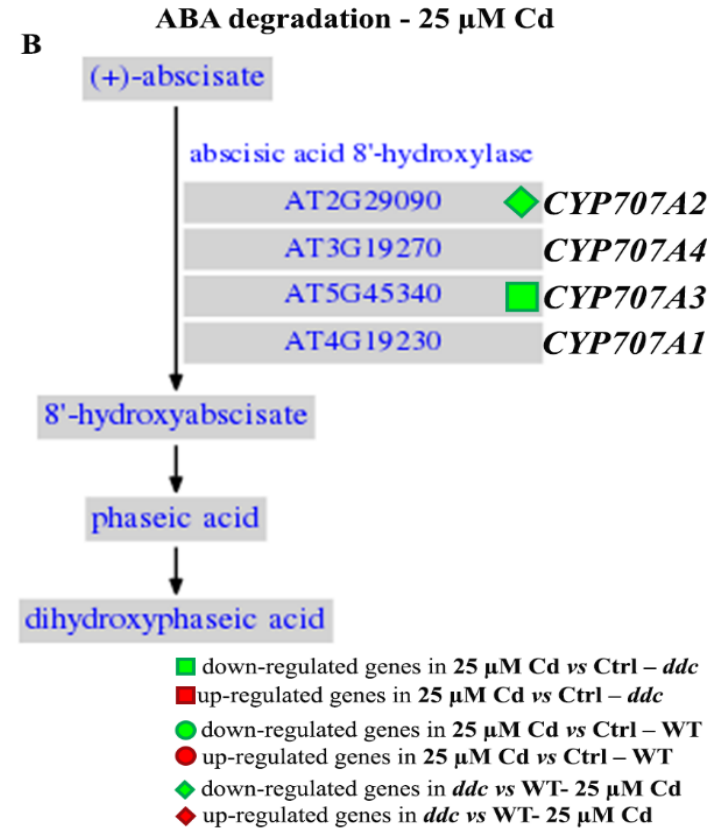
B
ABA degradation - 25 µM Cd
(+)-abscisate
abscisic acid 8'-hydroxylase
AT2G29090
CYP707A2
AT3G19270
CYP707A4
AT5G45340
CYP707A3
AT4G19230
CYP707A1
8'-hydroxyabscisate
phaseic acid
dihydroxyphaseic acid
down-regulated genes in 25 µM Cd vs Ctrl – ddc
up-regulated genes in 25 µM Cd vs Ctrl – ddc
down-regulated genes in 25 µM Cd vs Ctrl – WT
up-regulated genes in 25 µM Cd vs Ctrl – WT
down-regulated genes in ddc vs WT- 25 µM Cd
up-regulated genes in ddc vs WT- 25 µM Cd

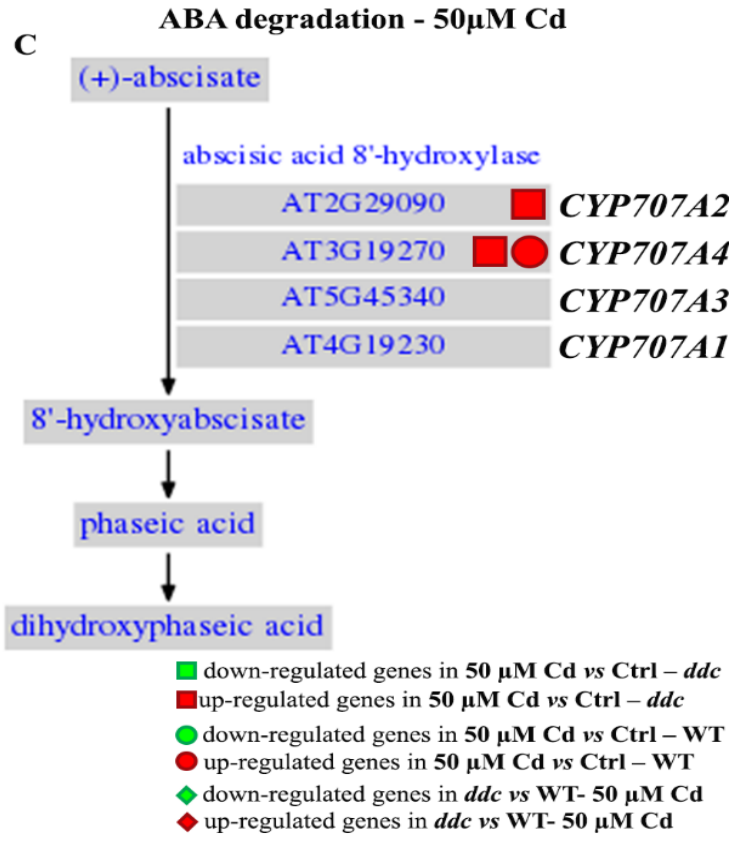
C
ABA degradation - 50µM Cd
(+)-abscisate
abscisic acid 8'-hydroxylase
AT2G29090
CYP707A2
AT3G19270
CYP707A4
AT5G45340
CYP707A3
AT4G19230
CYP707A1
8'-hydroxyabscisate
phaseic acid
dihydroxyphaseic acid
down-regulated genes in 50 µM Cd vs Ctrl – ddc
up-regulated genes in 50 µM Cd vs Ctrl – ddc
down-regulated genes in 50 µM Cd vs Ctrl – WT
up-regulated genes in 50 µM Cd vs Ctrl – WT
down-regulated genes in ddc vs WT- 50 µM Cd
up-regulated genes in ddc vs WT- 50 µM Cd

Figure 3.21: Genes differentially expressed (DEGs) along the pathway of abscisic acid degradation in *ddc* and WT seedlings identified through a transcriptomic approach. Seedling grown **(A)** in Ctrl condition, **(B)** under treatment with 25 µM Cd and **(C)** 50 µM Cd.

Concerning the genetic pathway related to ABA inactivation through glucose conjugation (ABA glucose ester (ABA-GE) biosynthesis), under Ctrl condition it wasn't differentially modulated in *ddc* mutant compared to WT (comparison ***ddc vs* WT- Ctrl)** (Fig. 3.22 A). It was instead differentially impacted by Cd treatment in the two samples. Namely, following 25 µM Cd treatment *ddc* mutant showed an up-regulation of *AT4G15260* and a down-regulation of *UGT71C3* expression (comparison **25 µM Cd *vs* Ctrl – *ddc)***, while no differences were induced in the WT (comparison **25 µM Cd *vs* Ctrl –WT)** (Fig. 3.22 B). However, no significant differences were highlighted when comparing *ddc vs* WT at 25 µM Cd (comparison ***ddc vs* WT -25 µM Cd)** (Fig. 3.22 B). Under 50 µM Cd treatment, the expression pattern of genetic pathway related to AGE-GE biosynthesis was impacted in both WT and *ddc* mutant in a similar way. In fact, in the WT such impact resulted into a down-regulation of *UGT71C1* and *UGT2* genes and an up-regulation of *UGT71B5*, *AT4G5260, AT5G49690* and *UGT71B6* (comparison **50 µM Cd *vs* Ctrl –WT)** (Fig. 3.22 C); in *ddc* mutant *UGT71C1* and *UGT2* were down-regulated, whereas *UGT71B5, AT5G49690* and *UGT71B6* were up-regulated (comparison **50 µM Cd *vs* Ctrl – *ddc)*** (Fig. 3.22 C).

From these data it's possible to conclude that Cd exposition determined a slight down-regulation of ABA biosynthesis in both *ddc* and WT samples, independently from the heavy metal concentration that was applied. ABA catabolic pathway was lightly down-regulated in *ddc* mutant at the lower Cd concentration, while in both samples it was up-regulated under 50 µM Cd treatment. We suggest that the down-regulation of ABA degradation detected in *ddc* mutant exposed to 25 µM Cd could be an early compensatory mechanism for ABA biosynthesis down-regulation determined by Cd exposition.

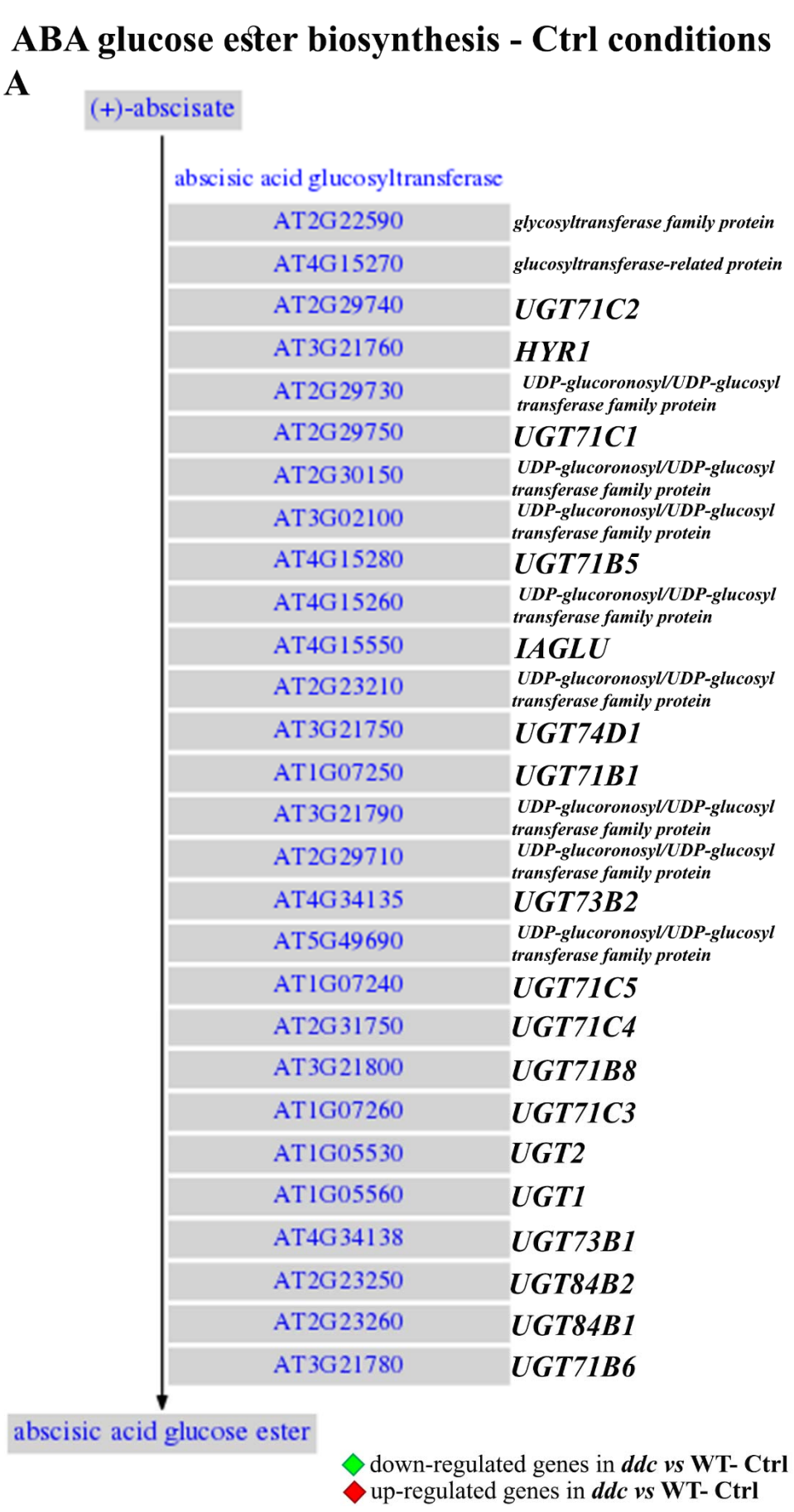
ABA glucose ester biosynthesis - Ctrl conditions
A
(+)-abscisate
abscisic acid glucosyltransferase
AT2G22590 glycosyltransferase family protein
AT4G15270 glucosyltransferase-related protein
AT2G29740 UGT71C2
AT3G21760 HYR1
AT2G29730 UDP-glucoronosyl/UDP-glucosyl transferase family protein
AT2G29750 UGT71C1
AT2G30150 UDP-glucoronosyl/UDP-glucosyl transferase family protein
AT3G02100 UDP-glucoronosyl/UDP-glucosyl transferase family protein
AT4G15280 UGT71B5
AT4G15260 UDP-glucoronosyl/UDP-glucosyl transferase family protein
AT4G15550 IAGLU
AT2G23210 UDP-glucoronosyl/UDP-glucosyl transferase family protein
AT3G21750 UGT74D1
AT1G07250 UGT71B1
AT3G21790 UDP-glucoronosyl/UDP-glucosyl transferase family protein
AT2G29710 UDP-glucoronosyl/UDP-glucosyl transferase family protein
AT4G34135 UGT73B2
AT5G49690 UDP-glucoronosyl/UDP-glucosyl transferase family protein
AT1G07240 UGT71C5
AT2G31750 UGT71C4
AT3G21800 UGT71B8
AT1G07260 UGT71C3
AT1G05530 UGT2
AT1G05560 UGT1
AT4G34138 UGT73B1
AT2G23250 UGT84B2
AT2G23260 UGT84B1
AT3G21780 UGT71B6
abscisic acid glucose ester
down-regulated genes in ddc vs WT- Ctrl
up-regulated genes in ddc vs WT- Ctrl

B

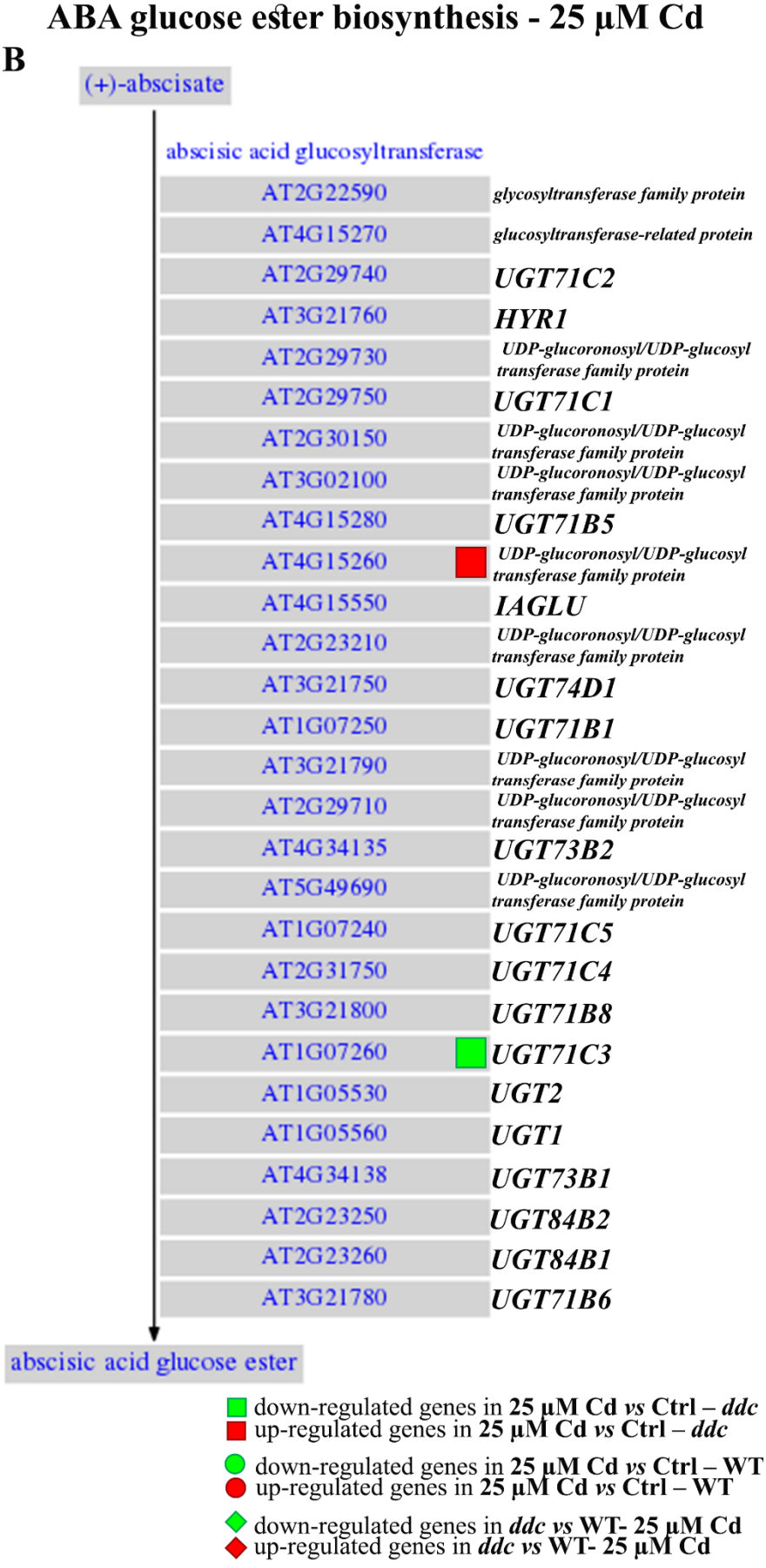
ABA glucose ester biosynthesis - 25 µM Cd
(+)-abscisate
abscisic acid glucosyltransferase
AT2G22590 glycosyltransferase family protein
AT4G15270 glucosyltransferase-related protein
AT2G29740 UGT71C2
AT3G21760 HYR1
AT2G29730 UDP-glucoronosyl/UDP-glucosyl transferase family protein
AT2G29750 UGT71C1
AT2G30150 UDP-glucoronosyl/UDP-glucosyl transferase family protein
AT3G02100 UDP-glucoronosyl/UDP-glucosyl transferase family protein
AT4G15280 UGT71B5
AT4G15260 UDP-glucoronosyl/UDP-glucosyl transferase family protein
AT4G15550 IAGLU
AT2G23210 UDP-glucoronosyl/UDP-glucosyl transferase family protein
AT3G21750 UGT74D1
AT1G07250 UGT71B1
AT3G21790 UDP-glucoronosyl/UDP-glucosyl transferase family protein
AT2G29710 UDP-glucoronosyl/UDP-glucosyl transferase family protein
AT4G34135 UGT73B2
AT5G49690 UDP-glucoronosyl/UDP-glucosyl transferase family protein
AT1G07240 UGT71C5
AT2G31750 UGT71C4
AT3G21800 UGT71B8
AT1G07260 UGT71C3
AT1G05530 UGT2
AT1G05560 UGT1
AT4G34138 UGT73B1
AT2G23250 UGT84B2
AT2G23260 UGT84B1
AT3G21780 UGT71B6
abscisic acid glucose ester
down-regulated genes in 25 µM Cd vs Ctrl – ddc
up-regulated genes in 25 µM Cd vs Ctrl – ddc
down-regulated genes in 25 µM Cd vs Ctrl – WT
up-regulated genes in 25 µM Cd vs Ctrl – WT
down-regulated genes in ddc vs WT- 25 µM Cd
up-regulated genes in ddc vs WT- 25 µM Cd

C

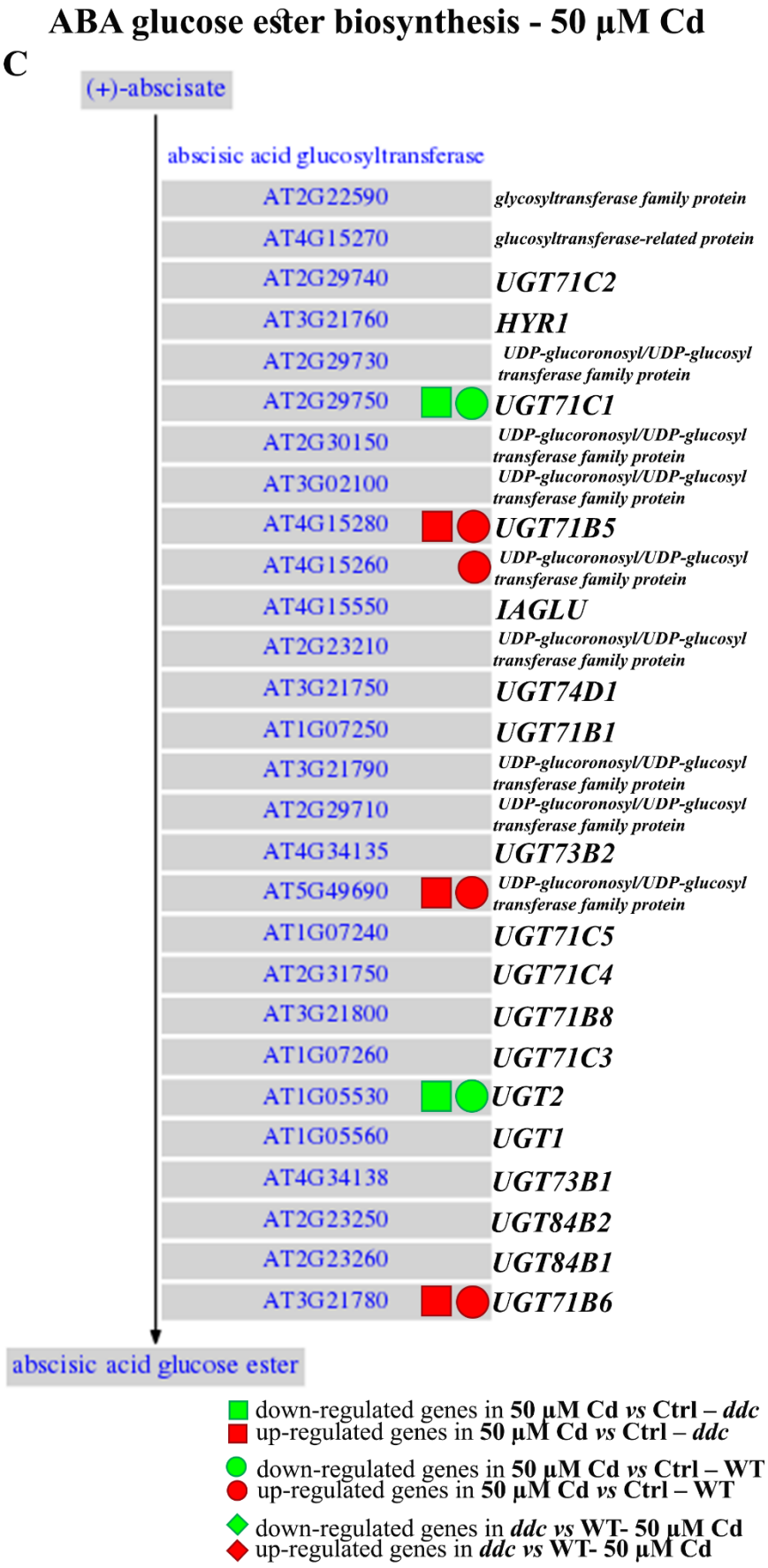
ABA glucose ester biosynthesis - 50 µM Cd
(+)-abscisate
abscisic acid glucosyltransferase
AT2G22590 glycosyltransferase family protein
AT4G15270 glucosyltransferase-related protein
AT2G29740 UGT71C2
AT3G21760 HYR1
AT2G29730 UDP-glucoronosyl/UDP-glucosyl transferase family protein
AT2G29750 UGT71C1
AT2G30150 UDP-glucoronosyl/UDP-glucosyl transferase family protein
AT3G02100 UDP-glucoronosyl/UDP-glucosyl transferase family protein
AT4G15280 UGT71B5
AT4G15260 UDP-glucoronosyl/UDP-glucosyl transferase family protein
AT4G15550 IAGLU
AT2G23210 UDP-glucoronosyl/UDP-glucosyl transferase family protein
AT3G21750 UGT74D1
AT1G07250 UGT71B1
AT3G21790 UDP-glucoronosyl/UDP-glucosyl transferase family protein
AT2G29710 UDP-glucoronosyl/UDP-glucosyl transferase family protein
AT4G34135 UGT73B2
AT5G49690 UDP-glucoronosyl/UDP-glucosyl transferase family protein
AT1G07240 UGT71C5
AT2G31750 UGT71C4
AT3G21800 UGT71B8
AT1G07260 UGT71C3
AT1G05530 UGT2
AT1G05560 UGT1
AT4G34138 UGT73B1
AT2G23250 UGT84B2
AT2G23260 UGT84B1
AT3G21780 UGT71B6
abscisic acid glucose ester
down-regulated genes in 50 µM Cd vs Ctrl – ddc
up-regulated genes in 50 µM Cd vs Ctrl – ddc
down-regulated genes in 50 µM Cd vs Ctrl – WT
up-regulated genes in 50 µM Cd vs Ctrl – WT
down-regulated genes in ddc vs WT- 50 µM Cd
up-regulated genes in ddc vs WT- 50 µM Cd

Figure 3.22: Genes differentially expressed (DEGs) along the pathway of abscisic acid glucose ester biosynthesis in *ddc* and WT seedlings identified through a transcriptomic approach. Seedling grown **(A)** in Ctrl condition, **(B)** under treatment with 25 µM Cd and **(C)** 50 µM Cd.

3.3.3.6 Ethylene

Box 6

Ethylene biosynthetic pathway

Ethylene is a gaseous plant hormone involved in both plant growth and development and biotic and abiotic stress responses. Even though its production is not tissue-specific, ethylene biosynthesis is tightly controlled in response to environmental and internal stimuli (Yang and Hoffman, 1984; Kende, 1993; Fluhr *et al.,*1996;).

In higher plants, ethylene is synthetized from S-adenosylmethionine (SAM), an activated form of the amino acid methionine (Met). SAM is the substrate of 1-aminocyclopropane-1-carboxylate synthase (ACC synthase, ACS) enzyme, that catalyse the formation of ACC. Subsequently, ACC is converted in ethylene by ACC oxidase (ACO), that oxidases ACC to ethylene, CO_2, and cyanide (Yang and Hoffmann, 1984).

ACS and ACO are codified by small gene families which expression is regulated at both transcriptional and post-transcriptional level (Xu and Zhang, 2014). In particular, ACS genes codify the rate-limiting enzymes in ethylene biosynthesis and are strictly regulated throughout plant development and in response to stresses (Lin *et al.,*2009). Many environmental stresses can induce ethylene production by *ACS* genes transcription up-regulation and different *ACS* genes present different expression patterns in response to different stresses (Peng *et al.,*2005; Han *et al.,*2010; Li *et al.,*2012).

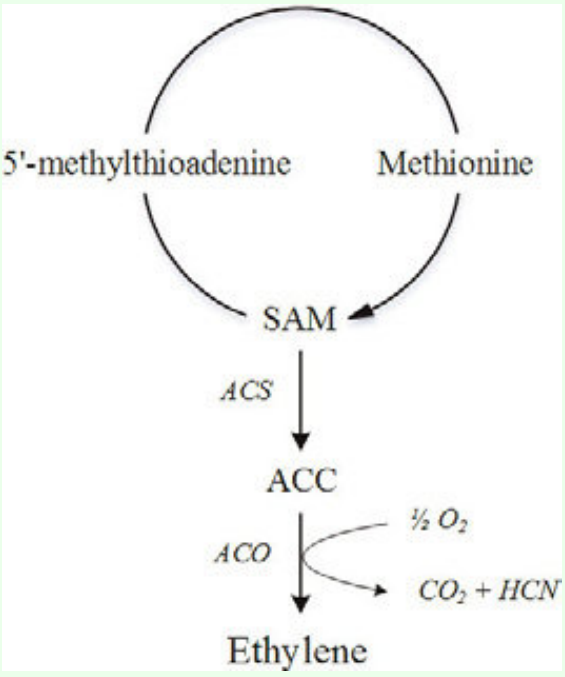

Figure B5: Ethylene biosynthesis in higher plants. Ethylene is synthetized from S-adenosylmethionine (SAM), an activated form of the amino acid methionine (Met). SAM is the substrate of ACC synthase, that catalyses the formation of ACC. Subsequently, ACC is converted in ethylene by ACC oxidase (ACO), that oxidases ACC to ethylene, CO_2, and cyanide (Mohsenzadeh *et al.,*2017).

Under Ctrl condition, an up-regulation of *ACS8* and *ACS11* genes working along ethylene biosynthesis pathway was observed in *ddc* compared to the WT (comparison ***ddc vs* WT- Ctrl)** (Fig. 3.23 A). Along this pathway, Cd treatment, at 25 µM Cd, was found to determine an up-regulation of *ACS4* gene in the WT (comparison **25 µM Cd *vs* Ctrl –WT)** (Fig. 3.23 B) and a down-regulation of two genes along the pathway, *ACS8* and *ACO5,* in *ddc* mutant (comparison **25 µM Cd *vs* Ctrl – *ddc)*** (Fig. 3.23 B). Moreover, under 25 µM Cd exposure, a down-regulation involving only *ACO1* gene was observed in *ddc* mutant compared to the WT (comparison ***ddc vs* WT -25 µM Cd)** (Fig. 3.23 B).

Globally, an up-regulation of this pathway was also found in WT exposed to 50 µM which exhibited an overexpression of *ACS2, ACS7* and *ACS11* (comparison **50 µM Cd *vs* Ctrl –WT)** (Fig. 3.23 C); a different impact was observed in *ddc* exposed to the same Cd concentration (50 µM) where an up-regulation of *ACS7* gene and a down-regulation of *ACO5* gene was detected (comparison **50 µM Cd *vs* Ctrl – *ddc)*** (Fig. 3.23 C). No differences were found when comparing the effects of 50 µM Cd treatment on *ddc vs* WT (comparison ***ddc vs* WT -50 µM Cd)** (Fig. 3.23 C)**.**

In summary, in Ctrl condition the genetic pathway related to ethylene biosynthesis was up-regulated in *ddc* compared to the WT. Cd treatment determined a general up-regulation of this genetic pathway in the WT, and its down-regulation in *ddc* mutant.

A

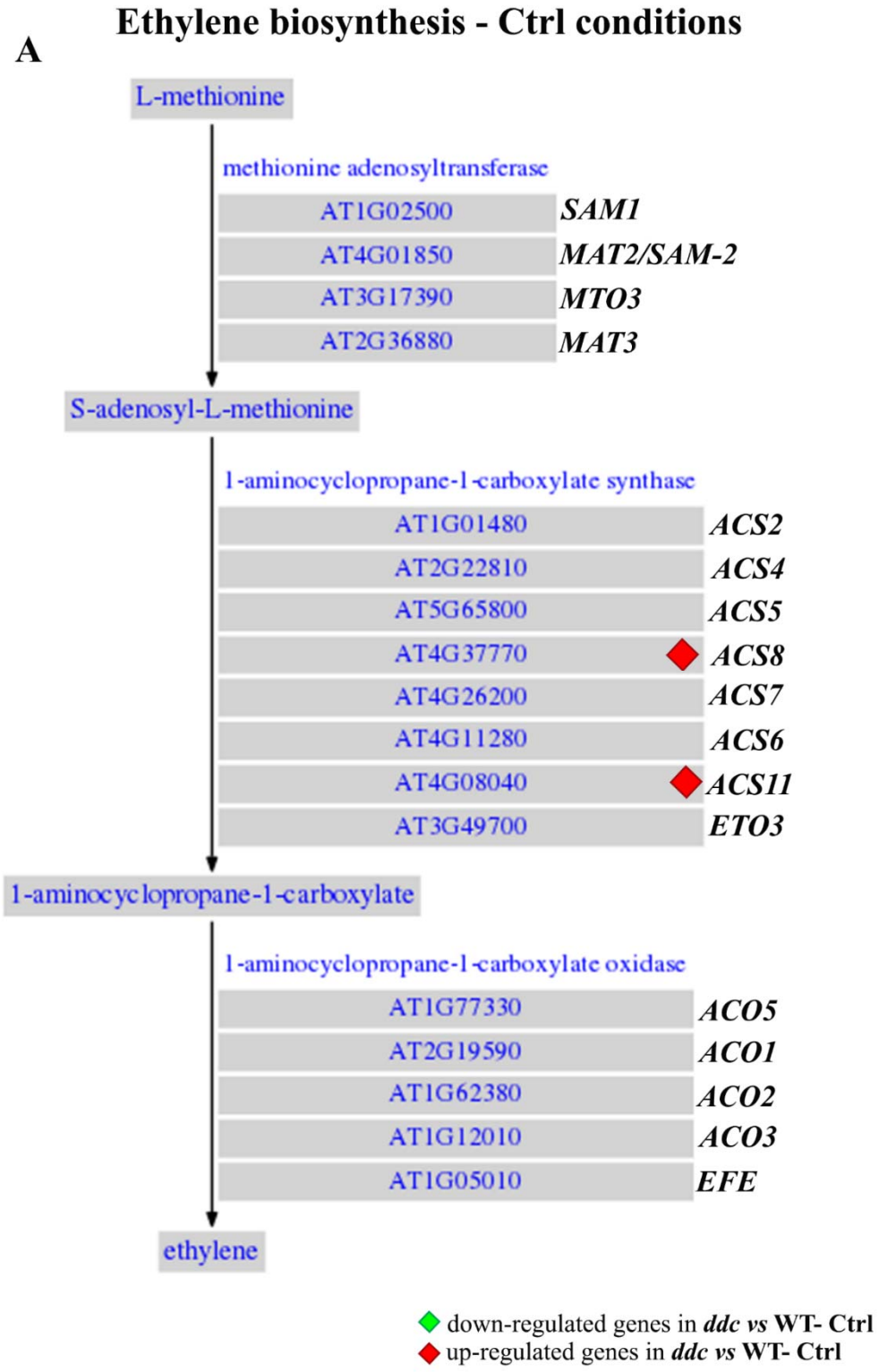
Ethylene biosynthesis - Ctrl conditions
L-methionine
methionine adenosyltransferase
AT1G02500 SAM1
AT4G01850 MAT2/SAM-2
AT3G17390 MTO3
AT2G36880 MAT3
S-adenosyl-L-methionine
1-aminocyclopropane-1-carboxylate synthase
AT1G01480 ACS2
AT2G22810 ACS4
AT5G65800 ACS5
AT4G37770 ACS8
AT4G26200 ACS7
AT4G11280 ACS6
AT4G08040 ACS11
AT3G49700 ETO3
1-aminocyclopropane-1-carboxylate
1-aminocyclopropane-1-carboxylate oxidase
AT1G77330 ACO5
AT2G19590 ACO1
AT1G62380 ACO2
AT1G12010 ACO3
AT1G05010 EFE
ethylene
down-regulated genes in ddc vs WT- Ctrl
up-regulated genes in ddc vs WT- Ctrl

B

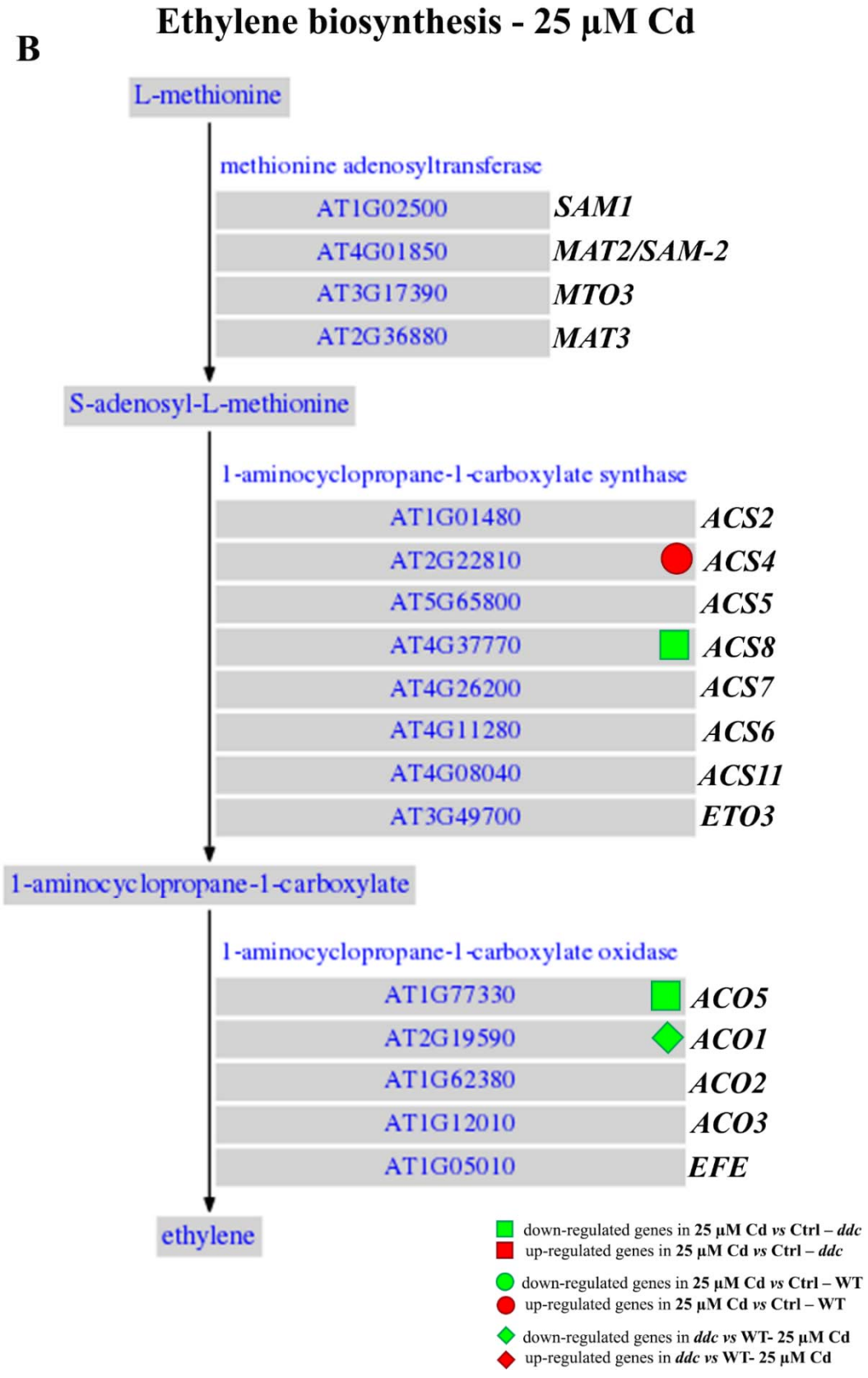
Ethylene biosynthesis - 25 µM Cd
L-methionine
methionine adenosyltransferase
AT1G02500 SAM1
AT4G01850 MAT2/SAM-2
AT3G17390 MTO3
AT2G36880 MAT3
S-adenosyl-L-methionine
1-aminocyclopropane-1-carboxylate synthase
AT1G01480 ACS2
AT2G22810 ACS4
AT5G65800 ACS5
AT4G37770 ACS8
AT4G26200 ACS7
AT4G11280 ACS6
AT4G08040 ACS11
AT3G49700 ETO3
1-aminocyclopropane-1-carboxylate
1-aminocyclopropane-1-carboxylate oxidase
AT1G77330 ACO5
AT2G19590 ACO1
AT1G62380 ACO2
AT1G12010 ACO3
AT1G05010 EFE
ethylene
down-regulated genes in 25 µM Cd vs Ctrl – ddc
up-regulated genes in 25 µM Cd vs Ctrl – ddc
down-regulated genes in 25 µM Cd vs Ctrl – WT
up-regulated genes in 25 µM Cd vs Ctrl – WT
down-regulated genes in ddc vs WT- 25 µM Cd
up-regulated genes in ddc vs WT- 25 µM Cd

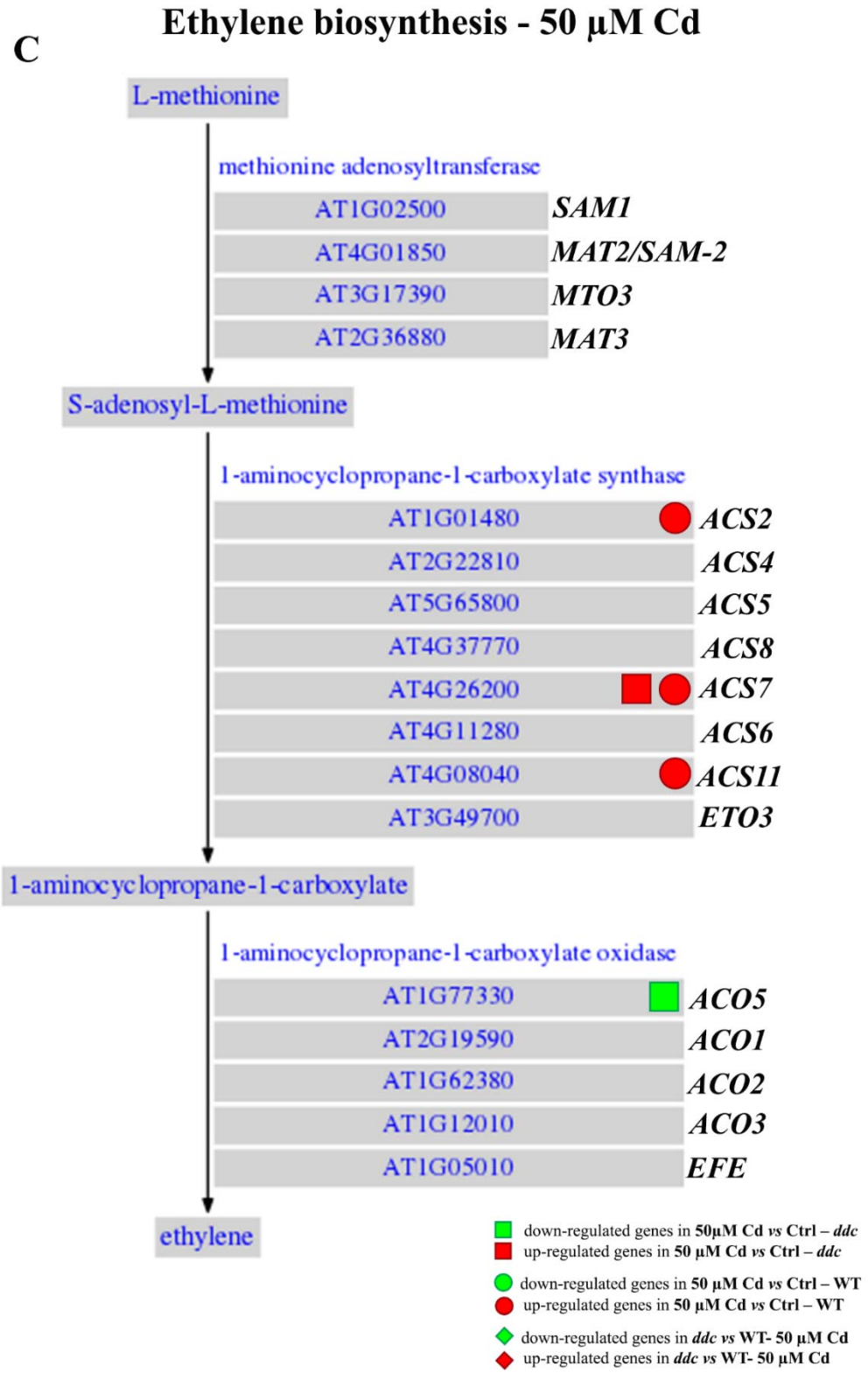

Figure 3.23: Genes differentially expressed (DEGs) along the pathway of ethylene biosynthesis in *ddc* and WT seedlings identified through a transcriptomic approach. Seedling grown **(A)** in Ctrl condition, **(B)** under treatment with 25 µM Cd and **(C)** 50 µM Cd.

3.3.4 Differential expression of genes involved in hormones signalling in *ddc* mutant and WT under Cd treatment.

Transcriptomic analysis evidenced that also the genetic pathways related to hormones signalling were differentially modulated in *ddc* mutant and WT plants under both Ctrl condition and Cd treatment.

To describe and discuss smoothly the obtained results, brief description of hormones signalling pathways will be included as boxes.

3.3.4.1 Auxin

Box 7

Auxin signalling pathway

Auxin signalling is initiated by modifications in auxin concentration, that are perceived by auxin receptors TIR1/AFB family (TRANSPORT INHIBITOR RESPONSE/AUXIN SIGNALING F-BOX). TIR1/AFB binds a regulatory protein of the AUX/IAA family, forming a co-receptor complex, and this interaction determines the ubiquitination and subsequently, the degradation of the AUX/IAA protein. (Korasick *et al.,*2015; Powers and Strader, 2016; Wang and Estelle, 2014). The effect is dose-dependent. Namely, different concentrations of IAA are sensed by different TIR1/AFB:Aux/IAA coreceptor combinations, determining different rates of Aux/IAA degradation (Dinesh *et al.,*2016).

In presence of low auxin concentration, AUX/IAA proteins interact with AUXIN RESPONSE FACTORS (ARFs) transcription factors and repress ARFs function by sequestering them away from their target promoters. This can occur through the binding of ARFs to the ARF auxin-responsive promoter elements (AuxREs) (Guilfoyle and Hagen, 2007), and by the recruitment of TOPLESS (TPL)/TPL-RELATED (TPR) corepressors, leading to chromatin inactivation and silencing of ARFs target genes (Long *et al.,*2006; Szemenyei *et al.,*2008; Kagale and Rozwadowski, 2011; Causier *et al.,*2012). ARFs are positive regulators of *AUX/IAA* genes, that are up-regulated in response to auxin in a negative feedback mechanism, and of *GH3* and *SAUR* family genes, that act downstream IAA signalling and promote plant growth (Tian *et al.,*2004; Li *et al.,*2016).

With respect to auxin signalling, no significant differences were detected at the transcriptomic level between *ddc* and WT under Ctrl condition (comparison ***ddc vs* WT-Ctrl)** (Fig. 3.24 A). However, a down-regulation of *SAUR* genes, belonging to the largest family of IAA responsive genes in plants (Ren and Gray, 2015), was observed in *ddc* mutant compared to the WT, suggesting a decrease of auxin response in the mutant. Under 25 µM Cd treatment, an overexpression of *AUX/IAA,* which acts as signalling repressor, was observed in the WT, suggesting a down-regulation of IAA signalling (comparison **25 µM Cd *vs* Ctrl –WT)** (Fig. 3.24 B). On the contrary, in *ddc* mutant the genetic pathway related to the signalling was globally up-regulated, as evidenced by the up-regulation of *SAUR* genes and the down-regulation of the repressor *AUX/IAA* and also of *GH3* genes which catalyse IAA conjugation (comparison **25 µM Cd *vs* Ctrl – *ddc)*** (Fig. 3.24 B). When comparing the effect of 25 µM Cd treatment on *ddc* mutant *vs* WT, a reduced expression of *AUX1, AUX/IAA, GH3* and *SAUR* was found. Note that *SAUR* down-regulation was due to the initial low level of expression of these family genes in the *ddc* compared to the WT under Ctrl condition (comparison ***ddc vs* WT -25 µM Cd)** (Fig. 3.24 A, B). At the highest Cd concentration, a similar expression pattern consisting in the down-regulation of *AUX/IAA* and *GH3* genes and the up-regulation of *SAUR* genes was observed in both *ddc* and WT, suggesting that at this concentration an up-regulation of IAA signalling pathway occurred in both samples (comparisons: **50 µM Cd *vs* Ctrl –WT*;* 50 µM Cd *vs* Ctrl – *ddc)*** (Fig. 3.24 C). No differences were found between *ddc* and WT (comparison ***ddc vs* WT -50 µM Cd)** (Fig. 3.24 C).

In summary, Cd treatment induced an increase of IAA signalling both in *ddc* mutant and in WT. Interestingly, only in *ddc* mutant this effect was already evident at 25 µM Cd concentration, suggesting that the mutant could present a more efficient response to Cd stress.

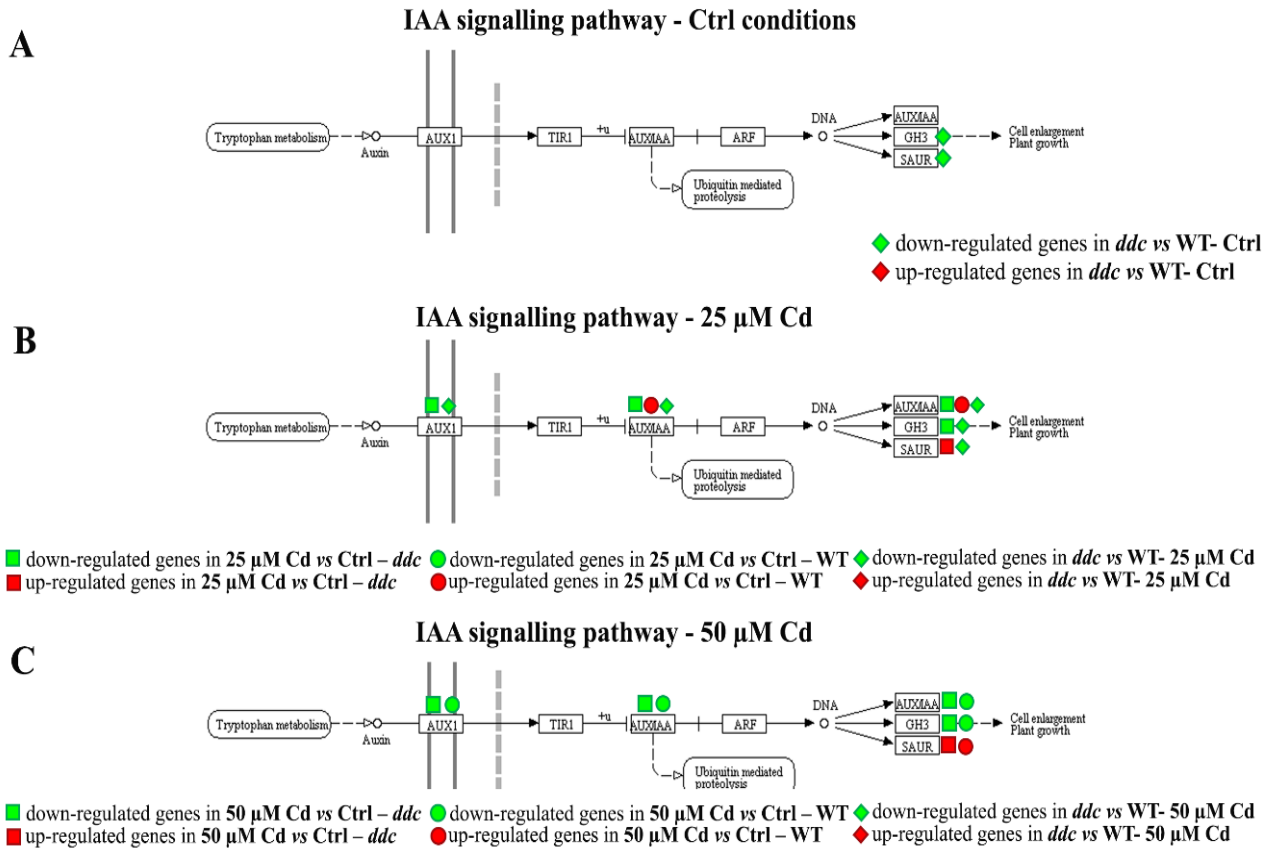

Figure 3.24: Genes differentially expressed (DEGs) along the pathway of auxin signalling in *ddc* and WT seedlings identified through a transcriptomic approach. Seedling grown **(A)** in Ctrl condition, **(B)** under treatment with 25 µM Cd and **(C)** 50 µM Cd.

3.3.4.2 Cytokinins

Box 8

Cytokinins signalling pathway

Cytokinins signalling involves the sequential transfer of phosphoryl groups from the receptors to the downstream components (Hwang and Sheen, 2001; Schaller *et al.,*2011; Sheen, 2002; To and Kieber, 2008).

Cytokinin receptors are histidine kinanes (AHKs) localized predominantly in endoplasmic reticulum (ER) membranes (Caesar *et al.,*2011; Lomin *et al.,*2011; Wulfetange *et al.,*2011). In *A. thaliana*, three AHKs were found: AHK2, AHK3 and AHK4 (also called CRE1 or WOODENLEG), the first cytokinin receptor identified through the "shoot formation assay" (Inoue *et al.,*2001). After cytokinin binding, these receptors are activated by autophosphorylation and activate in turn histidine phosphotransferase (HPt)

proteins (AHP1 to AHP5), that act as positive regulators of cytokinin signalling. AHPs activate type-A and type-B *A. thaliana* response regulators (ARRs) transcription factors (Suzuki *et al.,*1998, 2001, 2002; Imamura *et al.,*2001;).

Type-B ARRs are MYB-class transcription factors whose activity mediates primary plant response to cytokinin and, consequently, plant growth and development, through the activation of target genes (D'Agostino *et al.,*2000; Sakai *et al.,*2001). Type-A ARRs are negative regulators of cytokinin signalling. Their transcription, partially regulated by type-B ARRs transcription factors, is rapidly up-regulated in response to cytokinin (Hwang and Sheen, 2001; Sakai *et al.,*2001).

Clear differences were observed with respect to CKs signalling pathway. In particular, transcriptome data showed that under Ctrl condition it was up-regulated in *ddc* compared to the WT, as suggested by the down-regulation of A-ARRs encoding-genes (comparison ***ddc vs* WT- Ctrl)** (Fig. 3.25 A). Following 25 µM Cd treatment, no changes in the expression of genes involved in CKs signalling were observed in the WT (comparison **25 µM Cd *vs* Ctrl –WT)** (Fig. 3.25 B), while in *ddc* mutant the down-expression of genes codifying the B-ARRs transcription factors suggested a diminished CKs signalling (comparison **25 µM Cd *vs* Ctrl – *ddc)*** (Fig. 3.25 A). This hypothesis is supported by the evidence that the expression of *AHPs,* which encode positive regulators of CKs signalling was down-regulated in *ddc vs* WT, while *A-ARR* genes, which encode receptors working as negative regulators of cytokinin signalling, were overexpressed (comparison ***ddc vs* WT -25 µM Cd)** (Fig. 3.25 B). Finally, under 50 µM Cd concentration, *ddc* and WT showed a reduced expression of *A-ARR*, supposedly leading to an up-regulation of the pathway (comparisons: **50 µM Cd *vs* Ctrl –WT*;* 50 µM Cd *vs* Ctrl – *ddc)*** (Fig. 3.25 C). Again, no differences were found between *ddc* and WT (comparison ***ddc vs* WT -50 µM Cd)** (Fig. 3.25 C).

Globally, these results evidenced that Cd treatment induced a different modulation of CKs signalling in relation to both the samples (*ddc vs* WT) and heavy metal concentration. In fact, at 25 µM Cd, CKs signalling pathway was down-regulated only in the *ddc* mutant, while at 50 µM Cd concentration both *ddc* and WT put in place an enhancement of the pathway through the down-regulation of genes encoding A-ARR receptors.

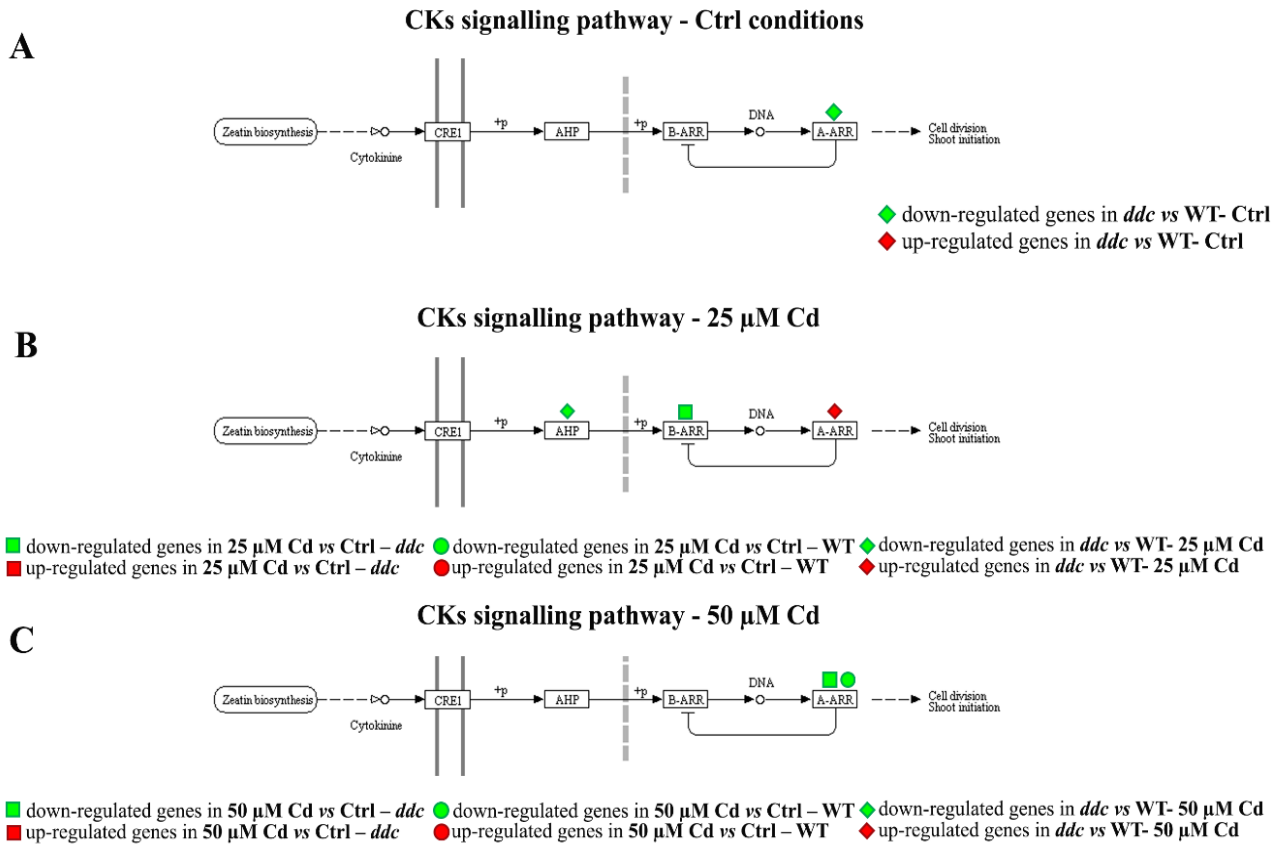

Figure 3.25: Genes differentially expressed (DEGs) along the pathway of cytokinin signalling in *ddc* and WT seedlings identified through a transcriptomic approach. Seedling grown **(A)** in Ctrl condition, **(B)** under treatment with 25 µM Cd and **(C)** 50 µM Cd.

3.3.4.3 Gibberellins

Box 9

Gibberellins signalling pathway

In *A. thaliana*, GAs receptors are codified by three different genes, *GID1a*, *GID1b*, and *GID1c,* which are ubiquitously expressed and fulfil both overlapping and specific roles in growth and development (Griffiths *et al.,*2006; Iuchi *et al.,*2007). The binding of a bioactive GA to the receptor induces conformational changes in GID1 protein and the formation of a GA-GID1 complex, that interacts with DELLA proteins and determine the formation of the stable GA-GID1-DELLA protein complex (Ueguchi-Tanaka *et al.,*2007). DELLA proteins are growth repressors belonging to a sub-family of plant-specific *GRAS* gene family of putative transcription factors, which includes among its members *GAI, RGA,* and *SCARECROW (SCR)* genes. DELLA proteins regulate the expression of the

target genes by: i) interacting with DNA-binding domains of transcription factors, thus hindering their DNA-binding activity and, consequently, the expression of their target genes; ii) interacting with other transcription factors as co-activators or co-repressors to modulate the expression of downstream genes (Yoshida and Ueguchi-Tanaka, 2014). The GA-GID1-DELLA protein complex binds the E3 ubiquitin-ligase SCFSLY1/GID2 complex (Griffiths *et al.,*2006), determining DELLA proteins degradation by the 26S proteasome (Daviere *et al.,*2008; Hartweck, 2008; Shimada *et al.,*2008; Gao *et al.,*2011; Xu *et al.,*2014), suppressing the growth inhibition caused by DELLAs and resulting in the activation of the GA-promoted responses.

Concerning the genetic pathway related to GA signalling, no differences were found between *ddc* and WT under Ctrl condition (comparison ***ddc vs* WT- Ctrl)** (Fig. 3.26 A). When treated with 25 µM Cd, only *ddc* plants showed an enhancing of GAs signalling pathway related to the down-regulation of genes encoding the repressors DELLA proteins (comparisons: **25 µM Cd *vs* Ctrl –WT; 25 µM Cd *vs* Ctrl – *ddc)*** (Fig. 3.26 B). Notably, under 25 µM Cd treatment, these genes were down-regulated also in *ddc vs* WT (comparison ***ddc vs* WT -25 µM Cd)** (Fig. 3.26 B). Under 50 µM Cd treatment, a reduced expression of DELLA-codifying genes was detected in *ddc* and WT, suggesting an up-regulation of GAs signalling pathway (comparisons: **50 µM Cd *vs* Ctrl –WT*; 50 µM Cd *vs* Ctrl – *ddc)*** (Fig. 3.26 C). As expected, under this Cd treatment *ddc* and WT didn't show any significant difference (comparison ***ddc vs* WT -50 µM Cd)** (Fig. 3.26 C).

Altogether, the obtained results evidenced that, in response to Cd, in *ddc* an up-regulation of GAs signalling was already observed at 25 µM Cd, while in the WT it occurred only when treated at 50 µM Cd.

Taking into account the Cd-induced decrease in GAs production (Fig. 3.34 B), it is tempting to suggest that the up-regulation of GAs signalling in the mutant could be a compensatory mechanism implemented by the plant to cope with the Cd stress.

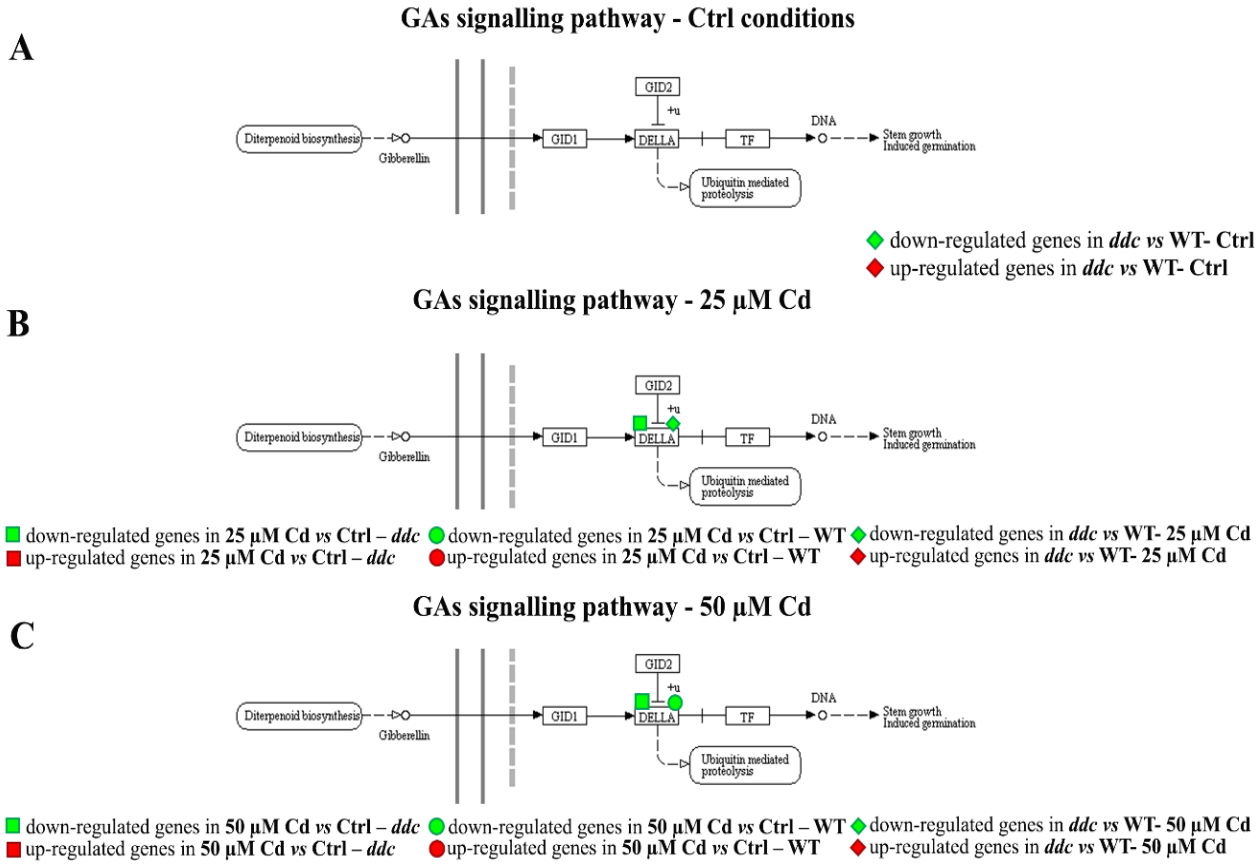

Figure 3.26: Genes differentially expressed (DEGs) along the pathway of gibberellins signalling in *ddc* and WT seedlings identified through a transcriptomic approach. Seedling grown **(A)** in Ctrl condition, **(B)** under treatment with 25 µM Cd and **(C)** 50 µM Cd.

3.3.4.4 Jasmonic acid

Box 10

Jasmonic acid signalling pathway

Jasmonic acid signalling is mediated by a core module composed of 4 principal components: CORONATINE INSENSITIVE 1 (COI1) protein, the Skp-Cullin-F-box (SCF) E3 ubiquitin ligase complex, the JASMONATE-ZIM DOMAIN (JAZ) proteins and various transcription factors that modulate the expression of JA-responsive genes (reviewed by Zhai *et al.,*2017).

COI1 is part of a SCF E3 ubiquitin ligase complex (SCF^{COI1}). This protein, by perceiving bioactive hormone jasmonoyl-isoleucine (JA-Ile), determines the recruiting of the repressor proteins of JA signalling for degradation (Yan *et al.,*2013). JAZ proteins, whose principal function consists in the repression of MYC2 transcription factor (Abe *et*

*al.,*1997; Boter *et al.,*2004; Dombrecht *et al.,*2007; Fernández-Calvo *et al.,*2011; Saijo *et al.,*1997), are also target of SCF^{COI1} complex in presence of active JA (Chini *et al.,*2007; Thines *et al.,*2007; Yan *et al.,*2007). MYC2 regulates 2 different branches of JA-mediated responses: plant responses to wounding and plant responses to pathogen infection (Boter *et al.,*2004; Lorenzo *et al.,*2004). MYC2 also directly regulates the expression of JAZs and JA biosynthetic genes (Chini *et al.,*2007; Grunewald *et al.,*2009).

Concerning JAs signalling, in Ctrl condition it was up-regulated in *ddc* as compared to the WT, as showed by the decreased expression of JAZ genes encoding proteins, which act as repressor of JAs signalling (comparison ***ddc vs* WT- Ctrl)** (Fig. 3.27 A). Notably, this gene family is the only one impacted by Cd exposure. In particular, under 25 µM Cd the expression of JAZ genes was up-regulated and down-regulated in *ddc* mutant and WT, respectively (comparisons: **25 µM Cd *vs* Ctrl – *ddc;* 25 µM Cd *vs* Ctrl –WT)** (Fig. 3.27 B). In line with the above described results, no differences were shown in *ddc* vs WT comparison (comparison ***ddc vs* WT -25 µM Cd)** (Fig. 3.27 B). Under 50 µM Cd concentration, JAZ genes were overexpressed in both *ddc* and WT (comparisons: **50 µM Cd *vs* Ctrl –WT; 50 µM Cd *vs* Ctrl – *ddc)*** (Fig. 3.27 C). No significant differences were observed under this same Cd concentration between the mutant and the WT (comparison ***ddc vs* WT -50 µM Cd)** (Fig. 3.27 C).

Briefly, Cd impacted on genes related to JA signalling more in *ddc* mutant than in WT. In fact, the down-regulation of these genes in *ddc* mutant was already evident under 25 µM Cd treatment, while in the WT it occurred only under 50 µM Cd concentration.

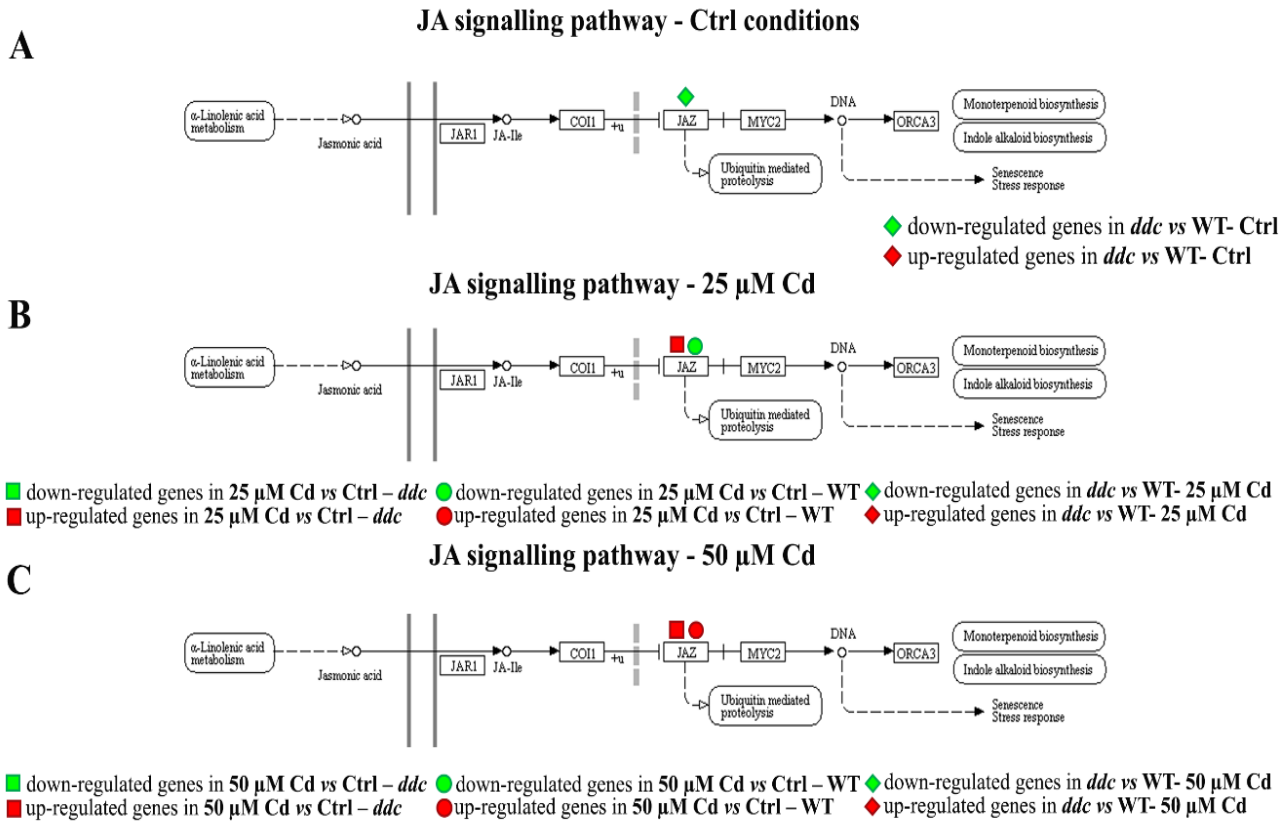

Figure 3.27: Genes differentially expressed (DEGs) along the pathway of jasmonic acid signalling in *ddc* and WT seedlings identified through a transcriptomic approach. Seedling grown **(A)** in Ctrl condition, **(B)** under treatment with 25 µM Cd and **(C)** 50 µM Cd.

3.3.4.5 Abscisic acid

Box 11

Abscisic acid signalling pathway

ABA signal transduction is carried on by three principal protein classes: ABA receptors, coreceptors, and kinases proteins, that are responsible for the earliest events of ABA signalling. In absence of ABA, phosphoprotein phosphatase 2Cs (PP2Cs) are active and act as negative regulators of ABA signalling. PP2Cs are also considered ABA coreceptors. (reviewed by Li *et al.,*2017).

A. thaliana steroidogenic acute regulatory (StAR)-related lipid transfer domain proteins PYR/PYL/RCARs were identified as soluble ABA receptors by two different working groups in 2009 (Ma *et al.,*2009; Park *et al.,*2009). In presence of ABA, these proteins deactivate PP2Cs, thus determining the activation of several classes of protein kinases, which regulate ABA signalling. Between these, SNF1-related protein kinases 2

(SnRK2s) are of particular importance as core components for ABA-dependent regulation of gene expression (Fujii *et al.,*2009).

SnRK2s activate the ABA-responsive element/ABRE-binding factors (AREBs/ABFs) belonging to the bZIP family of TFs, the key transcription factors in ABA signalling pathway, which modulate specific gene expression (Uno *et al.,*2000; Furihata *et al.,*2006; Fujii *et al.,*2005; Fujii *et al.,*2009). ABA signalling can be also mediated by mitogen-activated protein kinases (MAPKs), which signalling module usually comprehends at least 3 protein kinases: an MAP3K (MAPKKK), an MAP2K (MAPKK, MKK, or MEK), and an MAPK (MPK) (reviewed in de Zelicourt *et al.,*2016). In fact, MPK1 and MPK2 activity can be increased by ABA (Ortiz-Masia *et al.,*2007), while the ABA-dependent activation of MPK6 occurs in response to *CATALASE1* (*CAT1*) expression and H_2O_2 production (Xing *et al.,*2008). Moreover, MPK9 and MPK12 enhance the ROS-mediated ABA signalling in stomata guard cells (Jammes *et al.,*2009).

Concerning genetic pathways related to ABA signalling, no differences were detected between *ddc* and WT when grown in Ctrl condition (comparison ***ddc vs* WT-Ctrl)** (Fig. 3.28 A). In WT plants 25 µM Cd treatment enhanced the expression of gene family encoding PYR/PYL/RCARs ABA receptors and decreased the expression of *PP2Cs* gene family, whose encoded products acts as a negative regulators of ABA signalling (comparison **25 µM Cd *vs* Ctrl –WT)** (Fig. 3.28 B). This result is consistent with an up-regulation of ABA signalling. Under this same Cd treatment, the gene expression pattern of *ddc* mutant resulted rather more complex. In particular, like in the WT, *PYR/PYL/RCARs* genes were overexpressed and *PP2Cs* were down-regulated also in *ddc* plants. Moreover, the genes *AREBs/ABFs*, codifying the key transcription factors in ABA signalling pathway, were up-regulated, while *SnRK2s* genes, codifying proteins which activate the AREBs/ABFs transcription factors, were down-regulated. Starting from this scenario, it is likely that globally ABA signalling pathway was down-regulated in *ddc* plants treated with 25 µM Cd (comparison **25 µM Cd *vs* Ctrl – *ddc)*** (Fig. 3.28 B). In the *ddc vs* WT comparison, only *SnRK2s* were down-regulated (comparison ***ddc vs* WT -25 µM Cd)** (Fig. 3.28 B). When analysing the pattern induced by 50 µM Cd treatment, in WT plants, an up-regulation of *PYR/PYL/RCAR* and *AREBs/ABF* and a down-regulation of *SnRKs* were observed (comparison **50 µM Cd *vs* Ctrl –WT)** (Fig. 3.28 C). In a comparable

way, in *ddc* mutant *PYR/PYL/RCAR* genes were up-regulated and *PP2Cs* and *SnRKs* were down-regulated (comparison **50 µM Cd *vs* Ctrl – *ddc)*** (Fig. 3.28 C). Under this Cd treatment no differences were detected when comparing *ddc vs* WT (comparison ***ddc vs* WT -50 µM Cd)** (Fig. 3.28 C).

In summary, an up-regulation of genetic pathway related to ABA signalling was observed in WT at least at 25 µM Cd, while in *ddc* mutant it was found to be down-regulated whatever heavy metal concentration was used. This last result was very surprising, considering the role of ABA as a stress-related hormone.

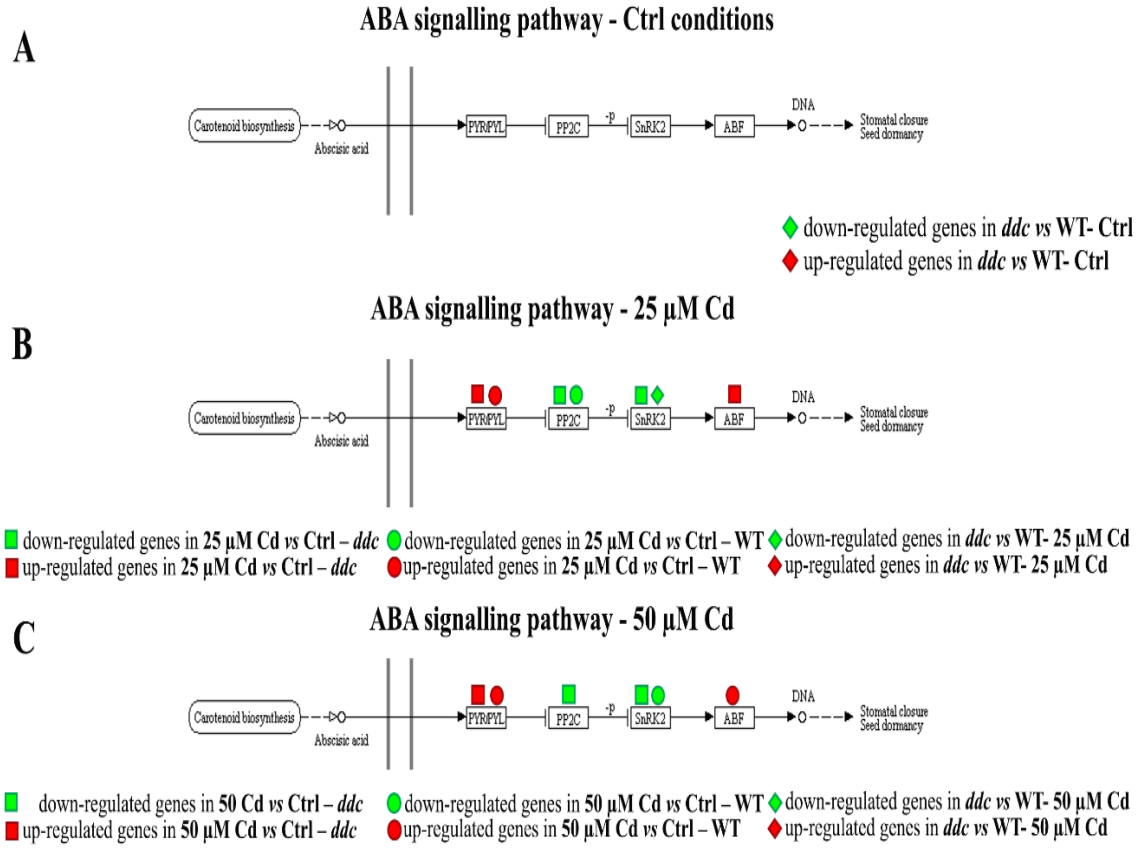

Figure 3.28: Genes differentially expressed (DEGs) along the pathway of abscisic acid signalling in *ddc* and WT seedlings identified through a transcriptomic approach. Seedling grown **(A)** in Ctrl condition, **(B)** under treatment with 25 µM Cd and **(C)** 50 µM Cd.

3.3.4.6 Ethylene

Box 12

Ethylene signalling pathway

Ethylene is perceived by a family of ER-localized receptor complexes that in *A. thaliana* includes 5 members: ETR1, ETR2, ERS1, ERS2, and EIN4 (Chang *et al.,*1993; Hua and Meyerowitz, 1998; Sakai *et al.,*1998).

CONSTITUTIVE TRIPLE RESPONSE 1 (CTR1), a negative regulator of ethylene signal transduction (Kieber *et al.,*1993), physically interacts with the ethylene receptors, suggesting that the initial step of signal transduction could involve the existence of a negative signalling complex that comprises the receptor and CTR1 (Gao *et al.,*2003). In absence of ethylene, this complex is inactive while, after ethylene binding, the complex function is inhibited, and the ethylene signalling is activated (reviewed by Gao *et al.,*2003). Moreover, CTR1 physically interacts with ETHYLENE INSENSITIVE 2 (EIN2) (Ju *et al.,*2012), a key component in ethylene signalling pathway. EIN2 protein is encoded by a single-copy gene in *A. thaliana*, whose loss-of-function confers complete insensitivity to ethylene (Alonso *et al.,*1999). After its activation by CTR1-mediated phosphorylation of the C-terminal domain, EIN2 is cleaved and transferred to the nucleus (Ju *et al.,*2012; Qiao *et al.,*2012; Wen *et al.,*2012). In the nucleus, EIN2 stabilizes ETHYLENE INSENSITIVE 3/ EIN3-LIKE 1 (EIN3/EIL1) transcription factors by inhibiting EIN3-BINDING PROTEIN 1)/EBF2 (EBF1), that in absence of ethylene directs EIN3/EIL1 proteasomal degradation (Guo and Ecker, 2003). EIN3/EIL1 proteins are necessary and sufficient to activate the ethylene response and, consequently, enhance the transcription of ethylene-induced genes (Zhao and Guo, 2011).

No differences in the expression of genes related to ethylene signalling were detected in *ddc* and WT under Ctrl condition (comparison ***ddc vs* WT- Ctrl)** (Fig. 3.29 A). Almost no differences were also found following 25 µM Cd treatment, where only WT plants displayed an up-regulation of *ETR*s genes, codifying ethylene receptors (comparisons: **25 µM Cd *vs* Ctrl –WT; 25 µM Cd *vs* Ctrl – *ddc)*** (Fig. 3.29 B). On the contrary, under 50 µM Cd treatment, both *ddc* and WT exhibited an up-regulation of *ETRs* and *ETHYLENE RESPONSE FACTORS (ERFs)* genes, suggesting an up-regulation of

ethylene signalling (comparisons: **50 µM Cd *vs* Ctrl –WT; 50 µM Cd *vs* Ctrl – *ddc)*** (Fig. 3.29 C). Under this Cd concentration, *ddc* and WT didn't exhibit any significant difference (***ddc vs* WT -50 µM Cd)** (Fig. 3.29 C).

Briefly, the analysed data showed that only the higher Cd concentration induced a differential expression of genes related to ethylene signalling in *ddc* and WT, that shared a similar response consisting in the up-regulation of ethylene-receptor genes and ethylene response genes.

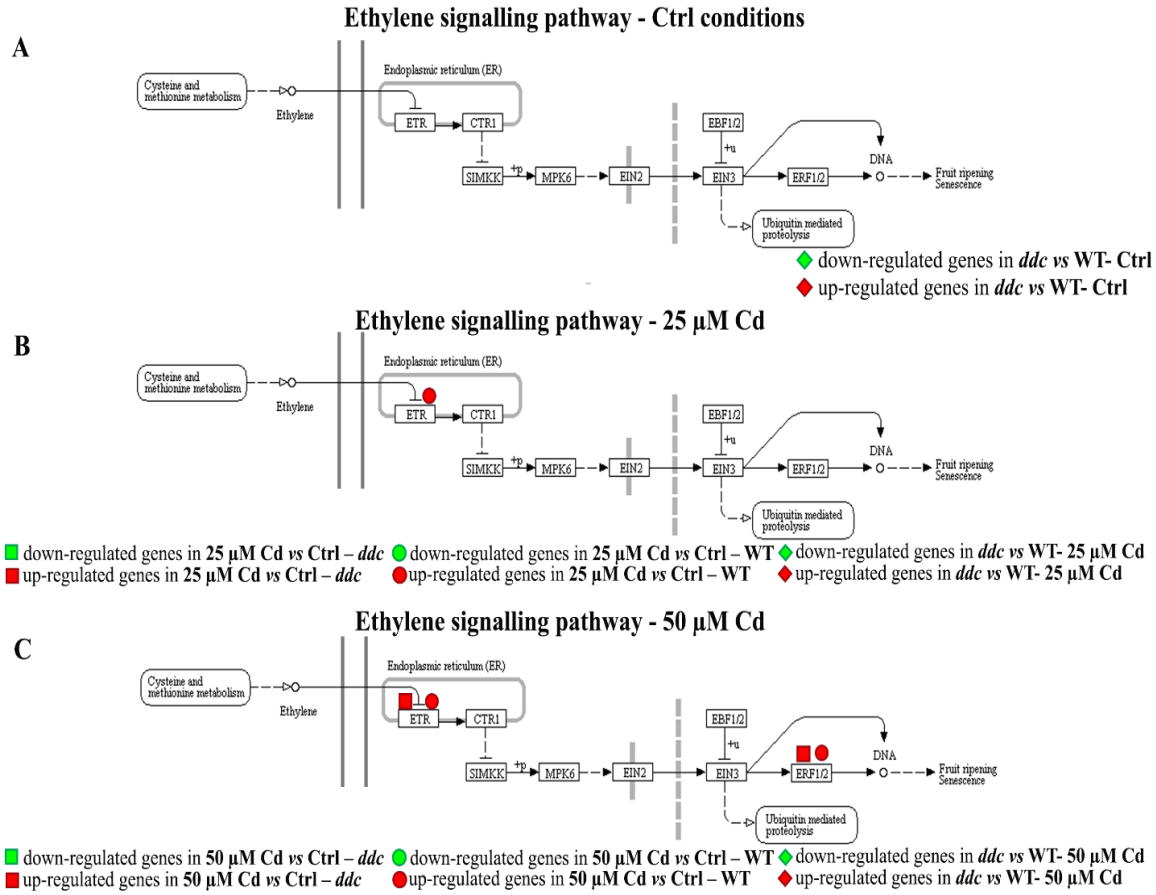

Figure 3.29: Genes differentially expressed (DEGs) along the pathway of ethylene signalling in *ddc* and WT seedlings identified through a transcriptomic approach. Seedling grown **(A)** in Ctrl condition, **(B)** under treatment with 25 µM Cd and **(C)** 50 µM Cd.

3.3.4.7 Brassinosteroids

Box 13

Brassinosteroids signalling pathway

Brassinosteroids (BRs) signalling is initiated by their perception from BRs receptor BRASSINOSTEROID-INSENSITIVE 1 (BRI1) and its co-receptor *BRI1*-ASSOCIATED RECEPTOR KINASE 1 (BAK1), which directly interacts with BRI1 leading the two proteins to their mutual *trans*- phosphorylation (Li *et al.,*2002; Nam and Li, 2002; Karlova *et al.,*2009; Wang *et al.,*2014). BRI1 kinase inhibitor 1 (BKI1) can interact with BRI1 and inhibits its activity by hindering its interaction with BAK1(Wang and Chory, 2006). The GSK3-like protein kinase BR-INSENSITIVE 2 (BIN2) negatively regulates BRs signalling by catalysing the phosphorylation of BRI1-EMS-SUPPRESSOR (BES1) and BRASSINAZOLE-RESISTANT 1 (BZR1) transcription factors. The phosphorylation of BES1 and BZR1 proteins reduces their DNA binding activity, leading to the inhibition of BRs signalling (Vert and Chory, 2006). In presence of BRs, the BRI1/BAK1 activate the BRs signalling kinase (BSK) and constitutive differential growth (CDG) proteins, that in turn activate BRI1 suppressor 1 (BSU1), which role is BIN2 deactivation. BIN2 can be also degraded by 26S proteasome or transported out of the nucleus (Anne *et al.,*2015). Consequently, the inhibitory effect of BIN2 on BES1 and BZR1, the two major downstream transcription factors in BRs signalling, is eliminated and BR-responsive genes expression will be induced (reviewed by Wang *et al.,*2017).

Concerning the genetic pathway related to BRs signalling, transcriptomic analysis didn't show any significative differences (Fig. 3.30 A-C). However, at 25 µM Cd, some differences were observed with respect to genes which act downstream BRs signalling. For example, *ddc* mutant showed a down-regulation of the gene encoding cyclin D-type protein CYCD3 which is also under the control of CKs signalling (comparison **25 µM Cd *vs* Ctrl-*ddc*)** (Fig. 3.30 B).

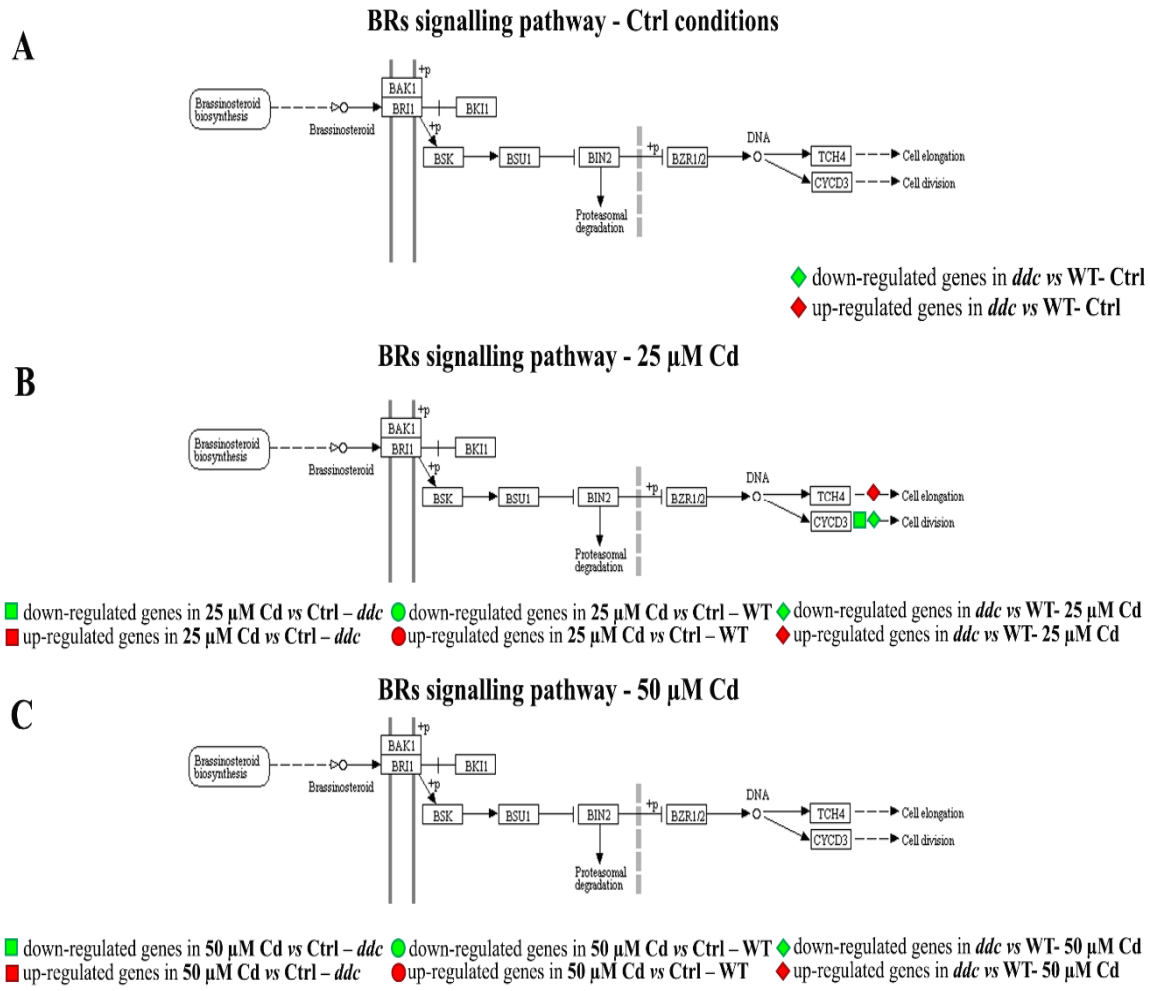

Figure 3.30: Genes differentially expressed (DEGs) along the pathway of brassinosteroids signalling in *ddc* and WT seedlings identified through a transcriptomic approach. Seedling grown **(A)** in Ctrl condition, **(B)** under treatment with 25 µM Cd and **(C)** 50 µM Cd.

Box 14

Salycilic acid signalling pathway

Salicylic acid is perceived by that NONEXPRESSER OF PATHOGENESIS-RELATED PROTEIN 1 (NPR1) receptors, which are responsible of SA-dependent defence signalling pathways (Cao *et al.,*1997). This protein is a transcriptional co-regulator that, in presence of SA, interacts with transcription factors like TGACG Sequence-specific Binding Proteins (TGAs), to activate expression of disease resistance genes (Després *et al.,*2000; 2003; Fan and Dong, 2002; Rochon *et al.,*2006).

Concerning SA signalling, in Ctrl condition no differences were evidenced between *ddc* and WT. Only *PATHOGENESIS-RELATED GENE 1 (PR-1)* gene was down-regulated (***ddc vs* WT- Ctrl)** (Fig. 3.31 A). Note that this gene is a useful molecular marker for the SAR (systemic acquired resistance) response usually induced in response to pathogens (Chern *et al.,*2008). No differences were found in WT under 25 µM Cd (**25 µM Cd *vs* Ctrl –WT) (**Fig. 3.31 B**)**, while under the same Cd concentration *ddc* showed a decrease of SA signalling pathway, as evidenced by the down-regulation of genes codifying TGAs transcription factors (**25 µM Cd *vs* Ctrl – *ddc)*** (Fig. 3.31 B). Under the treatment with the higher Cd concentration, in both *ddc* and WT, *TGAs* and *PR-1* gene were down-regulated, suggesting a decrease in SA signalling (comparisons: **50 µM Cd *vs* Ctrl –WT; 50 µM Cd *vs* Ctrl – *ddc)*** (Fig. 3.31 C). No differences were found between *ddc* and WT (comparison ***ddc vs* WT -50 µM Cd)** (Fig. 3.31 C).

Altogether, these results showed that Cd-related reduction of SA signalling was stronger in *ddc* mutant than in WT. In fact, under 25 µM Cd treatment, SA signalling was already impaired in *ddc* mutant, while such decrease was shown in WT only at the higher Cd concentration.

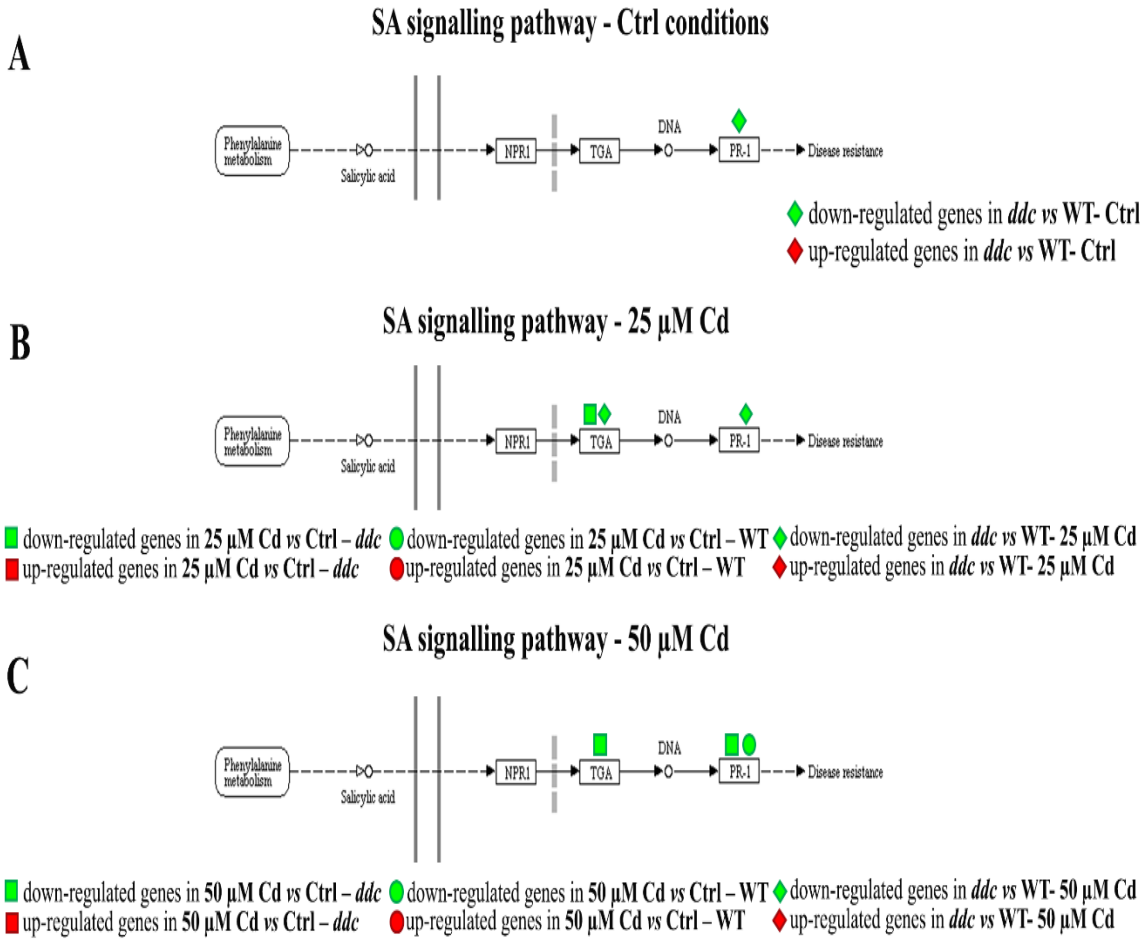

Figure 3.31: Genes differentially expressed (DEGs) along the pathway of salicylic acid signalling in *ddc* and WT seedlings identified through a transcriptomic approach. Seedling grown **(A)** in Ctrl condition, **(B)** under treatment with 25 µM Cd and **(C)** 50 µM Cd.

3.4 Libraries results validation: quantification of the expression levels of genes related to hormone biosynthesis and signalling in *ddc* mutant and WT in Ctrl condition and under Cd treatment by qRT-PCR.

For libraries results validation, 14 key genes related to hormone biosynthesis and signalling were selected for qRT-PCR, and the gene expression levels obtained from the transcriptomic and qRT-PCR analyses were compared by using Pearson correlation coefficient (Annese *et al.,*2018).

The qPCR analysis confirmed the differential expression emerged in RNA-seq analyses for all 14 genes (Fig. 3.32 A), and the estimates of fold change in expression level were highly consistent with those from RNA-Seq ($R^2 = 0.9736$) (Fig. 3.32 B).

A

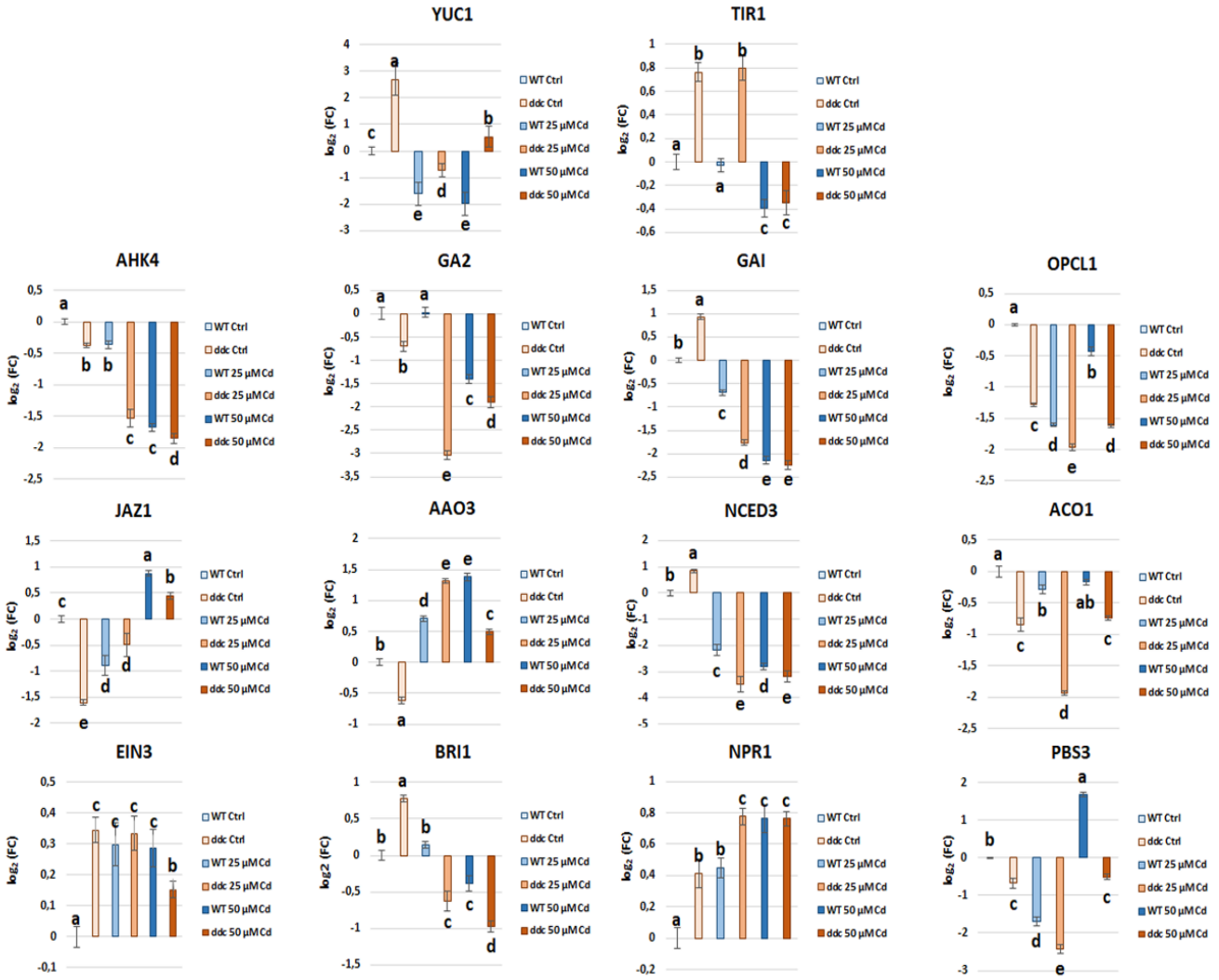
YUC1
TIR1
AHK4
GA2
GAI
OPCL1
JAZ1
AAO3
NCED3
ACO1
EIN3
BRI1
NPR1
PBS3
log2 (FC)
WT Ctrl
ddc Ctrl
WT 25 µM Cd
ddc 25 µM Cd
WT 50 µM Cd
ddc 50 µM Cd

B

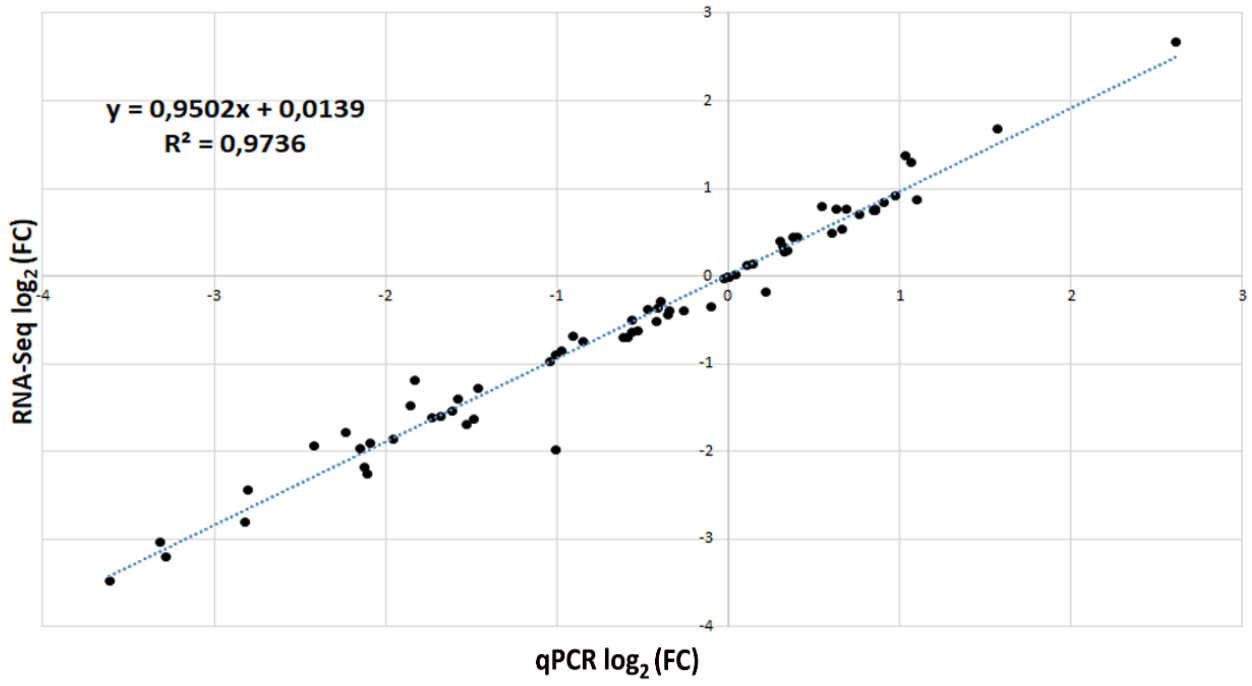
y = 0,9502x + 0,0139
R² = 0,9736
RNA-Seq log2 (FC)
qPCR log2 (FC)

Figure 3.32: Relative expression level by qRT-PCR of **(A)** 14 selected DEGs involved in hormones metabolism and signalling. Data present the mean ± standard error (SE) of three independent experiments. Statistical analysis was performed by using two-way ANOVA with Tukey post hoc test ($P \leq 0.05$) after Shapiro–Wilk normality test. Means with the same letter are not significantly different at $P \leq 0.05$; **(B)** Linear correlation between $\log_2$ (FC) values computed on RNA-Seq data and $\log_2$ (FC) values detected by qRT-PCR for 14 selected genes.

3.5 Phytohormones quantification in ddc mutant and WT under Cd treatment.

In view of the results of transcriptomic analysis showing a differential modulation in *ddc* mutant *vs* WT of the hormones genetic pathways, it appeared of interest to estimate the level of hormone classes in both *ddc* mutant and WT under Ctrl conditions and Cd treatment. For these analyses, only 25 µM Cd concentration was selected, since at the transcriptomic level the major differences between *ddc* mutant and WT plants were observed just under such treatment. The results so far obtained, dealing with indole 3-acetic acid (IAA), gibberellins (GAs), jasmonic acid (JA), salicylic acid (SA) and abscisic acid (ABA).

3.5.1 IAA quantification

Among different auxins, indole 3-acetic acid (IAA) was estimated, as the most relevant one. As evident in the Fig. 3.33, under Ctrl conditions, IAA amount was higher in *ddc* mutant than WT, although at not significant level. After Cd treatment, a trend to decrease was observed in the WT, while the amount remained unchanged in *ddc* mutant, resulting in a significant difference between the two samples.

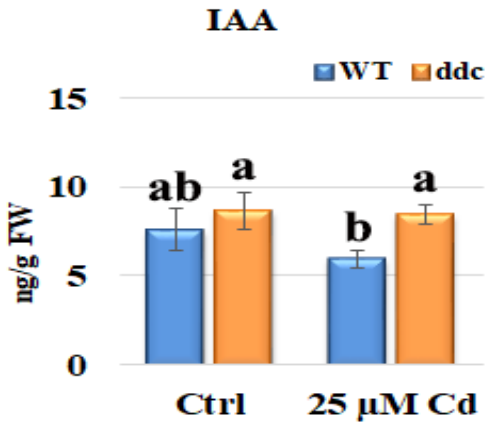

Figure 3.33: Indole 3-acetic acid (IAA) amount in *A. thaliana ddc* mutant and WT seedlings grown in Ctrl conditions and treated with 25 µM Cd estimated by GC–MS. The results represent the mean value (± standard deviation) of three independent biological replicates. Statistical analysis was performed by using two-way ANOVA with Tukey post hoc test ($p \leq 0.05$) after Shapiro–Wilk normality test. Means with the same letter are not significantly different at $p \leq 0.05$.

3.5.2 GAs quantification

Concerning GAs, we analysed both precursors (GA_9, GA_{19}, GA_{20}) and biologically active forms (GA_1, GA_3, GA_4, GA_7) as well as their catabolites (GA_8, GA_{34}, GA_{29}, GA_{51}), which were differentially related each other (Fig. 3.34 B). The precursors "*in serie*" of hydroxylated forms, GA_{19} and, at less extent, GA_{20}, were differentially modulated in *ddc* mutant and WT. In particular, under Ctrl condition, a very higher amount of GA_{19} was observed *in ddc* mutant compared to the WT. Following Cd treatment, an opposite behaviour was observed in GA_{19} amount, that significantly increased in the WT, while a slight downtrend was observed in *ddc* mutant, leading at the end of the treatment to comparable values in the two samples (Fig. 3.34 B a, b). Concerning the active hydroxylated forms, GA_1 and GA_3, under Ctrl conditions both exhibited higher amounts in the WT than in *ddc*. However, following Cd treatment, a decrease of their amount was detected only in the WT, globally leading to a higher amount of these active forms in *ddc* mutant compared to the WT (Fig 3.34 B c, d). In addition, in *ddc* mutant, the catabolites GA_8 and GA_{29} were globally lower compared to the WT, under both Ctrl condition and Cd treatment (Fig 3.34 B e, f).

Differences were observed also for GA_9, precursor of non-hydroxylated GAs: under Cd treatment its amount decreased in the WT and was instead induced in *ddc* mutant, resulting in a quite comparable value between the two samples (Fig. 3.34 B g). Concerning

the active non-hydroxylated forms, GA_4 and GA_7, their amount was found to increase under Cd treatment only in *ddc* mutant; also, in this case, at the end of heavy metal treatment, comparable values were detected in both *ddc* and WT (Fig. 3.34 B h, i). In agreement with these results, following Cd treatment, the amount of catabolites GA_{51} and GA_{34} did not change in the WT, whereas in *ddc* mutant it increased and decreased, respectively (Fig. 3.34 B j, k).

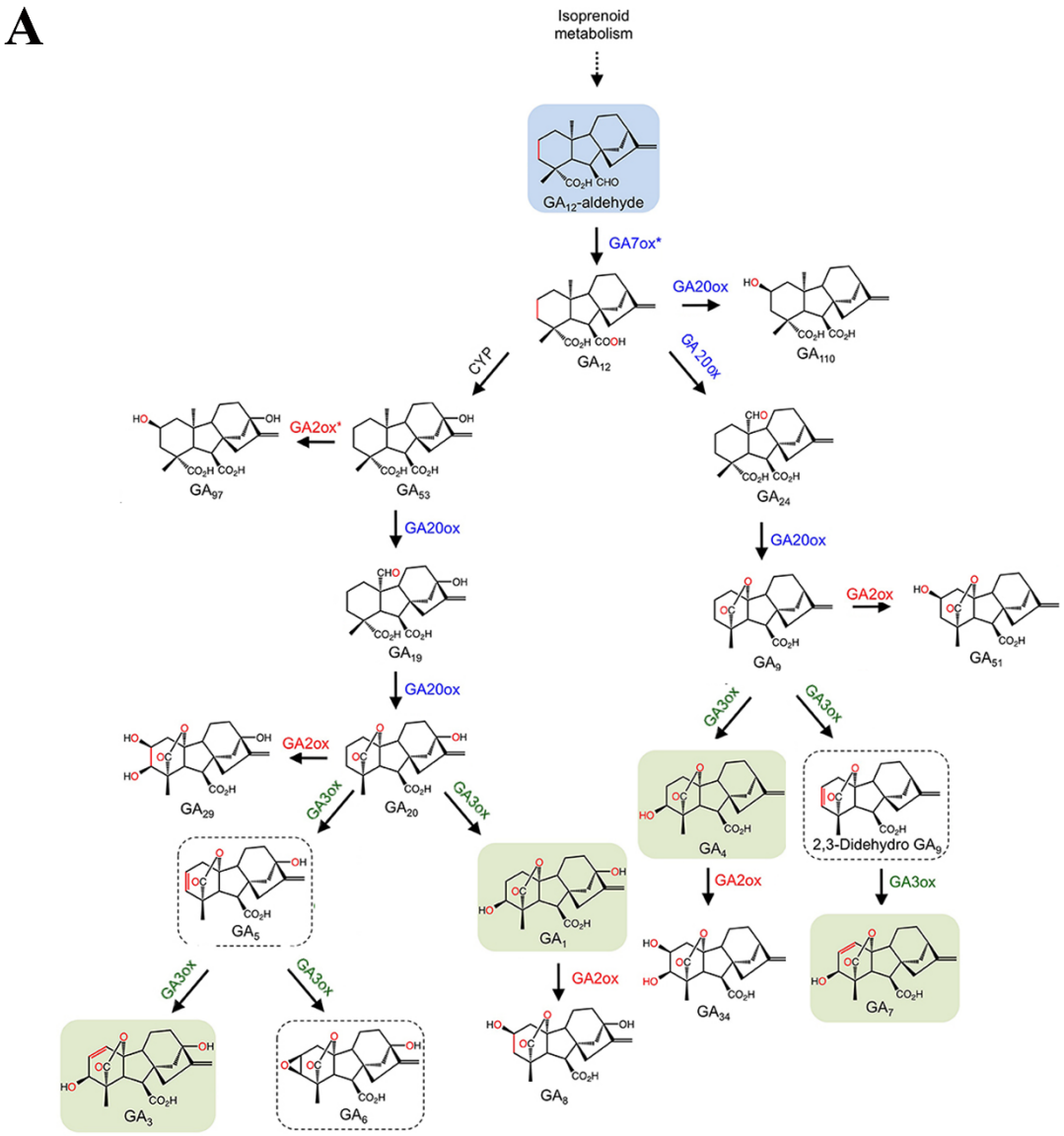
A
Isoprenoid metabolism
GA12-aldehyde
GA7ox*
GA12
GA20ox
GA110
CYP
GA20ox
GA97
GA2ox*
GA53
GA24
GA20ox
GA20ox
GA19
GA9
GA2ox
GA51
GA20ox
GA3ox
GA3ox
GA29
GA2ox
GA20
GA3ox
GA3ox
GA4
2,3-Didehydro GA9
GA5
GA1
GA2ox
GA2ox
GA3ox
GA34
GA7
GA3ox
GA3ox
GA3
GA6
GA8

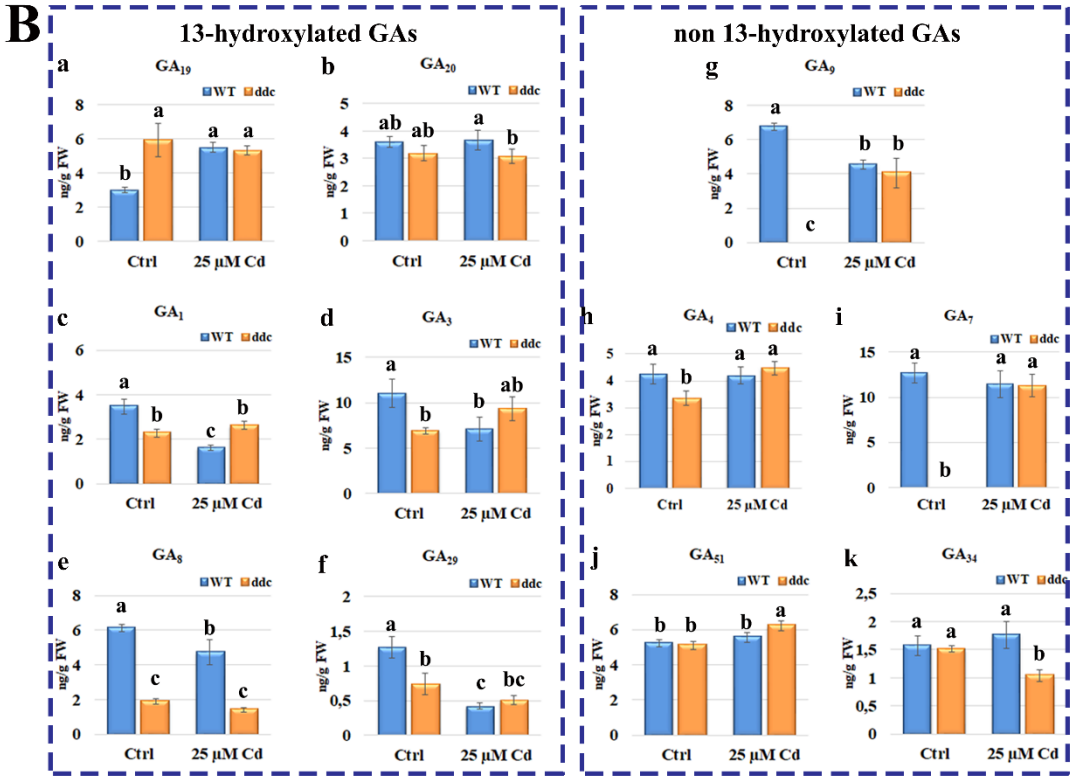
B
13-hydroxylated GAs
non 13-hydroxylated GAs
GA19
GA20
GA9
GA1
GA3
GA4
GA7
GA8
GA29
GA51
GA34
WT
ddc
ng/g FW
Ctrl
25 µM Cd

Figure 3.34: A) Gibberellins biosynthetic pathways in higher plants. GA_{12}, that lies at a branch-point in the pathway, is the precursor of the non-13-hydroxylated GAs. Moreover, due to its hydroxylation on C-13, it can be converted to GA_{53}, the precursor of 13-hydroxylated gibberellins (Hedden and Thomas, 2012). Blue labelled enzymes are involved in the major routes leading to active GAs, while red and green labelled enzymes are responsible of GA deactivation and activation, respectively. The blue box highlights the central intermediate of all GAs; green boxes highlight the active GAs (Adapted from: Farrow and Facchini, 2014). **B) (a-f)** 13-hydroxylated and **(g-k)** non-13-hydroxylated gibberellins (GAs) amount in *A. thaliana ddc* mutant and WT seedlings grown in Ctrl conditions and treated with 25 µM Cd estimated by GC–MS. The results represent the mean value (± standard deviation) of three independent biological replicates (n = 45). Statistical analysis was performed by using two-way ANOVA with Tukey post hoc test ($p \leq 0.05$) after Shapiro–Wilk normality test. Means with the same letter are not significantly different at $p \leq 0.05$.

3.5.3 JA quantification

As evident in Fig. 3.35, under Ctrl conditions, JA amount was significantly lower in *ddc* mutant than WT. However, following Cd treatment, JA amount significantly decreased in the WT while in *ddc* mutant a light, but not significant, increase was observed, leading to quite comparable values in the two samples (Fig. 3.35).

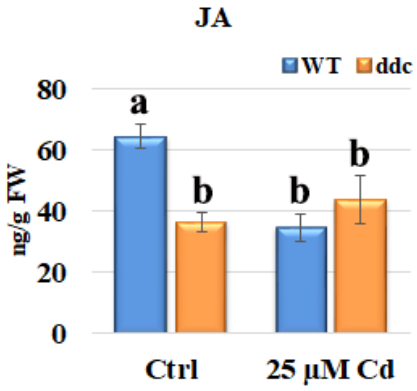

Figure 3.35: Jasmonic acid (JA) amount in *A. thaliana ddc* mutant and WT seedlings grown in Ctrl conditions and treated with 25 µM Cd estimated by GC–MS. The results represent the mean value (± standard deviation) of three independent biological replicates. Statistical analysis was performed by using two-way ANOVA with Tukey post hoc test ($p \leq 0.05$) after Shapiro–Wilk normality test. Means with the same letter are not significantly different at $p \leq 0.05$.

3.5.4 ABA quantification

As evident in Fig. 3.36, under Ctrl conditions, also ABA amount was significantly lower in *ddc* mutant than in WT. Following Cd treatment JA amount significantly decreased only in the WT. Notwithstanding, in *ddc* mutant the ABA amount remained lower than in WT (Fig. 3.36).

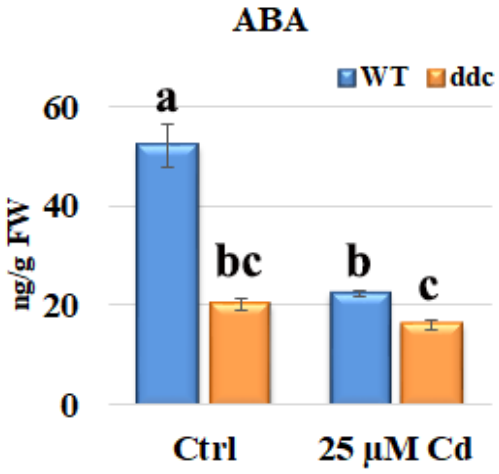

Figure 3.36: Abscisic acid (ABA) amount in *A. thaliana ddc* mutant and WT seedlings grown in Ctrl conditions and treated with 25 µM Cd estimated by GC–MS. The results represent the mean value (± standard deviation) of three independent biological replicates. Statistical analysis was performed by using two-way ANOVA with Tukey post hoc test ($p \leq 0.05$) after Shapiro–Wilk normality test. Means with the same letter are not significantly different at $p \leq 0.05$.

3.5.5 SA quantification

Both SA and its glycosylated form SAG were evaluated. As evident in Fig. A 5, under Ctrl conditions both SA and SAG amounts were significantly higher in *ddc* mutant than in WT. Following Cd treatment, their amounts significantly decreased more in *ddc* mutant than in in the WT, leading to an opposite condition (Fig. 3.37).

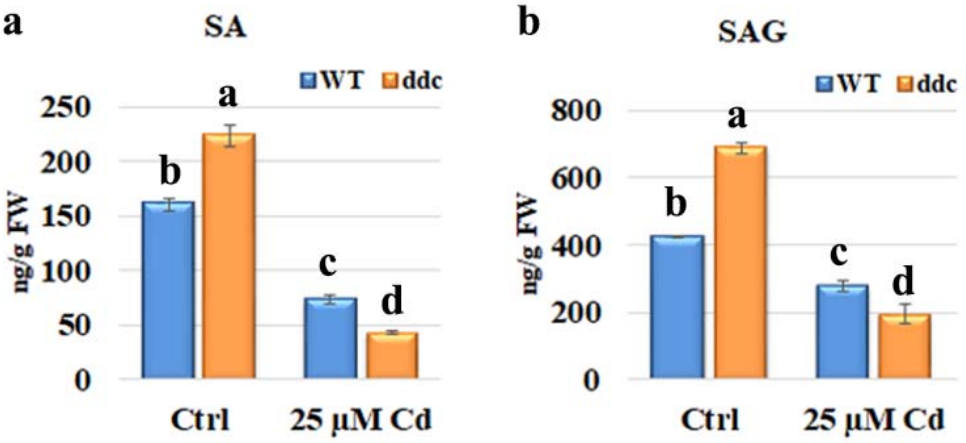

Figure 3.37: a) Salicylic acid (SA) and b) salicylic acid glucoside (SAG) amount in *A. thaliana ddc* mutant and WT seedlings grown in Ctrl conditions and treated with 25 µM Cd estimated by GC–MS. The results represent the mean value (± standard deviation) of three independent biological replicates. Statistical analysis was performed by using two-way ANOVA with Tukey post hoc test ($p \leq 0.05$) after Shapiro–Wilk normality test. Means with the same letter are not significantly different at $p \leq 0.05$.

3.6 How are the detected alteration in hormone pathways linked to the phenotype and differential response to Cd of *ddc* mutant?

3.6.1 An insight into the involvement of auxin distribution pathway

As mentioned, auxin is one of the most relevant phytohormones for plant growth and development and its role as a morphogen has been largely assessed. Namely, localized accumulations of auxin have been demonstrated to drive embryonic axis specification, organ formation and positioning, root meristem maintenance, vascular tissue differentiation, differential growth responses, fruit development, apical hook formation and apical dominance (reviewed by Davies, 2004). This control is mainly exercised thanks a strict regulation of its distribution pattern (van Berkel *et al.,*2013). Therefore, understanding how mechanisms of auxin distribution are modulated in *ddc* mutant could provide new insights into the role played by auxin in *ddc* phenotype.

Box 15

Polar auxin transport in *A. thaliana* plants

Auxin distribution pattern in plant undergoes to a strict regulation. In fact, at the low pH in cell walls, the weak acid auxin is protonated, thus can passively enter cells through the plasma membrane (PM). In addition, influx carriers of the AUX/LAX family pump auxin into cells. However, at the higher pH present in the cytosol, cellular auxin loses its ability to cross the membrane and needs to be actively pumped out of cells by efflux carriers such as PIN-FORMED (PIN) efflux carriers. In this way, the directionality of auxin flow is established by the distribution of its transporters (Estelle, 1998; Kramer and Bennett, 2006; Balzan *et al.,*2014).

Until now, a strong correlation between the polar subcellular localization and the known or predicted directions of auxin flow has been evidenced for PIN efflux carriers, confirming that cellular PINs positioning is a determining factor in polar auxin transport directionality (Friml *et al.,*2004).

The PIN proteins are a family of 8 integral membrane proteins that exhibit two conserved domains forming transmembrane helices and a central hydrophilic loop with variable length. Based on this discriminant characteristic, they are classified o in "long" and "short" PINs (Krecek *et al.,*2009; Ganguly *et al.,*2012). "Long" PINs (namely, PIN1, PIN2, PIN3, PIN4 and PIN7) are generally inserted into the PM, while "short" PINs (PIN5 and PIN8) and PIN6, that presents an intermediate form, are localised in the endoplasmic reticulum (ER), contributing to intracellular IAA homeostasis (Krecek *et al.,*2009; Mravec *et al.,*2009; Ganguly *et al.,*2010; Viaene *et al.,*2013; Cazzonelli *et al.,*2013). Depending on cell type and developmental stage, also PIN5 can be found into the PM (Sawchuk *et al.,*2013; Balzan *et al.,*2014; Ganguly *et al.,*2014;).

The constant cycle of PIN proteins to and from the PM allows the maintenance of their correct polarity and also the possibility to undergo to a quick redistribution in response to endogenous or exogenous stimuli (Geldner *et al.,*2001; Dhonukshe *et al.,*2007). Furthermore, auxin presence influences PIN cycling inhibiting PINs endocytosis and, consequently, determining the presence of a higher number of carriers on the PM (Paciorek *et al.,*2005; Robert *et al.,*2010).

In the epidermis of the shoot apical meristem, PIN distribution determines the formation of different auxin maxima, which prelude for the formation of primordia and the

production of phyllotactic patterns (Reinhardt *et al.,*2003). In the root tip and the lateral root primordia, PINs in the outer layer transport auxin away from the maximum, whereas PINs in the inner layers transport auxin toward the maximum, creating a "fountain-like" pattern (Blilou *et al.,*2005). The distal auxin maximum correlates with pattern formation and the orientation and extent of cell division, and the inhibition of polar auxin transport strongly affects these processes (Sabatini *et al.,*1999). Recently, a coordinated auxin efflux/influx activity, by PIN1 and LAX3, has been demonstrated to generate the IAA gradient and maxima required for a proper initiation and development of lateral and adventitious roots in *A. thaliana* (Swarup *et al.,*2008; Della Rovere *et al.,*2013).

Among the major players involved in the auxin distribution there are the members of the large family of PIN-FORMED (PIN) proteins (Box 15), which act as relevant rate-limiting efflux carriers (Zhou and Luo, 2018; Box 15). The results of transcriptomic analysis performed on the whole seedlings evidenced a general down-regulation of genes encoding these proteins following Cd treatment, even though at different level when comparing *ddc* mutant and WT plants (data not shown). However, it is known that PINs proteins acts in an organ- and tissue-specific way. Thus, it seemed to us more advisable to investigate PINs expression and auxin distribution at the level of single organs. So far, our analysis was focused on the roots which, as mentioned at the beginning of Results section, exhibited a Cd-dependent growth reduction less pronounced in *ddc* compared to the WT.

PINs expression was analysed at transcriptional level, by qRT-PCR of encoding genes and through protein detection by using the following transgenic reporter lines of *Arabidopsis thaliana*: *pPIN1::PIN1-GFP* (Blilou *et al.,*2005), *ddc X pPIN1::PIN1-GFP, pPIN7::PIN7-GFP* (Blilou *et al.,*2005), *and ddc X pPIN7::PIN7-GFP*. Based on data in literature showing their modulation in response to Cd stress (Yuan and Huang, 2015), PIN1 and PIN 7 were selected to be investigated. Auxin distribution was evaluated by using *pDR5::GFP* (Ottenschläger *et al.,*2003) and *ddc X pDR5::GFP* transgenic lines *of A. thaliana,* in which the GFP is expressed under the control of an auxin-induced promoter. For all the above analyses, seedlings at 8 DAG of both transgenic lines were grown either under Ctrl condition and exposed to 25 and 50 μM Cd.

Concerning *PIN* genes expression, a global down-regulation was found in both *ddc* and WT plants (Fig. 3.43 A, B). Namely, Cd exposition determined a dose-dependent

decrease of *PIN1* transcripts in the WT, while in *ddc* mutant transcript level was affected only at 50 µM Cd treatment (Fig. 3.43 A). However, note that under Ctrl condition *PIN1* was found to be down-expressed in *ddc vs* WT (Fig. 3.43 A). Under Ctrl condition, no differences in *ddc vs* WT were instead detected for *PIN7,* which expression was also strongly down-regulated in the WT whatever treatment was used (Fig. 3.43 B). In *ddc* mutant a strong *PIN7* down-regulation was found only under 50 µM Cd treatment (Fig. 3.43 B).

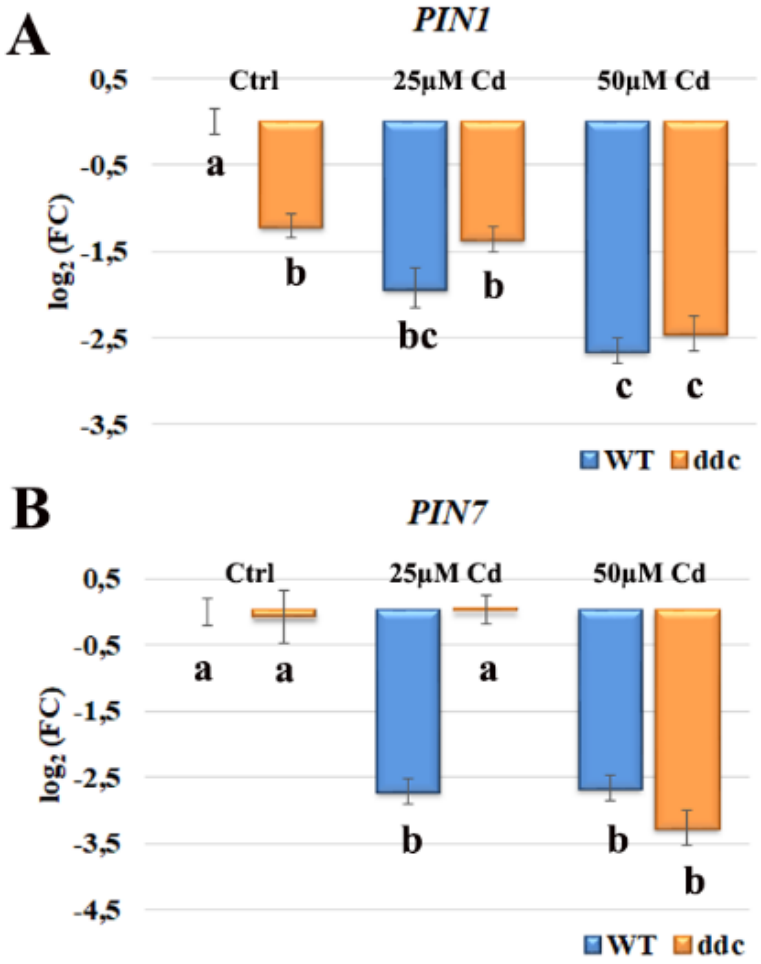

Figure 3.43: Relative expression by qRT-PCR of **(A)** *PIN1* and **(B)** *PIN7* in primary roots of *A. thaliana* seedlings grown **(i)** on control medium (Ctrl), **(ii)** on medium added with 25 µM Cd and **(iii)** on medium added with 50 µM Cd for 8 DAG. Data present the mean ± standard error (SE) of three independent experiments. Statistical analysis was performed by using two-way ANOVA with Tukey post hoc test ($P \leq 0.05$) after Shapiro–Wilk normality test. Means with the same letter are not significantly different at $P \leq 0.05$.

Concerning PINs distribution, in the roots of WT and *ddc* seedlings grown in Ctrl condition, a canonical GFP signal was observed for PIN1, whose presence extended from

the basal end of provascular cells to the SCN (Friml *et al.,*2009). However, in *ddc* mutant, the intensity of GFP signal was lower than in the WT (Fig. 3.44 A, D, G-I). Under Cd treatment, a dose-dependent reduction of GFP signal was observed in both mutant and WT (Fig. 3.44 B, C, E-I). However, despite the initial lower signal in *ddc*, under 50 µM Cd treatment, it resulted higher in the mutant compared to the WT (Fig. 3.44 C, F-I). Altogether, our results point out a differential impact of Cd on PIN1 expression on *ddc* and WT at both transcriptional and translation level.

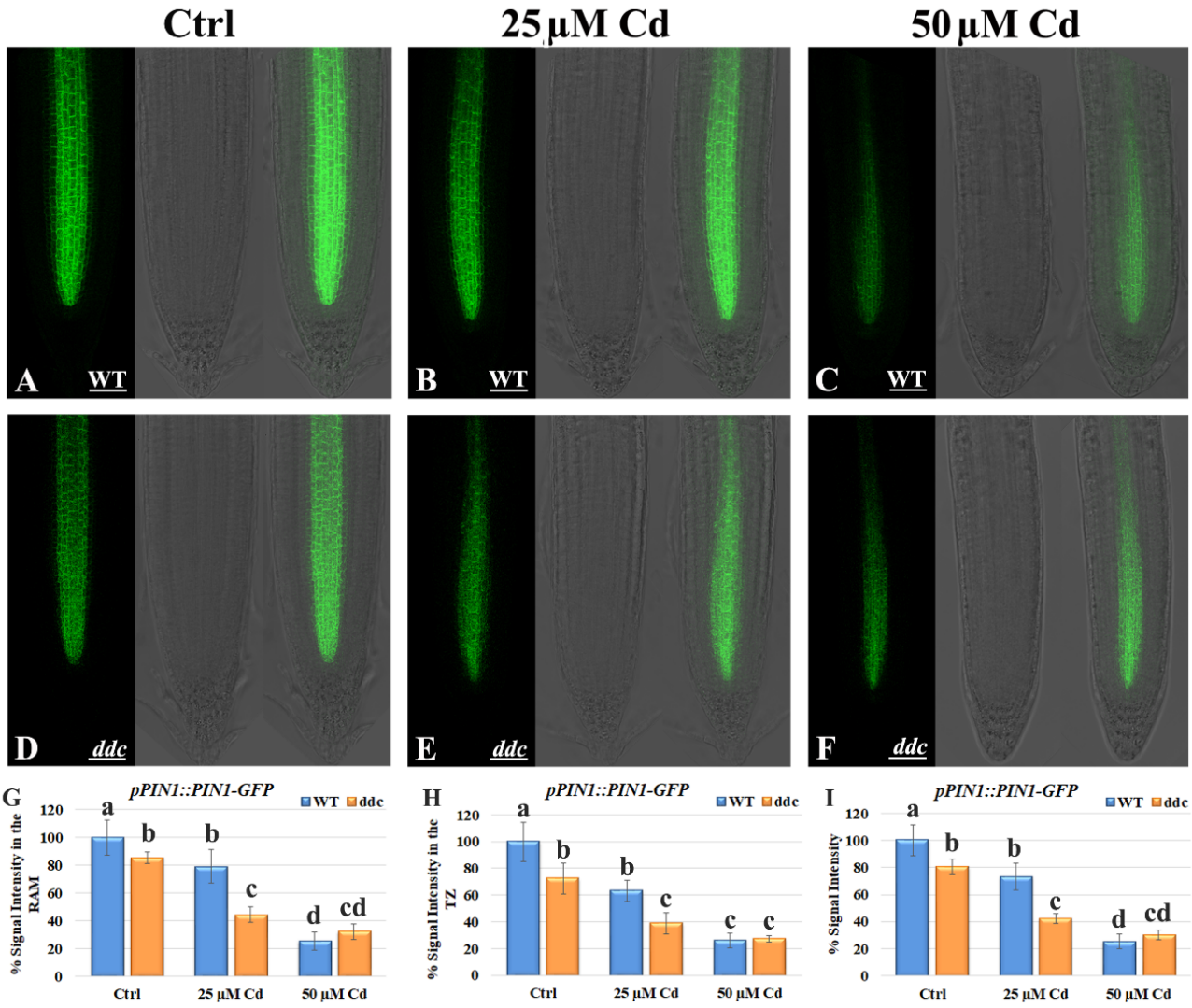

Figure 3.44: (A-F) Primary root tip in seedlings of *A. thaliana pPIN1::PIN1-GFP* and *ddc X pPIN1::PIN1-GFP*, transgenic lines grown**(A, D)** on control medium (Ctrl), **(B, E)** on medium added with 25 µM Cd and **(C, F)** on medium added with 50 µM Cd for 8 DAG. From left to right: confocal laser image; transmission image; merged image. **(G-I)** GFP relative signal intensities (normalized to Ctrl), in **(G)** the RAM, **(H)** the TZ and **(I)** the whole root apex, of above-mentioned Ctrl and Cd-treated roots. The results represent the mean

value (± standard deviation) of three independent biological replicates (n = 50). Statistical analysis was performed by using two-way ANOVA with Tukey post hoc test ($p \leq 0.05$) after Shapiro–Wilk normality test. Means with the same letter are not significantly different at $p \leq 0.05$. Scale bars 46 µm.

Concerning PIN7, in WT roots grown under Ctrl condition, GFP signal was typically localised in columella and in provascular cells (Fig. 3.40 A, D). Under the same condition, *ddc* roots exhibited a stronger GFP signal in the columella cells, whereas in provascular cells the signal was weaker and extended further from proximal meristem, compared to the WT (Fig. 3.40 A, D, G-J). Following exposure to 25 µM Cd, a general lowering of GFP signal was observed in WT roots, while in *ddc* mutant signal intensity was reduced only in the columella cells and remained unchanged and normally extended in the provascular strands. (Fig. 3.40 B, E, G-J). Under 50 µM Cd treatment, a further reduction of GFP signal was observed, more in WT than in *ddc* mutant (Fig. 3.40 C, F, G-J).

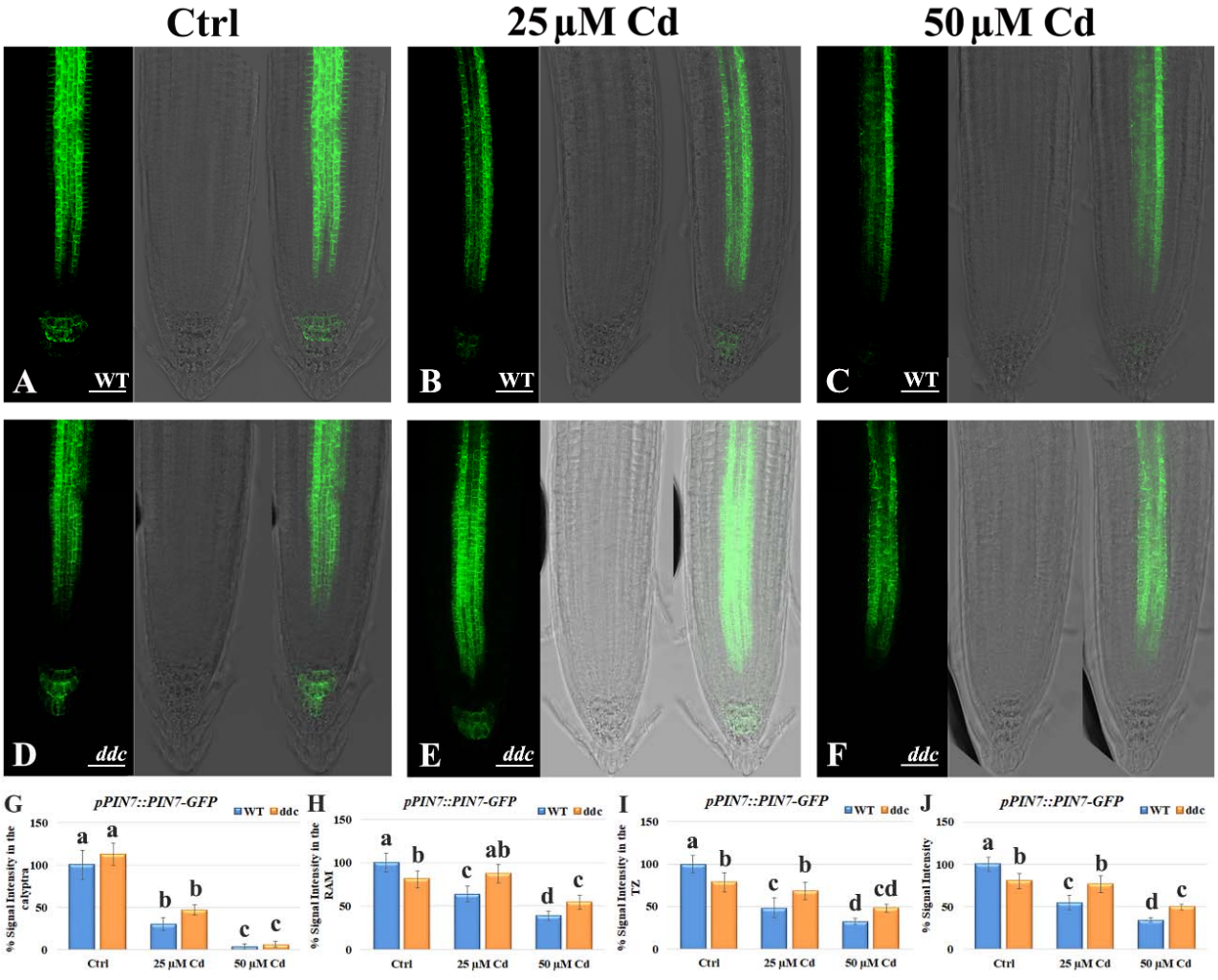

Figure 3.40: (A-F) Primary root tip in seedlings of *A. thaliana pPIN7::PIN7-GFP* and *ddc X pPIN7::PIN7-GFP*, transgenic lines grown **(A, D)** on control medium (Ctrl), **(B, E)** on medium added with 25 µM Cd and **(C, F)** on medium added with 50 µM Cd for 8 DAG. From left to right: confocal laser image; transmission image; merged image. **(G-J)** GFP relative signal intensities (normalized to Ctrl), in **(G)** the calyptra, **(H)** the RAM, **(I)** the TZ and **(J)** the whole root apex, of above-mentioned Ctrl and Cd-treated roots. The results represent the mean value (± standard deviation) of three independent biological replicates (n = 50). Statistical analysis was performed by using two-way ANOVA with Tukey post hoc test ($p \leq 0.05$) after Shapiro–Wilk normality test. Means with the same letter are not significantly different at $p \leq 0.05$.
Scale bars 46 µm.

Thereafter, auxin distribution was estimated by using *pDR5::GFP* and *ddc X pDR5::GFP* transgenic lines *of A. thaliana*. At this respect, confocal analyses evidenced that, under Ctrl condition, GFP signal was lower in *ddc* roots compared to the WT, especially along the stele which appeared almost deprived of signal (Fig. 3.41 A, D, G-J). Following Cd treatment, in WT roots a dose-dependent reduction of GFP signal was observed mostly in the stele, while in *ddc* mutant the signal intensity decreased only in roots exposed to 50 µM Cd concentration (Fig. 3.41 B, C, E-J).

Globally, these data showed that auxin distribution was impaired in both *ddc* mutant and WT under Cd treatment, although at different extent. Moreover, a link with Cd-toxicity on *PINs* gene expression and these efflux carriers distribution was also clearly established.

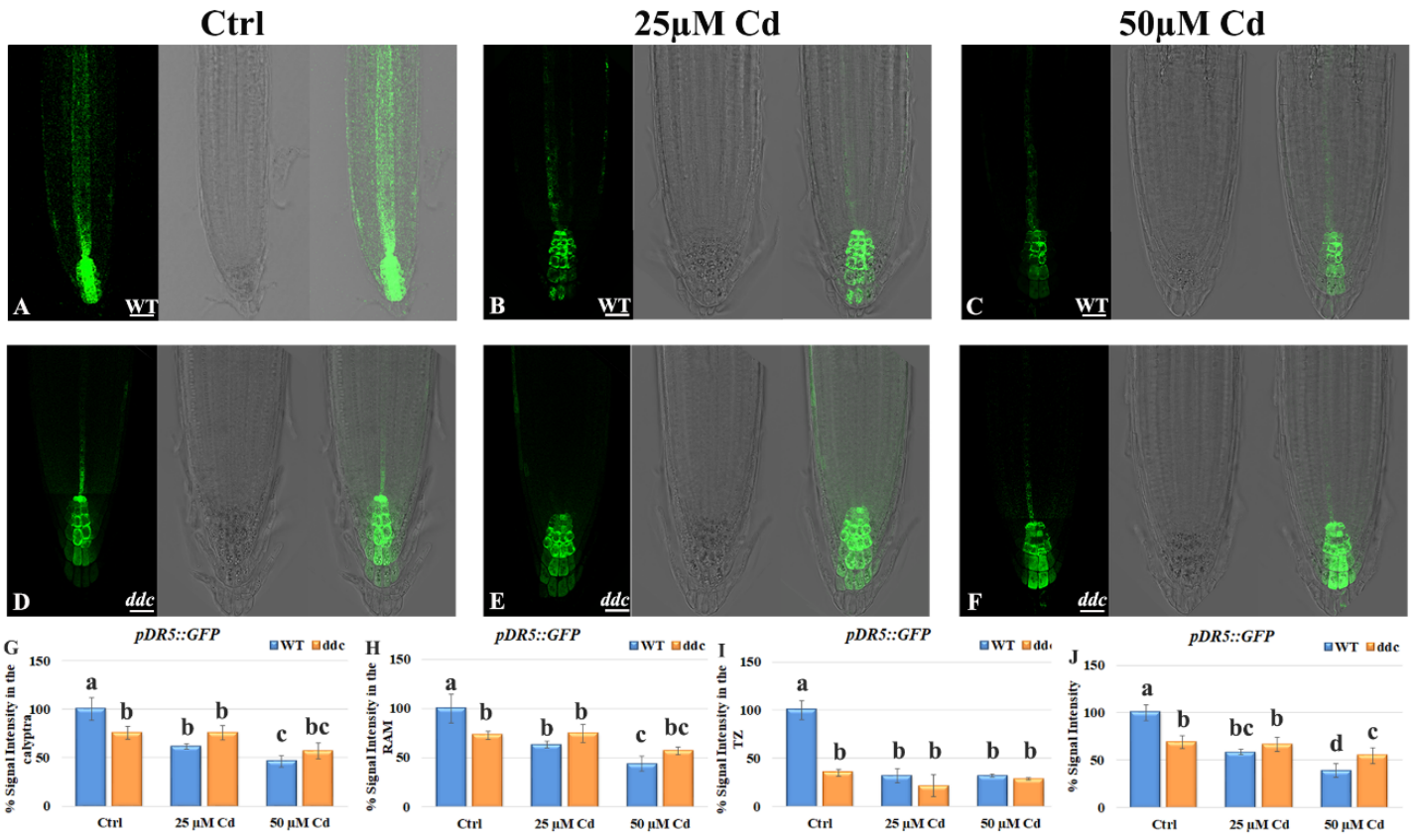

Figure 3.41: (A-F) Images of primary root apex in seedlings of *A. thaliana pDR5::GFP and ddc X pDR5::GFP* transgenic line grown **(A, D)** on growth medium as control (Ctrl), **(B)** on medium added with 25 µM Cd and **(C)** on medium added with 50 µM Cd for 8 days after germination. From left to right: confocal laser image; transmission image; merged image. **(G-J)** GFP relative signal intensities (normalized to Ctrl), in **(G)** the calyptra, **(H)** the RAM, **(I)** the TZ and **(J)** the whole root apex, of above-mentioned Ctrl and Cd-treated roots. The results represent the mean value (± standard deviation) of three independent biological replicates (n = 50). Statistical analysis was performed by using two-way ANOVA with Tukey post hoc test ($p \leq 0.05$) after Shapiro–Wilk normality test. Means with the same letter are not significantly different at $p \leq 0.05$. Scale bars 46 µm.

3.6.2 Effects of Cd toxicity on Root Apical Meristem pattern in *ddc* mutant and WT *A. thaliana* seedlings.

The involvement of auxin in root growth starts from the definition of the root apical meristem (RAM) during embryogenesis to its maintenance during post-embryonic development, both determined by maximum auxin accumulation (Bhalerao and Bennett, 2003; Leyser 2006; Prusinkiewicz and Rolland-Lagan, 2006; Tanaka *et al.,*2006; Benjamins and Scheres, 2008).

Starting from the Cd-related effects on phenotype, transcriptome and auxin distribution, we planned to analyse whether and how the patterning of the primary root could be affected by Cd both in WT plants and *ddc* mutant.

Firstly, we analysed root meristem size and pattern. Preliminarily, to define the full accomplishment of RAM development, we monitored when root meristem reached a fixed number of cells: in both WT and *ddc* mutant it occurred at 5/6 DAG and 7/8 DAG under Ctrl condition and Cd exposure, respectively. Therefore, in order to examine roots at comparable stages of development, seedlings at 8 DAG were used (Fig. 3.42 A-G; Fig. 3.43 A-G and A'-G').

Meristem size was estimated in both longitudinal and radial direction. To this aim, we estimated the root meristem length by measuring, along the single cortex layer, the distance from QC to TZ, where cell elongation is starting (Fig. 3.43 A-G). It resulted quite comparable in all the conditions analysed (Fig. 3.42 A; Fig. 3.43 A-G). The number of cortex cells present in the region extending from QC to TZ was also estimated. The cell number did not differ between *ddc* and WT under Ctrl condition (Fig. 3.42 B; Fig. 3.43 A, B), while a dose-dependent reduction was evident in Cd-treated roots of both *ddc* mutant and WT. However, under 25 µM Cd treatment, this effect was somehow different in *ddc vs* WT since cell number was lower in the former (Fig. 3.42 B; Fig. 3.43 C, D), while under 50 µM Cd treatment the cell number was similar (Fig. 3.42 B; Fig. 3.43 E, G). In all the cases, the reduction of cell number was associated to an increase of cell size, which accounts for the similar root meristem length detected in all the samples (Fig. 3.43 C, D, E, G).

For evaluating the meristem width, we measured the cross diameter of both whole root and stele at the level of TZ (Fig. 3.42 C, D; Fig. 3.43 A-G); limited to root stele, the number of cell files was also evaluated. The obtained results showed that under Ctrl condition both the root and stele width as well as the cell file number were comparable in *ddc vs* WT (Fig. 3.42 C, D, E; Fig. 3.43 A, B). As for Cd effect, on the whole it negatively affected all these parameters but in a different way when comparing *ddc vs* WT. In particular, the effect of Cd exposure on the root and stele width already started at 25 µM Cd concentration (Fig. 3.42 C, D; Fig. 3.43 C, D) and only at 50 µM Cd concentration in *ddc* mutant and WT, respectively (Fig. 3.42 C, D; Fig. 3.43 E, G). A dose-dependent

reduction of cell files number was instead observed in the stele of both *ddc* and WT (Fig. 3.42 E; Fig. 3.43 C, D, E, G).

Attention was then payed to the quiescent centre (QC), formed by a limited number of cells, which is the organizing centre of stem cell niche (SCN) and root meristem, by preventing the differentiation of surrounding cells (van den Berg *et al.,*1997; Stahl and Rüdiger, 2010). According to literature (van den Berg *et al.,*1997), under Ctrl condition, the QC of WT roots was typically arranged and formed by 4 equally-sized cells (Fig. 3.43 A, A'), while in *ddc* roots some QC cells were slightly bigger than others, thus impairing a correct SCN stratification (Fig. 3.43 B, B'). When exposed to Cd, a dose-dependent effect was observed in both WT and *ddc* roots, consisting in a progressive reduction of QC cell number and cell size increase causing also in these cases an evident alteration of SCN stratification pattern (Fig. 3.42 F; Fig. 3.43 C-G, C'-G'). Moreover, in WT roots exposed to 50 µM Cd in few cases the QC cells were totally undetectable and the SCN pattern fully compromised (Fig. 3.43 F, F').

Alterations were also observed in root cap. Namely, under Cd treatment a reduction of statocytes accumulation was observed in both *ddc* and WT root cap, suggesting a Cd-induced delay of columella cells differentiation (Fig. 3.43 C-G, C'-G'). In addition, 3-4 layers of cells devoid of statocytes were found in place of calyptrogen in the WT roots where QC was undetectable (Fig. 3.43 F, F').

Altogether, these results suggested that the QC cells exposed to Cd toxicity undergo to a progressive loss of their identity.

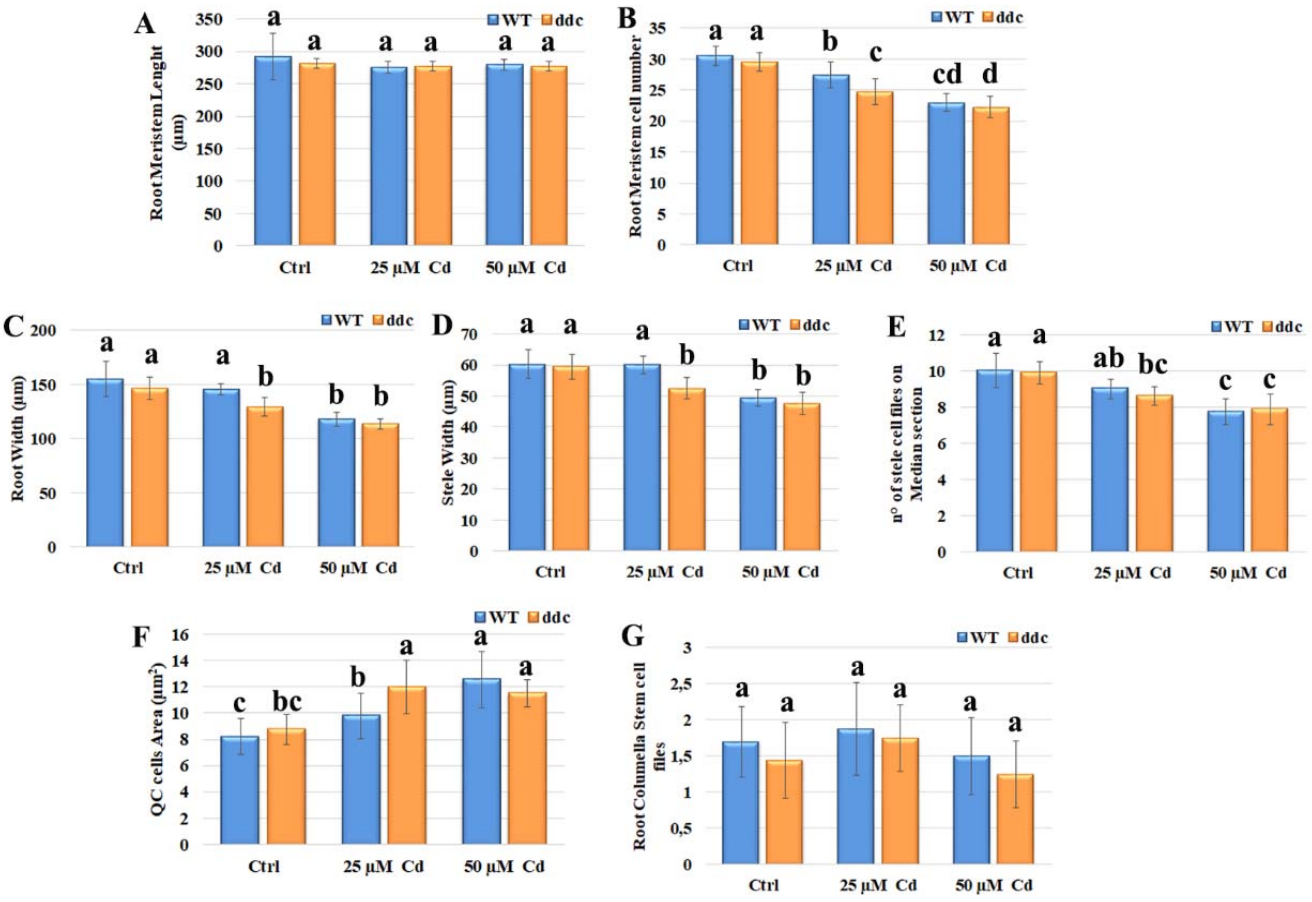

Figure 3.42: **(A)** Meristem length (µm), **(B)** meristem cell number, **(C)** meristem width (µm), **(D)** stele width (µm), **(E)** stele cell files number, **(F)** quiescent centre cell area (µm^2) **(G)** calyptrogen layers number, in primary roots of *A. thaliana* seedlings germinated **(i)** on growth medium as control (Ctrl) **(ii)** on medium added with 25 µM Cd and on medium added with 50 µM Cd for 8 days after germination. Data present the mean ± standard deviation (SD) of three independent experiments (n=70). Statistical analysis was performed by using two-way ANOVA with Tukey post hoc test ($p \leq 0.05$) after Shapiro–Wilk normality test. Means with the same letter are not significantly different at $p \leq 0.05$.

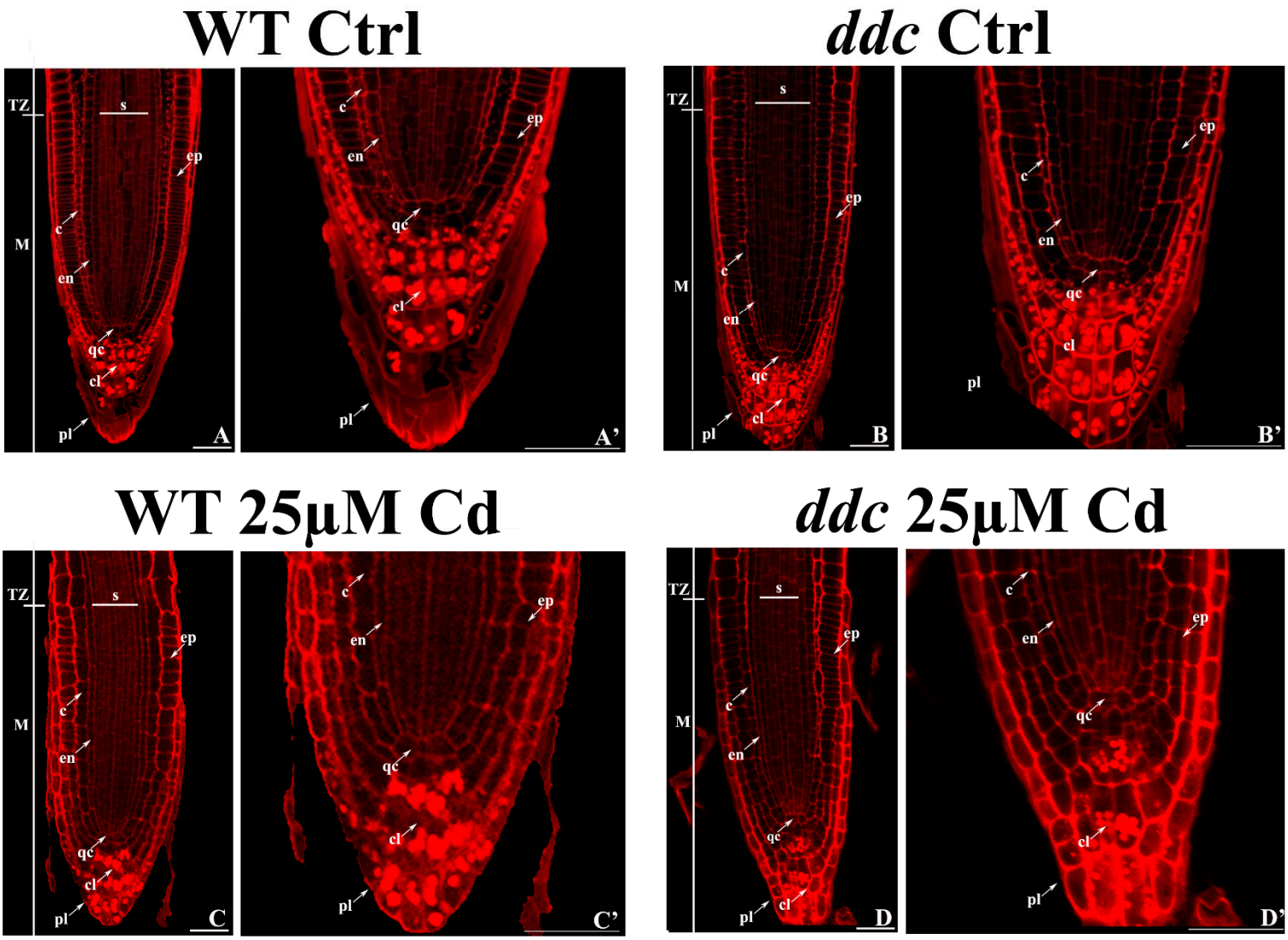
WT Ctrl
ddc Ctrl
WT 25µM Cd
ddc 25µM Cd
TZ
M
s
ep
c
en
qc
cl
pl
A
A'
B
B'
C
C'
D
D'

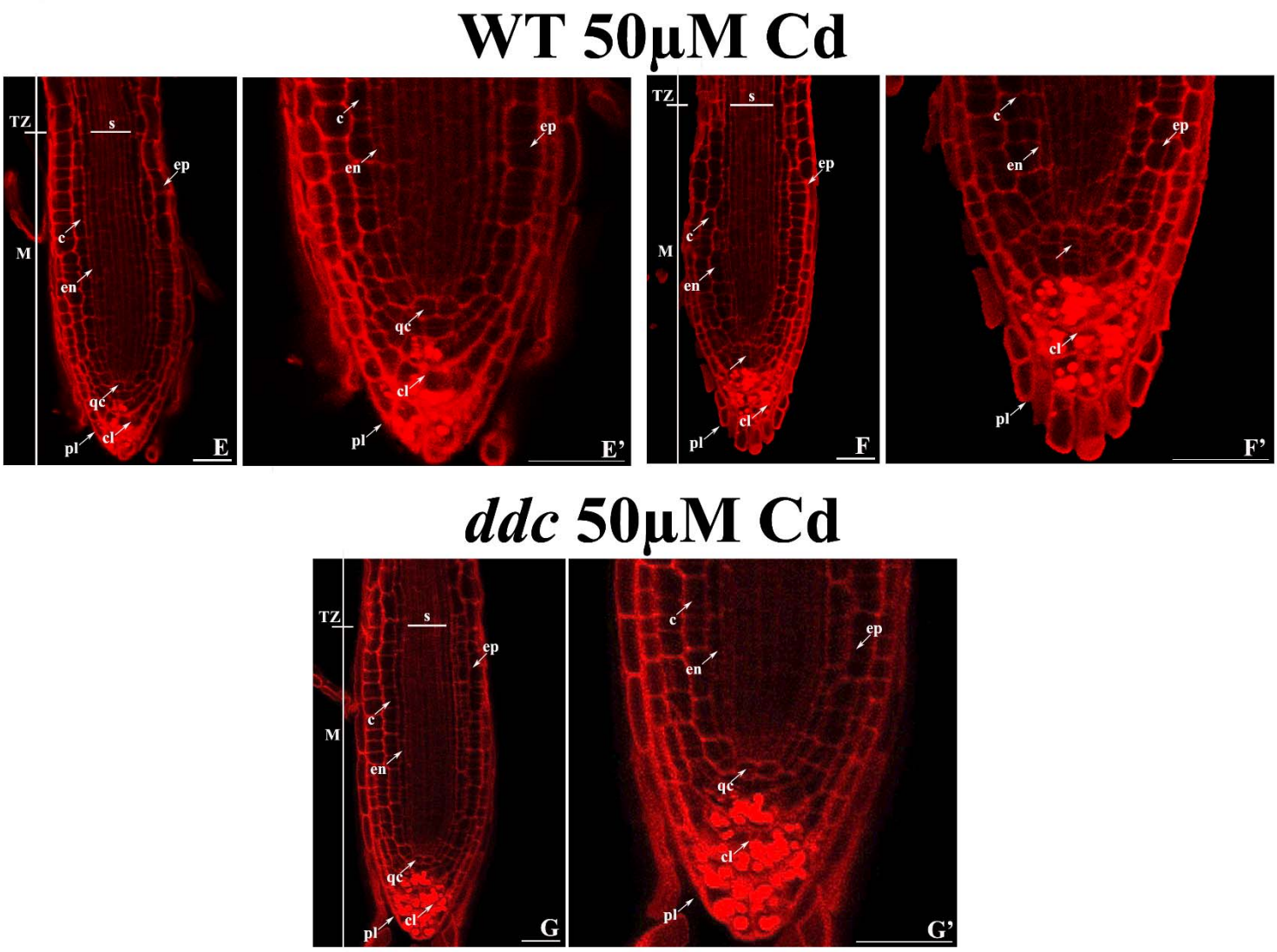

Figure 3.43: Confocal laser images of primary root tip of *ddc* mutant and WT seedlings of *A. thaliana* grown **(A, B)** on control medium **(Ctrl)**, **(C, D)** on medium added with 25 and **(E, F, G)** on medium added with 50 µM Cd, for 8 days after germination. **(A'–G')** Higher magnification of **(A–G)**, respectively.
cl, columella; c, cortex; en, endodermis; ep, epidermis; pl, cap peripheral layers; qc, quiescent center; s, stele; M, meristematic zone; TZ, transition zone. Scale bars **(A–G)** 46 µm; **(A'–G')** 53 µm.

3.6.3 Cd Impact on SCARECROW expression pattern in *ddc* mutant and WT *A. thaliana* seedlings.

From literature, it is known that the specification of QC identity and stem cell activity in the RAM is strictly dependent on the activity of SCR transcription factor of the GRAS family, which acts through a fine control of hormonal signalling in the RAM (Di

Laurenzio *et al.,*1996; Pysh *et al.,*1999; Wysocka-Diller *et al.,*2000). Indeed, SCR modulate auxin pathway and in turn itself is induced from auxin (Salvi *et al.,*2018). In particular, SCR, which is specifically expressed in the QC and the endodermis, suppresses ARR1 expression in QC cells, thus blocking cytokinin signalling and enhancing auxin production (Moubayidin *et al.,*2013). The auxin, in turn, keeps the division rate in the stem cells under control and, thanks to its polar transport, an auxin gradient is created along the RAM, from the QC to the transition zone, where ARR1 synthesis is not suppressed and the cells differentiation process can begin. This way, SCR acts as the principal spatial coordinator of RAM size and pattern (Moubayidin *et al.,*2013).

All these evidences, together with the above described results, prompted us to investigate whether SCR expression pattern was somehow affected by Cd exposure in both *ddc* and WT roots. To this aim, *pSCR::SCR-GFP* and *ddc X pSCR::SCR-GFP* transgenic lines of *A. thaliana* were used and seedling at 8 DAG of both transgenic lines were either grown under Ctrl condition and exposed to 25 and 50 µM Cd.

In line with data in literature, confocal analysis performed on GFP lines confirmed that in the WT roots grown under Ctrl condition, SCR expression was typically confined to QC cells, the cortex/endodermis initials and the endodermis, as evidenced by GFP signal (Malamy and Benfey, 1997; Moubayidin *et al.,*2013; Moubayidin *et al.,*2016) (Fig. 3.44 A, Fig. 3.44 A'). The same pattern was observed also in the root of *ddc* mutant grown in Ctrl condition, but in this case GFP signal resulted weaker as compared to WT, mainly at the level of QC (Fig. 3.44 D, Fig. 3.44 E'). Following Cd exposure, a pronounced reduction of *SCR* expression was observed in both *ddc* and WT roots. Indeed, in WT roots exposed to 25 µM Cd, GFP signal appeared almost absent in several endodermis cells, in the region extending from the proximal meristem to the transition zone (Fig. 3.44 B). A further reduction of GFP signal was observed in WT roots exposed to 50 µM Cd, together with its mislocalisation in the stele at the level of TZ and also in some committed cortex cells (Fig. 3.44 C, arrow; Fig. 3.44 C', D', arrows). A somehow different picture was induced by Cd in *ddc* roots. In particular, under 25 µM Cd treatment, in these roots GFP signal along endodermis was quite comparable to that detected under Ctrl conditions, but QC cells resulted almost deprived of signal (Fig. 3.44 E, Fig. 3.44 B'). A reduction of GFP signal involving also endodermis cells was instead observed in *ddc* roots exposed to 50 µM Cd

(Fig. 3.44 F). Moreover, also for *ddc* mutant an ectopic localization of GFP signal was observed, dealing only with caliptrogen cells (Fig. 3.44 G', arrow).

In summary, a diminished expression of *SCR* and its ectopic expression in the TZ and in the committed cortex cells was evidenced in both *ddc* mutant and WT roots under Cd treatment. Altogether, these data suggested that the modifications in RAM pattern observed in *ddc* and WT under Cd treatment were related to an impairment of *SCR* expression that likely determined a partial loss of QC identity.

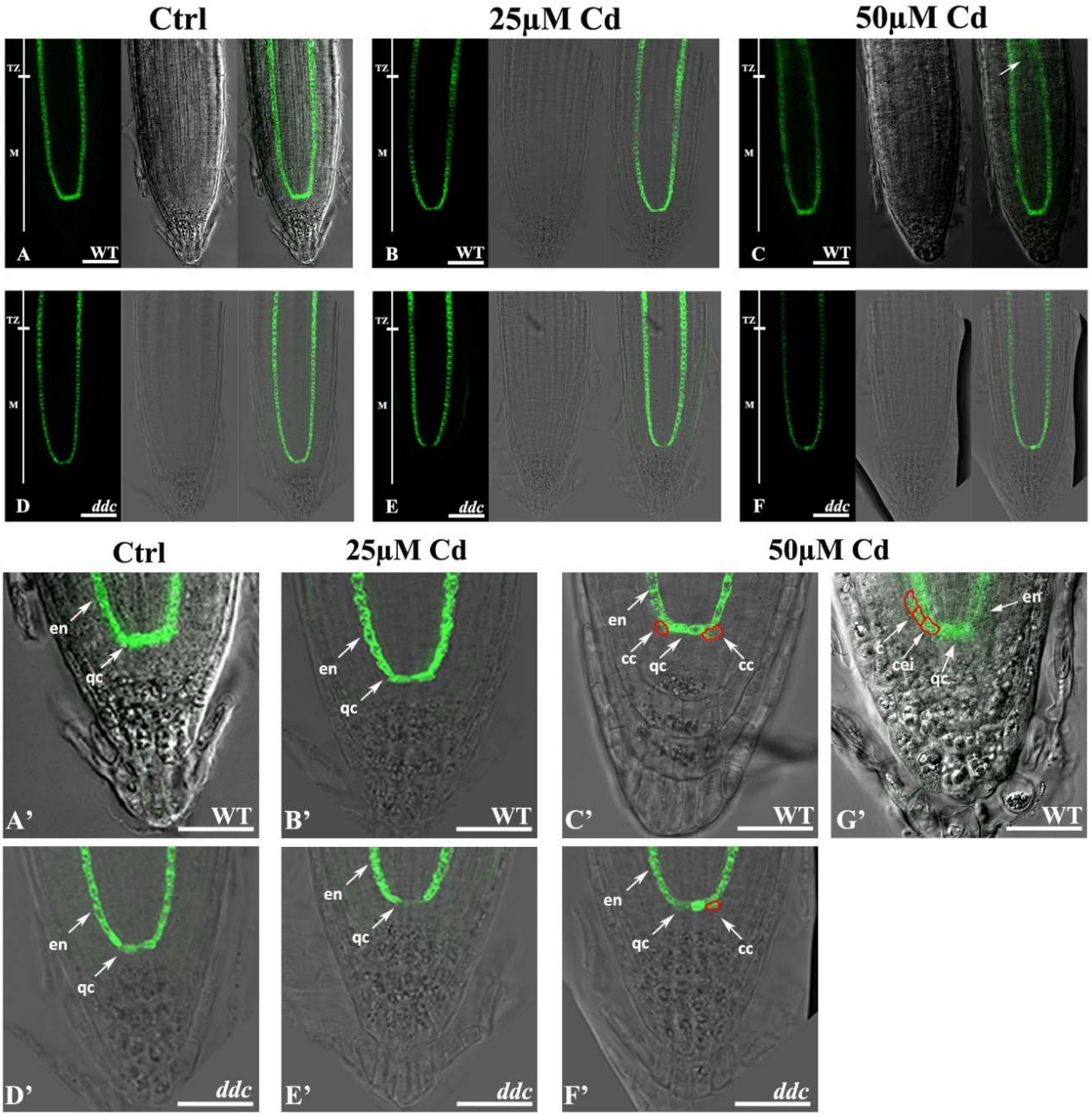

Figure 3.44: Expression of *SCARECROW* in the primary root of seedlings of *A. thaliana pSCR::SCR-GFP* and *ddc X pSCR::SCR-GFP* transgenic lines grown **(A, D)** on control medium (Ctrl), **(B, E)** on medium added with 25 µM Cd and **(C, F)** on medium added with 50 µM Cd, for 8 days after germination. From left to right: confocal laser image; transmission image; merged image; **(A'-F')** Higher magnification of A-F, and **(G')** additional picture showing the mislocalization of SCR expression in the proximal meristem.

Scale bars **(A-F)** 110 µm; **(A'-G')** 42 µm.

M, meristematic zone; TZ, transition zone. en, endodermis; qc, quiescent centre; cc, calyptrogen cells; c, cortex; cei, cortex and endodermis initial.

CHAPTER 4: DISCUSSION

Due to their sessile life style, plants are continuously exposed to a wide range of stresses. For this reason, a promptly conversion of stress signal perception into appropriate responses and adaptive modifications is fundamental for their survival (Chinnusamy and Zhu, 2009).

Recently, numerous studies underlined the importance of epigenetic, and mainly of DNA methylation, in the control of plant growth plasticity and stress response, as an effect of their capacity to put in place a simultaneous and extensive regulation of gene expression (Chinnusamy and Zhu, 2009). Despite this information, the complex mechanisms by which DNA methylation modulates plant stress response is yet largely unresolved, mainly with respect to heavy metal stress, for which a metal- and species-specific response was evidenced (Aina *et al.,*2004).

In order to contribute to fulfil this gap, in the present work we performed a comparative analysis on the effects of Cd treatment on *ddc* mutant of *A. thaliana*, defective in both maintenance and *de novo* methylation processes, and WT plants through a transcriptomic approach. We focused our attention on Cd, since it is one of the most toxic pollutants, widespread in both terrestrial and marine environment (Pinto *et al.,*2004).

Preliminarily, several growth parameters were analysed, since it is known that Cd toxicity impairs plant growth and development by affecting several physiological and metabolic processes (Sanità di Toppi *et al.,*2003; Dal Corso *et al.,*2010). This effect was confirmed in our work, since both germination and vegetative development were negatively affected by Cd in both *ddc* mutant and WT. In particular, a dose-dependent decrease of germinative energy, as well as of root length and leaf area was observed in Cd-treated seedlings (Fig. 3.1; Fig. 3.2 A, B; Fig 3.4 A, B). However, and very interestingly, all these growth parameters were impaired at higher extent in the WT than in *ddc* mutant. Therefore, although in Ctrl condition the growth rate was lower in the mutant than in the WT, under Cd treatment a better growth performance was exhibited by *ddc* mutant as compared to the WT, especially at 25 µM Cd concentration (Fig. 3.2; Fig 3.4).

Transcriptomic analysis, allowing the identification of the genetic pathways which undergo to a differential modulation under Cd treatment in *ddc vs* WT, provided some interesting and robust explanations to the different behaviour observed at the morphophysiological level. Namely, clear differences in gene expression were observed in

ddc vs WT under Ctrl condition and, above all, under Cd treatment (Fig. 3.8 A-G). In particular, GO term enrichment highlighted that the genetic pathways more impacted by Cd treatment dealt with photosynthesis, stress responses and hormone biosynthesis and signalling, which are all highly relevant for plant development (Fig. 3.8 A-G).

Then, a more detailed analysis was carried out on the pathways related to hormones, since these signal molecules, beside their role in plant development, are strongly involved in plant response to stress. However, concerning the other pathways, we would like at least to mention that, consistently with the better growth performance of *ddc* mutant, photosynthesis genetic pathways were globally upregulated in *ddc* mutant compared to the WT (data not shown).

Concerning the genetic pathways related to hormones, under Cd treatment, they resulted all differentially modulated in *ddc vs* WT, although at different extent. The most relevant differences were detected for those related to the metabolism and signalling of auxin (IAA), cytokinins (CKs) and gibberellins (GAs), that is consistent with several data in literature. Namely, it has been evidenced that many signalling molecules and plant hormones are involved in cadmium sensing and downstream plant response (Sanità Di Toppi *et al.,*2003; Sofo *et al.,*2013; Chmielowska-Bąk *et al.,*2014; Yue *et al.,*2016; Fattorini *et al.,*2017). However, the general picture is somehow controversial differing in relation to species, plant organ, heavy metal concentration and treatment duration (reviewed by Chmielowska-Bąk *et al.,*2014).

In our case, in *ddc* mutant both Cd concentrations were found to induce a significant down-regulation of the genes involved in the IPA pathway, which, as already mentioned, in *Arabidopsis thaliana* is the main auxin biosynthetic pathway (Mashiguchi *et al.,*2011; Brumos *et al.,*2014; Zhao *et al.,*2014; Kasahara, 2016) (Fig. 3.9 B, C). A higher transcription of genes involved in IAOX auxiliary pathway of auxin biosynthesis was also detected in *ddc* mutant at both Cd concentrations (Fig. 3.9 B, C). Whereas, in the WT a similar modulation of gene expression was reported only under 50 µM Cd treatment (Fig. 3.9 C). Interestingly, in *ddc* mutant, a down-regulation of genes involved in IAA inactivation was also observed when treated with 25 µM Cd (Fig. 3.10 B, Fig. 3.11 B). All these evidences suggested that, at least under 25 µM Cd treatment, *ddc* mutant could be able to produce and/or maintain a higher level of bioactive IAA compared to the WT. This hypothesis was fully verified through the quantification of this hormone (Fig. 3.33), that

evidenced a higher IAA level in *ddc* mutant, compared to the WT, under 25 μM Cd treatment. Moreover, under the same Cd concentration (25 μM), the genetic pathway related to IAA signalling was enhanced only in the *ddc* mutant, resulting in an up-regulation of *SAUR* auxin-responsive genes (Fig. 3.24 B) whose products are implicated in the regulation of a wide range of cellular, physiological, and developmental processes, including leaf and root growth (Ren and Gray, 2015).

Therefore, these results showing a different modulation of both auxin biosynthesis and signalling provided a suitable explanation for the better growth performance of the *ddc* mutant exposed to 25 μM Cd treatment, as highlighted by the rates of root and leaves growth. In this context, it is worth to recall that, as reported by Hu *et al.* (2013), in *A. thaliana* seedlings Cd induces a decrease of IAA content, associated to an increase of IAA oxidase activity, resulting into a down-regulation of numerous auxin-responsive genes, relevant for plant growth. Moreover, data in literature also showed that, under Cd exposure, high level of IAA prevented growth inhibition and increase heavy metal tolerance (Srivastava *et al.,*2014).

A second hormone class whose genetic pathways resulted affected by Cd is represented by CKs. It is known that CKs homeostasis relies on the balance between biosynthesis and catabolism and/or conjugation, which occurs through cleavage by CK oxidases or glycosylation, respectively (Hou *et al.,*2004; Wang *et al.,*2011, Wang *et al.,*2013). Previous literature data evidenced an enhancement of CKs oxidation/degradation in *Triticum durum* seedlings exposed to 0.04 mM Cd treatment (Veselov *et al.,*2003), whereas an overproduction of such hormones was detected by Sofo *et al.* (2013) in both root and shoot of Cd- treated plants of *A. thaliana.* In our work, an up-regulation of the genetic pathways related to CKs inactivation through glycosylation was observed in both the mutant and the WT when exposed to Cd (Fig. 3.14 B, C; Fig. 3.15 B, C). However, under 25 μM Cd treatment, the genetic pathway related to CKs *O*-glycosylation was up-regulated only in *ddc* mutant (Fig. 3.15 B). Notably, while *N*-glycosylation inactivates cytokinins in a definitive way (Feng *et al.,*2017), *O*-glycosylated CKs represent the stable hormone fraction, available for storage and transport, that can be re-converted in active CKs by β-glucosidases (Brzobohaty *et al.,*1993). Moreover, a down-regulation of the genes involved in cytokinin cleavage was also observed in *ddc* under 25 μM Cd (Fig. 3.13 B). All these results lead to hypothesize that the genetic modulation

detected in the mutant under such Cd concentration could be addressed to preserve CKs pool. As such, this mechanism could represent an important strategy to enhance plant resistance to Cd stress. In fact, CKs have a fundamental role in counteracting leaf senescence, as well as in protecting photosystems and enhance photosynthetic activity both under normal and Cd stress condition. (Al-Hakimi, 2007; Piotrowska-Niczyporuk *et al.,*2012). Accordingly, under Cd treatment, leaf growth was less impaired in *ddc* mutant than in WT plants (Fig. 3.4 B).

Concerning GAs, altogether, the results that we obtained evidenced that the pathways related to their biosynthesis were down-regulated by Cd treatment more rapidly in *ddc* mutant than in WT. In fact, under 25 µM Cd treatment both the early GAs biosynthetic pathway and the GAs biosynthesis super pathway, leading to active forms, were down-regulated in the mutant, while GAs inactivation was down-regulated (Fig. 3.16 B; Fig. 3.17 B, Fig. 3.18 B). By contrast, in the WT a down-regulation of only GAs biosynthesis super pathway was detected at 50 µM Cd concentration (Fig. 3.17 C). We suggest that the strong down-regulation of the genetic pathway related to GAs inactivation in the *ddc* mutant observed under 25 µM Cd treatment could represent a compensatory mechanism to counteract Cd-induced decrease of GAs production. This hypothesis was confirmed by the higher content of active GAs, and above all to the 13-hydroxylated GAs, detected in the mutant *vs* the WT under 25 µM Cd treatment (Fig. 3.34 B c, d, h, i). Furthermore, under 25 µM Cd an up-regulation of genetic network related to GAs signalling was found only in the *ddc* mutant (Fig. 3.26 B). It is known that GAs, in synergy with other hormones, play a relevant role in leaf development, by enhancing mitotic activity and promoting carbohydrate metabolism (Mansour and Kamel, 2005). Therefore, our results reporting a higher level of GAs and an enhancement of its signalling in the *ddc* mutant *vs* WT when exposed to 25 µM Cd are consistent with the higher number and area of leaves formed by *ddc* mutant under this treatment (Fig. 3.4 A, B).

Differences dealing with JA, SA, ABA and ethylene-related pathways were also detected through the transcriptomic analysis. Interestingly, all these plant growth regulators are strongly involved in the perception and downstream response of plants to different abiotic stresses, including heavy metals. Going into major details, regarding JA, we observed that in Ctrl condition the pathway related to the biosynthesis was down-regulated in the *ddc* mutant compared to the WT (Fig. 3.19 A), resulting in a lower

hormone amount (Fig. 3.35). Moreover, a down-regulation was induced by 25 µM Cd treatment, more pronounced in the WT than in *ddc* (Fig. 3.19 B), leading to comparable levels of JA in the two samples (Fig. 3.35). An opposite pattern was detected for the genetic pathway related to JA signalling, which under 25 µM Cd treatment was more impacted in *ddc* mutant than in WT (Fig. 3.27 B).

In the case of SA, we observed that the genetic pathway related to its biosynthesis wasn't differentially modulated in *ddc* mutant and WT (Fig. 3.31 A-C), even though under Ctrl condition significantly higher levels of SA and SAG were found in *ddc* mutant *vs* WT (Fig. 3.37). Following Cd treatments, the amount of both hormone forms significantly decreased, more in *ddc* mutant than in the WT, leading to an opposite condition (Fig. 3.37). SA signalling pathway resulted down-regulated in the mutant, compared to the WT, already under 25 µM Cd treatment (Fig. 3.31 B), while in the WT the pathway was down-regulated only at the higher Cd concentration (Fig. 3.31 C).

Finally, concerning ABA, at the transcriptomic level no differences were observed between *ddc* and WT under Ctrl condition (Fig. 3.20 A). However, its amount was significantly lower in *ddc* mutant *vs* WT (Fig. 3.36), suggesting a post-transcriptional regulation of hormone levels, as reported in literature (Shu *et al.,*2018). Moreover, at both Cd concentrations, a slight down-regulation of genetic network related to ABA biosynthesis was detected in both *ddc* and WT (Fig. 3.20 B, C), while ABA degradation was down-regulated in *ddc* mutant compared to the WT (Fig. 3.21 B, C). These results are consistent with the strong decrease of ABA amount induced by Cd in the WT (Fig. 3.36). Concerning ABA signalling, while in the WT an up-regulation was observed at 25 µM Cd, in *ddc* mutant it was found to be down-regulated whatever heavy metal concentration was used.

Globally, the results dealing with JA, SA and ABA evidenced that Cd treatment induced a down-regulation of biosynthesis and/or signalling of these three stress-related hormones, which resulted more evident in *ddc* mutant than in WT. This scenario was somehow unexpected, since there is large evidence that the level and activity of these hormones usually increases following abiotic stress, including heavy metal (Maksymiec *et al.,*2007; Tuteja 2007; Cutler *et al.,*2010; Ashger *et al.,*2015). However, as already mentioned, the exact mechanisms of hormone action in response to stress, and mainly in relation to their crosstalk with the whole signalling network of plant, are yet to be fully

clarified. In addition, the hormone effects are largely dependent on the species, the plant organ, the plant growth stage, the intensity and the duration of stress (Asgher *et al.,*2015; Bücker-Neto *et al.,*2017). For example, concerning JA, in several plant species, including *A. thaliana*, Cd treatment was found to induce an accumulation of this hormone strongly depending on the species and the plant growth stages (Rodríguez-Serrano *et al.,*2006; Maksymiec *et al.,*2007). Moreover, such accumulation exhibited a biphasic model, with an early accumulation of JA, followed by cyclic decreases and increases (Maksymiec *et al.,*2005). In this context, it must be underlined that low concentrations of JA have been found to be effective as protectant against Cd stress, while at higher concentrations toxic effects, such as ROS accumulation, root growth inhibition, lipid peroxidation can be induced (Ranjan and Lewak, 1992; Adams and Turner, 2010; Liu *et al.,*2010; Soares *et al.,*2010). Similar toxic effects can be caused also by high levels of SA, which has been proposed as the "life or death switch" of cells (Gust and Nürnberger, 2012). Moreover, negative effects on plant growth can be exerted also by high levels of ABA, which acts as an antagonist of GAs action (Li and Huang, 2011; Shu *et al.,*2018). Based on all these evidences, it is likely that under the prolonged Cd treatment (21 DAG) that we applied, plant activity was directed to avoid toxic effects related to a long-lasting activation of all these hormones, by decreasing their level and/or down-regulating their signalling. Interestingly, in *ddc* mutant, which exhibited the best growth performance, both these adaptive responses are more pronounced.

A different behaviour was derived for ethylene. Namely, under Ctrl condition the genetic pathway related to its biosynthesis was up-regulated in *ddc* compared to the WT (Fig. 3.23 A), while under Cd treatment it was globally up-regulated in the WT and down-regulated in the *ddc* mutant (Fig. 3.23 B, C). Interestingly, genetic studies evidenced an antagonistic interaction between ethylene and ABA, with respect to both the biosynthesis and signalling pathways (Li and Huang, 2011). Therefore, the results obtained for ethylene are consistent with the pattern above described for ABA and provided further support to the better growth performance of *ddc* mutant (Fig. 3.3; Fig. 3.4). Indeed, the interaction of the ethylene and ABA pathways has been found to be crucial in regulating the plant development as well as its capacity to cope with stress (Li and Huang, 2011).

In summary, transcriptomic analysis evidenced that stress sensing and response related to the action of major hormone classes was somehow anticipated in *ddc* mutant,

compared to the WT, occurring at the lower Cd concentration. This result prompted us to suggest an involvement of the DNA hypomethylated status of *ddc* mutant in inducing its prompter response to stress, compared to the WT.

The successive step of our work was to gain further insights in the relationship between the differential alterations in hormone pathways detected through the transcriptomic analysis and the different growth response of *ddc* mutant *vs* WT under Cd treatment. In particular, attention was focused on the hormone auxin and root was selected as study system. Several cytophysiological parameters involved in root growth and related to auxin action have been considered, such as: auxin distribution and transport along the root, RAM size and pattern, expression pattern of SCR transcription factor involved in specifying SCN and root radial pattern. Part of these results, dealing with WT plants, have been already published (Bruno *et al.,*2017). Here, we report on the comparison between *ddc* mutant and WT plants.

In particular, the analysis performed using transgenic *pDR5::GFP* line allowed us to verify that the auxin distribution gradient along the RAM was affected by Cd treatment more in the WT than in *ddc* mutant (Fig. 3.41 B, C, E, F). That it's consistent with both transcriptomic analysis and hormone quantification (see Appendix), although performed on the whole seedlings.

Our results also showed that the impairment in auxin distribution in Cd-treated roots was related to an altered presence and distribution of PIN1 and PIN7 proteins (Fig. 3.39 B, C, E, F; Fig. 3.40 B, C, E, F) belonging to the large PINs family of membrane transporters, which are central rate-limiting components of auxin transport and in turn are under auxin-mediated transcriptional control (Blilou *et al.,*2005; Grieneisen *et al.,*2007; Petrásek and Friml, 2009). Once again, the alterations in distribution pattern of PIN1 and PIN 7 were less pronounced in *ddc* mutant.

These results are consistent with data in literature showing that Cd inhibitory effect on both primary, lateral and adventitious roots was linked to an impairment of auxin optimal accumulation at the root tip, due to the down-regulation, at both transcriptional and post-transcriptional level, of both PIN and LAX proteins which act as auxin efflux and influx carriers, respectively (Hu *et al.,*2013; Yuan and Huang, 2016, Fattorini *et al.,*2017; Sofo *et al.,* 2017). In this context, it must be mentioned that an increased level of auxin was found in the whole root of *A. thaliana* at low Cd concentration, in association with a higher

root branching (Sofo *et al.,*2013) likely as compensatory mechanism to the reduced growth of primary root. Although obtained under different treatment conditions, altogether these results strongly suggested that an alteration of auxin distribution, more than its total level, was the most relevant effect of Cd treatment. Namely, the establishment of auxin maximum at the root tip is essential for the maintenance of RAM, on which relies root growth (Aida *et al.,*2004; Galinha *et al.,*2007; Overvoorde *et al.,*2010). Therefore, the minor impairment of auxin accumulation in the tip of Cd-treated roots of *ddc* mutant *vs* WT is fully consistent with its better growth under this treatment.

In line with the altered auxin gradient, root meristem size and pattern were negatively and differentially affected by Cd in *ddc* mutant *vs* WT. As a general effect of Cd treatment in both *ddc* mutant and WT, despite a similar RAM length, the cell number along the cortex was lower in the roots exposed to the heavy metal compared with Ctrl ones (Fig. 3.42 A, B; Fig. 3.43 C, D, E, G). Moreover, these cells were bigger in treated than in Ctrl roots (Fig. 3.43 A-G), suggesting that they are losing the meristematic features as verified also in the ground meristem of *A. thaliana* lateral roots, even applying a lower Cd concentration (Fattorini *et al.,*2017). Therefore, the increase in cell area could represent a kind of compensatory mechanism to a reduced potential for proliferation.

The major alterations were observed at the level of the quiescent centre (QC), which acts as the organizing centre of stem cell niche (SCN), formed by initials which divide continuously, producing at each division one cell that continues to act as an initial (Dolan *et al.,*1993; van den Berg *et al.,*1997; Sabatini *et al.,*2003). The number of RAM initials varies according to species (Webster and MacLeod, 1980), but they are almost permanent in position and include the QC, which represents the generating centre of root pattern and architecture. In *A. thaliana* root, QC is formed by 4 equally-sized cells (van den Berg *et al.,*1997) and such condition was typically observed in the WT roots under Ctrl condition (Fig. 3.43 A-A'), whereas in *ddc* roots some QC cells were slightly bigger than others, thus impairing a correct SCN stratification (Fig. 3.43 B-B'). When exposed to Cd, a dose-dependent effect was observed in both WT and *ddc* roots, consisting in a progressive reduction of QC cell number and an increase of cell size, resulting once again into an alteration of SCN stratification pattern (Fig. 3.42 F; Fig. 3.43 C-G, C'-G'). Moreover, in WT roots exposed to 50 μM Cd, in few cases the QC cells were totally undetectable and the SCN pattern was fully altered (Fig. 3.43 F-F'). Similar alteration in QC cell

specification have been observed also in lateral and adventitious Cd-treated roots of *A. thaliana* by Fattorini *et al.* (2017).

In Cd-treated roots, alterations in root pattern were observed in both proximal and distal direction (Fig. 3.43 C-G). Indeed, a delayed differentiation of columella cells, sometimes associated to three/four-layered calyptrogen formed by large isodiametric cells, was observed in WT Cd-treated roots (Fig. 3.43 F-F'). On the other side, we observed that Cd exposure caused a reduction of cell files in the stele in both *ddc* and WT, likely related to the reduction of QC cell number, thus affecting also the radial pattern of the root (Fig. 3.42 E; Fig. 3.43 C-G). Altogether, these results suggested that under Cd toxicity the QC cells underwent to a progressive loss of their identity, likely representing the principal cause of RAM pattern alteration and root growth inhibition in both *ddc* and WT plants, even though the mutant seemed to be less affected by the heavy metal exposure.

It is known that the specification of QC identity is strictly dependent on the activity of SCR transcription factor (Sabatini *et al.,*2003; Moubayidin *et al.,*2016) which modulates auxin pathway and in turn itself is induced by auxin (Salvi *et al.,*2018). Based on the Cd-induced effect on hormone distribution and RAM pattern organization, we used transgenic GFP lines *pSCR::SCR-GFP* and *ddc X pSCR::SCR-GFP* to investigate whether SCR expression pattern was somehow affected in Cd-treated roots of *ddc* and WT. Through confocal analysis, we were able to observe a clear reduction of SCR expression in Cd-treated roots of both *ddc* and WT plants, more pronounced in the WT (Fig. 3.44 B, C, E, F), especially under 25 μM Cd treatment (Fig. 3.44 B, C). Moreover, and very interestingly, in both *ddc* and WT an ectopic expression of SCR was observed in some cap committed cells and at the level of some cortex committed cells and in the stele under 50 μM Cd treatment, respectively (Fig. 3.44 C, Fig. 3.44 C', D', G').

These results showed, for the first time, that Cd toxicity on root growth and pattern was related to a misexpression of SCR transcription factor. We propose that Cd treatment determined a partial loss of QC centre identity by affecting SCR expression pattern and auxin gradient impairment, with consequent alteration of RAM size and root growth. Moreover, it is worth to note that SCR transcription factor is known to interplay with auxin/cytokinin cross-talk in the control of RAM maintenance and activity (Salvi *et al.,*2018). Indeed, SCR is involved in formative stem cell division by regulating auxin levels through the suppression of cytokinin signalling, by inhibiting the cytokinin-

dependent *ARABIDOPSIS* RESPONSE REGULATOR 1 (ARR1), thus preventing post embryonic root stem cells differentiation (Moubayidin *et al.,*2013, 2016). Whereas, at the TZ, SCR modulates non-autonomously the ARR1 transcript levels via auxin and by sustaining gibberellin signals from the endodermis (Moubayidin *et al.,*2013, 2016). Interestingly, in line with this picture, in Cd-treated roots SCR signal was somehow weak in some cell of the stem niche, whereas it was ectopically expressed in the stele.

CHAPTER 5: CONCLUSIONS

In summary, the analyses performed in this work clearly showed that, under a prolonged Cd treatment (21 DAG) and within a specific threshold concentration (i.e. 25 µM Cd), the *ddc* triple mutant of *Arabidopsis thaliana*, defective in both *de novo* and maintenance DNA methylation, exhibited a different response compared to the WT, globally resulting into a better growth performance.

The reason of such behaviour likely relies on a higher genome plasticity of *ddc* mutant conferred by DNA hypomethylated status, which allowed it to better respond to Cd toxicity through an early modulation of gene expression. Namely, pathways relevant for plant development and its interaction with environment, such as photosynthesis, stress response, hormone metabolism and signalling, have been found to be differentially modulated at the transcriptomic level in *ddc* triple mutant compared to the WT.

In the framework of the pathways so far analysed, dealing specifically with the diverse classes of phytohormones, the following scheme is proposed that link transcriptomic differences and hormone quantification (see Appendix) to the morphophysiological features of *ddc* mutant and WT.

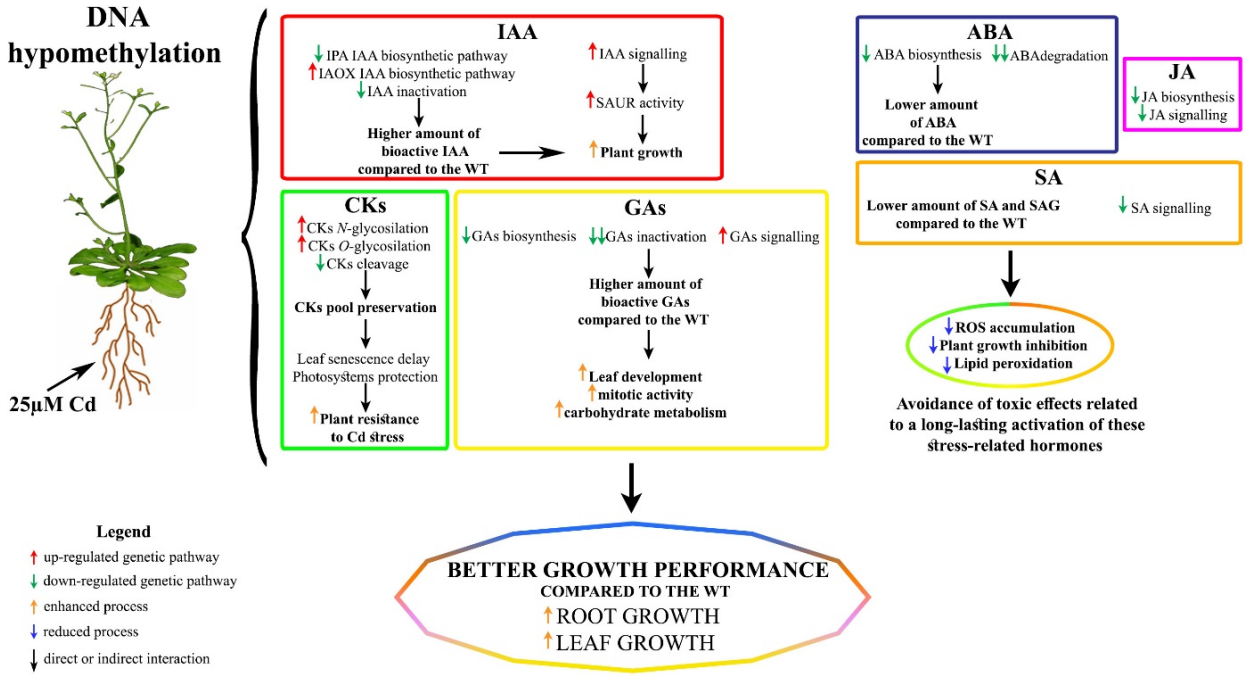

Figure 5.1: Scheme summarizing the modifications in hormone-related genetic pathways in *ddc* mutant plants under 25 µM Cd stress. The related effects of these modifications are also indicated.

The emerging picture suggests that, under a prolonged heavy metal exposure, plants activity is directed to enhance and/or maintain the level and signalling of hormones which are relevant in sustaining the growth more than those of hormones specifically related to stress response. This could represent the plant strategy, more effective in *ddc* than in WT, to avoid the negative effects of long-lasting activity of stress-related hormones. This result appears relevant at theorical and applicative level, in view of the emerging relationship between the phytohormone action and epigenetic mechanisms.

Further analysis of transcriptomic data, providing information on the other players of plant whole signalling network, such as the MAPK, ROS and NO pathways, tightly related to hormones action, could provide a more complete picture on the role of methylation status on modulating plant strategy for "life or death switch" under stress condition.

REFERENCES

Abbas, M., Hernández-García, J., Pollmann, S., Samodelov, S. L., Kolb, M., Friml, J., … Alabadí, D. (2018). Auxin methylation is required for differential growth in *Arabidopsis*. *Proceedings of the National Academy of Sciences,* 115(26), 6864-6869. https://doi.org/10.1073/pnas.1806565115

Abe, H., Yamaguchi-Shinozaki, K., Urao, T., Iwasaki, T., Hosokawa, D., & Shinozaki, K. (1997). Role of *Arabidopsis* MYC and MYB homologs in drought- and abscisic acid-regulated gene expression. *The Plant Cell*, *9*(10), 1859 LP-1868.

Adams, E., & Turner, J. (2010). COI1, a jasmonate receptor, is involved in ethylene-induced inhibition of *Arabidopsis* root growth in the light. *Journal of Experimental Botany*, *61*(15), 4373–4386. https://doi.org/10.1093/jxb/erq240

Aida, M., Beis, D., Heidstra, R., Willemsen, V., Blilou, I., Galinha, C., … Scheres, B. (2004). The PLETHORA Genes Mediate Patterning of the *Arabidopsis* Root Stem Cell Niche. *Cell*, *119*(1), 109–120. https://doi.org/10.1016/j.cell.2004.09.018

Aina, R., Sgorbati, S., Santagostino, A., Labra, M., Ghiani, A., & Citterio, S. (2004). Specific hypomethylation of DNA is induced by heavy metals in white clover and industrial hemp. *Physiologia Plantarum*, *121*(3), 472–480. https://doi.org/10.1111/j.1399-3054.2004.00343.x

Akhter, M. F., Omelon, C. R., Gordon, R. A., Moser, D., & Macfie, S. M. (2014). Localization and chemical speciation of cadmium in the roots of barley and lettuce. *Environmental and Experimental Botany*, *100*, 10–19. https://doi.org/10.1016/J.ENVEXPBOT.2013.12.005

Alcántara, E., Romera, F. J., Cañete, M., & De la Guardia, M. D. (1994). Effects of heavy metals on both induction and function of root Fe(lll) reductase in Fe-deficient cucumber (*Cucumis sativus* L.) plants. *Journal of Experimental Botany*, *45*(12), 1893–1898. https://doi.org/10.1093/jxb/45.12.1893

Al-Hakimi, A. M. A. (2007). Modification of cadmium toxicity in pea seedlings by kinetin. *Plant Soil and Environment*, *53*, 129–135.

Alleman, M., Sidorenko, L., McGinnis, K., Seshadri, V., Dorweiler, J. E., White, J., … Chandler, V. L. (2006). An RNA-dependent RNA polymerase is required for paramutation in maize. *Nature*, *442*(7100), 295–298. https://doi.org/10.1038/nature04884

Alonso, J. M., Hirayama, T., Roman, G., Nourizadeh, S., & Ecker, J. R. (1999). EIN2, a Bifunctional Transducer of Ethylene and Stress Responses in *Arabidopsis*. *Science*, *284*(5423), 2148 LP-2152.

An, F., Zhang, X., Zhu, Z., Ji, Y., He, W., Jiang, Z., … Guo, H. (2012). Coordinated regulation of apical hook development by gibberellins and ethylene in etiolated *Arabidopsis* seedlings. *Cell Research*, *22*(5), 915–927. https://doi.org/10.1038/cr.2012.29

Angers, B., Castonguay, E., & Massicotte, R. (2010). Environmentally induced phenotypes and DNA methylation: how to deal with unpredictable conditions until the next generation and after. *Molecular Ecology*, *19*(7), 1283–1295. https://doi.org/10.1111/j.1365-294X.2010.04580.x

Anne, P., Azzopardi, M., Gissot, L., Beaubiat, S., Hématy, K., & Palauqui, J.-C. (2015). OCTOPUS Negatively Regulates BIN2 to Control Phloem Differentiation in *Arabidopsis thaliana*. *Current Biology*, *25*(19), 2584–2590. https://doi.org/10.1016/j.cub.2015.08.033

Annese, A., Manzari, C., Lionetti, C., Picardi, E., Horner, D. S., Chiara, M., … D'Erchia, A. M. (2018). Whole transcriptome profiling of Late-Onset Alzheimer's Disease patients provides insights into the molecular changes involved in the disease. *Scientific Reports*, *8*(1), 4282. https://doi.org/10.1038/s41598-018-22701-2

Arasimowicz-Jelonek, M., Floryszak-Wieczorek, J., & Gwóźdź, E. A. (2011). The message of nitric oxide in cadmium challenged plants. *Plant Science*, *181*(5), 612–620. https://doi.org/https://doi.org/10.1016/j.plantsci.2011.03.019

Argueso, C. T., Ferreira, F. J., Epple, P., To, J. P. C., Hutchison, C. E., Schaller, G. E., … Kieber, J. J. (2012). Two-component elements mediate interactions between cytokinin and salicylic acid in plant immunity. *PLOS Genetics*, *8*(1), e1002448.

Asgher, M., Khan, M. I. R., Anjum, N. A., & Khan, N. A. (2015). Minimising toxicity of cadmium in plants—role of plant growth regulators. *Protoplasma*, *252*(2), 399–413. https://doi.org/10.1007/s00709-014-0710-4

Asseng, S., Ewert, F., Martre, P., Rötter, R. P., Lobell, D. B., Cammarano, … Zhu, Y. (2014). Rising temperatures reduce global wheat production. *Nature Climate Change*, *5*, 143.

Bajrami, E., & Spiroski, M. (2016). Genomic Imprinting. *Open Access Macedonian Journal of Medical Sciences*, *4*(1), 181. https://doi.org/10.3889/oamjms.2016.028

Baker, A. J. M., & Proctor, J. (1990). The influence of cadmium, copper, lead, and zinc on the distribution and evolution of metallophytes in the British Isles. *Plant Systematics and Evolution*, *173*(1–2), 91–108. https://doi.org/10.1007/BF00937765

Balzan, S., Johal, G. S., & Carraro, N. (2014). The role of auxin transporters in monocots development. *Frontiers in Plant Science*, *5*, 393. https://doi.org/10.3389/fpls.2014.00393

Barratt, N. M., Dong, W., Gage, D. A., Magnus, V., & Town, C. D. (1999). Metabolism of exogenous auxin by *Arabidopsis thaliana*: Identification of the conjugate N_{α}-(indol-3-ylacetyl)-glutamine and initiation of a mutant screen. *Physiologia Plantarum*, *105*(2), 207–217. https://doi.org/10.1034/j.1399-3054.1999.105204.x

Barrero, J. M., Piqueras, P., González-Guzmán, M., Serrano, R., Rodríguez, P. L., Ponce, M. R., & Micol, J. L. (2005). A mutational analysis of the ABA1 gene of *Arabidopsis thaliana* highlights the involvement of ABA in vegetative development. *Journal of Experimental Botany*, *56*(418), 2071–2083.

Bartee, L., Malagnac, F., & Bender, J. (2001). *Arabidopsis* CMT3 chromomethylase mutations block non-CG methylation and silencing of an endogenous gene. *Genes & Development*, *15*(14), 1753–1758. https://doi.org/10.1101/gad.905701

Bartel, B., & Fink, G. R. (1994). Differential regulation of an auxin-producing nitrilase gene family in *Arabidopsis thaliana*. *Proceedings of the National Academy of Sciences of the United States of America*, *91*(14), 6649–6653.

Bartels, D., & Sunkar, R. (2005). Drought and Salt Tolerance in Plants. *Critical Reviews in Plant Sciences*, *24*(1), 23–58. https://doi.org/10.1080/07352680590910410

Becker, C., Hagmann, J., Müller, J., Koenig, D., Stegle, O., Borgwardt, K., & Weigel, D. (2011). Spontaneous epigenetic variation in the *Arabidopsis thaliana* methylome. *Nature*, *480*(7376), 245–249. https://doi.org/10.1038/nature10555

Bell, A. C., & Felsenfeld, G. (2000). Methylation of a CTCF-dependent boundary controls imprinted expression of the IGF2 gene. *Nature*, *405*(6785), 482–485. https://doi.org/10.1038/35013100

Bell, E., Creelman, R. A., & Mullet, J. E. (1995). A chloroplast lipoxygenase is required for wound-induced jasmonic acid accumulation in *Arabidopsis. Proceedings of the National Academy of Sciences of the United States of America*, *92*(19), 8675–8679.

Bellard, C., Bertelsmeier, C., Leadley, P., Thuiller, W., & Courchamp, F. (2012). Impacts of climate change on the future of biodiversity. *Ecology Letters*, *15*(4), 365–377. https://doi.org/10.1111/j.1461-0248.2011.01736.x

Ben Rejeb, I., Pastor, V., & Mauch-Mani, B. (2014). Plant responses to simultaneous biotic and abiotic stress: molecular mechanisms. *Plants*, *3*(4), 458–475. https://doi.org/10.3390/plants3040458

Benavides, M. P., Gallego, S. M., & Tomaro, M. L. (2005). Cadmium toxicity in plants. *Brazilian Journal of Plant Physiology*, *17*(1), 21–34. https://doi.org/10.1590/S1677-04202005000100003

Benjamins, R., & Scheres, B. (2008). Auxin: The Looping Star in Plant Development. *Annual Review of Plant Biology*, *59*(1), 443–465. https://doi.org/10.1146/annurev.arplant.58.032806.103805

Besson-Bard, A., Gravot, A., Richaud, P., Auroy, P., Duc, C., Gaymard, F., … Wendehenne, D. (2009). Nitric oxide contributes to cadmium toxicity in *Arabidopsis* by promoting cadmium accumulation in roots and by up-regulating genes related to iron uptake. *Plant Physiology*, *149*(3), 1302–1315. https://doi.org/10.1104/pp.108.133348

Bewick, A. J., & Schmitz, R. J. (2017). Gene body DNA methylation in plants. *Current Opinion in Plant Biology*, *36*, 103–110. https://doi.org/10.1016/j.pbi.2016.12.007

Bhalerao, R. P., & Bennett, M. J. (2003). The case for morphogens in plants. *Nature Cell Biology*, *5*(11), 939–943. https://doi.org/10.1038/ncb1103-939

Bindea, G., Mlecnik, B., Hackl, H., Charoentong, P., Tosolini, M., Kirilovsky, A., Fridman, W., Pagès, H. F., Trajanoski, Z., Galon, J. (2009). ClueGO: a Cytoscape plug-in to decipher functionally grouped gene ontology and pathway annotation networks. *Bioinformatics*, *25*(8), 1091–1093. https://doi.org/10.1093/bioinformatics/btp101

Bingham, F. T., Page, A. L., Mahler, R. J., & Ganje, T. J. (1976). Yield and cadmium accumulation of forage species in relation to cadmium content of sludge-amended soil. *Journal of Environmental Quality*, *5*, 57–60. https://doi.org/10.2134/jeq1976.00472425000500010012x

Bitonti, M. B., Cozza, R., Wang, G., Ruffini-Castiglione, M., Mazzuca, S., Castiglione, S., … Innocenti, A. M. (1996). Nuclear and genomic changes in floating and submerged buds and leaves of heterophyllous waterchestnut (*Trapa natans*). *Physiologia Plantarum*, *97*(1), 21–27. https://doi.org/10.1111/j.1399-3054.1996.tb00473.x

Bitonti, M. B., Cozza, R., Chiappetta, A., Giannino, D., Ruffini Castiglione, M., Dewitte, W., … Innocenti, A. M. (2002). Distinct nuclear organization, DNA methylation pattern and cytokinin distribution mark juvenile, juvenile-like and adult vegetative apical meristems in peach (*Prunus persica* (L.) Batsch). *Journal of Experimental Botany*, *53*(371), 1047–1054.

Bittner, F., Oreb, M., & Mendel, R. R. (2001). ABA3 is a molybdenum cofactor sulfurase required for activation of aldehyde oxidase and xanthine dehydrogenase in *Arabidopsis thaliana*. *Journal of Biological Chemistry*, *276*(44), 40381–40384. https://doi.org/10.1074/JBC.C100472200

Blasco, M. A. (2007). The epigenetic regulation of mammalian telomeres. *Nature Reviews Genetics*, *8*, 299.

Blilou, I., Xu, J., Wildwater, M., Willemsen, V., Paponov, I., Friml, J., … Scheres, B. (2005). The PIN auxin efflux facilitator network controls growth and patterning in *Arabidopsis* roots. *Nature*, *433*, 39.

Blum, W. H. (1997). Cadmium uptake by higher plants. In *Proceedings of extended abstracts from the Fourth International Conference on the Biogeochemistry of Trace Elements* (pp. 109–110). Berkeley, USA. University of California.

Bohnert, H. J., Ostrem, J. A., Cushman, J. C., Michalowski, C. B., Rickers, J., Meyer, G., … Schmitt, J. M. (1988). *Mesembryanthemum crystallinum*, a higher plant model for the study of environmentally induced changes in gene expression. *Plant Molecular Biology Reporter*, *6*(1), 10–28. https://doi.org/10.1007/BF02675305

Boter, M., Ruíz-Rivero, O., Abdeen, A., & Prat, S. (2004). Conserved MYC transcription factors play a key role in jasmonate signaling both in tomato and *Arabidopsis*. *Genes & Development*, *18*(13), 1577–1591. https://doi.org/10.1101/gad.297704

Boyes, D. C., Zayed, A. M., Ascenzi, R., Mccaskill, A. J., Hoffman, N. E., Davis, K. R., & Görlach, J. (2001). Growth stage-based phenotypic analysis of *Arabidopsis*: A model for high throughput functional genomics in plants. *The Plant Cell* (Vol. 13).

Boyes, J., & Bird, A. (1991). DNA methylation inhibits transcription indirectly via a methyl-CpG binding protein. *Cell*, *64*(6), 1123–1134. https://doi.org/10.1016/0092-8674(91)90267-3

Bray, E.A., Bailey-Serres, J., Weretilnyk, E. (2000). Responses to abiotic stresses. In W. Buchanan, B., Gruissem (Ed.), *Biochemistry and Molecular Biology of Plant* (p. 1160). American Society of Plant Physiologists.

Brumos, J., Alonso, J. M., & Stepanova, A. N. (2013). Genetic aspects of auxin biosynthesis and its regulation. *Physiologia Plantarum*, *151*(1), 3–12. https://doi.org/10.1111/ppl.12098

Bruno, L., Pacenza, M., Forgione, I., Lamerton, L. R., Greco, M., Chiappetta, A., & Bitonti, M. B. (2017). In *Arabidopsis thaliana* cadmium impact on the growth of primary root by altering scr expression and auxin-cytokinin cross-talk. *Frontiers in Plant Science*, *8*, 1323. https://doi.org/10.3389/fpls.2017.01323

Brzobohatý, B., Moore, I., Kristoffersen, P., Bako, L., Campos, N., Schell, J., … Palme, K. (1993). Release of active cytokinin by a beta-glucosidase localized to the maize root meristem. *Science*, *262*(5136), 1051 LP-1054. https://doi.org/10.1126/SCIENCE.8235622

Bücker-Neto, L., Paiva, A. L. S., Machado, R. D., Arenhart, R. A., & Margis-Pinheiro, M. (2017). Interactions between plant hormones and heavy metals responses. *Genetics and Molecular Biology*, *40*(1 suppl 1), 373–386. https://doi.org/10.1590/1678-4685-GMB-2016-0087

Burnett, E. C., Desikan, R., Moser, R. C., & Neill, S. J. (2000). ABA activation of an MBP kinase in *Pisum sativum* epidermal peels correlates with stomatal responses to ABA. *Journal of Experimental Botany*, *51*(343), 197–205.

Cabrera, D., Young, S. D., & Rowell, D. L. (1988). The toxicity of cadmium to barley plants as affected by complex formation with humic acid. *Plant and Soil*, *105*(2), 195–204. https://doi.org/10.1007/BF02376783

Caesar, K., Thamm, A. M. K., Witthöft, J., Elgass, K., Huppenberger, P., Grefen, C., … Harter, K. (2011). Evidence for the localization of the *Arabidopsis* cytokinin receptors AHK3 and AHK4 in the endoplasmic reticulum. *Journal of Experimental Botany*, *62*(15), 5571–5580. https://doi.org/10.1093/jxb/err238

Caldelari, D., Wang, G., Farmer, E. E., & Dong, X. (2011). *Arabidopsis lox3 lox4* double mutants are male sterile and defective in global proliferative arrest. *Plant Molecular Biology*, *75*(1–2), 25–33. https://doi.org/10.1007/s11103-010-9701-9

Campanero, M. R., Armstrong, M. I., & Flemington, E. K. (2000). CpG methylation as a mechanism for the regulation of E2F activity. *Proceedings of the National Academy of Sciences*, *97*(12), 6481–6486. https://doi.org/10.1073/pnas.100340697

Candaele, J., Demuynck, K., Mosoti, D., Beemster, G. T. S., Inzé, D., & Nelissen, H. (2014). Differential Methylation during Maize Leaf Growth Targets Developmentally Regulated Genes. *Plant Physiology*, *164*(3), 1350–1364. https://doi.org/10.1104/pp.113.233312

Cao, H., Glazebrook, J., Clarke, J. D., Volko, S., & Dong, X. (1997). The *Arabidopsis NPR1* gene that controls systemic acquired resistance encodes a novel protein containing ankyrin repeats. *Cell*, *88*(1), 57–63. https://doi.org/10.1016/S0092-8674(00)81858-9

Cao, X., & Jacobsen, S. E. (2002a). Role of the *Arabidopsis* DRM Methyltransferases in De Novo DNA Methylation and Gene Silencing. *Current Biology*, *12*(13), 1138–1144. https://doi.org/10.1016/S0960-9822(02)00925-9

Cao, X., & Jacobsen, S. E. (2002b). Locus-specific control of asymmetric and CpNpG methylation by the DRM and CMT3 methyltransferase genes. *Proceedings of the National Academy of Sciences of the United States of America*, *99*(Suppl 4), 16491–16498. https://doi.org/10.1073/pnas.162371599

Causier, B., Ashworth, M., Guo, W., & Davies, B. (2012). The TOPLESS Interactome: a framework for gene repression in *Arabidopsis*. *Plant Physiology*, *158*(1), 423–438. https://doi.org/10.1104/pp.111.186999

Cazzonelli, C. I., Vanstraelen, M., Simon, S., Yin, K., Carron-Arthur, A., Nisar, N., … Pogson, B. J. (2013). Role of the *Arabidopsis* PIN6 Auxin Transporter in Auxin Homeostasis and Auxin-Mediated Development. *PLOS ONE*, *8*(7), e70069.

Chan, S. R. W. L., & Blackburn, E. H. (2004). Telomeres and telomerase. *Philosophical Transactions of the Royal Society of London. Series B, Biological Sciences*, *359*(1441), 109–121. https://doi.org/10.1098/rstb.2003.1370

Chandler, J. W. (2009). Local auxin production: a small contribution to a big field. *BioEssays*, *31*(1), 60–70. https://doi.org/10.1002/bies.080146

Chang, C., Kwok, S. F., Bleecker, A. B., & Meyerowitz, E. M. (1993). *Arabidopsis* ethylene-response gene ETR1: similarity of product to two-component regulators. *Science (New York, N.Y.)*, *262*(5133), 539–544.

Chauvin, A., Caldelari, D., Wolfender, J.-L., & Farmer, E. E. (2012). Four 13-lipoxygenases contribute to rapid jasmonate synthesis in wounded *Arabidopsis thaliana* leaves: a role for lipoxygenase 6 in responses to long-distance wound signals. *New Phytologist*, *197*(2), 566–575. https://doi.org/10.1111/nph.12029

Chen, J., Yan, Z., & Li, X. (2014). Effect of methyl jasmonate on cadmium uptake and antioxidative capacity in Kandelia obovata seedlings under cadmium stress. *Ecotoxicology and Environmental Safety*, *104*, 349–356. https://doi.org/https://doi.org/10.1016/j.ecoenv.2014.01.022

Cheng, W.-H., Endo, A., Zhou, L., Penney, J., Chen, H.-C., Arroyo, A., … Sheen, J. (2002). A Unique Short-Chain Dehydrogenase/Reductase in *Arabidopsis* Glucose Signaling and Abscisic Acid Biosynthesis and Functions. *The Plant Cell*, *14*(11), 2723–2743. https://doi.org/10.1105/tpc.006494

Chern, M., Canlas, P. E., & Ronald, P. C. (2008). Strong Suppression of Systemic Acquired Resistance in *Arabidopsis* by NRR is Dependent on its Ability to Interact with NPR1and its Putative Repression Domain. *Molecular Plant*, *1*(3), 552–559. https://doi.org/10.1093/mp/ssn017

Chini, A., Fonseca, S., Fernández, G., Adie, B., Chico, J. M., Lorenzo, O., … Solano, R. (2007). The JAZ family of repressors is the missing link in jasmonate signalling. *Nature*, *448*, 666.

Chinnusamy, V., & Zhu, J.-K. (2009). Epigenetic regulation of stress responses in plants. *Current Opinion in Plant Biology*, *12*(2), 133–139. https://doi.org/10.1016/j.pbi.2008.12.006

Chmielowska-Bąk, J., Lefèvre, I., Lutts, S., & Deckert, J. (2013). Short term signaling responses in roots of young soybean seedlings exposed to cadmium stress. *Journal of Plant Physiology*, *170*(18), 1585–1594. https://doi.org/https://doi.org/10.1016/j.jplph.2013.06.019

Clarkson, D. T. (1996). Marschner H. 1995. Mineral nutrition of higher plants. second edition. 889pp. London: Academic Press, £29.95 (paperback). *Annals of Botany*, *78*(4), 527–528.

Cokus, S. J., Feng, S., Zhang, X., Chen, Z., Merriman, B., Haudenschild, C. D., … Jacobsen, S. E. (2008). Shotgun bisulphite sequencing of the *Arabidopsis* genome reveals DNA methylation patterning. *Nature*, *452*, 215.

Consortium, T. G. O., Ashburner, M., Ball, C. A., Blake, J. A., Botstein, D., Butler, H., … Sherlock, G. (2000). Gene Ontology: tool for the unification of biology. *Nature Genetics*, *25*(1), 25–29. https://doi.org/10.1038/75556

Cowling, R. J., Kamiya, Y., Seto, H., & Harberd, N. P. (1998). Gibberellin dose-response regulation of ga4 gene transcript levels in *Arabidopsis*. *Plant Physiology*, *117*(4), 1195–1203.

Cramer, G. R., Urano, K., Delrot, S., Pezzotti, M., & Shinozaki, K. (2011). Effects of abiotic stress on plants: a systems biology perspective. *BMC Plant Biology*, *11*, 163. https://doi.org/10.1186/1471-2229-11-163

Curie, C., Cassin, G., Couch, D., Divol, F., Higuchi, K., Le Jean, M., … Mari, S. (2009). Metal movement within the plant: contribution of nicotianamine and yellow stripe 1-like transporters. *Annals of Botany*, *103*(1), 1–11. https://doi.org/10.1093/aob/mcn207

Cutler, A. J., & Krochko, J. E. (1999). Formation and breakdown of ABA. *Trends in Plant Science*, *4*(12), 472–478. https://doi.org/10.1016/S1360-1385(99)01497-1

Cutler, S. R., Rodriguez, P. L., Finkelstein, R. R., & Abrams, S. R. (2010). Abscisic Acid: Emergence of a Core Signaling Network. *Annual Review of Plant Biology*, *61*(1), 651–679. https://doi.org/10.1146/annurev-arplant-042809-112122

D'Agostino, I. B., Deruère, J., & Kieber, J. J. (2000). Characterization of the Response of the *Arabidopsis* Response Regulator Gene Family to Cytokinin. *Plant Physiology*, *124*(4), 1706–1717.

DalCorso, G., Farinati, S., & Furini, A. (2010). Regulatory networks of cadmium stress in plants. *Plant Signaling & Behavior*, *5*(6), 663–667. https://doi.org/10.4161/psb.5.6.11425

Danquah, A., de Zelicourt, A., Colcombet, J., & Hirt, H. (2014). The role of ABA and MAPK signaling pathways in plant abiotic stress responses. *Biotechnology Advances*, *32*(1), 40–52. https://doi.org/https://doi.org/10.1016/j.biotechadv.2013.09.006

Das, P., Samantaray, S., & Rout, G. R. (1997). Studies on cadmium toxicity in plants: A review. *Environmental Pollution*, *98*(1), 29–36. https://doi.org/https://doi.org/10.1016/S0269-7491(97)00110-3

Dat, J., Vandenabeele, S., Vranová, E., Van Montagu, M., Inzé, D., & Van Breusegem, F. (2000). Dual action of the active oxygen species during plant stress responses. *Cellular and Molecular Life Sciences CMLS*, *57*(5), 779–795. https://doi.org/10.1007/s000180050041

Dat, J. F., Capelli, N., Folzer, H., Bourgeade, P., & Badot, P.-M. (2004). Sensing and signalling during plant flooding. *Plant Physiology and Biochemistry*, *42*(4), 273–282. https://doi.org/https://doi.org/10.1016/j.plaphy.2004.02.003

Davière, J.-M., & Achard, P. (2016). A Pivotal Role of DELLAs in Regulating Multiple Hormone Signals. *Molecular Plant*, *9*(1), 10–20. https://doi.org/10.1016/j.molp.2015.09.011

Davière, J.-M., de Lucas, M., & Prat, S. (2008). Transcriptional factor interaction: a central step in DELLA function. *Current Opinion in Genetics & Development*, *18*(4), 295–303. https://doi.org/https://doi.org/10.1016/j.gde.2008.05.004

Davies, P. J. (2004). *Plant hormones: biosynthesis, signal transduction, action!* Kluwer Academic.

de Zelicourt, A., Colcombet, J., & Hirt, H. (2016). The role of MAPK modules and aba during abiotic stress signaling. *Trends in Plant Science*, *21*(8), 677–685. https://doi.org/10.1016/j.tplants.2016.04.004

Della Rovere, F., Fattorini, L., D'Angeli, S., Veloccia, A., Falasca, G., & Altamura, M. M. (2013). Auxin and cytokinin control formation of the quiescent centre in the adventitious root apex of arabidopsis. *Annals of Botany*, *112*(7), 1395–1407. https://doi.org/10.1093/aob/mct21

Dello Ioio, R., Linhares, F. S., Scacchi, E., Casamitjana-Martinez, E., Heidstra, R., Costantino, P., & Sabatini, S. (2007). Cytokinins determine *Arabidopsis* root-meristem size by controlling cell differentiation. *Current Biology*, *17*(8), 678–682. https://doi.org/10.1016/j.cub.2007.02.047

Deng, X., Song, X., Wei, L., Liu, C., & Cao, X. (2016). Epigenetic regulation and epigenomic landscape in rice. *National Science Review*, *3*(3), 309–327. https://doi.org/10.1093/nsr/nww042

Després, C., Chubak, C., Rochon, A., Clark, R., Bethune, T., Desveaux, D., & Fobert, P. R. (2003). The *Arabidopsis* NPR1 disease resistance protein is a novel cofactor that confers redox regulation of DNA binding activity to the basic domain/leucine zipper transcription factor TGA1. *The Plant Cell*, *15*(9), 2181–2191. https://doi.org/10.1105/tpc.012849

Després, C., DeLong, C., Glaze, S., Liu, E., & Fobert, P. R. (2000). The *Arabidopsis* NPR1/NIM1 protein enhances the dna binding activity of a subgroup of the TGA family of bZIP transcription factors. *The Plant Cell*, *12*(2), 279–290.

Dhonukshe, P., Aniento, F., Hwang, I., Robinson, D. G., Mravec, J., Stierhof, Y.-D., & Friml, J. (2007). Clathrin-mediated constitutive endocytosis of pin auxin efflux carriers in *Arabidopsis. Current Biology*, *17*(6), 520–527. https://doi.org/10.1016/j.cub.2007.01.052

Di Laurenzio, L., Wysocka-Diller, J., Malamy, J. E., Pysh, L., Helariutta, Y., Freshour, G., … Benfey, P. N. (1996). The *SCARECROW* gene regulates an asymmetric cell division that is essential for generating the radial organization of the *Arabidopsis* Root. *Cell*, *86*(3), 423–433. https://doi.org/10.1016/S0092-8674(00)80115-4

Dinesh, D. C., Villalobos, L. I. A. C., & Abel, S. (2016). Structural Biology of Nuclear Auxin Action. *Trends in Plant Science*, *21*(4), 302–316. https://doi.org/10.1016/j.tplants.2015.10.019

Dixon, S. C., Martin, R. C., Mok, M. C., Shaw, G., & Mok, D. W. S. (1989). Zeatin glycosylation enzymes in phaseolus: isolation of o-glucosyltransferase from *P. lunatus* and comparison to o-xylosyltransferase from *P. vulgaris. Plant Physiology*, *90*(4), 1316–1321.

Doerfler, W. (1983). DNA Methylation and Cene Activity. *Annual Review of Biochemistry*, *52*(1), 93–124. https://doi.org/10.1146/annurev.bi.52.070183.000521

Doerfler, W. (1981). DNA Methylation-A Regulatory Signal in Eukaryotic Gene Expression. *Journal of General Virology*, *57*(1), 1–20. https://doi.org/10.1099/0022-1317-57-1-1

Dolan, L., Janmaat, K., Willemsen, V., Linstead, P., Poethig, S., Roberts, K., & Scheres, B. (1993). Cellular organisation of the *Arabidopsis thaliana* root. *Development (Cambridge, England)*, *119*(1), 71–84.

Dombrecht, B., Xue, G. P., Sprague, S. J., Kirkegaard, J. A., Ross, J. J., Reid, J. B., … Kazan, K. (2007). MYC2 differentially modulates diverse jasmonate-dependent functions in *Arabidopsis*. *The Plant Cell*, *19*(7), 2225 LP-2245.

Dong, X., Zhang, M., Chen, J., Peng, L., Zhang, N., Wang, X., & Lai, J. (2017). Dynamic and antagonistic allele-specific epigenetic modifications controlling the expression of imprinted genes in maize endosperm. *Molecular Plant*, *10*(3), 442–455. https://doi.org/10.1016/j.molp.2016.10.007

dos Santos, R. W., Schmidt, É. C., Martins, R. de P., Latini, A., Maraschin, M., Horta, P. A., & Bouzon, Z. L. (2012). Effects of cadmium on growth, photosynthetic pigments, photosynthetic performance, biochemical parameters and structure of chloroplasts in the agarophyte *Gracilaria domingensis* (Rhodophyta, Gracilariales). *American Journal of Plant Sciences*, *03*(08), 1077–1084. https://doi.org/10.4236/ajps.2012.38129

Dowen, R. H., Pelizzola, M., Schmitz, R. J., Lister, R., Dowen, J. M., Nery, J. R., … Ecker, J. R. (2012). Widespread dynamic DNA methylation in response to biotic stress. *Proceedings of the National Academy of Sciences*, *109*(32), E2183–E2191. https://doi.org/10.1073/pnas.1209329109

Du, J., Johnson, L. M., Groth, M., Feng, S., Hale, C. J., Li, S., … Jacobsen, S. E. (2014). Mechanism of DNA methylation-directed histone methylation by KRYPTONITE. *Molecular Cell*, *55*(3), 495–504. https://doi.org/10.1016/j.molcel.2014.06.009

Duque, A. S., de Almeida, A. M., Bernardes da Silva, A., Marques da Silva, J., Farinha, A. P., Santos, D., de Sousa F. P., Araújo, S. (2013). Abiotic Stress Responses in Plants: Unraveling the Complexity of Genes and Networks to Survive. In *Abiotic*

Stress - Plant Responses and Applications in Agriculture. InTech. https://doi.org/10.5772/52779

Dyachenko, O. V., Zakharchenko, N. S., Shevchuk, T. V., Bohnert, H. J., Cushman, J. C., & Buryanov, Y. I. (2006). Effect of hypermethylation of CCWGG sequences in DNA of *Mesembryanthemum crystallinum* plants on their adaptation to salt stress. *Biochemistry (Moscow)*, *71*(4), 461–465. https://doi.org/10.1134/S000629790604016X

Eichten, S. R., Briskine, R., Song, J., Li, Q., Swanson-Wagner, R., Hermanson, P. J., … Springer, N. M. (2013). Epigenetic and genetic influences on DNA methylation variation in maize populations. *The Plant Cell*, *25*(8), 2783–2797. https://doi.org/10.1105/tpc.113.114793

Engels, W. R., Johnson-Schlitz, D. M., Eggleston, W. B., & Sved, J. (1990). High-frequency P element loss in *Drosophila* is homolog dependent. *Cell*, *62*(3), 515–525. https://doi.org/10.1016/0092-8674(90)90016-8

Erhard, K. F., Stonaker, J. L., Parkinson, S. E., Lim, J. P., Hale, C. J., & Hollick, J. B. (2009). RNA polymerase IV functions in paramutation in *Zea mays*. *Science (New York, N.Y.)*, *323*(5918), 1201–1205. https://doi.org/10.1126/science.1164508

Estelle, M. (1998). Polar auxin transport: new support for an old model. *The Plant Cell*, *10*(11), 1775 LP-1778.

Fambrini, M., Mariotti, L., Parlanti, S., Salvini, M., & Pugliesi, C. (2015). A GRAS-like gene of sunflower (*Helianthus annuus* L.) alters the gibberellin content and axillary meristem outgrowth in transgenic *Arabidopsis* plants. *Plant Biology*, *17*(6), 1123–1134. https://doi.org/10.1111/plb.12358

Fan, W., & Dong, X. (2002). In vivo interaction between npr1 and transcription factor tga2 leads to salicylic acid–mediated gene activation in *Arabidopsis. The Plant Cell*, *14*(6), 1377 LP-1389.

Farrow, S. C., & Facchini, P. J. (2014). Functional diversity of 2-oxoglutarate/Fe(II)-dependent dioxygenases in plant metabolism. *Frontiers in Plant Science*, *5*, 524. https://doi.org/10.3389/fpls.2014.00524

Fattorini, L., Ronzan, M., Piacentini, D., Della Rovere, F., De Virgilio, C., Sofo, A., … Falasca, G. (2017). Cadmium and arsenic affect quiescent centre formation and maintenance in *Arabidopsis thaliana* post-embryonic roots disrupting auxin biosynthesis and transport. *Environmental and Experimental Botany*, *144*, 37–48. https://doi.org/https://doi.org/10.1016/j.envexpbot.2017.10.005

Fedoroff, N. V, Battisti, D. S., Beachy, R. N., Cooper, P. J. M., Fischhoff, D. A., Hodges, C. N., … Zhu, J.-K. (2010). Radically Rethinking Agriculture for the 21st Century. *Science (New York, N.Y.)*, *327*(5967), 833–834. https://doi.org/10.1126/science.1186834

Feng, J., Shi, Y., Yang, S., & Zuo, J. (2017). 3 - Cytokinins. In J. Li, C. Li, & S. M. B. T.-H. M. and S. in P. Smith (Eds.) (pp. 77–106). Academic Press. https://doi.org/https://doi.org/10.1016/B978-0-12-811562-6.00003-7

Feng, S., Cokus, S. J., Zhang, X., Chen, P.-Y., Bostick, M., Goll, M. G., … Jacobsen, S. E. (2010). Conservation and divergence of methylation patterning in plants and animals. *Proceedings of the National Academy of Sciences of the United States of America*, *107*(19), 8689–8694. https://doi.org/10.1073/pnas.1002720107

Fernández-Calvo, P., Chini, A., Fernández-Barbero, G., Chico, J.-M., Gimenez-Ibanez, S., Geerinck, J., … Solano, R. (2011). The *Arabidopsis* bHLH Transcription Factors MYC3 and MYC4 Are Targets of JAZ Repressors and Act Additively with MYC2 in the Activation of Jasmonate Responses. *The Plant Cell*, *23*(2), 701 LP-715.

Finkelstein, R. (2013). Abscisic Acid Synthesis and Response. *The Arabidopsis Book / American Society of Plant Biologists*, *11*, e0166. https://doi.org/10.1199/tab.0166

Finnegan, E. J., & Dennis, E. S. (1993). Isolation and identification by sequence homology of a putative cytosine methyltransferase from *Arabidopsis thaliana*. *Nucleic Acids Research*, *21*(10), 2383–2388.

Finnegan, E. J., Peacock, W. J., & Dennis, E. S. (1996). Reduced DNA methylation in *Arabidopsis thaliana* results in abnormal plant development. *Proceedings of the National Academy of Sciences of the United States of America*, *93*(16), 8449–8454.

Fluhr, R., Mattoo, A. K., & Dilley, D. R. (1996). Ethylene - Biosynthesis and perception. *Critical Reviews in Plant Sciences*, *15*(5–6), 479–523. https://doi.org/10.1080/07352689609382368

Forgione, I., Woloszynska, M., Pacenza, M., Chiappetta, A., Greco, M., Araniti, F., Abenavoli, M.R., Van Lijsebettens, M., Bitonti, M.B., Bruno, L. (2018). Hypomethylated *drm1 drm2 cmt3* mutant phenotype of *Arabidopsis thaliana* is related to auxin pathway impairment. *Plant Science*.

Forgione, I. (2016). *Impact of DNA methylation on plant growth and development: a study on a methylation-defective mutant of Arabidopsis thaliana*. Università della Calabria.

Fray, R., & Zhong, S. (2015). 11 - Genome-wide DNA methylation in tomato. In P. Poltronieri & Y. B. T.-A. P. G. and B. Hong (Eds.) (pp. 179–193). Oxford: Woodhead Publishing. https://doi.org/https://doi.org/10.1016/B978-0-08-100068-7.00011-2

Frey, A., Effroy, D., Lefebvre, V., Seo, M., Perreau, F., Berger, A., … Marion-Poll, A. (2012). Epoxycarotenoid cleavage by NCED5 fine-tunes ABA accumulation and affects seed dormancy and drought tolerance with other NCED family members. *The Plant Journal*, *70*(3), 501–512. https://doi.org/10.1111/j.1365-313X.2011.04887.x

Friml, J. (2003). Auxin transport — shaping the plant. *Current Opinion in Plant Biology*, *6*(1), 7–12. https://doi.org/https://doi.org/10.1016/S1369526602000031

Friml, J., Yang, X., Michniewicz, M., Weijers, D., Quint, A., Tietz, O., … Offringa, R. (2004). A PINOID-dependent binary switch in apical-basal pin polar targeting directs auxin efflux. *Science*, *306*(5697), 862 LP-865.

Fujii, H., & Zhu, J.-K. (2009). *Arabidopsis* mutant deficient in 3 abscisic acid-activated protein kinases reveals critical roles in growth, reproduction, and stress. *Proceedings of the National Academy of Sciences of the United States of America*, *106*(20), 8380–8385. https://doi.org/10.1073/pnas.0903144106

Furihata, T., Maruyama, K., Fujita, Y., Umezawa, T., Yoshida, R., Shinozaki, K., & Yamaguchi-Shinozaki, K. (2006). Abscisic acid-dependent multisite phosphorylation regulates the activity of a transcription activator AREB1. *Proceedings of the National Academy of Sciences of the United States of America*, *103*(6), 1988 LP-1993.

Galinha, C., Hofhuis, H., Luijten, M., Willemsen, V., Blilou, I., Heidstra, R., & Scheres, B. (2007). PLETHORA proteins as dose-dependent master regulators of *Arabidopsis* root development. *Nature*, *449*(7165), 1053–1057. https://doi.org/10.1038/nature06206

Ganguly, A., Lee, S. H., Cho, M., Lee, O. R., Yoo, H., & Cho, H.-T. (2010). Differential auxin-transporting activities of PIN-FORMED proteins in *Arabidopsis* root hair cells. *Plant Physiology*, *153*(3), 1046–1061. https://doi.org/10.1104/pp.110.156505

Ganguly, A., Lee, S.-H., & Cho, H.-T. (2012). Functional identification of the phosphorylation sites of *Arabidopsis* PIN-FORMED3 for its subcellular localization and biological role. *The Plant Journal*, *71*(5), 810–823. https://doi.org/10.1111/j.1365-313X.2012.05030.x

Ganguly, A., Park, M., Kesawat, M. S., & Cho, H.-T. (2014). Functional analysis of the hydrophilic loop in intracellular trafficking of *Arabidopsis* PIN-FORMED proteins. *The Plant Cell*, *26*(4), 1570–1585. https://doi.org/10.1105/tpc.113.118422

Gao, X.-H., Xiao, S.-L., Yao, Q.-F., Wang, Y.-J., & Fu, X.-D. (2011). An updated GA signaling 'relief of repression' regulatory model. *Molecular Plant*, *4*(4), 601–606. https://doi.org/https://doi.org/10.1093/mp/ssr046

Gao, X., Zhang, Y., He, Z., & Fu, X. (2017). 4 - Gibberellins. In J. Li, C. Li, & S. M. B. T.-H. M. and S. in P. Smith (Eds.) (pp. 107–160). Academic Press. https://doi.org/https://doi.org/10.1016/B978-0-12-811562-6.00004-9

Gao, Z., Chen, Y.-F., Randlett, M. D., Zhao, X.-C., Findell, J. L., Kieber, J. J., & Schaller, G. E. (2003). Localization of the Raf-like Kinase CTR1 to the endoplasmic reticulum of *Arabidopsis* through participation in ethylene receptor signaling complexes. *Journal of Biological Chemistry*, *278*(36), 34725–34732. https://doi.org/10.1074/jbc.M305548200

Gehring, M., & Henikoff, S. (2008). DNA methylation and demethylation in *Arabidopsis. The Arabidopsis Book / American Society of Plant Biologists*, *6*, e0102. https://doi.org/10.1199/tab.0102

Geldner, N., Friml, J., Stierhof, Y.-D., Jürgens, G., & Palme, K. (2001). Auxin transport inhibitors block PIN1 cycling and vesicle trafficking. *Nature*, *413*, 425.

Genger, R. K., Kovac, K. A., Dennis, E. S., Peacock, W. J., & Finnegan, E. J. (1999). Multiple DNA methyltransferase genes in *Arabidopsis thaliana*. *Plant Molecular Biology*, *41*(2), 269–278. https://doi.org/10.1023/A:1006347010369

Glauser, G., Dubugnon, L., Mousavi, S. A. R., Rudaz, S., Wolfender, J.-L., & Farmer, E. E. (2009). Velocity estimates for signal propagation leading to systemic jasmonic acid accumulation in wounded *Arabidopsis*. *The Journal of Biological Chemistry*, *284*(50), 34506–34513. https://doi.org/10.1074/jbc.M109.061432

González-Guzmán, M., Apostolova, N., Bellés, J. M., Barrero, J. M., Piqueras, P., Ponce, M. R., … Rodríguez, P. L. (2002). The short-chain alcohol dehydrogenase ABA2 catalyzes the conversion of xanthoxin to abscisic aldehyde. *The Plant Cell*, *14*(8), 1833–1846.

Grebner, W., Stingl, N. E., Oenel, A., Mueller, M. J., & Berger, S. (2013). Lipoxygenase6-dependent oxylipin synthesis in roots is required for abiotic and biotic stress resistance of *Arabidopsis. Plant Physiology*, *161*(4), 2159–2170. https://doi.org/10.1104/pp.113.214544

Greco, M., Chiappetta, A., Bruno, L., & Bitonti, M. B. (2012). In *Posidonia oceanica* cadmium induces changes in DNA methylation and chromatin patterning. *Journal of Experimental Botany*, *63*(2), 695–709.

Grieneisen, V. A., Xu, J., Marée, A. F. M., Hogeweg, P., & Scheres, B. (2007). Auxin transport is sufficient to generate a maximum and gradient guiding root growth. *Nature*, *449*(7165), 1008–1013. https://doi.org/10.1038/nature06215

Griffith, J. S., & Mahler, H. R. (1969). DNA Ticketing Theory of Memory. *Nature*, *223*, 580.

Griffiths, J., Murase, K., Rieu, I., Zentella, R., Zhang, Z.-L., Powers, S. J., … Thomas, S. G. (2006). Genetic characterization and functional analysis of the GID1 gibberellin receptors in *Arabidopsis The Plant Cell*, *18*(12), 3399 LP-3414.

Grossniklaus, U., Vielle-Calzada, J. P., Hoeppner, M. A., & Gagliano, W. B. (1998). Maternal control of embryogenesis by *MEDEA*, a polycomb group gene in *Arabidopsis*. *Science (New York, N.Y.)*, *280*(5362), 446–450.

Grunewald, W., Vanholme, B., Pauwels, L., Plovie, E., Inzé, D., Gheysen, G., & Goossens, A. (2009). Expression of the *Arabidopsis* jasmonate signalling repressor

JAZ1/TIFY10A is stimulated by auxin. *EMBO Reports*, *10*(8), 923–928. https://doi.org/10.1038/embor.2009.103

Guerinot, M. Lou. (2000). The ZIP family of metal transporters. *Biochimica et Biophysica Acta (BBA) - Biomembranes*, *1465*(1), 190–198. https://doi.org/https://doi.org/10.1016/S0005-2736(00)00138-3

Guilfoyle, T. J., & Hagen, G. (2007). Auxin response factors. *Current Opinion in Plant Biology*, *10*(5), 453–460. https://doi.org/https://doi.org/10.1016/j.pbi.2007.08.014

Guo, H., & Ecker, J. R. (2003). Plant responses to ethylene gas are mediated by $SCF^{EBF1/EBF2}$-dependent proteolysis of EIN3 transcription factor. *Cell*, *115*(6), 667–677. https://doi.org/10.1016/S0092-8674(03)00969-3

Gust, A. A., & Nürnberger, T. (2012). A life or death switch. *Nature*, *486*, 198.

Gutiérrez-Marcos, J. F., Costa, L. M., Prà, M. D., Scholten, S., Kranz, E., Perez, P., & Dickinson, H. G. (2006). Epigenetic asymmetry of imprinted genes in plant gametes. *Nature Genetics*, *38*, 876.

Hąc-Wydro, K., Sroka, A., & Jabłońska, K. (2016). The impact of auxins used in assisted phytoextraction of metals from the contaminated environment on the alterations caused by lead (II) ions in the organization of model lipid membranes. *Colloids and Surfaces B: Biointerfaces*, *143*, 124–130. https://doi.org/https://doi.org/10.1016/j.colsurfb.2016.03.018

Han, F., & Zhu, B. (2011). Evolutionary analysis of three gibberellin oxidase genes in rice, *Arabidopsis*, and soybean. *Gene*, *473*(1), 23–35. https://doi.org/https://doi.org/10.1016/j.gene.2010.10.010

Han, L., Li, G.-J., Yang, K.-Y., Mao, G., Wang, R., Liu, Y., & Zhang, S. (2010). Mitogen-activated protein kinase 3 and 6 regulate Botrytis cinerea-induced ethylene production in *Arabidopsis*. *The Plant Journal*, *64*(1), 114–127. https://doi.org/10.1111/j.1365-313X.2010.04318.x

Hark, A. T., Schoenherr, C. J., Katz, D. J., Ingram, R. S., Levorse, J. M., & Tilghman, S. M. (2000). CTCF mediates methylation-sensitive enhancer-blocking activity at the H19/Igf2 locus. *Nature*, *405*(6785), 486–489. https://doi.org/10.1038/35013106

Hartweck, L. M. (2008). Gibberellin signalling. *Planta*, *229*(1), 1. https://doi.org/10.1007/s00425-008-0830-1

Hashem, H. A. (2013). Cadmium toxicity induces lipid peroxidation and alters cytokinin content and antioxidant enzyme activities in soybean. *Botany*, *92*(1), 1–7. https://doi.org/10.1139/cjb-2013-0164

Haun, W. J., Laoueillé-Duprat, S., O'Connell, M. J., Spillane, C., Grossniklaus, U., Phillips, A. R., … Springer, N. M. (2007). Genomic imprinting, methylation and

molecular evolution of maize Enhancer of zeste (Mez) homologs. *The Plant Journal*, *49*(2), 325–337. https://doi.org/10.1111/j.1365-313X.2006.02965.x

He, X.-J., Chen, T., & Zhu, J.-K. (2011). Regulation and function of DNA methylation in plants and animals. *Cell Research*, *21*(3), 442–465. https://doi.org/10.1038/cr.2011.23

Hedden, P., & Phillips, A. L. (2000). Gibberellin metabolism: new insights revealed by the genes. *Trends in Plant Science*, *5*(12), 523–530. https://doi.org/10.1016/S1360-1385(00)01790-8

Hedden, P., & Sponsel, V. (2015). A Century of Gibberellin Research. *Journal of Plant Growth Regulation*, *34*, 740–760. https://doi.org/10.1007/s00344-015-9546-1

Hedden, P., & Thomas, S. G. (2012). Gibberellin biosynthesis and its regulation. *Biochemical Journal*, *444*(1), 11 LP-25.

Helliwell, C. A., Chandler, P. M., Poole, A., Dennis, E. S., & Peacock, W. J. (2001). The CYP88A cytochrome P450, ent-kaurenoic acid oxidase, catalyzes three steps of the gibberellin biosynthesis pathway. *Proceedings of the National Academy of Sciences of the United States of America*, *98*(4), 2065–2070.

Helliwell, C. A., Sullivan, J. A., Mould, R. M., Gray, J. C., Peacock, W. J., & Dennis, E. S. (2001). A plastid envelope location of *Arabidopsis* ent-kaurene oxidase links the plastid and endoplasmic reticulum steps of the gibberellin biosynthesis pathway. *The Plant Journal*, *28*(2), 201–208. https://doi.org/10.1046/j.1365-313X.2001.01150.x

Helliwell, C. A., Poole, A., James Peacock, W., & Dennis, E. S. (1999). *Arabidopsis ent*-kaurene oxidase catalyzes three steps of gibberellin biosynthesis. *Plant Physiology*, *119*(2), 507–510.

Helliwell, C. A., Sheldon, C. C., Olive, M. R., Walker, A. R., Zeevaart, J. A. D., Peacock, W. J., & Dennis, E. S. (1998). Cloning of the *Arabidopsis ent*-kaurene oxidase gene GA3. *Proceedings of the National Academy of Sciences*, *95*(15), 9019 LP-9024.

Henderson, I. R., & Jacobsen, S. E. (2008). Tandem repeats upstream of the *Arabidopsis* endogene SDC recruit non-CG DNA methylation and initiate siRNA spreading. *Genes & Development*, *22*(12), 1597–1606. https://doi.org/10.1101/gad.1667808

Henderson, I. R., & Jacobsen, S. E. (2007). Epigenetic inheritance in plants. *Nature*, *447*, 418.

Henikoff, S., & Comai, L. (1998). A DNA methyltransferase homolog with a chromodomain exists in multiple polymorphic forms in *Arabidopsis*. *Genetics*, *149*(1), 307–318.

Hermon, P., Srilunchang, K., Zou, J., Dresselhaus, T., & Danilevskaya, O. N. (2007). Activation of the imprinted Polycomb Group *FIE1* gene in maize endosperm requires

demethylation of the maternal allele. *Plant Molecular Biology*, *64*(4), 387–395. https://doi.org/10.1007/s11103-007-9160-0

Hernandez, L. E., Carpena-Ruiz, R., & Gárate, A. (1996). Alterations in the mineral nutrition of pea seedlings exposed to cadmium. *Journal of Plant Nutrition*, *19*(12), 1581–1598. https://doi.org/10.1080/01904169609365223

Heyl, A., Riefler, M., Romanov, G. A., & Schmülling, T. (2012). Properties, functions and evolution of cytokinin receptors. *European Journal of Cell Biology*, *91*(4), 246–256. https://doi.org/https://doi.org/10.1016/j.ejcb.2011.02.009

Heyno, E., Klose, C., & Krieger-Liszkay, A. (2008). Origin of cadmium-induced reactive oxygen species production: mitochondrial electron transfer versus plasma membrane NADPH oxidase. *New Phytologist*, *179*(3), 687–699. https://doi.org/10.1111/j.1469-8137.2008.02512.x

Hirose, N., Takei, K., Kuroha, T., Kamada-Nobusada, T., Hayashi, H., & Sakakibara, H. (2007). Regulation of cytokinin biosynthesis, compartmentalization and translocation. *Journal of Experimental Botany*, *59*(1), 75–83. https://doi.org/10.1093/jxb/erm157

Holliday, R., & Pugh, J. E. (1975). DNA modification mechanisms and gene activity during development. *Science (New York, N.Y.)*, *187*(4173), 226–232.

Holliday, R. (1991). Mutations and epimutations in mammalian cells. *Mutation Research/Fundamental and Molecular Mechanisms of Mutagenesis*, *250*(1), 351–363. https://doi.org/https://doi.org/10.1016/0027-5107(91)90192-Q

Hotchkiss, R. D. (1948). The quantitative separation of purines, pyrimidines, and nucleosides by paper chromatography. *The Journal of Biological Chemistry*, *175*(1), 315–332.

Hou, B., Lim, E.-K., Higgins, G. S., & Bowles, D. J. (2004). *N* -Glucosylation of cytokinins by glycosyltransferases of *Arabidopsis thaliana*. *Journal of Biological Chemistry*, *279*(46), 47822–47832. https://doi.org/10.1074/jbc.M409569200

Hsieh, T.-F., Ibarra, C. A., Silva, P., Zemach, A., Eshed-Williams, L., Fischer, R. L., & Zilberman, D. (2009). Genome-wide demethylation of *Arabidopsis* endosperm. *Science*, *324*(5933), 1451–1454. https://doi.org/10.1126/science.1172417

Hu, Y. F., Zhou, G., Na, X. F., Yang, L., Nan, W. Bin, Liu, X., … Bi, Y. R. (2013). Cadmium interferes with maintenance of auxin homeostasis in *Arabidopsis* seedlings. *Journal of Plant Physiology*, *170*(11), 965–975. https://doi.org/https://doi.org/10.1016/j.jplph.2013.02.008

Hua, J., & Meyerowitz, E. M. (1998). Ethylene responses are negatively regulated by a receptor gene family in *Arabidopsis thaliana*. *Cell*, *94*(2), 261–271.

Huettel, B., Kanno, T., Daxinger, L., Aufsatz, W., Matzke, A. J. M., & Matzke, M. (2006). Endogenous targets of RNA-directed DNA methylation and Pol IV in *Arabidopsis*. *The EMBO Journal*, *25*(12), 2828–2836. https://doi.org/10.1038/sj.emboj.7601150

Hull, A. K., Vij, R., & Celenza, J. L. (2000). *Arabidopsis* cytochrome P450s that catalyse the first step of tryptophan-dependent indole-3-acetic acid biosynthesis. *Proceedings of the National Academy of Sciences*, *97*(5), 2379 LP-2384.

Hwang, I., & Sheen, J. (2001). Two-component circuitry in *Arabidopsis* cytokinin signal transduction. *Nature*, *413*(6854), 383. https://doi.org/10.1038/35096500

Hwang, I., Sheen, J., & Müller, B. (2012). Cytokinin signaling networks. *Annual Review of Plant Biology*, *63*(1), 353–380. https://doi.org/10.1146/annurev-arplant-042811-105503

Iakimova, E. T., Woltering, E. J., Kapchina-Toteva, V. M., Harren, F. J. M., & Cristescu, S. M. (2013). Cadmium toxicity in cultured tomato cells—Role of ethylene, proteases and oxidative stress in cell death signaling. *Cell Biology International*, *32*(12), 1521–1529. https://doi.org/10.1016/j.cellbi.2008.08.021

Ibarra, C. A., Feng, X., Schoft, V. K., Hsieh, T.-F., Uzawa, R., Rodrigues, J. A., … Zilberman, D. (2012). Active DNA Demethylation in Plant Companion Cells Reinforces Transposon Methylation in Gametes. *Science (New York, N.Y.)*, *337*(6100), 1360–1364. https://doi.org/10.1126/science.1224839

Iguchi-Ariga, S. M., & Schaffner, W. (1989). CpG methylation of the cAMP-responsive enhancer/promoter sequence TGACGTCA abolishes specific factor binding as well as transcriptional activation. *Genes & Development*, *3*(5), 612–619.

Ingouff, M., Selles, B., Michaud, C., Vu, T. M., Berger, F., Schorn, A. J., … Grimanelli, D. (2017). Live-cell analysis of DNA methylation during sexual reproduction in *Arabidopsis* reveals context and sex-specific dynamics controlled by noncanonical RdDM. *Genes & Development*, *31*(1), 72–83. https://doi.org/10.1101/gad.289397.116

Inoue, T., Higuchi, M., Hashimoto, Y., Seki, M., Kobayashi, M., Kato, T., … Kakimoto, T. (2001). Identification of CRE1 as a cytokinin receptor from *Arabidopsis*. *Nature*, *409*, 1060.

Iqbal, N., Trivellini, A., Masood, A., Ferrante, A., & Khan, N. A. (2013). Current understanding on ethylene signaling in plants: The influence of nutrient availability. *Plant Physiology and Biochemistry*, *73*, 128–138. https://doi.org/https://doi.org/10.1016/j.plaphy.2013.09.011

Iuchi, S., Suzuki, H., Kim, Y.-C., Iuchi, A., Kuromori, T., Ueguchi-Tanaka, M., … Nakajima, M. (2007). Multiple loss-of-function of *Arabidopsis* gibberellin receptor *AtGID1*s completely shuts down a gibberellin signal. *The Plant Journal*, *50*(6), 958–966. https://doi.org/10.1111/j.1365-313X.2007.03098.x

Jackson, R. G., Kowalczyk, M., Li, Y., Higgins, G., Ross, J., Sandberg, G., & Bowles, D. J. (2002). Over-expression of an *Arabidopsis* gene encoding a glucosyltransferase of indole-3-acetic acid: phenotypic characterisation of transgenic lines. *The Plant Journal*, *32*(4), 573–583. https://doi.org/10.1046/j.1365-313X.2002.01445.x

Jacobsen, S. E., Sakai, H., Finnegan, E. J., Cao, X., & Meyerowitz, E. M. (2000). Ectopic hypermethylation of flower-specific genes in *Arabidopsis*. *Current Biology*, *10*(4), 179–186. https://doi.org/10.1016/S0960-9822(00)00324-9

Jain, M., & Khurana, J. P. (2009). Transcript profiling reveals diverse roles of auxin-responsive genes during reproductive development and abiotic stress in rice. *The FEBS Journal*, *276*(11), 3148–3162. https://doi.org/10.1111/j.1742-4658.2009.07033.x

Jammes, F., Song, C., Shin, D., Munemasa, S., Takeda, K., Gu, D., … Kwak, J. M. (2009). MAP kinases MPK9 and MPK12 are preferentially expressed in guard cells and positively regulate ROS-mediated ABA signaling. *Proceedings of the National Academy of Sciences*, *106*(48), 20520 LP-20525.

Janeczko, A., Koscielniak, J., Pilipowicz, M., Szarek-Lukaszewska, G., & Skoczowski, A. (2005). Protection of winter rape photosystem 2 by 24-epibrassinolide under cadmium stress. *Photosynthetica*, *43*(2), 293–298. https://doi.org/10.1007/s11099-005-0048-4

Jeddeloh, J. A., Stokes, T. L., & Richards, E. J. (1999). Maintenance of genomic methylation requires a SWI2/SNF2-like protein. *Nature Genetics*, *22*, 94.

Jiang, Z., Li, J., & Qu, L.-J. (2017). Auxins. In *Hormone Metabolism and Signaling in Plants* (pp. 39–76). Elsevier. https://doi.org/10.1016/B978-0-12-811562-6.00002-5

Jiang, C., Mithani, A., Belfield, E. J., Mott, R., Hurst, L. D., & Harberd, N. P. (2014). Environmentally responsive genome-wide accumulation of *de novo Arabidopsis thaliana* mutations and epimutations. *Genome Research*, *24*(11), 1821–1829. https://doi.org/10.1101/gr.177659.114

Jin, S.-H., Ma, X.-M., Kojima, M., Sakakibara, H., Wang, Y.-W., & Hou, B.-K. (2013). Overexpression of glucosyltransferase UGT85A1 influences trans-zeatin homeostasis and trans-zeatin responses likely through *O*-glucosylation. *Planta*, *237*(4), 991–999. https://doi.org/10.1007/s00425-012-1818-4

Jones-Rhoades, M. W., & Bartel, D. P. (2004). Computational identification of plant microRNAs and their targets, including a stress-induced miRNA. *Molecular Cell*, *14*(6), 787–799. https://doi.org/10.1016/j.molcel.2004.05.027

Joung, J.-G., Corbett, A. M., Fellman, S. M., Tieman, D. M., Klee, H. J., Giovannoni, J. J., & Fei, Z. (2009). Plant MetGenMAP: an integrative analysis system for plant systems biology. *Plant Physiology*, *151*(4), 1758 LP-1768. https://doi.org/10.1104/pp.109.145169

Ju, C., Yoon, G. M., Shemansky, J. M., Lin, D. Y., Ying, Z. I., Chang, J., … Chang, C. (2012). CTR1 phosphorylates the central regulator EIN2 to control ethylene hormone signaling from the ER membrane to the nucleus in *Arabidopsis*. *Proceedings of the National Academy of Sciences of the United States of America*, *109*(47), 19486–19491. https://doi.org/10.1073/pnas.1214848109

Jullien, P. E., Kinoshita, T., Ohad, N., & Berger, F. (2006). Maintenance of DNA methylation during the *Arabidopsis* life cycle is essential for parental imprinting. *The Plant Cell*, *18*(6), 1360–1372. https://doi.org/10.1105/tpc.106.041178

Kagale, S., & Rozwadowski, K. (2011). EAR motif-mediated transcriptional repression in plants: An underlying mechanism for epigenetic regulation of gene expression. *Epigenetics*, *6*(2), 141–146. https://doi.org/10.4161/epi.6.2.13627

Kakutani, T., Jeddeloh, J. A., Flowers, S. K., Munakata, K., & Richards, E. J. (1996). Developmental abnormalities and epimutations associated with DNA hypomethylation mutations. *Proceedings of the National Academy of Sciences of the United States of America*, *93*(22), 12406–12411.

Kankel, M. W., Ramsey, D. E., Stokes, T. L., Flowers, S. K., Haag, J. R., Jeddeloh, J. A., … Richards, E. J. (2003). *Arabidopsis MET1* cytosine methyltransferase mutants. *Genetics*, *163*(3), 1109–1122.

Karlova, R., Boeren, S., van Dongen, W., Kwaaitaal, M., Aker, J., Vervoort, J., & de Vries, S. (2008). Identification of in vitro phosphorylation sites in the *Arabidopsis thaliana* somatic embryogenesis receptor-like kinases. *PROTEOMICS*, *9*(2), 368–379. https://doi.org/10.1002/pmic.200701059

Kasahara, H. (2016). Current aspects of auxin biosynthesis in plants. *Bioscience, Biotechnology, and Biochemistry*, *80*(1), 34–42. https://doi.org/10.1080/09168451.2015.1086259

Kawakatsu, T., Stuart, T., Valdes, M., Breakfield, N., Schmitz, R. J., Nery, J. R., … Ecker, J. R. (2016). Unique cell-type specific patterns of DNA methylation in the root meristem. *Nature Plants*, *2*(5), 16058. https://doi.org/10.1038/nplants.2016.58

Kende, H. (1993). Ethylene Biosynthesis. *Annual Review of Plant Physiology and Plant Molecular Biology*, *44*(1), 283–307. https://doi.org/10.1146/annurev.pp.44.060193.001435

Khan, M. I. R., & Khan, N. A. (2014). Ethylene reverses photosynthetic inhibition by nickel and zinc in mustard through changes in PS II activity, photosynthetic nitrogen use efficiency, and antioxidant metabolism. *Protoplasma*, *251*(5), 1007–1019. https://doi.org/10.1007/s00709-014-0610-7

Kieber, J. J., Rothenberg, M., Roman, G., Feldmann, K. A., & Ecker, J. R. (1993). CTR1, a negative regulator of the ethylene response pathway in *Arabidopsis*, encodes a

member of the Raf family of protein kinases. *Cell*, *72*(3), 427–441. https://doi.org/10.1016/0092-8674(93)90119-B

Kieber, J. J., & Schaller, G. E. (2014). Cytokinins. *The Arabidopsis Book / American Society of Plant Biologists*, *12*, e0168. https://doi.org/10.1199/tab.0168

Kim, M. Y., & Zilberman, D. (2014). DNA methylation as a system of plant genomic immunity. *Trends in Plant Science*, *19*(5), 320–326. https://doi.org/10.1016/j.tplants.2014.01.014

Kinoshita, T., Miura, A., Choi, Y., Kinoshita, Y., Cao, X., Jacobsen, S. E., … Kakutani, T. (2004). One-way control of *FWA* imprinting in *Arabidopsis e*ndosperm by DNA methylation. *Science*, *303*(5657), 521 LP-523.

Kiyosue, T., Ohad, N., Yadegari, R., Hannon, M., Dinneny, J., Wells, D., … Fischer, R. L. (1999). Control of fertilization-independent endosperm development by the *MEDEA* polycomb gene in *Arabidopsis*. *Proceedings of the National Academy of Sciences of the United States of America*, *96*(7), 4186–4191.

Knetsch, M. L. W., Wang, M., Snaar-Jagalska, B. E., & Heimovaara-Dijkstra, S. (1996). Abscisic acid induces mitogen-activated protein kinase activation in barley aleurone protoplasts. *The Plant Cell*, *8*(6), 1061–1067. https://doi.org/10.1105/tpc.8.6.1061

Kong, W., Li, Y., Zhang, M., Jin, F., & Li, J. (2015). A Novel *Arabidopsis* microrna promotes iaa biosynthesis via the indole-3-acetaldoxime pathway by suppressing *SUPERROOT1*. *Plant and Cell Physiology*, *56*(4), 715–726.

Korasick, D. A., Jez, J. M., & Strader, L. C. (2015). Refining *the Nuclear Auxin Response Pathway Through Structural Biology*. *Current Opinion in Plant Biology*, *27*, 22–28. https://doi.org/10.1016/j.pbi.2015.05.007

Koyro, H.-W., Ahmad, P., & Geissler, N. (2012). Abiotic stress responses in plants: an overview. In *Environmental Adaptations and Stress Tolerance of Plants in the Era of Climate Change* (pp. 1–28). New York, NY: Springer New York. https://doi.org/10.1007/978-1-4614-0815-4_1

Kramer, E. M., & Bennett, M. J. (2006). Auxin transport: a field in flux. *Trends in Plant Science*, *11*(8), 382–386. https://doi.org/10.1016/j.tplants.2006.06.002

Krecek, P., Skupa, P., Libus, J., Naramoto, S., Tejos, R., Friml, J., & Zazímalová, E. (2009). The PIN-FORMED (PIN) protein family of auxin transporters. *Genome Biology*, *10*(12), 249. https://doi.org/10.1186/gb-2009-10-12-249

Kriechbaumer, V., Park, W. J., Piotrowski, M., Meeley, R. B., Gierl, A., & Glawischnig, E. (2007). Maize nitrilases have a dual role in auxin homeostasis and β-cyanoalanine hydrolysis. *Journal of Experimental Botany*, *58*(15–16), 4225–4233.

Kumar, S., Cheng, X., Klimasauskas, S., Mi, S., Posfai, J., Roberts, R. J., & Wilson, G. G. (1994). The DNA (cytosine-5) methyltransferases. *Nucleic Acids Research*, *22*(1), 1–10.

Kurakawa, T., Ueda, N., Maekawa, M., Kobayashi, K., Kojima, M., Nagato, Y., … Kyozuka, J. (2007). Direct control of shoot meristem activity by a cytokinin-activating enzyme. *Nature*, *445*, 652.

Kushiro, T., Okamoto, M., Nakabayashi, K., Yamagishi, K., Kitamura, S., Asami, T., … Nambara, E. (2004). The *Arabidopsis* cytochrome P450 CYP707A encodes ABA 8′-hydroxylases: key enzymes in ABA catabolism. *The EMBO Journal*, *23*(7), 1647–1656. https://doi.org/10.1038/sj.emboj.7600121

Laibach, F. (1943). *Arabidopsis thaliana* (L.) Heynh. Als Objekt fu¨ r genetische und entwicklungsphysiologische Untersuchungen. In *Botanisches Archiv* (pp. 439–455).

Laibach, F. (1907). Zur frage nach der individualität der chromosomen im plfanzenreich. *Beihefte Zum Botanischen Centralblatt*, *22*, 19–210.

Lang, Z., Wang, Y., Tang, K., Tang, D., Datsenka, T., Cheng, J., … Zhu, J.-K. (2017). Critical roles of DNA demethylation in the activation of ripening-induced genes and inhibition of ripening-repressed genes in tomato fruit. *Proceedings of the National Academy of Sciences of the United States of America*, *114*(22), E4511–E4519. https://doi.org/10.1073/pnas.1705233114

Lange, T., Hedden, P., & Graebe, J. E. (1994). Expression cloning of a gibberellin 20-oxidase, a multifunctional enzyme involved in gibberellin biosynthesis. *Proceedings of the National Academy of Sciences of the United States of America*, *91*(18), 8552–8556.

Lauria, M., & Rossi, V. (2011). Epigenetic control of gene regulation in plants. *Biochimica et Biophysica Acta (BBA) - Gene Regulatory Mechanisms*, *1809*(8), 369–378. https://doi.org/10.1016/j.bbagrm.2011.03.002

Law, J. A., & Jacobsen, S. E. (2010). Establishing, maintaining and modifying DNA methylation patterns in plants and animals. *Nature Reviews. Genetics*, *11*(3), 204–220. https://doi.org/10.1038/nrg2719

Lazar, T. (2003). Taiz, L. and Zeiger, E. Plant physiology. 3rd edn. *Annals of Botany*, *91*(6), 750–751. https://doi.org/10.1093/aob/mcg079

Lee, K. H., Piao, H. L., Kim, H.-Y., Choi, S. M., Jiang, F., Hartung, W., … Hwang, I. (2006). Activation of glucosidase via stress-induced polymerization rapidly increases active pools of abscisic acid. *Cell*, *126*(6), 1109–1120. https://doi.org/10.1016/j.cell.2006.07.034

Lefebvre, V., North, H., Frey, A., Sotta, B., Seo, M., Okamoto, M., … Marion-Poll, A. (2006). Functional analysis of *Arabidopsis NCED6* and *NCED9* genes indicates that

ABA synthesized in the endosperm is involved in the induction of seed dormancy. *The Plant Journal*, *45*(3), 309–319. https://doi.org/10.1111/j.1365-313X.2005.02622.x

Leyser, O. (2006). Dynamic Integration of Auxin Transport and Signalling. *Current Biology*, *16*(11), R424–R433. https://doi.org/10.1016/J.CUB.2006.05.014

Li, Y., Kumar, S., & Qian, W. (2018). Active DNA demethylation: mechanism and role in plant development. *Plant Cell Reports*, *37*(1), 77–85. https://doi.org/10.1007/s00299-017-2215-z

Li, J., Wu, Y., Xie, Q., & Gong, Z. (2017). 5 - Abscisic acid. In J. Li, C. Li, & S. M. B. T.-H. M. and S. in P. Smith (Eds.) (pp. 161–202). Academic Press. https://doi.org/https://doi.org/10.1016/B978-0-12-811562-6.00005-0

Li, J., Huang, Q., Sun, M., Zhang, T., Li, H., Chen, B., … Wu, X. (2016). Global DNA methylation variations after short-term heat shock treatment in cultured microspores of *Brassica napus* cv. Topas. *Scientific Reports*, *6*(1), 38401. https://doi.org/10.1038/srep38401

Li, Z., & Huang, R. (2011). The reciprocal regulation of abscisic acid and ethylene biosyntheses. *Plant Signaling & Behavior*, *6*(11), 1647–1650. https://doi.org/10.4161/psb.6.11.17756

Li, C., Schilmiller, A. L., Liu, G., Lee, G. I., Jayanty, S., Sageman, C., … Howe, G. A. (2005). Role of β-Oxidation in Jasmonate Biosynthesis and Systemic Wound Signaling in Tomato. *The Plant Cell*, *17*(3), 971 LP-986.

Lichtenthaler, H. K. (1998). The Stress Concept in Plants: An Introduction. *Annals of the New York Academy of Sciences*, *851*(1), 187–198. https://doi.org/10.1111/j.1749-6632.1998.tb08993.x

Lichtenthaler, H. K. (1996). Vegetation Stress: an Introduction to the Stress Concept in Plants. *Journal of Plant Physiology*, *148*(1), 4–14. https://doi.org/https://doi.org/10.1016/S0176-1617(96)80287-2

Lin, C.-A. J., Yang, T.-Y., Lee, C.-H., Huang, S. H., Sperling, R. A., Zanella, M., … Chang, W. H. (2009). Synthesis, characterization, and bioconjugation of fluorescent gold nanoclusters toward biological labeling applications. *ACS Nano*, *3*(2), 395–401. https://doi.org/10.1021/nn800632j

Lindroth, A. M., Cao, X., Jackson, J. P., Zilberman, D., McCallum, C. M., Henikoff, S., & Jacobsen, S. E. (2001). Requirement of *CHROMOMETHYLASE3* for maintenance of CpXpG methylation. *Science*, *292*(5524), 2077 LP-2080.

Lippman, Z., Gendrel, A.-V., Black, M., Vaughn, M. W., Dedhia, N., Richard McCombie, W., … Martienssen, R. (2004). Role of transposable elements in heterochromatin and epigenetic control. *Nature*, *430*, 471.

Lippman, Z., May, B., Yordan, C., Singer, T., & Martienssen, R. (2003). Distinct mechanisms determine transposon inheritance and methylation via small interfering RNA and histone modification. *PLOS Biology*, *1*(3), e67.

Lister, R., Mukamel, E. A., Nery, J. R., Urich, M., Puddifoot, C. A., Johnson, N. D., … Ecker, J. R. (2013). Global epigenomic reconfiguration during mammalian brain development. *Science (New York, N.Y.)*, *341*(6146), 1237905. https://doi.org/10.1126/science.1237905

Lister, R., O'Malley, R. C., Tonti-Filippini, J., Gregory, B. D., Berry, C. C., Millar, A. H., & Ecker, J. R. (2008). Highly Integrated Single-Base Resolution Maps of the Epigenome in *Arabidopsis*. *Cell*, *133*(3), 523–536. https://doi.org/10.1016/j.cell.2008.03.029

Liu, K., Lv, J., He, W., Zhang, H., Cao, Y., & Dai, Y. (2015). Major factors influencing cadmium uptake from the soil into wheat plants. *Ecotoxicology and Environmental Safety*, *113*, 207–213. https://doi.org/10.1016/J.ECOENV.2014.12.005

Liu, Z.-W., Shao, C.-R., Zhang, C.-J., Zhou, J.-X., Zhang, S.-W., Li, L., … He, X.-J. (2014). The SET domain proteins SUVH2 and SUVH9 are required for Pol V occupancy at RNA-Directed DNA methylation loci. *PLoS Genetics*, *10*(1), e1003948. https://doi.org/10.1371/journal.pgen.1003948

Liu, F., Jiang, H., Ye, S., Chen, W.-P., Liang, W., Xu, Y., Sun, B., Sun, J., Wang, Q., Cohen, J. D., Li, C. (2010). The *Arabidopsis* P450 protein CYP82C2 modulates jasmonate-induced root growth inhibition, defense gene expression and indole glucosinolate biosynthesis. *Cell Research*, *20*(5), 539–552. https://doi.org/10.1038/cr.2010.36

Liu, K., Shen, L., & Sheng, J. (2008). Improvement in cadmium tolerance of tomato seedlings with an antisense dna for 1-aminocyclopropane-1-carboxylate synthase. *Journal of Plant Nutrition*, *31*(5), 809–827. https://doi.org/10.1080/01904160802043080

Ljung, K. (2013). Auxin metabolism and homeostasis during plant development. *Development*, *140*(5), 943 LP-950.

Lo, S.-F., Yang, S.-Y., Chen, K.-T., Hsing, Y.-I., Zeevaart, J. A. D., Chen, L.-J., & Yu, S.-M. (2008). A novel class of gibberellin 2-oxidases control semidwarfism, Tillering, and root development in rice. *The Plant Cell*, *20*(10), 2603–2618. https://doi.org/10.1105/tpc.108.060913

Lomin, S. N., Yonekura-Sakakibara, K., Romanov, G. A., & Sakakibara, H. (2011). Ligand-binding properties and subcellular localization of maize cytokinin receptors. *Journal of Experimental Botany*, *62*(14), 5149–5159. https://doi.org/10.1093/jxb/err220

Long, J. A., Ohno, C., Smith, Z. R., & Meyerowitz, E. M. (2006). TOPLESS Regulates Apical Embryonic Fate in *Arabidopsis. Science*, *312*(5779), 1520 LP-1523.

Lorenzo, O., Chico, J. M., Sánchez-Serrano, J. J., & Solano, R. (2004). JASMONATE-INSENSITIVE1 Encodes a MYC Transcription Factor Essential to Discriminate between Different Jasmonate-Regulated Defense Responses in *Arabidopsis*. *The Plant Cell*, *16*(7), 1938 LP-1950.

Ma, Y., Szostkiewicz, I., Korte, A., Moes, D., Yang, Y., Christmann, A., & Grill, E. (2009). Regulators of PP2C phosphatase activity function as abscisic acid sensors. *Science*, *324*(5930), 1064–1068. https://doi.org/10.1126/science.1172408

MADLUNG, A., & COMAI, L. (2004). The effect of stress on genome regulation and structure. *Annals of Botany*, *94*(4), 481–495. https://doi.org/10.1093/aob/mch172

Magome, H., Nomura, T., Hanada, A., Takeda-Kamiya, N., Ohnishi, T., Shinma, Y., … Yamaguchi, S. (2013). CYP714B1 and CYP714B2 encode gibberellin 13-oxidases that reduce gibberellin activity in rice. *Proceedings of the National Academy of Sciences of the United States of America*, *110*(5), 1947–1952. https://doi.org/10.1073/pnas.1215788110

Mahmoud, M., & Kamel, A.R. (2005). Interactive effect of heavy metals and gibberellic acid on mitotic activity and some metabolic changes of *Vicia faba* L. plants. *Cytologia : International Journal of Cytology*, *70*(3), 275–282.

Maksymiec, W. (2011). Effects of jasmonate and some other signalling factors on bean and onion growth during the initial phase of cadmium action. *Biologia Plantarum*, *55*(1), 112–118. https://doi.org/10.1007/s10535-011-0015-9

Maksymiec, W., Wójcik, M., & Krupa, Z. (2007). Variation in oxidative stress and photochemical activity in *Arabidopsis thaliana* leaves subjected to cadmium and excess copper in the presence or absence of jasmonate and ascorbate. *Chemosphere*, *66*(3), 421–427. https://doi.org/https://doi.org/10.1016/j.chemosphere.2006.06.025

Malamy, J. E., & Benfey, P. N. (1997). Analysis of SCARECROW expression using a rapid system for assessing transgene expression in *Arabidopsis* roots. *The Plant Journal: For Cell and Molecular Biology*, *12*(4), 957–963.

Mallory, A. C., Bartel, D. P., & Bartel, B. (2005). MicroRNA-directed regulation of *arabidopsis* auxin response factor17 is essential for proper development and modulates expression of early auxin response genes. *The Plant Cell*, *17*(5), 1360–1375. https://doi.org/10.1105/tpc.105.031716

Manara, A. (2012). Plant responses to heavy metal toxicity - Plants and Heavy Metals. In A. Furini (Ed.) (pp. 27–53). Dordrecht: Springer Netherlands. https://doi.org/10.1007/978-94-007-4441-7_2

Mano, Y., & Nemoto, K. (2012). The pathway of auxin biosynthesis in plants. *Journal of Experimental Botany*, *63*(8), 2853–2872.

Mano, Y., Nemoto, K., Suzuki, M., Seki, H., Fujii, I., & Muranaka, T. (2010). The *AMI1* gene family: indole-3-acetamide hydrolase functions in auxin biosynthesis in plants. *Journal of Experimental Botany*, *61*(1), 25–32.

Martin, R. C., Mok, M. C., Habben, J. E., & Mok, D. W. S. (2001). A maize cytokinin gene encoding an *O*-glucosyltransferase specific to cis-zeatin. *Proceedings of the National Academy of Sciences of the United States of America*, *98*(10), 5922–5926. https://doi.org/10.1073/pnas.101128798

Mashiguchi, K., Tanaka, K., Sakai, T., Sugawara, S., Kawaide, H., Natsume, M., … Kasahara, H. (2011). The main auxin biosynthesis pathway in *Arabidopsis*. *Proceedings of the National Academy of Sciences*, *108*(45), 18512 LP-18517.

Masood, A, Khan, N. (2013). ethylene and gibberellic acid interplay in regulation of photosynthetic capacity inhibition by cadmium. *Journal of Plant Biochemistry & Physiology*, *01*(03), 1–3. https://doi.org/10.4172/2329-9029.1000111

Masood, A., Iqbal, N., & Khan, N. A. (2011). Role of ethylene in alleviation of cadmium-induced photosynthetic capacity inhibition by sulphur in mustard. *Plant, Cell & Environment*, *35*(3), 524–533. https://doi.org/10.1111/j.1365-3040.2011.02432.x

Mathieu, O., Reinders, J., Čaikovski, M., Smathajitt, C., & Paszkowski, J. (2007). Transgenerational stability of the *Arabidopsis* epigenome is coordinated by CG Methylation. *Cell*, *130*(5), 851–862. https://doi.org/10.1016/j.cell.2007.07.007

Matzke, M. A., & Mosher, R. A. (2014). RNA-directed DNA methylation: an epigenetic pathway of increasing complexity. *Nature Reviews Genetics*, *15*, 394.

McCallum, C. M., Comai, L., Greene, E. A., & Henikoff, S. (2000). Targeted screening for induced mutations. *Nature Biotechnology*, *18*, 455.

Meinke, D. W., Cherry, J. M., Dean, C., Rounsley, S. D., & Koornneef, M. (1998). *Arabidopsis thaliana*: a model plant for genome analysis. *Science*, *282*(5389), 662 LP-682.

Mench, M., & Martin, E. (1991). Mobilization of cadmium and other metals from two soils by root exudates of *Zea mays* L., *Nicotiana tabacum* L. and *Nicotiana rustica* L. *Plant and Soil*, *132*(2), 187–196. https://doi.org/10.1007/BF00010399

Meyer, P., Niedenhof, I., & ten Lohuis, M. (1994). Evidence for cytosine methylation of non-symmetrical sequences in transgenic Petunia hybrida. *The EMBO Journal*, *13*(9), 2084–2088.

Mikkelsen, M. D., Hansen, C. H., Wittstock, U., & Halkier, B. A. (2000). Cytochrome P450 CYP79B2 from *Arabidopsis* catalyzes the conversion of tryptophan to indole-

3-acetaldoxime, a precursor of indole glucosinolates and indole-3-acetic acid. *Journal of Biological Chemistry*, *275*(43), 33712–33717. https://doi.org/10.1074/jbc.M001667200

Mitchell-Olds, T. (2001). *Arabidopsis thaliana* and its wild relatives: a model system for ecology and evolution. *Trends in Ecology & Evolution*, *16*(12), 693–700. https://doi.org/10.1016/S0169-5347(01)02291-1

Miyawaki, K., Tarkowski, P., Matsumoto-Kitano, M., Kato, T., Sato, S., Tarkowska, D., … Kakimoto, T. (2006). Roles of *Arabidopsis* ATP/ADP isopentenyltransferases and tRNA isopentenyltransferases in cytokinin biosynthesis. *Proceedings of the National Academy of Sciences of the United States of America*, *103*(44), 16598–16603. https://doi.org/10.1073/pnas.0603522103

Mockaitis, K., & Estelle, M. (2008). Auxin receptors and plant development: A New Signaling Paradigm. *Annual Review of Cell and Developmental Biology*, *24*(1), 55–80. https://doi.org/10.1146/annurev.cellbio.23.090506.123214

Mohsenzadeh, A., Zamani, A., & Taherzadeh, M. J. (2017). Bioethylene production from ethanol: a review and techno-economical evaluation. *ChemBioEng Reviews*, *4*(2), 75–91. https://doi.org/10.1002/cben.201600025

Mok, D. W. S., & Mok, M. C. (2001). Cytokinin metabolism and action. *Annual Review of Plant Physiology and Plant Molecular Biology*, *52*(1), 89–118. https://doi.org/10.1146/annurev.arplant.52.1.89

Moreno, J. L., Hernández, T., Pérez, A., & García, C. (2002). Toxicity of cadmium to soil microbial activity: effect of sewage sludge addition to soil on the ecological dose. *Applied Soil Ecology*, *21*(2), 149–158. https://doi.org/10.1016/S0929-1393(02)00064-1

Moritoh, S., Eun, C.-H., Ono, A., Asao, H., Okano, Y., Yamaguchi, K., … Terada, R. (2012). Targeted disruption of an orthologue of DOMAINS REARRANGED METHYLASE 2, *OsDRM2*, impairs the growth of rice plants by abnormal DNA methylation. *The Plant Journal*, *71*(1), 85–98. https://doi.org/10.1111/j.1365-313X.2012.04974.x

Moubayidin, L., Di Mambro, R., Sozzani, R., Pacifici, E., Salvi, E., Terpstra, I., … Sabatini, S. (2013). Spatial coordination between stem cell activity and cell differentiation in the root meristem. *Developmental Cell*, *26*(4), 405–415. https://doi.org/10.1016/j.devcel.2013.06.025

Moubayidin, L., Salvi, E., Giustini, L., Terpstra, I., Heidstra, R., Costantino, P., & Sabatini, S. (2016). A SCARECROW-based regulatory circuit controls *Arabidopsis thaliana* meristem size from the root endodermis. *Planta*, *243*(5), 1159–1168. https://doi.org/10.1007/s00425-016-2471-0

Mravec, J., Skůpa, P., Bailly, A., Hoyerová, K., Křeček, P., Bielach, A., … Friml, J. (2009). Subcellular homeostasis of phytohormone auxin is mediated by the ER-localized PIN5 transporter. *Nature*, *459*, 1136.

Mukhopadhyay, M., & Mondal, T. K. (2015). Effect of zinc and boron on growth and water relations of *Camellia sinensis* (L.) O. Kuntze cv. T-78. *National Academy Science Letters*, *38*(3), 283–286. https://doi.org/10.1007/s40009-015-0381-5

Murashige, T., & Skoog, F. (1962). A revised medium for rapid growth and bio assays with tobacco tissue cultures. *Physiologia Plantarum*, *15*(3), 473–497. https://doi.org/10.1111/j.1399-3054.1962.tb08052.x

Nam, K. H., & Li, J. (2002). BRI1/BAK1, a receptor kinase pair mediating brassinosteroid signaling. *Cell*, *110*(2), 203–212. https://doi.org/https://doi.org/10.1016/S0092-8674(02)00814-0

Nambara, E., & Marion-Poll, A. (2005). Abscisic acid biosynthesis and catabolism. *Annual Review of Plant Biology*, *56*(1), 165–185. https://doi.org/10.1146/annurev.arplant.56.032604.144046

Nasrallah, M. E., Yogeeswaran, K., Snyder, S., & Nasrallah, J. B. (2000). *Arabidopsis* species hybrids in the study of species differences and evolution of amphiploidy in plants. *Plant Physiology*, *124*(4), 1605 LP-1614.

Nemoto, K., Hara, M., Suzuki, M., Seki, H., Muranaka, T., & Mano, Y. (2008). The *NtAMI1* gene functions in cell division of tobacco BY-2 cells in the presence of indole-3-acetamide. *FEBS Letters*, *583*(2), 487–492. https://doi.org/10.1016/j.febslet.2008.12.049

Nies, D. H. (1999). Microbial heavy-metal resistance. *Applied Microbiology and Biotechnology*, *51*(6), 730–750. https://doi.org/10.1007/s002530051457

Nomura, T., Magome, H., Hanada, A., Takeda-Kamiya, N., Mander, L. N., Kamiya, Y., & Yamaguchi, S. (2013). Functional analysis of *Arabidopsis* CYP714A1 and CYP714A2 reveals that they are distinct gibberellin modification enzymes. *Plant and Cell Physiology*, *54*(11), 1837–1851.

Normanly, J., Cohen, J. D., & Fink, G. R. (1993). *Arabidopsis thaliana* auxotrophs reveal a tryptophan-independent biosynthetic pathway for indole-3-acetic acid. *Proceedings of the National Academy of Sciences of the United States of America*, *90*(21), 10355–10359.

Normanly, J. (2010). Approaching cellular and molecular resolution of auxin biosynthesis and metabolism. *Cold Spring Harbor Perspectives in Biology*, *2*(1), a001594. https://doi.org/10.1101/cshperspect.a001594

Okamoto, M., Kuwahara, A., Seo, M., Kushiro, T., Asami, T., Hirai, N., … Nambara, E. (2006). CYP707A1 and CYP707A2, which encode abscisic acid 8′-hydroxylases, are

indispensable for proper control of seed dormancy and germination in *Arabidopsis*. *Plant Physiology*, *141*(1), 97–107. https://doi.org/10.1104/pp.106.079475

Olszewski, N., Sun, T., & Gubler, F. (2002). Gibberellin signaling: biosynthesis, catabolism, and response pathways. *The Plant Cell*, *14*(Suppl), s61–s80. https://doi.org/10.1105/tpc.010476

Ortiz-Masia, D., Perez-Amador, M. A., Carbonell, J., & Marcote, M. J. (2007). Diverse stress signals activate the C1 subgroup MAP kinases of *Arabidopsis*. *FEBS Letters*, *581*(9), 1834–1840. https://doi.org/10.1016/j.febslet.2007.03.075

Östin, A., Kowalyczk, M., Bhalerao, R. P., & Sandberg, G. (1998). Metabolism of Indole-3-Acetic Acid in *Arabidopsis*. *Plant Physiology*, *118*(1), 285–296.

Ottaviani, A., Gilson, E., & Magdinier, F. (2008). Telomeric position effect: From the yeast paradigm to human pathologies? *Biochimie*, *90*(1), 93–107. https://doi.org/https://doi.org/10.1016/j.biochi.2007.07.022

Ottenschläger, I., Wolff, P., Wolverton, C., Bhalerao, R. P., Sandberg, G., Ishikawa, H., … Palme, K. (2003). Gravity-regulated differential auxin transport from columella to lateral root cap cells. *Proceedings of the National Academy of Sciences of the United States of America*, *100*(5), 2987–2991. https://doi.org/10.1073/pnas.0437936100

Overvoorde, P., Fukaki, H., & Beeckman, T. (2010). Auxin control of root development. *Cold Spring Harbor Perspectives in Biology*, *2*(6), a001537. https://doi.org/10.1101/cshperspect.a001537

Paciorek, T., Zažímalová, E., Ruthardt, N., Petrášek, J., Stierhof, Y.-D., Kleine-Vehn, J., … Friml, J. (2005). Auxin inhibits endocytosis and promotes its own efflux from cells. *Nature*, *435*, 1251.

Park, S.-Y., Fung, P., Nishimura, N., Jensen, D. R., Fujii, H., Zhao, Y., … Cutler, S. R. (2009). Abscisic acid inhibits type 2C protein phosphatases via the PYR/PYL family of START proteins. *Science*, *324*(5930), 1068–1071. https://doi.org/10.1126/science.1173041

Pavlopoulou, A., & Kossida, S. (2007). Plant cytosine-5 DNA methyltransferases: Structure, function, and molecular evolution. *Genomics*, *90*(4), 530–541. https://doi.org/https://doi.org/10.1016/j.ygeno.2007.06.011

Peng, H., & Zhang, J. (2009). Plant genomic DNA methylation in response to stresses: Potential applications and challenges in plant breeding. *Progress in Natural Science*, *19*(9), 1037–1045. https://doi.org/https://doi.org/10.1016/j.pnsc.2008.10.014

Peng, H.-P., Lin, T.-Y., Wang, N.-N., & Shih, M.-C. (2005). Differential expression of genes encoding 1-aminocyclopropane-1-carboxylate synthase in *Arabidopsis* during hypoxia. *Plant Molecular Biology*, *58*(1), 15–25. https://doi.org/10.1007/s11103-005-3573-4

Penterman, J., Zilberman, D., Huh, J. H., Ballinger, T., Henikoff, S., & Fischer, R. L. (2007). DNA demethylation in the *Arabidopsis* genome. *Proceedings of the National Academy of Sciences*, *104*(16), 6752–6757. https://doi.org/10.1073/pnas.0701861104

Pereira, A. (2016). Plant abiotic stress challenges from the changing environment. *Frontiers in Plant Science*, *7*, 1123. https://doi.org/10.3389/fpls.2016.01123

Perilli, S., & Sabatini, S. (2010). Analysis of root meristem size development - Plant Developmental Biology: Methods and Protocols. In L. Hennig & C. Köhler (Eds.) (pp. 177–187). Totowa, NJ: Humana Press. https://doi.org/10.1007/978-1-60761-765-5_12

Perrot-Rechenmann, C., & Napier, R. M. (2005). Auxins. In G. B. T.-V. & H. Litwack (Ed.), *Plant Hormones* (Vol. 72, pp. 203–233). Academic Press. https://doi.org/https://doi.org/10.1016/S0083-6729(04)72006-3

Petrasek, J., & Friml, J. (2009). Auxin transport routes in plant development. *Development*, *136*(16), 2675–2688. https://doi.org/10.1242/dev.030353

Pignatta, D., Erdmann, R. M., Scheer, E., Picard, C. L., Bell, G. W., & Gehring, M. (2014). Natural epigenetic polymorphisms lead to intraspecific variation in *Arabidopsis* gene imprinting. *ELife*, *3*, e03198. https://doi.org/10.7554/eLife.03198

Pikaard, C. S., Haag, J. R., Pontes, O. M. F., Blevins, T., & Cocklin, R. (2012). A transcription fork model for Pol IV and Pol V-dependent RNA-directed DNA methylation. *Cold Spring Harbor Symposia on Quantitative Biology*, *77*(0), 205–212. https://doi.org/10.1101/sqb.2013.77.014803

Pinto, A. P., Mota, A. M., Devarennes, A., Pinto, F. C., De Varennes, A., & Pinto, F. C. (2004). Influence of organic matter on the uptake of cadmium, zinc, copper and iron by sorghum plants. *Science of The Total Environment*, *326*(1), 239–247. https://doi.org/https://doi.org/10.1016/j.scitotenv.2004.01.004

Piotrowska-Niczyporuk, A., Bajguz, A., Zambrzycka, E., & Godlewska-Żyłkiewicz, B. (2012). Phytohormones as regulators of heavy metal biosorption and toxicity in green alga Chlorella vulgaris (Chlorophyceae). *Plant Physiology and Biochemistry*, *52*, 52–65. https://doi.org/https://doi.org/10.1016/j.plaphy.2011.11.009

Plackett, A. R. G., Thomas, S. G., Wilson, Z. A., & Hedden, P. (2011). Gibberellin control of stamen development: a fertile field. *Trends in Plant Science*, *16*(10), 568–578. https://doi.org/10.1016/j.tplants.2011.06.007

Pollmann, S., Müller, A., & Weiler, E. W. (2006). Many roads lead to "auxin": of nitrilases, synthases, and amidases. *Plant Biology, 8*(03), 326–333. https://doi.org/10.1055/s-2006-924075

Poonam, S., Kaur, H., & Geetika, S. (2013). Effect of Jasmonic Acid on Photosynthetic Pigments and Stress Markers in *Cajanus cajan* (L.) Millsp. Seedlings under Copper

Stress. *American Journal of Plant Sciences*, *04*(04), 817–823. https://doi.org/10.4236/ajps.2013.44100

Poorter, H. (2004). Larcher, W. Physiological plant ecology. 4th edn. *Annals of Botany*, *93*(5), 616–617. https://doi.org/10.1093/aob/mch084

Popova, L. P., Maslenkova, L. T., Yordanova, R. Y., Ivanova, A. P., Krantev, A. P., Szalai, G., & Janda, T. (2009). Exogenous treatment with salicylic acid attenuates cadmium toxicity in pea seedlings. *Plant Physiology and Biochemistry*, *47*(3), 224–231. https://doi.org/https://doi.org/10.1016/j.plaphy.2008.11.007

Pósfai, J., Bhagwat, A. S., Pósfai, G., & Roberts, R. J. (1989). Predictive motifs derived from cytosine methyltransferases. *Nucleic Acids Research*, *17*(7), 2421–2435.

Powers, S. K., & Strader, L. C. (2016). Up in the air: untethered factors of auxin response. *F1000Research*, *5*. https://doi.org/10.12688/f1000research.7492.1

Pray, L. (2008). Transposons: The Jumping Genes. *Nature Education*, *1*(1), 204.

Prusinkiewicz, P., & Rolland-Lagan, A.-G. (2006). Modeling plant morphogenesis. *Current Opinion in Plant Biology*, *9*(1), 83–88. https://doi.org/10.1016/j.pbi.2005.11.015

Pysh, L. D., Wysocka-Diller, J. W., Camilleri, C., Bouchez, D., & Benfey, P. N. (2002). The GRAS gene family in *Arabidopsis*: sequence characterization and basic expression analysis of the SCARECROW-LIKE genes. *The Plant Journal*, *18*(1), 111–119. https://doi.org/10.1046/j.1365-313X.1999.00431.x

Qiao, H., Shen, Z., Huang, S. C., Schmitz, R. J., Urich, M. A., Briggs, S. P., & Ecker, J. R. (2012). Processing and subcellular trafficking of er-tethered ein2 control response to ethylene gas. *Science (New York, N.Y.)*, *338*(6105), 390–393. https://doi.org/10.1126/science.1225974

Qiu, Z., Guo, J., Zhu, A., Zhang, L., & Zhang, M. (2014). Exogenous jasmonic acid can enhance tolerance of wheat seedlings to salt stress. *Ecotoxicology and Environmental Safety*, *104*, 202–208. https://doi.org/https://doi.org/10.1016/j.ecoenv.2014.03.014

Ramsahoye, B. H., Biniszkiewicz, D., Lyko, F., Clark, V., Bird, A. P., & Jaenisch, R. (2000). Non-CpG methylation is prevalent in embryonic stem cells and may be mediated by DNA methyltransferase 3a. *Proceedings of the National Academy of Sciences of the United States of America*, *97*(10), 5237–5242.

Ranjan, R., & Lewak, S. (1992). Jasmonic acid promotes germination and lipase activity in non-stratified apple embryos. *Physiologia Plantarum*, *86*(2), 335–339. https://doi.org/10.1034/j.1399-3054.1992.860222.x

Rao, X., Lai, D., & Huang, X. (2013). A New Method for Quantitative Real-Time Polymerase Chain Reaction Data Analysis. *Journal of Computational Biology*, *20*(9), 703–711. https://doi.org/10.1089/cmb.2012.0279

Rauser, W. E., & Dumbroff, E. B. (1981). Effects of excess cobalt, nickel and zinc on the water relations of Phaseolus vulgaris. *Environmental and Experimental Botany*, *21*(2), 249–255. https://doi.org/https://doi.org/10.1016/0098-8472(81)90032-0

Razin, A., & Cedar, H. (1993). DNA methylation and embryogenesis. *EXS*, *64*, 343–357.

Regnault, T., Davière, J.-M., Heintz, D., Lange, T., & Achard, P. (2014). The gibberellin biosynthetic genes *AtKAO1* and *AtKAO2* have overlapping roles throughout *Arabidopsis* development. *The Plant Journal*, *80*(3), 462–474. https://doi.org/10.1111/tpj.12648

Remans, T., Smeets, K., Opdenakker, K., Mathijsen, D., Vangronsveld, J., & Cuypers, A. (2008). Normalisation of real-time RT-PCR gene expression measurements in *Arabidopsis thaliana* exposed to increased metal concentrations. *Planta*, *227*(6), 1343–1349. https://doi.org/10.1007/s00425-008-0706-4

Ren, H., & Gray, W. M. M. (2015). SAUR proteins as effectors of hormonal and environmental signals in plant growth. *Molecular Plant*, *8*(8), 1153–1164. https://doi.org/10.1016/j.molp.2015.05.003

Riggs, A. D. (1975). X inactivation, differentiation, and DNA methylation. *Cytogenetic and Genome Research*, *14*(1), 9–25. https://doi.org/10.1159/000130315

Robert, S., Kleine-Vehn, J., Barbez, E., Sauer, M., Paciorek, T., Baster, P., … Friml, J. (2010). ABP1 mediates auxin inhibition of clathrin-dependent endocytosis in *Arabidopsis*. *Cell*, *143*(1), 111–121. https://doi.org/10.1016/j.cell.2010.09.027

Roberts, A., Pimentel, H., Trapnell, C., & Pachter, L. (2011). Identification of novel transcripts in annotated genomes using RNA-Seq. *Bioinformatics*, *27*(17), 2325–2329.

Rochon, A., Boyle, P., Wignes, T., Fobert, P. R., & Després, C. (2006). The coactivator function of *Arabidopsis* NPR1 requires the core of Its BTB/POZ domain and the oxidation of c-terminal cysteines. *The Plant Cell*, *18*(12), 3670 LP-3685.

Rock, C. D., Bowlby, N. R., Hoffmann-Benning, S., & Zeevaart, J. A. D. (1992). The aba Mutant of *Arabidopsis thaliana* (L.) Heynh. has reduced chlorophyll fluorescence yields and reduced thylakoid stacking. *Plant Physiology*, *100*(4), 1796–1801.

Rodrigues, J. A., & Zilberman, D. (2015). Evolution and function of genomic imprinting in plants. *Genes & Development*, *29*(24), 2517–2531. https://doi.org/10.1101/gad.269902.115

Rodríguez-Serrano, M., Romero-Puertas, M. C., Zabalza, A., Corpas, F. J., Gómez, M., Del Río, L. A., & Sandalio, L. M. (2006). Cadmium effect on oxidative metabolism of pea (*Pisum sativum* L.) roots. Imaging of reactive oxygen species and nitric oxide accumulation in vivo. *Plant, Cell & Environment*, *29*(8), 1532–1544.

Romanov, G. A., Lomin, S. N., & Schmülling, T. (2006). Biochemical characteristics and ligand-binding properties of *Arabidopsis* cytokinin receptor AHK3 compared to CRE1/AHK4 as revealed by a direct binding assay. *Journal of Experimental Botany*, *57*(15), 4051–4058.

Ronemus, M. J., Galbiati, M., Ticknor, C., Chen, J., & Dellaporta, S. L. (1996). Demethylation-induced developmental pleiotropy in *Arabidopsis*. *Science*, *273*(5275), 654 LP-657.

Sabatini, S., Heidstra, R., Wildwater, M., & Scheres, B. (2003). SCARECROW is involved in positioning the stem cell niche in the *Arabidopsis* root meristem. *Genes & Development*, *17*(3), 354–358. https://doi.org/10.1101/gad.252503

Sabatini, S., Beis, D., Wolkenfelt, H., Murfett, J., Guilfoyle, T., Malamy, J., … Scheres, B. (1999). An Auxin-Dependent Distal Organizer of Pattern and Polarity in the *Arabidopsis* Root. *Cell*, *99*(5), 463–472. https://doi.org/10.1016/S0092-8674(00)81535-4

Sahu, P. P., Pandey, G., Sharma, N., Puranik, S., Muthamilarasan, M., & Prasad, M. (2013). Epigenetic mechanisms of plant stress responses and adaptation. *Plant Cell Reports*, *32*(8), 1151–1159. https://doi.org/10.1007/s00299-013-1462-x

Saijo, Y., Uchiyama, B., Abe, T., Satoh, K., & Nukiwa, T. (2018). Contiguous four-guanosine sequence in c-myc antisense phosphorothioate oligonucleotides inhibits cell growth on human lung cancer cells: possible involvement of cell adhesion inhibition. *Japanese Journal of Cancer Research*, *88*(1), 26–33. https://doi.org/10.1111/j.1349-7006.1997.tb00297.x

Saito, S., Hirai, N., Matsumoto, C., Ohigashi, H., Ohta, D., Sakata, K., & Mizutani, M. (2004). *Arabidopsis* CYP707As Encode (+)-Abscisic acid 8′-hydroxylase, a key enzyme in the oxidative catabolism of abscisic acid. *Plant Physiology*, *134*(4), 1439–1449. https://doi.org/10.1104/pp.103.037614

Sakai, H., Hua, J., Chen, Q. G., Chang, C., Medrano, L. J., Bleecker, A. B., & Meyerowitz, E. M. (1998). ETR2 is an ETR1-like gene involved in ethylene signaling in *Arabidopsis*. *Proceedings of the National Academy of Sciences of the United States of America*, *95*(10), 5812–5817. https://doi.org/10.1073/PNAS.95.10.5812

Sakai, H., Honma, T., Aoyama, T., Sato, S., Kato, T., Tabata, S., & Oka, A. (2001). ARR1, a transcription factor for genes immediately responsive to cytokinins. *Science*, *294*(5546), 1519 LP-1521.

Sakamoto, T., Sakakibara, H., Kojima, M., Yamamoto, Y., Nagasaki, H., Inukai, Y., … Matsuoka, M. (2006). Ectopic expression of knotted1-like homeobox protein induces expression of cytokinin biosynthesis genes in rice. *Plant Physiology*, *142*(1), 54 LP-62.

Sakamoto, T., Miura, K., Itoh, H., Tatsumi, T., Ueguchi-Tanaka, M., Ishiyama, K., … Matsuoka, M. (2004). An overview of gibberellin metabolism enzyme genes and their related mutants in rice. *Plant Physiology*, *134*(4), 1642 LP-1653.

Salin, M. L. (1988). Toxic oxygen species and protective systems of the chloroplast. *Physiologia Plantarum*, *72*(3), 681–689. https://doi.org/10.1111/j.1399-3054.1988.tb09182.x

Salvi, E., Di Mambro, R., Pacifici, E., Dello Ioio, R., Costantino, P., Moubayidin, L., & Sabatini, S. (2018). SCARECROW and SHORTROOT control the auxin/cytokinin balance necessary for embryonic stem cell niche specification. *Plant Signaling & Behavior*, *13*(8), e1507402. https://doi.org/10.1080/15592324.2018.1507402

Sanchez, D. H., & Paszkowski, J. (2014). Heat-induced release of epigenetic silencing reveals the concealed role of an imprinted plant gene. *PLoS Genetics*, *10*(11), e1004806. https://doi.org/10.1371/journal.pgen.1004806

Sanders, P. M., Lee, P. Y., Biesgen, C., Boone, J. D., Beals, T. P., Weiler, E. W., & Goldberg, R. B. (2000). The *Arabidopsis DELAYED DEHISCENCE1* gene encodes an enzyme in the jasmonic acid synthesis pathway. *The Plant Cell*, *12*(7), 1041–1062.

Sanità Di Toppi, L., Gremigni, P., Pawlik-Skowroska, B., Prasad, M. N. V., Cobbett, C. S. (2003). Response to heavy metals in plants: a molecular approach. In B. Sanità Di Toppi, L., Pawlik-Skowroska (Ed.), *Abiotic Stresses in Plants* (pp. 133–156). Dordrecht: Kluwer Academic Publishers.

Sanità di Toppi, L., & Gabbrielli, R. (1999). Response to cadmium in higher plants. *Environmental and Experimental Botany*, *41*(2), 105–130. https://doi.org/https://doi.org/10.1016/S0098-8472(98)00058-6

Sasaki, A., Yamaji, N., Yokosho, K., & Ma, J. F. (2012). Nramp5 Is a major transporter responsible for manganese and cadmium uptake in rice. *The Plant Cell*, *24*(5), 2155–2167. https://doi.org/10.1105/tpc.112.096925

Sawchuk, M. G., Edgar, A., & Scarpella, E. (2013). Patterning of leaf vein networks by convergent auxin transport pathways. *PLOS Genetics*, *9*(2), e1003294.

Saze, H., Scheid, O. M., & Paszkowski, J. (2003). Maintenance of CpG methylation is essential for epigenetic inheritance during plant gametogenesis. *Nature Genetics*, *34*(1), 65. https://doi.org/10.1038/ng1138

Scartazza, A., Picciarelli, P., Mariotti, L., Curadi, M., Barsanti, L., & Gualtieri, P. (2017). The role of *Euglena gracilis* paramylon in modulating xylem hormone levels,

photosynthesis and water-use efficiency in Solanum lycopersicum L. *Physiologia Plantarum*, *161*(4), 486–501. https://doi.org/10.1111/ppl.12611

Schaller, G. E., Shiu, S.-H., & Armitage, J. P. (2011). Two-Component Systems and Their Co-Option for Eukaryotic Signal Transduction. *Current Biology*, *21*(9), R320–R330. https://doi.org/10.1016/j.cub.2011.02.045

Schat, H., Sharma, S. S., & Vooijs, R. (2006). Heavy metal-induced accumulation of free proline in a metal-tolerant and a nontolerant ecotype of *Silene vulgaris*. *Physiologia Plantarum*, *101*(3), 477–482. https://doi.org/10.1111/j.1399-3054.1997.tb01026.x

Schellingen, K., Van Der Straeten, D., Vandenbussche, F., Prinsen, E., Remans, T., Vangronsveld, J., & Cuypers, A. (2014). Cadmium-induced ethylene production and responses in *Arabidopsis thaliana* rely on *ACS2* and *ACS6* gene expression. *BMC Plant Biology*, *14*(1), 214. https://doi.org/10.1186/s12870-014-0214-6

Schilmiller, A. L., Koo, A. J. K., & Howe, G. A. (2007). Functional diversification of acyl-coenzyme A oxidases in jasmonic acid biosynthesis and action. *Plant Physiology*, *143*(2), 812–824. https://doi.org/10.1104/pp.106.092916

Schmitz, R. J., Schultz, M. D., Lewsey, M. G., O'Malley, R. C., Urich, M. A., Libiger, O., … Ecker, J. R. (2011). Transgenerational epigenetic instability is a source of novel methylation variants. *Science*, *334*(6054), 369–373. https://doi.org/10.1126/science.1212959

Schommer, C., Palatnik, J. F., Aggarwal, P., Chételat, A., Cubas, P., Farmer, E. E., … Weigel, D. (2008). Control of jasmonate biosynthesis and senescence by mir319 targets. *PLoS Biology*, *6*(9), e230. https://doi.org/10.1371/journal.pbio.0060230

Sekimoto, H., Seo, M., Dohmae, N., Takio, K., Kamiya, Y., & Koshiba, T. (1997). Cloning and molecular characterization of plant aldehyde oxidase. *The Journal of Biological Chemistry*, *272*(24), 15280–15285. https://doi.org/10.1074/JBC.272.24.15280

Seo, M., Akaba, S., Oritani, T., Delarue, M., Bellini, C., Caboche, M., & Koshiba, T. (1998). Higher activity of an aldehyde oxidase in the auxin-overproducing superroot1 mutant of *Arabidopsis thaliana*. *Plant Physiology*, *116*(2), 687–693.

Shan, C., Mei, Z., Duan, J., Chen, H., Feng, H., & Cai, W. (2014). OsGA2ox5, a gibberellin metabolism enzyme, is involved in plant growth, the root gravity response and salt stress. *PLoS ONE*, *9*(1), e87110. https://doi.org/10.1371/journal.pone.0087110

Shan, X., Wang, X., Yang, G., Wu, Y., Su, S., Li, S., … Yuan, Y. (2013). Analysis of the DNA methylation of maize (*Zea mays* L.) in response to cold stress based on methylation-sensitive amplified polymorphisms. *Journal of Plant Biology*, *56*(1), 32–38. https://doi.org/10.1007/s12374-012-0251-3

Shannon, P., Markiel, A., Ozier, O., Baliga, N. S., Wang, J. T., Ramage, D., … Ideker, T. (2003). Cytoscape: A Software Environment for Integrated Models of Biomolecular

Interaction Networks. *Genome Research*, *13*(11), 2498–2504. https://doi.org/10.1101/gr.1239303

Sheen, J. (2002). Phosphorelay and Transcription Control in Cytokinin Signal Transduction. *Science*, *296*(5573), 1650 LP-1652.

Shi, G. R., Cai, Q. S., Liu, Q. Q., & Wu, L. (2009). Salicylic acid-mediated alleviation of cadmium toxicity in hemp plants in relation to cadmium uptake, photosynthesis, and antioxidant enzymes. *Acta Physiologiae Plantarum*, *31*(5), 969–977. https://doi.org/10.1007/s11738-009-0312-5

Shimada, A., Ueguchi-Tanaka, M., Nakatsu, T., Nakajima, M., Naoe, Y., Ohmiya, H., … Matsuoka, M. (2008). Structural basis for gibberellin recognition by its receptor GID1. *Nature*, *456*, 520.

Shu, K., Zhou, W., Chen, F., Luo, X., & Yang, W. (2018). Abscisic acid and gibberellins antagonistically mediate plant development and abiotic stress responses. *Frontiers in Plant Science*, *9*, 416. https://doi.org/10.3389/fpls.2018.00416

Singh, S., & Prasad, S. M. (2014). Growth, photosynthesis and oxidative responses of *Solanum melongena L*. seedlings to cadmium stress: Mechanism of toxicity amelioration by kinetin, *Scientia Horticulturae, 176*, 1–10. https://doi.org/10.1016/j.scienta.2014.06.022

Slotkin, R. K., Vaughn, M., Tanurdžic, M., Borges, F., Becker, J. D., Feijó, J. A., & Martienssen, R. A. (2009). Epigenetic reprogramming and small RNA silencing of transposable elements in pollen. *Cell*, *136*(3), 461–472. https://doi.org/10.1016/j.cell.2008.12.038

Soares, A. M. dos S., Souza, T. F. de, Jacinto, T., & Machado, O. L. T. (2010). Effect of Methyl Jasmonate on antioxidative enzyme activities and on the contents of ROS and H_2O_2 in *Ricinus communis* leaves. *Brazilian Journal of Plant Physiology*, *22*(3), 151–158. https://doi.org/10.1590/S1677-04202010000300001

Sofo, A., Bochicchio, R., Amato, M., Rendina, N., Vitti, A., Nuzzaci, M., … Scopa, A. (2017). Plant architecture, auxin homeostasis and phenol content in Arabidopsis thaliana grown in cadmium- and zinc-enriched media. *Journal of Plant Physiology*, *216*, 174–180. https://doi.org/10.1016/J.JPLPH.2017.06.008

Sofo, A., Vitti, A., Nuzzaci, M., Tataranni, G., Scopa, A., Vangronsveld, J., … Sanità di Toppi, L. (2013). Correlation between hormonal homeostasis and morphogenic responses in *Arabidopsis thaliana* seedlings growing in a Cd/Cu/Zn multi-pollution context. *Physiologia Plantarum*, *149*(4), 487–498. https://doi.org/10.1111/ppl.12050

Song, Y., Jin, L., & Wang, X. (2017). Cadmium absorption and transportation pathways in plants. *International Journal of Phytoremediation*, *19*(2), 133–141. https://doi.org/10.1080/15226514.2016.1207598

Soppe, W. J. J., Jacobsen, S. E., Alonso-Blanco, C., Jackson, J. P., Kakutani, T., Koornneef, M., & Peeters, A. J. M. (2000). The late flowering phenotype of FWA mutants is caused by gain-of-function epigenetic alleles of a homeodomain gene. *Molecular Cell*, *6*(4), 791–802. https://doi.org/10.1016/S1097-2765(05)00090-0

Spíchal, L., Rakova, N. Y., Riefler, M., Mizuno, T., Romanov, G. A., Strnad, M., & Schmülling, T. (2004). Two cytokinin receptors of *Arabidopsis thaliana*, CRE1/AHK4 and AHK3, differ in their ligand specificity in a bacterial assay. *Plant and Cell Physiology*, *45*(9), 1299–1305.

Srivastava, R. K., Pandey, P., Rajpoot, R., Rani, A., & Dubey, R. S. (2014). Cadmium and lead interactive effects on oxidative stress and antioxidative responses in rice seedlings. *Protoplasma*, *251*(5), 1047–1065. https://doi.org/10.1007/s00709-014-0614-3

Stahl, Y., & Rüdiger, S. (2010). Plant primary meristems: shared functions and regulatory mechanisms. *Current Opinion in Plant Biology*, *13*(1), 53–58. https://doi.org/https://doi.org/10.1016/j.pbi.2009.09.008

Staswick, P. E., Serban, B., Rowe, M., Tiryaki, I., Maldonado, M. T., Maldonado, M. C., & Suza, W. (2005). Characterization of an *Arabidopsis* enzyme family that conjugates amino acids to indole-3-acetic acid. *The Plant Cell*, *17*(2), 616 LP-627.

Staswick, P. E., & Tiryaki, I. (2004). the oxylipin signal jasmonic acid is activated by an enzyme that conjugates it to isoleucine in *Arabidopsis*. *The Plant Cell*, *16*(8), 2117 LP-2127.

Staswick, P. E., Tiryaki, I., & Rowe, M. L. (2002). Jasmonate response locus JAR1 and several related *Arabidopsis* genes encode enzymes of the firefly luciferase superfamily that show activity on jasmonic, salicylic, and indole-3-acetic acids in an assay for adenylation. *The Plant Cell*, *14*(6), 1405–1415. https://doi.org/10.1105/tpc.000885

Stepanova, A. N., Robertson-Hoyt, J., Yun, J., Benavente, L. M., Xie, D.-Y., Doležal, K., … Alonso, J. M. (2008). TAA1-mediated auxin biosynthesis is essential for hormone crosstalk and plant development. *Cell*, *133*(1), 177–191. https://doi.org/10.1016/j.cell.2008.01.047

Stepanova, A. N., Yun, J., Robles, L. M., Novak, O., He, W., Guo, H., … Alonso, J. M. (2011). The *Arabidopsis* YUCCA1 flavin monooxygenase functions in the indole-3-pyruvic acid branch of auxin biosynthesis. *The Plant Cell*, *23*(11), 3961–3973. https://doi.org/10.1105/tpc.111.088047

Stintzi, A., & Browse, J. (2000). The *Arabidopsis* male-sterile mutant, opr3, lacks the 12-oxophytodienoic acid reductase required for jasmonate synthesis. *Proceedings of the National Academy of Sciences of the United States of America*, *97*(19), 10625–10630.

Stroud, H., Do, T., Du, J., Zhong, X., Feng, S., Johnson, L., … Jacobsen, S. E. (2014). The roles of non-CG methylation in *Arabidopsis*. *Nature Structural & Molecular Biology*, *21*(1), 64–72. https://doi.org/10.1038/nsmb.2735

Stroud, H., Greenberg, M. V. C., Feng, S., Bernatavichute, Y. V, & Jacobsen, S. E. (2013). Comprehensive analysis of silencing mutants reveals complex regulation of the *Arabidopsis* methylome. *Cell*, *152*(1–2), 352–364. https://doi.org/10.1016/j.cell.2012.10.054

Sugawara, S., Hishiyama, S., Jikumaru, Y., Hanada, A., Nishimura, T., Koshiba, T., … Kasahara, H. (2009). Biochemical analyses of indole-3-acetaldoxime-dependent auxin biosynthesis in *Arabidopsis*. *Proceedings of the National Academy of Sciences*, *106*(13), 5430 LP-5435.

Sun, T. (2011). The molecular mechanism and evolution of the GA-GID1-DELLA signaling module in plants. *Current Biology*, *21*(9), R338–R345. https://doi.org/10.1016/j.cub.2011.02.036

Sun, T., & Gubler, F. (2004). Molecular mechanism of gibberellin signaling in plants. *Annual Review of Plant Biology*, *55*(1), 197–223. https://doi.org/10.1146/annurev.arplant.55.031903.141753

Surani, M. A. H., Barton, S. C., & Norris, M. L. (1984). Development of reconstituted mouse eggs suggests imprinting of the genome during gametogenesis. *Nature*, *308*, 548.

Suzuki, T., Ishikawa, K., Yamashino, T., & Mizuno, T. (2002). An *Arabidopsis* histidine-containing phosphotransfer (HPt) factor implicated in phosphorelay signal transduction: overexpression of AHP2 in plants results in hypersensitiveness to cytokinin. *Plant & Cell Physiology*, *43*(1), 123–129.

Suzuki, T., Miwa, K., Ishikawa, K., Yamada, H., Aiba, H., & Mizuno, T. (2001). The *Arabidopsis* sensor His-kinase, AHk4, can respond to cytokinins. *Plant & Cell Physiology*, *42*(2), 107–113.

Suzuki, T., Imamura, A., Ueguchi, C., & Mizuno, T. (1998). Histidine-containing phosphotransfer (HPt) signal transducers implicated in His-to-Asp phosphorelay in *Arabidopsis*. *Plant & Cell Physiology*, *39*(12), 1258–1268.

Swarup, K., Benková, E., Swarup, R., Casimiro, I., Péret, B., Yang, Y., … Bennett, M. J. (2008). The auxin influx carrier LAX3 promotes lateral root emergence. *Nature Cell Biology*, *10*(8), 946–954. https://doi.org/10.1038/ncb1754

Szemenyei, H., Hannon, M., & Long, J. A. (2008). TOPLESS mediates auxin-dependent transcriptional repression during *Arabidopsis e*mbryogenesis. *Science*, *319*(5868), 1384 LP-1386.

Takuno, S., & Gaut, B. S. (2013). Gene body methylation is conserved between plant orthologs and is of evolutionary consequence. *Proceedings of the National Academy of Sciences of the United States of America*, *110*(5), 1797–1802. https://doi.org/10.1073/pnas.1215380110

Tam, Y. Y., Epstein, E., & Normanly, J. (2000). Characterization of Auxin Conjugates in *Arabidopsis*. Low steady-state levels of indole-3-acetyl-aspartate, indole-3-acetyl-glutamate, and indole-3-acetyl-glucose. *Plant Physiology*, *123*(2), 589–596.

Tan, B.-C., Joseph, L. M., Deng, W.-T., Liu, L., Li, Q.-B., Cline, K., & McCarty, D. R. (2003). Molecular characterization of the *Arabidopsis* 9-cis epoxycarotenoid dioxygenase gene family. *The Plant Journal For Cell and Molecular Biology*, *35*(1), 44–56.

Tanaka, H., Dhonukshe, P., Brewer, P. B., & Friml, J. (2006). Spatiotemporal asymmetric auxin distribution: a means to coordinate plant development. *Cellular and Molecular Life Sciences*, *63*(23), 2738–2754. https://doi.org/10.1007/s00018-006-6116-5

Tao, Y., Ferrer, J.-L., Ljung, K., Pojer, F., Hong, F., Long, J. A., … Chory, J. (2008). Rapid synthesis of auxin via a new tryptophan-dependent pathway is required for shade avoidance in plants. *Cell*, *133*(1), 164–176. https://doi.org/10.1016/j.cell.2008.01.049

Taya, Y., Tanaka, Y., & Nishimura, S. (1978). 5′-AMP is a direct precursor of cytokinin in Dictyostelium discoideum. *Nature*, *271*, 545.

Thines, B., Katsir, L., Melotto, M., Niu, Y., Mandaokar, A., Liu, G., … Browse, J. (2007). JAZ repressor proteins are targets of the SCFCOI1 complex during jasmonate signalling. *Nature*, *448*, 661.

Tian, C., Muto, H., Higuchi, K., Matamura, T., Tatematsu, K., Koshiba, T., & Yamamoto, K. T. (2004). Disruption and overexpression of auxin response factor 8 gene of *Arabidopsis* affect hypocotyl elongation and root growth habit, indicating its possible involvement in auxin homeostasis in light condition. *The Plant Journal*, *40*(3), 333–343. https://doi.org/10.1111/j.1365-313X.2004.02220.x

To, J. P. C., & Kieber, J. J. (2008). Cytokinin signaling: two-components and more. *Trends in Plant Science*, *13*(2), 85–92. https://doi.org/10.1016/j.tplants.2007.11.005

Tognetti, V. B., Van Aken, O., Morreel, K., Vandenbroucke, K., van de Cotte, B., De Clercq, I., … Van Breusegem, F. (2010). Perturbation of indole-3-butyric acid homeostasis by the udp-glucosyltransferase ugt74e2 modulates *Arabidopsis* architecture and water stress tolerance. *The Plant Cell*, *22*(8), 2660–2679. https://doi.org/10.1105/tpc.109.071316

Truernit, E., Bauby, H., Dubreucq, B., Grandjean, O., Runions, J., Barthélémy, J., & Palauqui, J.-C. (2008). High-resolution whole-mount imaging of three-dimensional tissue organization and gene expression enables the study of Phloem development

and structure in *Arabidopsis*. *The Plant Cell*, *20*(6), 1494–1503. https://doi.org/10.1105/tpc.107.056069

Tuteja, N. (2007). Abscisic Acid and abiotic stress signaling. *Plant Signaling & Behavior*, *2*(3), 135–138.

Ueguchi-Tanaka, M., Nakajima, M., Katoh, E., Ohmiya, H., Asano, K., Saji, S., … Matsuoka, M. (2007). Molecular interactions of a soluble gibberellin receptor, gid1, with a rice DELLA protein, SLR1, and gibberellin. *The Plant Cell*, *19*(7), 2140–2155. https://doi.org/10.1105/tpc.106.043729

Uno, Y., Furihata, T., Abe, H., Yoshida, R., Shinozaki, K., & Yamaguchi-Shinozaki, K. (2000). *Arabidopsis* basic leucine zipper transcription factors involved in an abscisic acid-dependent signal transduction pathway under drought and high-salinity conditions. *Proceedings of the National Academy of Sciences of the United States of America*, *97*(21), 11632–11637.

Van Belleghem, F., Cuypers, A., Semane, B., Smeets, K., Vangronsveld, J., d'Haen, J., & Valcke, R. (2006). Subcellular localization of cadmium in roots and leaves of *Arabidopsis thaliana*. *New Phytologist*, *173*(3), 495–508. https://doi.org/10.1111/j.1469-8137.2006.01940.x

van Berkel, K., de Boer, R. J., Scheres, B., & ten Tusscher, K. (2013). Polar auxin transport: models and mechanisms. *Development*, *140*(11), 2253 LP-2268.

Van De Mortel, J. E., Schat, H., Moerland, P. D., Van Themaat, E. V. L. E. R. L., Van Der Ent, S., Blankestijn, H., … Aarts, M. G. M. M. (2007). Expression differences for genes involved in lignin, glutathione and sulphate metabolism in response to cadmium in *Arabidopsis thaliana* and the related Zn/Cd-hyperaccumulator Thlaspi caerulescens. *Plant, Cell & Environment*, *31*(3), 301–324. https://doi.org/10.1111/j.1365-3040.2007.01764.x

van den Berg, C., Willemsen, V., Hendriks, G., Weisbeek, P., & Scheres, B. (1997). Short-range control of cell differentiation in the *Arabidopsis* root meristem. *Nature*, *390*, 287.

Varbanova, M., Yamaguchi, S., Yang, Y., McKelvey, K., Hanada, A., Borochov, R., … Pichersky, E. (2007). Methylation of gibberellins by *Arabidopsis* GAMT1 and GAMT2. *The Plant Cell*, *19*(1), 32 LP-45.

Veach, Y. K., Martin, R. C., Mok, D. W. S., Malbeck, J., Vankova, R., & Mok, M. C. (2003). *O*-Glucosylation of *cis*-zeatin in maize. characterization of genes, enzymes, and endogenous cytokinins. *Plant Physiology*, *131*(3), 1374–1380. https://doi.org/10.1104/pp.017210

Velitchkova, M., & Fedina, I. (1998). Response of photosynthesis of *Pisum sativum* to salt stress as affected by methyl jasmonate. *Photosynthetica*, *35*(1), 89–97. https://doi.org/10.1023/A:1006878016556

Vera-Sirera, F., Gomez, M. D., & Perez-Amador, M. A. (2016). Chapter 20 - DELLA proteins, a group of GRAS transcription regulators that mediate gibberellin signaling. In D. H. B. T.-P. T. F. Gonzalez (Ed.) (pp. 313–328). Boston: Academic Press. https://doi.org/https://doi.org/10.1016/B978-0-12-800854-6.00020-8

Verma, V., Ravindran, P., & Kumar, P. P. (2016). Plant hormone-mediated regulation of stress responses. *BMC Plant Biology*, *16*, 86. https://doi.org/10.1186/s12870-016-0771-y

Verslues, P. E., Agarwal, M., Katiyar-Agarwal, S., Zhu, J., & Zhu, J.-K. (2006). Methods and concepts in quantifying resistance to drought, salt and freezing, abiotic stresses that affect plant water status. *The Plant Journal*, *45*(4), 523–539. https://doi.org/10.1111/j.1365-313X.2005.02593.x

Vert, G., & Chory, J. (2006). Downstream nuclear events in brassinosteroid signalling. *Nature*, *441*, 96.

Veselov, D., Kudoyarova, G., Symonyan, M., & Veselov, S. (2003). Effect of cadmium onion uptake, transpiration and cytokinin content in wheat seedlings. *Bulgarian Journal of Plant Physiology,* Special Issue*, 353–359*

Viaene, T., Delwiche, C. F., Rensing, S. A., & Friml, J. (2013). Origin and evolution of PIN auxin transporters in the green lineage. *Trends in Plant Science*, *18*(1), 5–10. https://doi.org/10.1016/j.tplants.2012.08.009

Villiers, F., Jourdain, A., Bastien, O., Leonhardt, N., Fujioka, S., Tichtincky, G., … Hugouvieux, V. (2012). Evidence for functional interaction between brassinosteroids and cadmium response in *Arabidopsis thaliana*. *Journal of Experimental Botany*, *63*(3), 1185–1200.

Vitti, A., Nuzzaci, M., Scopa, A., Tataranni, G., Remans, T., Vangronsveld, J., & Sofo, A. (2013). Auxin and cytokinin metabolism and root morphological modifications in *Arabidopsis thaliana* seedlings infected with Cucumber mosaic virus (CMV) or exposed to cadmium. *International Journal of Molecular Sciences*, *14*(4), 6889–6902. https://doi.org/10.3390/ijms14046889

von Mering, C., Jensen, L. J., Snel, B., Hooper, S. D., Krupp, M., Foglierini, M., … Bork, P. (2004). STRING: known and predicted protein-protein associations, integrated and transferred across organisms. *Nucleic Acids Research*, *33*(Database issue), D433–D437. https://doi.org/10.1093/nar/gki005

Vrbsky, J., Akimcheva, S., Watson, J. M., Turner, T. L., Daxinger, L., Vyskot, B., … Riha, K. (2010). siRNA–mediated methylation of *Arabidopsis* telomeres. *PLOS Genetics*, *6*(6), e1000986.

Wang, B., Chu, J., Yu, T., Xu, Q., Sun, X., Yuan, J., … Li, J. (2015). Tryptophan-independent auxin biosynthesis contributes to early embryogenesis in *Arabidopsis*.

Proceedings of the National Academy of Sciences of the United States of America, *112*(15), 4821–4826. https://doi.org/10.1073/pnas.1503998112

Wang, H., Wei, Z., Li, J., & Wang, X. (2017). Brassinosteroids. In *Hormone Metabolism and Signaling in Plants* (pp. 291–326). Elsevier. https://doi.org/10.1016/B978-0-12-811562-6.00009-8

Wang, J., Ma, X.-M., Kojima, M., Sakakibara, H., & Hou, B.-K. (2011). *N*-glucosyltransferase UGT76C2 is involved in cytokinin homeostasis and cytokinin response in *Arabidopsis thaliana*. *Plant and Cell Physiology*, *52*(12), 2200–2213.

Wang, J., Ma, X.-M., Kojima, M., Sakakibara, H., & Hou, B.-K. (2013). Glucosyltransferase UGT76C1 finely modulates cytokinin responses via cytokinin N-glucosylation in *Arabidopsis thaliana*. *Plant Physiology and Biochemistry*, *65*, 9–16. https://doi.org/https://doi.org/10.1016/j.plaphy.2013.01.012

Wang, R., & Estelle, M. (2014). Diversity and specificity: auxin perception and signaling through the TIR1/AFB pathway. *Current Opinion in Plant Biology*, *0*, 51–58. https://doi.org/10.1016/j.pbi.2014.06.006

Wang, X., & Chory, J. (2006). Brassinosteroids regulate dissociation of BKI1, a negative regulator of BRI1 signaling, from the plasma membrane. *Science*, *313*(5790), 1118 LP-1122. https://doi.org/10.1126/science.1127593

Weast, R. C. (1984). *CRC Handbook of Chemistry and Physics* (64th ed.). CRC Press, Boca Raton.

Weber, M., Trampczynska, A., & Clemens, S. (2006). Comparative transcriptome analysis of toxic metal responses in *Arabidopsis thaliana* and the Cd^{2+}-hypertolerant facultative metallophyte Arabidopsis halleri. *Plant, Cell & Environment*, *29*(5), 950–963. https://doi.org/10.1111/j.1365-3040.2005.01479.x

Webster, P. L., & MacLeod, R. D. (1980). Characteristics of root apical meristem cell population kinetics: A review of analyses and concepts. *Environmental and Experimental Botany*, *20*(4), 335–358. https://doi.org/10.1016/0098-8472(80)90227-0

Wei, L., Gu, L., Song, X., Cui, X., Lu, Z., Zhou, M., … Cao, X. (2014). Dicer-like 3 produces transposable element-associated 24-nt siRNAs that control agricultural traits in rice. *Proceedings of the National Academy of Sciences of the United States of America*, *111*(10), 3877–3882. https://doi.org/10.1073/pnas.1318131111

Wen, X., Zhang, C., Ji, Y., Zhao, Q., He, W., An, F., … Guo, H. (2012). Activation of ethylene signaling is mediated by nuclear translocation of the cleaved EIN2 carboxyl terminus. *Cell Research*, *22*(11), 1613–1616. https://doi.org/10.1038/cr.2012.145

Wibowo, A., Becker, C., Marconi, G., Durr, J., Price, J., Hagmann, J., … Gutierrez-Marcos, J. (2016). Hyperosmotic stress memory in *Arabidopsis* is mediated by

distinct epigenetically labile sites in the genome and is restricted in the male germline by DNA glycosylase activity. *ELife*, *5*, e13546. https://doi.org/10.7554/eLife.13546

Wilen, R. W., Ewan, B. E., & Gusta, L. V. (1994). Interaction of abscisic acid and jasmonic acid on the inhibition of seed germination and the induction of freezing tolerance. *Canadian Journal of Botany*, *72*(7), 1009–1017. https://doi.org/10.1139/b94-127

Wohrmann, H. J. P., Gagliardini, V., Raissig, M. T., Wehrle, W., Arand, J., Schmidt, A., … Grossniklaus, U. (2012). Identification of a DNA methylation-independent imprinting control region at the *Arabidopsis* MEDEA locus. *Genes & Development*, *26*(16), 1837–1850. https://doi.org/10.1101/gad.195123.112

Woodward, A. W., & Bartel, B. (2005). Auxin: Regulation, Action, and Interaction. *Annals of Botany*, *95*(5), 707–735.

Wulfetange, K., Lomin, S. N., Romanov, G. A., Stolz, A., Heyl, A., & Schmülling, T. (2011). The cytokinin receptors of *Arabidopsis* are located mainly to the endoplasmic reticulum. *Plant Physiology*, *156*(4), 1808 LP-1818.

Wysocka-Diller, J. W., Helariutta, Y., Fukaki, H., Malamy, J. E., & Benfey, P. N. (2000). Molecular analysis of SCARECROW function reveals a radial patterning mechanism common to root and shoot. *Development*, *127*(3), 595 LP-603.

Xiao, W., Custard, K. D., Brown, R. C., Lemmon, B. E., Harada, J. J., Goldberg, R. B., & Fischer, R. L. (2006). DNA methylation is critical for *Arabidopsis* embryogenesis and seed viability. *The Plant Cell*, *18*(4), 805–814. https://doi.org/10.1105/tpc.105.038836

Xing, Y., Jia, W., & Zhang, J. (2008). AtMKK1 mediates ABA-induced CAT1 expression and H_2O_2 production via AtMPK6-coupled signaling in *Arabidopsis*. *The Plant Journal*, *54*(3), 440–451. https://doi.org/10.1111/j.1365-313X.2008.03433.x

Xiong, L., Ishitani, M., Lee, H., & Zhu, J.-K. (2001). The *Arabidopsis* LOS5/ABA3 locus encodes a molybdenum cofactor sulfurase and modulates cold stress– and osmotic stress–responsive gene expression. *The Plant Cell*, *13*(9), 2063 LP-2083.

Xu, H., Liu, Q., Yao, T., & Fu, X. (2014). Shedding light on integrative GA signaling. *Current Opinion in Plant Biology*, *21*, 89–95. https://doi.org/https://doi.org/10.1016/j.pbi.2014.06.010

Xu, J., & Zhang, S. (2014). Regulation of ethylene biosynthesis and signaling by protein kinases and phosphatases. *Molecular Plant*, *7*(6), 939–942. https://doi.org/10.1093/mp/ssu059

Xu, R., Wang, Y., Zheng, H., Lu, W., Wu, C., Huang, J., … Zheng, C. (2015). Salt-induced transcription factor MYB74 is regulated by the RNA-directed DNA methylation pathway in *Arabidopsis*. *Journal of Experimental Botany*, *66*(19), 5997–6008. https://doi.org/10.1093/jxb/erv312

Xu, Z.-Y., Lee, K. H., Dong, T., Jeong, J. C., Jin, J. B., Kanno, Y., … Hwang, I. (2012). A vacuolar β-Glucosidase homolog that possesses glucose-conjugated abscisic acid hydrolyzing activity plays an important role in osmotic stress responses in *ArabidopsisThe Plant Cell*, *24*(5), 2184 LP-2199.

Yamada, M., Greenham, K., Prigge, M. J., Jensen, P. J., & Estelle, M. (2009). The TRANSPORT INHIBITOR RESPONSE2 gene is required for auxin synthesis and diverse aspects of plant development. *Plant Physiology*, *151*(1), 168–179. https://doi.org/10.1104/pp.109.138859

Yamaguchi, N., Mori, S., Baba, K., Kaburagi-Yada, S., Arao, T., Kitajima, N., … Terada, Y. (2011). Cadmium distribution in the root tissues of solanaceous plants with contrasting root-to-shoot Cd translocation efficiencies. *Environmental and Experimental Botany*, *71*(2), 198–206. https://doi.org/https://doi.org/10.1016/j.envexpbot.2010.12.002

Yamaguchi, S., & Kamiya, Y. (2000). Gibberellin biosynthesis: its regulation by endogenous and environmental signals. *Plant & Cell Physiology*, *41*(3), 251–257.

Yamaguchi, S. (2008). Gibberellin metabolism and its regulation. *Annual Review of Plant Biology*, *59*(1), 225–251. https://doi.org/10.1146/annurev.arplant.59.032607.092804

Yamamuro, C., Miki, D., Zheng, Z., Ma, J., Wang, J., Yang, Z., … Zhu, J.-K. (2014). Overproduction of stomatal lineage cells in *Arabidopsis* mutants defective in active DNA demethylation. *Nature Communications*, *5*, 4062. https://doi.org/10.1038/ncomms5062

Yamamuro, C., Zhu, J.-K., & Yang, Z. (2016). Epigenetic modifications and plant hormone action. *Molecular Plant*, *9*(1), 57–70. https://doi.org/10.1016/j.molp.2015.10.008

Yamasaki, S., Fujii, N., & Takahashi, H. (2005). Hormonal Regulation of Sex Expression in Plants. In G. B. T.-V. & H. Litwack (Ed.), *Plant Hormones* (Vol. 72, pp. 79–110). Academic Press. https://doi.org/https://doi.org/10.1016/S0083-6729(05)72003-3

Yan, J., Li, H., Li, S., Yao, R., Deng, H., Xie, Q., & Xie, D. (2013). The *Arabidopsis* F-Box Protein CORONATINE INSENSITIVE1 Is Stabilized by SCF(COI1) and Degraded via the 26S Proteasome Pathway. *The Plant Cell*, *25*(2), 486–498. https://doi.org/10.1105/tpc.112.105486

Yan, Y., Stolz, S., Chételat, A., Reymond, P., Pagni, M., Dubugnon, L., & Farmer, E. E. (2007). A downstream mediator in the growth repression limb of the jasmonate pathway. *The Plant Cell*, *19*(8), 2470 LP-2483.

Yang, D.-L., Li, Q., Deng, Y.-W., Lou, Y.-G., Wang, M.-Y., Zhou, G.-X., … He, Z.-H. (2008). Altered disease development in the eui mutants and eui overexpressors indicates that gibberellins negatively regulate rice basal disease resistance. *Molecular Plant*, *1*(3), 528–537. https://doi.org/10.1093/mp/ssn021

Yang, S. F., & Hoffman, N. E. (1984). Ethylene biosynthesis and its regulation in higher plants. *Annual Review of Plant Physiology*, *35*(1), 155–189. https://doi.org/10.1146/annurev.pp.35.060184.001103

Ye, J., Coulouris, G., Zaretskaya, I., Cutcutache, I., Rozen, S., & Madden, T. L. (2012). Primer-BLAST: a tool to design target-specific primers for polymerase chain reaction. *BMC Bioinformatics*, *13*, 134. https://doi.org/10.1186/1471-2105-13-134

Yong-Villalobos, L., González-Morales, S. I., Wrobel, K., Gutiérrez-Alanis, D., Cervantes-Peréz, S. A., Hayano-Kanashiro, C., … Herrera-Estrella, L. (2015). Methylome analysis reveals an important role for epigenetic changes in the regulation of the *Arabidopsis* response to phosphate starvation. *Proceedings of the National Academy of Sciences of the United States of America*, *112*(52), E7293–E7302. https://doi.org/10.1073/pnas.1522301112

Yoshida, H., & Ueguchi-Tanaka, M. (2014). DELLA and SCL3 balance gibberellin feedback regulation by utilizing INDETERMINATE DOMAIN proteins as transcriptional scaffolds. *Plant Signaling & Behavior*, *9*, e29726. https://doi.org/10.4161/psb.29726

Yuan, H.-M., & Huang, X. (2015). Inhibition of root meristem growth by cadmium involves nitric oxide-mediated repression of auxin accumulation and signalling in *Arabidopsis*. *Plant, Cell & Environment*, *39*(1), 120–135. https://doi.org/10.1111/pce.12597

Yue, R., Lu, C., Qi, J., Han, X., Yan, S., Guo, S., … Tie, S. (2016). Transcriptome analysis of cadmium-treated roots in maize (*Zea mays* L.). *Frontiers in Plant Science*, *7*, 1298. https://doi.org/10.3389/fpls.2016.01298

Zemach, A., Kim, M. Y., Hsieh, P.-H., Coleman-Derr, D., Eshed-Williams, L., Thao, K., … Zilberman, D. (2013). The nucleosome remodeler DDM1 allows DNA methyltransferases to access H1-containing heterochromatin. *Cell*, *153*(1), 193–205. https://doi.org/10.1016/j.cell.2013.02.033

Zhai, Q., Yan, C., Li, L., Xie, D., & Li, C. (2017). 7 - Jasmonates. In J. Li, C. Li, & S. M. B. T.-H. M. and S. in P. Smith (Eds.) (pp. 243–272). Academic Press. https://doi.org/https://doi.org/10.1016/B978-0-12-811562-6.00007-4

Zhang, H., Lang, Z., & Zhu, J.-K. (2018). Dynamics and function of DNA methylation in plants. *Nature Reviews Molecular Cell Biology*, *19*(8), 489–506. https://doi.org/10.1038/s41580-018-0016-z

Zhang, B., Tieman, D. M., Jiao, C., Xu, Y., Chen, K., Fei, Z., … Klee, H. J. (2016). Chilling-induced tomato flavor loss is associated with altered volatile synthesis and transient changes in DNA methylation. *Proceedings of the National Academy of Sciences of the United States of America*, *113*(44), 12580–12585. https://doi.org/10.1073/pnas.1613910113

Zhang, H., & Zhu, J.-K. (2011). RNA-directed DNA Methylation. *Current Opinion in Plant Biology*, *14*(2), 142–147. https://doi.org/10.1016/j.pbi.2011.02.003

Zhang, X., & Jacobsen, S. E. (2006). Genetic Analyses of DNA Methyltransferases in *Arabidopsis thaliana*. *Cold Spring Harbor Symposia on Quantitative Biology* , *71*, 439–447.

Zhao, Y. (2014). Auxin Biosynthesis. *The Arabidopsis Book / American Society of Plant Biologists*, *12*, e0173. https://doi.org/10.1199/tab.0173

Zhao, Z., Zhang, Y., Liu, X., Zhang, X., Liu, S., Yu, X., … Wan, J. (2013). A role for a dioxygenase in auxin metabolism and reproductive development in rice. *Developmental Cell*, *27*(1), 113–122. https://doi.org/10.1016/j.devcel.2013.09.005

Zhao, Y. (2010). Auxin biosynthesis and its role in plant development. *Annual Review of Plant Biology*, *61*, 49–64. https://doi.org/10.1146/annurev-arplant-042809-112308

Zhao, Q., & Guo, H.-W. (2011). Paradigms and paradox in the ethylene signaling pathway and interaction network. *Molecular Plant*, *4*(4), 626–634. https://doi.org/10.1093/mp/ssr042

Zhao, Y., Hull, A. K., Gupta, N. R., Goss, K. A., Alonso, J., Ecker, J. R., … Celenza, J. L. (2002). Trp-dependent auxin biosynthesis in *Arabidopsis*: involvement of cytochrome P450s CYP79B2 and CYP79B3. *Genes & Development*, *16*(23), 3100–3112. https://doi.org/10.1101/gad.1035402

Zhong, S., Fei, Z., Chen, Y.-R., Zheng, Y., Huang, M., Vrebalov, J., … Giovannoni, J. J. (2013). Single-base resolution methylomes of tomato fruit development reveal epigenome modifications associated with ripening. *Nature Biotechnology*, *31*, 154.

Zhou, J.-J., & Luo, J. (2018). The PIN-FORMED Auxin Efflux Carriers in Plants. *International Journal of Molecular Sciences*, *19*(9), 2759. https://doi.org/10.3390/ijms19092759

Zhu, J.-K. (2016). Abiotic Stress Signaling and Responses in Plants. *Cell*, *167*(2), 313–324. https://doi.org/10.1016/j.cell.2016.08.029

Zhu, X. F., Wang, Z. W., Dong, F., Lei, G. J., Shi, Y. Z., Li, G. X., & Zheng, S. J. (2013). Exogenous auxin alleviates cadmium toxicity in *Arabidopsis thaliana* by stimulating synthesis of hemicellulose 1 and increasing the cadmium fixation capacity of root cell walls. *Journal of Hazardous Materials*, *263*, 398–403. https://doi.org/10.1016/j.jhazmat.2013.09.018

Zhu, J.-K. (2009). Active DNA demethylation mediated by DNA glycosylases. *Annual Review of Genetics*, *43*(1), 143–166. https://doi.org/10.1146/annurev-genet-102108-134205

Zhu, Y. (2010). The epigenetic involvement in plant hormone signaling. *Chinese Science Bulletin*, *55*(21), 2198–2203. https://doi.org/10.1007/s11434-010-3193-2

Zilberman, D. (2008). The evolving functions of DNA methylation. *Current Opinion in Plant Biology*, *11*(5), 554–559. https://doi.org/10.1016/j.pbi.2008.07.004

Zilberman, D., & Henikoff, S. (2007). Genome-wide analysis of DNA methylation patterns. *Development*, *134*(22), 3959 LP-3965.

ACKNOWLEDGEMENTS

I would like to express my sincere gratitude to my advisor Prof. Maria Beatrice Bitonti for the continuous support of my Ph.D and related research. Besides my advisor, I would like to thank Dott. Ernesto Picardi for his precious contribution in conducting transcriptomic analyses. Finally, a special thanks goes to Prof. Piero Picciarelli and Dott. Lorenzo Mariotti, who performed hormones quantification.